BANDWIDTH CONSTRAINED SIGNATURE WAVEFORMS FOR CDMA SYSTEMS

by

Ha H. Nguyen

SUBMITTED IN PARTIAL FULFILLMENT OF THE
REQUIREMENTS FOR THE DEGREE OF
DOCTOR OF PHILOSOPHY
AT
THE UNIVERSITY OF MANITOBA
WINNIPEG, MANITOBA
AUGUST, 2001

THE UNIVERSITY OF MANITOBA

FACULTY OF GRADUATE STUDIES

*****

COPYRIGHT PERMISSION

BANDWIDTH CONSTRAINED SIGNATURE WAVEFORMS FOR CDMA SYSTEMS

BY

HA H. NGUYEN

A Thesis/Practicum submitted to the Faculty of Graduate Studies of The University of Manitoba in partial fulfillment of the requirement of the degree

of

DOCTOR OF PHILOSOPHY

To my parents, Hanh and NamCa.

Acknowledgements

I am extremely grateful to my advisor, Professor E. Shwedyk, for his endless support and guidance throughout my doctoral studies at the University of Manitoba. His technical expertise and moral encouragement have always been a great source of motivation. I would like to thank Professors G. O. Martens, M. Pawlak, and N. Popplewell for serving on my dissertation committee and for their helpful comments and suggestions on my thesis work. I would also like to thank Professor H. Leib for acting as an external examiner.

The financial support from the University of Manitoba Graduate Fellowship (UMGF), Natural Sciences and Engineering Research Council of Canada (NSERC) operating grant, the Faculty of Graduate Studies and the Department of Electrical and Computer Engineering are gratefully acknowledged. These financial sources have made my dream of pursuing a Ph.D. degree possible.

I am also grateful to all the teachers I had the privilege to learn from during the many years I spent in school, first in my home country Vietnam, then in Thailand and lately in Canada. Their help, inspiration and encouragement are always remembered and appreciated.

Finally, I would like to express my deepest love and gratitude to my parents, my wife and my son for their understanding, support, encouragement and sacrifices. I am deeply indebted to my parents for so much. They always provided me with the best opportunities in education, regardless of many difficulties in the past. I thank Hanh and NamCa for allowing me to put our lives on hold for many years to complete my degree and for always being there for me. To them I dedicate this dissertation.

Abstract

Code-division multiple access (CDMA) increases the spectral efficiency of a communication system by allowing all users to share a common channel at the same time. To provide multiple access, CDMA systems require a family of distinct signature waveforms to be assigned to different users. Since the limiting factor for such a system is the inevitable multiple-access interference (MAI) present at the receiver, it is important to suppress the MAI in CDMA systems. This thesis focuses mainly on signature waveform design as a means of suppressing the MAI. The novelty in the approach is that the available bandwidth of the systems is explicitly incorporated into the design process. In this way, this precious resource is most efficiently utilized and hence a benefit is achieved.

In the first part of the thesis, signature waveform design is considered for *synchronous* CDMA systems equipped with either correlation or minimum mean-square error (MMSE) receivers. The design criterion can be either to maximize the network capacity (i.e., the maximum number of users) for a specified level of MAI, or to minimize the average MAI for a given number of users. Both the fractional out-of-band energy (FOBE) and the root-mean-square (RMS) bandwidth measures are examined. Comparisons to signature waveforms constructed using different approaches are made to quantify the superiority of the proposed signature waveforms. When the FOBE bandwidth criterion is used, the generation of the proposed signature waveforms at the receivers is quite complicated due to the involvement of the prolate spheroidal wave functions. Thus a simplified receiver structure based on a Walsh signal space is also developed for a practical use.

In the second part, signature waveforms are designed to minimize the MAI in *asynchronous* CDMA systems. The series expansion method is first applied to find the optimal signature waveforms, where no special restriction is imposed on the structure of the signature waveforms. For a special class of asynchronous CDMA systems, known as direct-sequence CDMA (DS-CDMA), the signature waveforms are constructed by modulating a given chip waveform with the corresponding *signature sequences*. Furthermore, when random signature sequences are assumed, the MAI in DS-CDMA systems is only affected by the shape of the chip waveform. In this thesis, the use of *multiple* chip waveforms is also introduced as a means of suppressing MAI in DS-CDMA systems. Optimal multiple chip waveforms are obtained using the series expansion method. Finally, to evaluate the error performance of DS-CDMA systems using random signature sequences and multiple chip waveforms, an expression for error probabilities is derived based on Holtzman's approximation and its accuracy is verified with simulation results.

Contents

List of Tables

List of Figures

This page is intentionally left blank.

List of Symbols and Abbreviations

α	The SIR requirement level
γ	The Signal-to-background noise ratio
$\epsilon(s_k(t))$	The fraction of the energy of $s_k(t)$ lying outside the frequency W
$\epsilon(\mathbf{s}(t))$	The average fraction of the energy of $\mathbf{s}(t)$ lying outside the frequency W
η	The fractional out-of-band energy parameter
$\mathbf{\Lambda}$	The diagonal matrix of the ordered eigenvalues of the correlation matrix $\mathbf{R}$
$\mathbf{\Xi}$	The diagonal matrix whose kth diagonal element equals $1-\chi_{k-1}$
$\mathbf{\Pi}$	The diagonal matrix whose kth diagonal element equals k^2
σ^2	The variance of the background noise
τ_k	The delay of the kth user's signal
$\mathbf{\Phi}(t)$	The vector of time-truncated sinusoids as orthonormal basis functions
$\mathbf{\Psi}(t)$	The vector of shifted, normalized and time-truncated prolate spheroidal wave functions as orthonormal basis functions
φ_k	The overall phase shift of the kth user's signal
$\varphi_i(t,c)$	The ith prolate spheroidal wave function
$\widehat{\varphi}_i(t,c)$	The ith shifted, normalized and time-truncated prolate spheroidal wave function

χ_i	The ith eigenvalue correponding to the ith prolate spheroidal wave function
b_k	The information symbol of the kth user
$b(s_k(t))$	The RMS bandwidth of a signal $s_k(t)$
$b(\mathbf{s}(t))$	The average RMS bandwidth of a signal set vector $\mathbf{s}(t)$
$\mathbf{b}$	The vector of the information symbols of all users
$\widehat{\mathbf{b}}$	The estimate of $\mathbf{b}$
$\mathbf{C}$	The matrix of the linear filter in the linear multiuser receiver
$\mathbf{c}_k^\top$	The kth row of matrix $\mathbf{C}$
E_b	The energy per symbol
$\mathcal{F}\{\cdot\}$	The Fourier transform operation
f_c	The carrier frequency
G	The asymptotic gain in network capacity
$g_m(t)$	The mth chip waveform
$\mathbf{H}$	The Hadamard matrix
$h_{m,n}(r)$, $\widehat{h}_{m,n}(r)$	The cross-correlation functions between the mth and the nth chip waveforms
$h_m(r)$, $\widehat{h}_m(r)$	The cross-correlation functions of the mth chip waveform
$\mathbf{I}$	The identity matrix
I	The normalized interference parameter
$I_{k,i}$	The interference caused by the ith user to the kth user
J	The normalized average MAI variance
K	The number of users
$\mathbf{m}$	The Gaussian vector of zero-mean and identity covariance matrix
$m_1,\ \widehat{m}_1,\ w_1,\ \widehat{w}_1$	The correlation parameters of a single chip waveform
$\mathbf{n}$	The Gaussian vector of zero-mean and covariance matrix $\mathbf{R}$
N	The processing gain
$N_0/2$	The variance of the background noise

p_k	The received power of the kth user
P	The common received power
$P(f)$	The power spectral density function
$Q(\cdot)$	The complementary unit cumulative Gaussian distribution
$R_{k,i}(\tau)$, $\widehat{R}_{k,i}(\tau)$	The cross-correlation functions between the kth and the ith signature waveforms
$R_k(\tau)$, $\widehat{R}_k(\tau)$	The cross-correlation functions of the kth signature waveform
$\mathbf{R}$	The correlation matrix of the signature waveforms
$\mathbf{R}_k$	The kth column of correlation matrix $\mathbf{R}$
$\mathbf{R}_{i,j}$	The (i,j) element of correlation matrix $\mathbf{R}$
$\widehat{\mathbf{R}}$	The power-weighted correlation matrix
$s_k(t)$	The signature waveform of the kth user
$\mathbf{s}(t)$	The signature vector
$\mathbf{s}_k$	The signature sequence of the kth user
$\mathbf{S}$	The signature matrix
T	The symbol duration
T_c	The chip duration
$\mathbf{v}_k$	The kth eigenvector of the correlation matrix $\mathbf{R}$
$\mathbf{V}$	The matrix of the eigenvectors of the correlation matrix $\mathbf{R}$
W	The transmission bandwidth
$\mathbf{W}$	The diagonal matrix of the received powers of all users
$w_k(t)$	The kth Walsh function
$\mathbf{w}(t)$	The vector of the first L Walsh functions
$y(t)$	The received signal
y_k	The output of a filter matched to $s_k(t)$
$\mathbf{y}$	The vector of sufficient statistic

AWGN	Additive white Gaussian noise
A-CDMA	Asynchronous code division multiple access

BER	Bit error rate
CDMA	Code division multiple access
DS-CDMA	Direct sequence code division multiple access
FDMA	Frequency division multiple access
FOBE	Fractional out-of-band energy
FOBP	Fractional out-of-band power
GA	Gaussian approximation
ICI	Inter-chip interference
IGA	Improved Gaussian approximation
ISI	Inter-chip-symbol interference
MAI	Multiple access interference
MMSE	Minimum mean-square error
MSE	Mean-square error
MTSC	Minimum total squared correlation
PSD	Power spectral density
PSWF	Prolate spheroidal wave function
RMS	Root-mean-square
S-CDMA	Synchronous code division multiple access
SIR	Signal-to-interference ratio
SRRC	Squared-root raised cosine
TDMA	Time division multiple access
TIP	Total interference parameter
TMSE	Total mean squared error
TSC	Total squared correlation
UGP	Uniformly good property
WBE	Welch bound equality

Chapter 1

Introduction

The need for multiple access techniques arises when more than one user transmits over the same medium. As an example, a multiple access technique is required in cellular telephony. In this example, the users are cellular telephone customers and the common medium is the range of radio frequencies allocated for use by cellular subscribers. Without multiple access techniques, only one caller would be able to make a call at a given time. There are three common forms of multiple access, namely frequency division multiple access (FDMA), time division multiple access (TDMA), and code division multiple access (CDMA).

With the FDMA technique, the available frequency band is divided into disjoint sub-bands and each of these sub-bands is used to carry a single user's signal at the same time. In a TDMA system, time slots are allocated to the users such that only one user can transmit in a particular time slot over the same frequency band. It is important to point out that in both FDMA and TDMA systems, different users do not incur any mutual interference from each other. This is made possible by ensuring that the signals transmitted by various users are mutually orthogonal, either in frequency or in time. For a given signaling duration T and a transmission bandwidth W, the number of orthogonal users in both FDMA and TDMA systems is approximately $2WT$, which is a fixed number [1].

In a CDMA system, users are assigned different *signature waveforms* (or *codes*, an older terminology from which the term CDMA originated [2]). Each user sends her/his narrow-band data stream by modulating her/his own signature waveform. All user signals are then transmitted over the same frequency band and at the same time. The signature waveforms are used to spread the bandwidth of the transmitted signals over the entire frequency band, and if they are well chosen, the corresponding receivers (which have knowledge of these waveforms) can de-spread the received signal and recover the intended narrow-band data streams.

Technically, the users in CDMA systems can also be orthogonal if their signature waveforms are orthogonal. However the important (and interesting) feature of CDMA communications is that users are not necessarily orthogonal. This implies that the number of users in CDMA systems is not hard-limited by $2WT$ as in FDMA or TDMA systems and users can be added and removed from a CDMA system quite easily. This property makes network planning and management in CDMA systems much simpler.

Since the users are not necessarily orthogonal in CDMA systems, there is interuser interference or multiple access interference (MAI) apart from the background noise. This additional interference limits performance, but due to the way time and bandwidth resources are allocated, CDMA systems offer higher capacity compared to FDMA and TDMA systems [3]. The flexibility and higher spectral efficiency has made CDMA the standard of choice for the air-interface in the third and fourth generations (3G and 4G) of wireless mobile systems [4, 5].

To further improve the spectral efficiency of CDMA systems, it is important to suppress the MAI. Loosely speaking, there are three different methods for suppressing MAI in CDMA systems: i) to design signature waveforms with MAI-suppression capability for a given type of receiver; ii) to design efficient receivers for a given set of signature waveforms and iii) to jointly design transmitters and receivers.

The topic of receiver design for CDMA systems has been very active in the past fifteen years under the name of *multiuser detection*. Perhaps this research area was pioneered by the work of Verdú in 1986 [6]. In [6] the author derives the optimal multiuser receiver based on a maximum likelihood criterion and shows that there is, in general, a huge gap in the performance between the conventional correlation receiver and the optimal receiver. It has also been shown that the complexity of the optimal multiuser detector is exponential in the number of users and hence it is not practical for implementation, even for a system with a moderate number of users [7]. To reduce the complexity of multiuser receivers, many different suboptimal detectors have been proposed in the literature (see [8] and [9] for extensive reviews). It should be noted, however, that when the suboptimal receivers are used, they are very sensitive to the signature waveforms and this makes signature waveform design a more crucial task in CDMA systems. Regarding joint transmitter and receiver design, this research topic has just been recently introduced and there is relatively little work done on this topic [10, 11, 12]. This thesis concentrates on signature waveform design as a means of suppressing MAI in CDMA systems. The design considers both synchronous and asynchronous CDMA systems and under different bandwidth criteria.

1.1 Previous Work and Thesis Contribution

CDMA systems can be either *synchronous* (S-CDMA) or *asynchronous* (A-CDMA) and signature waveform design must be considered for a particular system. Synchronous systems assume that the users' bit epochs are perfectly aligned at the receiver. This requires closed-loop timing control or providing the transmitters with access to a common clock (such as the Global Positioning System) [2]. In asynchronous CDMA systems, the users' time epochs are not aligned. The design of CDMA systems is considerably simplified if the users need not be synchronized. However the spectral efficiency of asynchronous CDMA systems is significantly lower than that of

the synchronous ones.

Conceptually, it is not necessary to place any specific structure on the signature waveforms, as long as they satisfy the duration, bandwidth and energy constraints. There is, however, a common and popular approach to constructing the signature waveforms for both synchronous and asynchronous CDMA systems. This approach assumes that the space of signature waveforms is spanned by some set of orthonormal basis functions. Each signature waveform is then constructed as a linear combination of basis functions weighted by a *signature sequence*. The length of each signature sequence equals the dimensionality of the signature space (commonly referred to as the *processing gain* N) which is controlled by the available bandwidth of the system. Thus, given N and a set of basis functions, the design of signature waveforms is essentially the design of signature sequences.

Signature sequence designs for S-CDMA systems are studied in [13, 14, 15], where it is shown that the optimal sequences are the Welch bound equality (WBE) sequences since they satisfy Welch's bound on the sum of the squared cross correlations of equal energy sequences [13, 16]. The performance measure in [14] is the the (information) sum capacity of a S-CDMA system, whereas the network capacity, i.e., the maximum number of users that can be accommodated in a system, is the performance criterion in [15]. Recently, a generalization of the work in [14] has been presented in [17] to include the case of unequal-power users. It should be noted that the bandwidth consideration is not explicitly specified in all of the above mentioned work, but rather is taken into account through the dimensionality of the signature space. In this thesis we will extend the results of [15] by considering the bandwidth constraint to better exploit this system resource. Using the property of the WBE sequences, the optimal orthonormal basis functions for the construction of signature waveforms can be easily identified.

Signature waveform designs for S-CDMA systems are also considered in [18, 19,

20, 21], where either the root-mean-square (RMS) or fractional out-of-band energy (FOBE) bandwidth constraint [22] is explicitly specified in the design problems. In particular, the authors in [18] and [19] found the information capacity region of a two-user synchronous CDMA system and the optimal pairs of signature waveforms that achieve any point inside the capacity region. In [20] the authors derive the signature waveforms that maximize the total information capacity and asymptotic efficiency of a S-CDMA system under the RMS bandwidth constraint. Similar work considering the FOBE bandwidth constraint appears in [21].

Unlike the above mentioned work which was concerned with the information theory aspects of a CDMA communications channel, in this thesis the signature waveforms are designed to minimize the MAI at the outputs of the receivers. The bandwidth constraint (which can be either RMS or FOBE bandwidth) is also explicitly incorporated into the design process. The design is carried out for two different types of receivers, namely the conventional correlation receiver and the minimum mean-square error (MMSE) receiver. Furthermore, since under the FOBE bandwidth criterion, the optimal signature waveforms are constructed from the prolate spheroidal wave functions (PSWFs) [23, 24], the implementation of receivers operating with these signature waveforms is complicated. To overcome this disadvantage, a simplified receiver is also developed based on the Walsh signal space.

In A-CDMA systems, the signature waveforms are usually generated using signature sequences shaped by an elementary chip waveform. In binary transmission, the signature sequences are binary sequences, whereas in M-ary modulation, the signature sequences are polyphase sequences (whose symbols are the complex Mth roots of unity). The most popular polyphase sequences are the quadriphase sequences, corresponding to quadrature phase shift keying (PSK) modulation. Analysis of A-CDMA systems leads to the consideration of various correlation functions of the spreading sequences [25, 26, 27]. For signature sequences in A-CDMA systems, there are also

Welch bounds on the maximum magnitude ($C_{\max}$) and root-mean-square (RMS) magnitude (C_{rms}) of their correlation functions [27, 28]. The sequences that achieves the Welch lower bound on C_{rms} are referred to as Welch-bound-equality (WBE) sequences and they are of particularly importance in A-CDMA systems [14, 27]. It was shown in [29] that finding WBE sequences is almost trivially easy, for example *almost all* linear codes (and their cosets) form a WBE sequence set. In contrast, signal sets that meet Welch bound on $C_{\max}$ are not easy to find. Two examples are the binary Gold code family [25] and the two families (families $\mathcal{A}$ and $\mathcal{B}$) of quadriphase sequences found in [30]. In [27] the optimal phases of family $\mathcal{A}$ sequences are also obtained so that the family satisfies the Welch bounds on $C_{\max}$ and C_{rms} simultaneously.

A different method of designing signature waveforms for A-CDMA systems that does not rely on binary or polyphase sequences has also appeared in [31]. The signature waveforms obtained in [31] are constrained to have a flat amplitude spectrum and they are complex signals in general. Such a constraint requires that the cardinality of the signature set be fairly low so that they have good cross-correlation values.

This thesis also considers signature waveform design for A-CDMA systems. The signature waveforms are not assumed to have any specific structure and they are designed to minimize the average MAI at the outputs of the correlation receiver. The correlation receiver is preferred to other multiuser receivers in A-CDMA systems because the complexity of any multiuser detection is usually prohibitive in asynchronous systems with a large number of users. Analogous to the design for S-CDMA systems, here the bandwidth is also explicitly incorporated into the design process.

Although there are signature sequences that perform better than the random signature sequences [26, 27, 30], the use of random signature sequences has been widely adopted to analyze the performance of A-CDMA systems [32, 33, 34, 35]. With random signature sequences, the MAI variance at the output of a correlation receiver

depends only on the chip pulse shape. Generally, the chip pulse can be either a time-limited or a band-limited waveform. Commonly used time-limited chip waveforms are rectangular and half-sine pulses [36, 37]. Other time-limited chip waveforms are introduced and evaluated in [35, 38, 39]. On the other hand, the square root raised cosine pulse is the most popular band-limited waveform [4, 5, 35]. It is widely expected that the band-limited chip waveforms are more bandwidth efficient than the time-limited ones, however this is not always true as shown in [35]. Another contribution of this thesis is the proposal of using multiple chip waveforms instead of a single chip waveform as a means of suppressing MAI. The study is restricted to the family of time-limited chip waveforms but the idea can be easily extended to band-limited waveforms. Optimal multiple chip waveforms are obtained for the RMS bandwidth constraint, although the methodology is also applicable for the FOBE bandwidth criterion. The combinations of some commonly used chip waveforms are also evaluated to investigate the advantage of the proposed scheme. Finally, to evaluate the performance of A-CDMA systems employing random signature sequences and multiple chip waveforms, an extension of Holtzman's approximation for error probabilities is also derived.

1.2 Thesis Outline

The rest of this thesis is organized as follows. Chapter 2 first describes the system models for both S-CDMA and A-CDMA communications systems. For S-CDMA systems, both the correlation and MMSE receivers are discussed in detail. For A-CDMA systems, only the correlation receiver is considered. The chapter also defines the RMS and FOBE bandwidths for CDMA systems, which will be used throughout the rest of the thesis.

In Chapter 3, signature waveforms for maximizing the network capacity of S-CDMA systems are obtained under both the RMS and FOBE bandwidth constraints.

Based on the results in [15], the signature waveforms are constructed from the Welch-bound-equality (WBE) sequences [13]. It is first shown that using the property of the WBE sequences, the constraint on the bandwidth of signature waveforms can be transformed into the bandwidth constraint of the orthonormal basis functions. Then the optimal orthonormal bases are identified to be used with the WBE sequences. Performance of the proposed signature waveforms is compared to that of the suboptimal signature waveforms (constructed from suboptimal basis functions) to quantify the gain achieved by the proposed signature waveforms.

Chapter 4 also studies signature waveform design for S-CDMA systems but under a slightly different scenario. Here the number of users is fixed and the signature waveforms to minimize the multiple access interference (MAI) are found. The design is first carried out for the correlation receiver under both RMS and FOBE bandwidth constraints. Then it is extended to include the MMSE receiver. Comparison to suboptimal signature waveforms that are constructed from WBE sequences is also made to quantify the superiority of the proposed signature waveforms.

Chapter 5 is concerned with the practical implementation of the linear receivers when the signature waveforms are constructed from prolate spheroidal wave functions (this happens when the FOBE bandwidth criterion is used). The structure of the simplified receiver in a Walsh signal space is first developed. Then its performance is evaluated based on the exact expression of error probability for S-CDMA communications.

Chapter 6 is devoted to the design of signature and multiple chip waveforms for A-CDMA systems. The chapter begins with the evaluation of the signal-to-interference ratio (SIR) at the output of a correlation receiver in terms of the Fourier transforms of the signature and chip waveforms respectively. These expressions suggest a method to obtain the signature and chip waveforms through series expansion. The series expansion method can be applied for both RMS and FOBE bandwidth constraints, but

for simplicity only the optimal signature waveforms and multiple chip waveforms are presented for the case of RMS bandwidth. Additionally, this chapter also investigates the combinations of several commonly used chip waveforms to study the gain achieved by using multiple chip waveforms.

An error probability calculation for A-CDMA systems using random signature sequences and double chip waveforms is the topic of Chapter 7. The main contribution of this chapter is to extend and evaluate the accuracy of an approximation previously proposed by Holtzman [40]. This approximation is first extended to include an arbitrary *single* chip waveform. The accuracy of Holtzman's approximation for this case is verified with the exact calculation derived in [34]. Holtzman's approximation is then developed for A-CDMA systems using double chip waveforms and its accuracy is verified using computer simulation.

Finally Chapter 8 draws conclusions and gives suggestions for further study.

Chapter 2

Signalling Over CDMA Channels

This chapter reviews basic concepts in CDMA systems and serves as background material for the subsequent chapters. Both the synchronous and asynchronous CDMA channel models are discussed. Various receivers, including optimal, correlation and minimum mean-square error (MMSE) receivers are explained for S-CDMA systems. For A-CDMA systems, only the correlation receiver is considered. The importance of signature waveform design for system performance is highlighted. This chapter also discusses the bandwidth criteria used in the thesis.

2.1 S-CDMA System Model

In a synchronous CDMA system, each user transmits an information symbol in a time interval T and over a bandwidth W by modulating its own distinct signature waveform. Let K be the number of users and $s_k(t)$, $0 \leq t \leq T$, be the signature waveform of the kth user whose energy is normalized to unity. Then the received *baseband* signal in one symbol interval can be expressed as

$$y(t) = \sum_{k=1}^{K} \sqrt{p_k} b_k s_k(t) + n(t), \qquad 0 \leq t \leq T \tag{2.1}$$

where b_k is the information symbol of the kth user ($b_k \in A_k$ for some finite set of amplitudes A_k), p_k is the received power of the kth user's signal and $n(t)$ is additive

white Gaussian noise of spectral strength $\sigma^2 = N_0/2$. To simplify the analysis it is assumed that $E[b_k^2] = 1$ (by scaling the set of amplitudes A_k appropriately).

It can be shown that a sufficient statistic for demodulating the information symbols of K users is given by the K-vector $\mathbf{y}$ whose kth component is the output of a filter matched to $s_k(t)$ [2], i.e.,

$$y_k = \int_0^T y(t)s_k(t)\mathrm{d}t, \qquad k = 1, \ldots, K. \tag{2.2}$$

The sufficient statistic vector $\mathbf{y} = [y_1, \ldots, y_K]^\top$ can be written as

$$\mathbf{y} = \mathbf{R}\mathbf{W}^{1/2}\mathbf{b} + \sigma\mathbf{n} \tag{2.3}$$

where one has the following:

- $\mathbf{R}$ denotes the correlation matrix of the set of signature waveforms

$$\mathbf{R} = [\mathbf{R}_{ij}] = \int_0^T \mathbf{s}(t)\mathbf{s}^\top(t)\mathrm{d}t \tag{2.4}$$

  where $\mathbf{s}(t) = [s_1(t), \ldots, s_K(t)]^\top$ is the signal set vector.

- $\mathbf{b} \in \{[b_1, b_2, \ldots, b_K]^\top | b_k \in A_k\}$ is the vector of information symbols of all users. For a binary data symbol $A_k = \{+1, -1\}$.

- $\mathbf{n}$ is a Gaussian vector of zero-mean and covariance matrix $\mathbf{R}$, independent of the transmitted symbols.

- $\mathbf{W} = \mathrm{diag}(p_1, p_2, \ldots, p_K)$.

When the signature space is spanned by an orthonormal set $\{\psi_1(t), \ldots, \psi_N(t)\}$, $0 \le t \le T$, a different N-vector $\mathbf{r}$ of sufficient statistic can be obtained by projecting the received signal $y(t)$ onto the orthonormal set. Let each user waveform be written as

$$s_k(t) = \sum_{i=1}^{N} s_k(i)\psi_i(t), \qquad 0 \le t \le T \tag{2.5}$$

then

$$\mathbf{r} = \sum_{k=1}^{K} \sqrt{p_k} b_k \mathbf{s}_k + \sigma \mathbf{m} = \mathbf{S}\mathbf{W}^{1/2}\mathbf{b} + \sigma \mathbf{m} \tag{2.6}$$

where $\mathbf{s}_k = [s_k(1), \ldots, s_k(N)]^\top$ is the signature sequence of user k, $\mathbf{S} = [\mathbf{s}_1, \mathbf{s}_2, \ldots, \mathbf{s}_K]$ is an $N \times K$ signature matrix and $\mathbf{m}$ is a Gaussian vector of zero-mean and identity covariance matrix, independent of $\mathbf{b}$. Note that since $\mathbf{R} = \mathbf{S}^\top\mathbf{S}$, it is easy to see from (2.3) and (2.6) that

$$\mathbf{y} = \mathbf{S}^\top \mathbf{r} \tag{2.7}$$

The output of the matched filter in (2.2) can be decomposed into three components as follows:

$$\begin{aligned} y_k &= \int_0^T y(t) s_k(t) \mathrm{d}t \\ &= \sqrt{p_k} b_k + \underbrace{\sum_{\substack{i=1 \\ i \neq k}}^{K} \sqrt{p_i} b_i \int_0^T s_i(t) s_k(t) \mathrm{d}t}_{\text{MAI}} + \int_0^T n(t) s_k(t) \mathrm{d}t. \end{aligned} \tag{2.8}$$

In (2.8) the first component contains the desired signal of user k, the second component is due to multiple-access interference (MAI) from all other $(K-1)$ users and the last component is due to the background noise.

Though the vector $\mathbf{y}$ in (2.3) is a sufficient statistic for detecting one or more user information symbols, the conventional approach for demodulating the vector $\mathbf{b}$ in (2.3) has been to rely on correlation receivers (or single-user matched filters) as follows:

$$\widehat{b}_k = \mathrm{sgn}(y_k), \quad k = 1, \ldots, K; \qquad \text{or} \quad \widehat{\mathbf{b}} = \mathrm{sgn}(\mathbf{y}). \tag{2.9}$$

This approach simply neglects the presence of MAI since it assumes that the statistical properties of MAI are similar to additive white Gaussian noise, and therefore a correlation receiver should be near-optimal to combat such interference. This assumption was proven wrong by the derivation and analysis of the optimal multiuser detector in [6].

The optimal multiuser detector searches for the most likely $\mathbf{b}$ in (2.3) that minimizes the error probability, or equivalently maximizes the likelihood function

$$\Omega(\mathbf{b}) = 2\mathbf{b}^\top \mathbf{W}^{1/2}\mathbf{y} - \mathbf{b}^\top \widehat{\mathbf{R}}\mathbf{b} \tag{2.10}$$

where $\widehat{\mathbf{R}} = \mathbf{W}^{1/2}\mathbf{R}\mathbf{W}^{1/2}$, is the power weighted correlation matrix. Unfortunately, for an arbitrary correlation matrix, no search algorithm is known for the optimal multiuser detection whose computational complexity is polynomial in the number of users. In fact the complexity of the search in (2.10) is exponential in the number of users ($O(2^K)$ for binary transmission). The following structural constraints on the correlation matrix or the signature waveforms are known to lead to polynomial complexity of the optimal multiuser detection.

(i) Band-diagonal correlation matrix with small number of non-zero diagonals [2, 41].

(ii) Non-positive cross-correlation among all pairs of signature waveforms [42].

(iii) Tree structure of the signature waveforms where the signature waveforms in the same subset are orthogonal [43].

However, the above constraints are rather restrictive and can be satisfied only in some special scenarios of CDMA communication.

Recently, there has been considerable interest in linear multiuser detection [44, 45, 46, 47], where a linear filter, $\mathbf{C}$, is introduced between the the bank of matched filters and the bank of hard limiters (for detection of binary information) as shown in Fig. 2.1. Although the linear multiuser detector does not achieve minimum bit-error-rate, it has been shown to satisfy alternative optimization criteria such as asymptotic efficiency or near-far resistance [44].

Note that the correlation receiver is the simplest linear multiuser detector obtained by choosing linear filter $\mathbf{C}$ to be an identity matrix. i.e., $\mathbf{C} = \mathbf{I}$. On the other

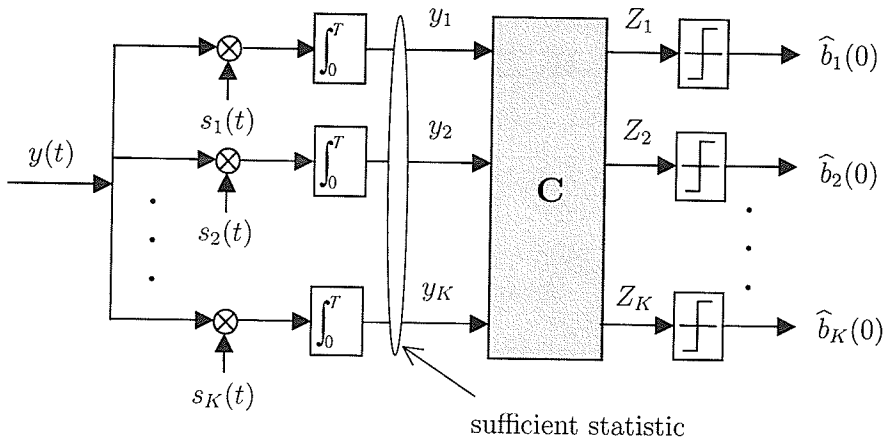

Figure 2.1: Linear multiuser receiver

hand, the decorrelating receiver [44] is realized by setting $\mathbf{C} = \mathbf{R}^{-1}$. In this manner, the decorrelating receiver totally removes the MAI simultaneously enhances the background noise [44]. Another important linear multiuser receiver is the minimum mean square error (MMSE) detector, whose linear filter $\mathbf{C}$ is obtained as follows (see also [2] for a different treatment).

Let $\mathbf{c}_k^\top = [C_{k1}, \ldots, C_{kK}]$ be the kth row of matrix $\mathbf{C}$. The linear receiver for user k can be written as

$$c_k(t) = \sum_{j=1}^{K} C_{kj} s_j(t) = \mathbf{c}_k^\top \mathbf{s}(t). \tag{2.11}$$

The output of the linear detector for user k is,

$$\begin{aligned} Z_k &= \langle c_k(t), y(t) \rangle = \mathbf{c}_k^\top \mathbf{y} \\ &= \sqrt{p_k} b_k \mathbf{c}_k^\top \mathbf{R}_k + \sum_{\substack{j=1 \\ j \neq k}}^{K} \sqrt{p_j} b_j \mathbf{c}_k^\top \mathbf{R}_j + \sigma \mathbf{c}_k^\top \mathbf{n} \end{aligned} \tag{2.12}$$

where $\mathbf{R}_k$ is the kth column of correlation matrix $\mathbf{R}$. The mean-square value of Z_k can be decomposed into three different components as follows

$$E\left\{Z_k^2\right\} = p_k \left(\mathbf{c}_k^\top \mathbf{R}_k\right)^2 + \sum_{j=1, j \neq k}^{K} p_j \left(\mathbf{c}_k^\top \mathbf{R}_j\right)^2 + \sigma^2 \mathbf{c}_k^\top \mathbf{R} \mathbf{c}_k. \tag{2.13}$$

The first component accounts for the power of the desired signal of user k, the second component is due to MAI and the last component is caused by the background noise due to correlation with $\mathbf{c}_k$. As mentioned before, the correlation receiver neglects the MAI and chooses the linear filter to minimize the background noise, whereas the decorrelating receiver neglects the background noise and chooses the linear filter to minimize the MAI. In contrast, the MMSE receiver chooses the filter to minimize the mean squared error $E\left\{\left(\mathbf{c}_k^\top \mathbf{y} - \sqrt{p_k}b_k\right)^2\right\}$. Using (2.3) and the assumption that the data symbols from different users are independent of each other and of the background noise, one then obtains

$$\begin{aligned}
\mathrm{MSE}_k &= E\left\{\left(\mathbf{c}_k^\top \mathbf{y} - \sqrt{p_k}b_k\right)^2\right\} \\
&= E\left\{\left[\mathbf{c}_k^\top\left(\mathbf{R}\mathbf{W}^{1/2}\mathbf{b} + \sigma\mathbf{n}\right) - \sqrt{p_k}b_k\right]\left[\left(\sigma\mathbf{n}^\top + \mathbf{b}^\top\mathbf{W}^{1/2}\mathbf{R}\right)\mathbf{c}_k - \sqrt{p_k}b_k\right]\right\} \\
&= E\left\{\mathbf{c}_k^\top\mathbf{R}\mathbf{W}^{1/2}\mathbf{b}\mathbf{b}^\top\mathbf{W}^{1/2}\mathbf{R}\mathbf{c}_k - 2\mathbf{c}_k^\top\mathbf{R}\mathbf{W}^{1/2}\mathbf{b}\sqrt{p_k}b_k + \sigma^2\mathbf{c}_k^\top\mathbf{n}\mathbf{n}^\top\mathbf{c}_k + p_k b_k^2\right\} \\
&= \mathbf{c}_k^\top\left(\mathbf{R}\mathbf{W}\mathbf{R} + \sigma^2\mathbf{R}\right)\mathbf{c}_k + p_k - 2p_k\mathbf{c}_k^\top\mathbf{R}_k. \qquad (2.14)
\end{aligned}$$

Setting $\partial\mathrm{MSE}_k/\partial\mathbf{c}_k = 0$ gives

$$\mathbf{c}_k = \left(\mathbf{R}\mathbf{W}\mathbf{R} + \sigma^2\mathbf{R}\right)^{-1} p_k\mathbf{R}_k \qquad (2.15)$$

from which the linear filter $\mathbf{C}$ is

$$\mathbf{C} = \mathbf{C}^\top = \left(\mathbf{R}\mathbf{W}\mathbf{R} + \sigma^2\mathbf{R}\right)^{-1}\mathbf{R}\mathbf{W} = \left(\mathbf{R} + \sigma^2\mathbf{W}^{-1}\right)^{-1}. \qquad (2.16)$$

Note that to obtain the above identity it has been assumed that the correlation matrix $\mathbf{R}$ is invertible (or non-singular). If this is not the case, the p-inverse (pseudo-inverse[1]) should be used to give

$$\mathbf{c}_k = \left(\mathbf{R}\mathbf{W}\mathbf{R} + \sigma^2\mathbf{R}\right)^{-} p_k\mathbf{R}_k. \qquad (2.17)$$

[1]For each $m \times n$ matrix $\mathbf{A}$, there exists a unique $n \times m$ matrix $\mathbf{A}^-$ satisfying the four properties:

(1) $\mathbf{A}^-\mathbf{A}\mathbf{A}^- = \mathbf{A}^-$ (2) $\mathbf{A}\mathbf{A}^-\mathbf{A} = \mathbf{A}$
(3) $(\mathbf{A}^-\mathbf{A})^{\mathrm{H}} = \mathbf{A}^-\mathbf{A}$ (4) $(\mathbf{A}\mathbf{A}^-)^{\mathrm{H}} = \mathbf{A}\mathbf{A}^-$ (H means Hermitian)

If $\mathbf{A}$ is diagonal then $\mathbf{A}^-_{kk} = 1/\mathbf{A}_{kk}$ if $\mathbf{A}_{kk} \neq 0$, and $\mathbf{A}^-_{kk} = 0$ if $\mathbf{A}_{kk} = 0$.

From the expressions of the matrix $\mathbf{C}$ for all the linear receivers discussed above the following observation can be made regarding the required information for their implementation. The advantage of the correlation receiver is that its implementation requires only the signature waveform of the the user to be demodulated. The decorrelator, on the other hand, requires knowledge of all users' signature waveforms to demodulate any given user. The MMSE receiver too requires knowledge of all users' signature waveforms, as well as requiring knowledge of the signal-to-noise ratios of all users. The benefit obtained from the requirement of more information for the receiver implementation is the superiority in bit-error-rate performance of the corresponding receiver [47].

One performance measure used in this thesis is the signal-to-interference ratio (SIR) at the output of the linear multiuser detector. This parameter is defined as the ratio of the power in the decision statistic due to the desired signal to the total power due to the interfering users plus the background noise. Thus, it follows from (2.13) that the SIR is given by

$$\mathrm{SIR}_k = \frac{p_k \left(\mathbf{c}_k^\top \mathbf{R}_k\right)^2}{\sigma^2 \mathbf{c}_k^\top \mathbf{R} \mathbf{c}_k + \sum_{\substack{j=1 \\ j \neq k}}^{K} p_j \left(\mathbf{c}_k^\top \mathbf{R}_j\right)^2}. \tag{2.18}$$

This is an intuitively useful measure of performance, particularly when error control coding is implemented. Among all linear receivers, the MMSE receiver maximizes the signal-to-interference ratio [2]. For the correlation and decorrelating receivers, the SIR simplifies to

$$\mathrm{SIR}_k = \frac{p_k}{\sigma^2 + \sum_{\substack{j=1 \\ j \neq k}}^{K} p_j \mathbf{R}_{kj}^2} \tag{2.19}$$

and

$$\mathrm{SIR}_k = \frac{p_k}{\sigma^2 \left(\mathbf{R}^{-1}\right)_{kk}} \tag{2.20}$$

respectively.

Next it is shown that for the MMSE receiver, the SIR_k can be expressed in terms of MMSE_k, which is the MSE_k in (2.14) corresponding to the MMSE receiver. Rewrite the SIR in (2.18) as follows

$$\mathrm{SIR}_k = \frac{p_k \left(\mathbf{c}_k^\top \mathbf{R}_k\right)^2}{E\left\{Z_k^2\right\} - p_k \left(\mathbf{c}_k^\top \mathbf{R}_k\right)^2}. \tag{2.21}$$

From the definition of the minimum mean-square error (MSE) in (2.14), the minimum MSE at the output of the MMSE receiver for user k is

$$\begin{aligned} \mathrm{MMSE}_k &= E\left\{\left(\mathbf{c}_k^\top \mathbf{y} - \sqrt{p_k} b_k\right)^2\right\} \\ &= E\left\{(\mathbf{c}_k^\top \mathbf{y})^2\right\} - 2E\left\{\mathbf{c}_k^\top \mathbf{y} \sqrt{p_k} b_k\right\} + E\left\{p_k b_k^2\right\} \\ &= E\left\{Z_k^2\right\} - 2p_k \mathbf{c}_k^\top \mathbf{R}_k + p_k. \end{aligned} \tag{2.22}$$

On the other hand, by substituting $\mathbf{c}_k$ from (2.15) into (2.14), MMSE_k can be found to be

$$\mathrm{MMSE}_k = p_k - p_k^2 \mathbf{R}_k^\top \left(\mathbf{RWR} + \sigma^2 \mathbf{R}\right)^{-1} \mathbf{R}_k = p_k \left(1 - \mathbf{c}_k^\top \mathbf{R}_k\right). \tag{2.23}$$

It then follows from (2.22) and (2.23) that $E\left\{Z_k^2\right\} = p_k \mathbf{c}_k^\top \mathbf{R}_k$. Hence (2.21) becomes

$$\begin{aligned} \mathrm{SIR}_k &= \frac{p_k \left(\mathbf{c}_k^\top \mathbf{R}_k\right)^2}{p_k \mathbf{c}_k^\top \mathbf{R}_k - p_k \left(\mathbf{c}_k^\top \mathbf{R}_k\right)^2} = \frac{\mathbf{c}_k^\top \mathbf{R}_k}{1 - \mathbf{c}_k^\top \mathbf{R}_k} \\ &= \frac{1}{1 - \mathbf{c}_k^\top \mathbf{R}_k} - 1 = \frac{p_k}{\mathrm{MMSE_k}} - 1. \end{aligned} \tag{2.24}$$

From equations (2.19), (2.20), (2.23) and (2.24) it is obvious that the SIR at the output of each linear receiver can be further maximized by carefully selecting the correlation matrix $\mathbf{R}$ through the design of signature waveforms $\{s_1(t), \ldots, s_K(t)\}$. This design problem will be addressed in Chapter 4 for the cases of correlation and MMSE receivers[2].

[2]Signature waveform design for the decorrelating receiver can be carried out similarly.

As is common in CDMA system analysis, it is the average performance rather than the maximum (or worst case) performance that is of most interest as a performance measure. The parameters that reflect this average performance are introduced next for both correlation and MMSE receivers. For the correlation receiver, it follows from (2.19) that maximizing SIR_k is equivalent to minimizing $\left(\sigma^2 + \sum_{\substack{j=1 \\ j\neq k}}^{K} p_j \mathbf{R}_{kj}^2\right)$. However, to design the signature waveforms to minimize this quantity for *every* user k is a very difficult, if not an impossible task. Thus the alternative criterion is to minimize the total interference parameter (TIP), defined as follows

$$\begin{aligned} \mathrm{TIP} &= \sum_{k=1}^{K} \left(\sigma^2 + \sum_{\substack{j=1 \\ j\neq k}}^{K} p_j \mathbf{R}_{kj}^2 \right) \\ &= K\sigma^2 + \sum_{k=1}^{K} \sum_{\substack{j=1 \\ j\neq k}}^{K} p_j \mathbf{R}_{kj}^2. \end{aligned} \tag{2.25}$$

Similarly, for the MMSE linear detector, although it is desirable to minimize MMSE_k in (2.24) for every k, the alternative criterion is to minimize the total mean squared error (TMSE), which is defined as

$$\begin{aligned} \mathrm{TMSE} &= \sum_{k=1}^{K} \mathrm{MMSE}_k = \sum_{k=1}^{K} \left(p_k - p_k^2 \mathbf{R}_k^{\top} \left(\mathbf{RWR} + \sigma^2 \mathbf{R} \right)^{-1} \mathbf{R}_k \right) \\ &= \mathrm{tr}(\mathbf{W}) - \mathrm{tr}\left(\left[\mathbf{I} + \sigma^2 \left(\mathbf{WR} \right)^{-1} \right]^{-1} \mathbf{W} \right). \end{aligned} \tag{2.26}$$

To conclude this section, the formulas to calculate the error probability for binary signaling over synchronous CDMA channels are given next. Without loss of generality, consider the detection of the first user. The exact error probability is [47]

$$P_1 = 2^{1-K} \sum_{b_2,\ldots,b_K \in \{-1,+1\}^{K-1}} Q\left(\frac{\sqrt{p_1}}{\sigma} \frac{(\mathbf{CR})_{1,1} \left(1 + \omega_2 b_2 + \cdots + \omega_K b_K\right)}{\sqrt{(\mathbf{CRC})_{1,1}}} \right) \tag{2.27}$$

where $\omega_k = \sqrt{p_k/p_1}\,(\mathbf{CR})_{1,k} / (\mathbf{CR})_{1,1}$ for $k = 2, 3, \ldots, K$. For large K the evaluation of the above equation is time consuming and the Gaussian approximation to P_1 can

be used [47]

$$\widetilde{P}_1 = Q\left(\left[\frac{\sigma^2\left(\mathbf{CRC}\right)_{1,1}}{p_1\left(\mathbf{CR}\right)_{1,1}} + \omega_2^2 + \cdots + \omega_K^2\right]^{-1/2}\right) \tag{2.28}$$

where $Q(\cdot)$ is the complementary unit cumulative Gaussian distribution, defined as

$$Q(x) = \frac{1}{\sqrt{2\pi}}\int_x^\infty e^{-t^2/2}\mathrm{d}t, \quad x \geq 0. \tag{2.29}$$

It has also been shown in [47] that the Gaussian approximation in (2.28) is very accurate for the MMSE receiver. This is in contrast to the bit-error-rate of the correlation receiver where the Gaussian approximation is quite loose for all but very low signal-to-noise ratios [48].

2.2 A-CDMA System Model

The model for asynchronous CDMA systems considered in this thesis is similar to the one in [36, 37]. It should be noted, however, that there is a major difference in the way the signature waveforms are constructed. Here, each signature waveform is not constrained to consist of a sequence of rectangular pulses as in [36, 37], but rather it can be of any shape. Later, the case where signature waveforms are constructed from signature sequences and chip pulse(s) is also investigated. There are K users sharing the same channel. The kth user transmits the following *passband* spread-spectrum signal over the channel of bandwidth W

$$y_k(t) = \sum_{i=-\infty}^{\infty} \sqrt{2P}b_k(i)s_k(t - iT)\cos(2\pi f_c t + \theta_k). \tag{2.30}$$

In (2.30), P is the signal power (the common power assumption $p_1 = \ldots = p_k = P$ is made for simplicity but can be relaxed); f_c is the carrier frequency; θ_k is the phase introduced by the kth modulator and T is the symbol duration. The sequence $\{b_k(i)\}$ is the binary data sequence of user k, which is modeled as a sequence of independent and identically distributed (i.i.d.) random variables such that $\Pr\{b_k(i) = +1\} =$

$\Pr\{b_k(i) = -1\} = 1/2$. The signature waveforms $s_k(t)$, $1 \leq k \leq K$, are time-limited to T whose spectrum can occupy the entire bandwidth W. Furthermore these signature waveforms are normalized so that[3]

$$\int_0^T s_k^2(t)\mathrm{d}t = T, \qquad k = 1, \ldots, K. \tag{2.31}$$

The received signal is

$$y(t) = \sum_{k=1}^{K} \sum_{i=-\infty}^{\infty} \sqrt{2P} b_k(i) s_k(t - iT - \tau_k) \cos(2\pi f_c t + \varphi_k) + n(t) \tag{2.32}$$

where τ_k and $\varphi_k = \theta_k - 2\pi f_c \tau_k$ are the delay and the overall phase shift of the kth user, which can be modeled as uniform random variables over $[0, T]$ and $[0, 2\pi]$ respectively. The noise $n(t)$ is additive white Gaussian noise (AWGN) with a two-sided power spectral density of $\sigma^2 = N_0/2$.

As with S-CDMA systems, many multiuser receivers have been developed for A-CDMA systems. However, only the correlation receiver is considered in this thesis. The correlation receiver is preferred to other multiuser receivers because the complexity of multiuser detection is usually prohibitive in systems with a large number of users and therefore a correlation receiver is still the only practical solution in many A-CDMA systems.

Without loss of generality, consider the detection of the first information symbol of the kth user, i.e., $b_k(0)$. Also, since only relative delays and phases are important one can set $\tau_k = 0$ and $\varphi_k = 0$ and the delays and phase shifts of all other users are interpreted with reference to the kth user. Ignoring the double frequency component

[3]Note that this normalization is different from the one in Section 2.1, where the signature waveforms are normalized to have unit energy. These different normalizations are convenient when comparing our results with previous results for S-CDMA and A-CDMA systems, respectively.

at $2f_c$, the output of the kth correlation receiver is [37]

$$\begin{aligned} Z_k &= \int_0^T y(t)s_k(t)\cos(2\pi f_c t)\mathrm{d}t \\ &= \sqrt{P/2}b_k(0)T + \sqrt{P/2}\sum_{i=1,i\neq k}^{K} I_{k,i} + n \end{aligned} \tag{2.33}$$

where n is a Gaussian random variable with zero mean and variance $N_0T/4$ and $I_{k,i}$ is the interference caused by the ith user, given by

$$I_{k,i} = \left[b_i(-1)R_{k,i}(\tau_i) + b_i(0)\widehat{R}_{k,i}(\tau_i)\right]\cos\varphi_i. \tag{2.34}$$

The functions $R_{k,i}(\tau)$ and $\widehat{R}_{k,i}(\tau)$ are the continuous-time partial cross-correlation functions between the kth and the ith signature waveforms. These functions were originally introduced in [36] and can be written here as

$$R_{k,i}(\tau) = \int_0^{\tau} s_k(t)s_i(t+T-\tau)\mathrm{d}t \tag{2.35}$$

$$\widehat{R}_{k,i}(\tau) = \int_{\tau}^{T} s_k(t)s_i(t-\tau)\mathrm{d}t \tag{2.36}$$

for $0 \leq \tau \leq T$. If $k = i$, then denote $R_k(\tau) = R_{k,k}(\tau)$ and $\widehat{R}_k(\tau) = \widehat{R}_{k,k}(\tau)$.

In (2.33), the first term is the desired signal component, the second term is the multiple access interference (MAI) and the last term is due to the background noise. It is obvious from (2.33) and (2.34) that the signature waveforms directly influence the MAI. To maximize the SIR, it is desired to have signature waveforms that minimize the MAI. This problem will be addressed in Chapter 6.

2.3 Bandwidth Considerations

When designing the set of signature waveforms for both S-CDMA and A-CDMA systems, an important constraint is the available bandwidth. The issue of bandwidth definition is discussed in this section.

The bandwidth of a communication system is usually judged based on the power spectral density (PSD) of the transmitted signal. Two commonly used bandwidth measures are the root-mean-square (RMS) and fractional out-of-band power (FOBP) bandwidth [22]. Let $P(f)$ be the PSD of the equivalent *baseband* transmitted signal of either (2.1) (with equal-power users) or (2.32). The RMS bandwidth W of the system is defined as

$$W = \left(\frac{\int_{-\infty}^{\infty} f^2 P(f) \mathrm{d}f}{\int_{-\infty}^{\infty} P(f) \mathrm{d}f} \right)^{1/2}. \tag{2.37}$$

The system is said to have FOBE bandwidth W at level η, $0 < \eta < 1$, if

$$\frac{\int_{|f|>W} P(f) \mathrm{d}f}{\int_{-\infty}^{\infty} P(f) \mathrm{d}f} \leq \eta. \tag{2.38}$$

When the user's data symbols are equally likely and independent of each other and from the other user's data symbols, it can be shown that $P(f)$ is proportional to $\sum_{k=1}^{K} |S_k(f)|^2$ [49]. Thus the bandwidth of the received signal is determined by the *average* bandwidth of the set of signature waveforms.

Let $S_k(f) = \mathcal{F}\{s_k(t)\}$, where $\mathcal{F}\{\cdot\}$ denotes the Fourier transform. The RMS bandwidth of the signature waveform $s_k(t)$ is defined as,

$$b\left(s_k(t)\right) = \left[\frac{\int_{-\infty}^{\infty} f^2 |S_k(f)|^2 \mathrm{d}f}{\int_{-\infty}^{\infty} |S_k(f)|^2 \mathrm{d}f} \right]^{1/2}. \tag{2.39}$$

Let $\mathbf{s}(t) = [s_1(t), \ldots, s_K(t)]^{\top}$ be the signal set vector, then the *average* RMS bandwidth $b\left(\mathbf{s}(t)\right)$ of the signal set satisfies

$$b^2\left(\mathbf{s}(t)\right) = \frac{1}{K} \sum_{k=1}^{K} b^2\left(s_k(t)\right) = \frac{1}{K} \sum_{k=1}^{K} \frac{\int_{-\infty}^{\infty} f^2 |S_k(f)|^2 \mathrm{d}f}{\int_{-\infty}^{\infty} |S_k(f)|^2 \mathrm{d}f}. \tag{2.40}$$

On the other hand the *maximum* RMS bandwidth $b_{\max}\left(\mathbf{s}(t)\right)$ of the set is

$$b_{\max}\left(\mathbf{s}(t)\right) = \max\left\{b\left(s_1(t)\right), \ldots, b\left(s_K(t)\right)\right\}. \tag{2.41}$$

The fraction of the energy of $s_k(t)$ lying outside the frequency interval $[-W, W]$ is given by

$$\epsilon\left(s_k(t)\right) = \frac{\int_{|f|>W} |S_k(f)|^2 \mathrm{d}f}{\int_{-\infty}^{\infty} |S_k(f)|^2 \mathrm{d}f}. \tag{2.42}$$

Let $0 < \eta < 1$ be arbitrary. The signal $s_k(t)$ is said to have FOBE bandwidth of W at level η if $\epsilon\left(s_k(t)\right) \leq \eta$ and therefore the signal set is said to have a *maximum* FOBE bandwidth W at level η if

$$\max\left\{\epsilon\left(s_1(t)\right), \ldots, \epsilon\left(s_K(t)\right)\right\} \leq \eta. \tag{2.43}$$

Similarly, the signal set has *average* FOBE bandwidth W at level η if

$$\epsilon\left(\mathbf{s}(t)\right) = \frac{1}{K}\sum_{k=1}^{K} \epsilon\left(s_k(t)\right) = \frac{1}{K}\sum_{k=1}^{K} \frac{\int_{|f|>W} |S_k(f)|^2 \mathrm{d}f}{\int_{-\infty}^{\infty} |S_k(f)|^2 \mathrm{d}f} \leq \eta \tag{2.44}$$

Given a correlation matrix $\mathbf{R}$, the sets of signals that achieve either minimum average RMS or minimum average FOBE bandwidth are of particular importance for the designs in Chapter 4. The following proposition specifies these sets under the RMS bandwidth constraint [50].

Proposition 2.1 *(Nuttall, 1968).* Among all sets of vectors $\mathbf{s}(t)$ that have the same prescribed $K \times K$ *unit-diagonal* correlation matrix $\mathbf{R}$, the optimal signal set vector that achieves the minimum average RMS bandwidth is given by

$$\mathbf{s}(t) = \mathbf{V}\boldsymbol{\Lambda}^{1/2}\boldsymbol{\Phi}(t) \tag{2.45}$$

where $\boldsymbol{\Lambda} = \mathrm{diag}\left(\lambda_1, \ldots, \lambda_K\right), \lambda_i \geq \lambda_{i+1}$, are the ordered eigenvalues of $\mathbf{R}$, $\mathbf{V}$ is the matrix of eigenvectors of $\mathbf{R}$ in its singular-value decomposition $\mathbf{R} = \mathbf{V}\boldsymbol{\Lambda}\mathbf{V}^{\top}$ and the vector of basis functions $\boldsymbol{\Phi}(t)$ is

$$\boldsymbol{\Phi}(t) = \sqrt{\frac{2}{T}}\left[\sin\left(\frac{\pi t}{T}\right), \sin\left(\frac{2\pi t}{T}\right), \ldots, \sin\left(\frac{K\pi t}{T}\right)\right]^{\top}, \quad 0 \leq t \leq T. \tag{2.46}$$

Furthermore the individual and average RMS bandwidths of the signals are given by

$$b^2\left(s_k(t)\right) = \frac{1}{(2T)^2}\left(\mathbf{V}\mathbf{\Lambda}\mathbf{\Pi}\mathbf{V}^\top\right)_{kk} \tag{2.47}$$

$$b^2\left(\mathbf{s}(t)\right) = \frac{1}{K(2T)^2}\mathrm{tr}(\mathbf{\Lambda}\mathbf{\Pi}) \tag{2.48}$$

where $\mathbf{\Pi}$ is a diagonal matrix with $\mathbf{\Pi}_{kk} = k^2$. Δ

A similar result has also been shown for the FOBE bandwidth constraint. Since the result is given in terms of prolate spheroidal wave functions, this family of functions is reviewed next. It was shown in [23, 24] that the solutions to the following integral equation

$$\int_{-T/2}^{T/2} \frac{\sin 2\pi W(t-s)}{\pi(t-s)} f(s)\mathrm{d}s = \chi f(t) \tag{2.49}$$

are the prolate spheroidal wave functions (PSWFs) $\{\varphi_i(t;c)\}_{i=0}^{\infty}$, where $c = \pi WT$. The corresponding eigenvalues $\{\chi_i(c)\}_{i=0}^{\infty}$ are ordered so that $1 > \chi_0(c) > \chi_1(c) > \ldots > 0$. The PSWFs form a complete orthonormal basis for the space of all square-integrable functions band-limited to $[-W, W]$. The fraction of energy of $\varphi_i(t;c)$ in the interval $[-T/2, T/2]$ equals $\chi_i(c)$; thus the first PSWF $\varphi_0(t;c)$ is the one most concentrated in $[-T/2, T/2]$. Moreover, among all the band-limited signals orthogonal to $\varphi_0(t)$, $\varphi_1(t)$ is the most concentrated in $[-T/2, T/2]$ and so on. Further let

$$\widehat{\varphi}_i(t;c) = \begin{cases} \dfrac{\varphi_i\left(t-\dfrac{T}{2};c\right)}{\sqrt{\chi_i}}, & 0 \le t \le T \\ 0, & \text{otherwise} \end{cases}$$

be the shifted, normalized and time-truncated version of $\varphi_i(t)$, then $\{\widehat{\varphi}_i(t;c)\}_{i=0}^{\infty}$ form a complete orthonormal basis for the space of time-limited (to $[0, T]$), real square-integrable functions. The function $\widehat{\varphi}_i(t;c)$ has out-of-band energy (outside $[-W, W]$) equal to $1-\chi_i$, i.e., $\epsilon(\widehat{\varphi}_i(t;c)) = 1-\chi_i$. Also $\widehat{\varphi}_0(t;c)$ is the one most concentrated in $[-W, W]$ and among all the time-limited signals orthogonal to $\widehat{\varphi}_0(t)$, $\widehat{\varphi}_1(t)$ is the

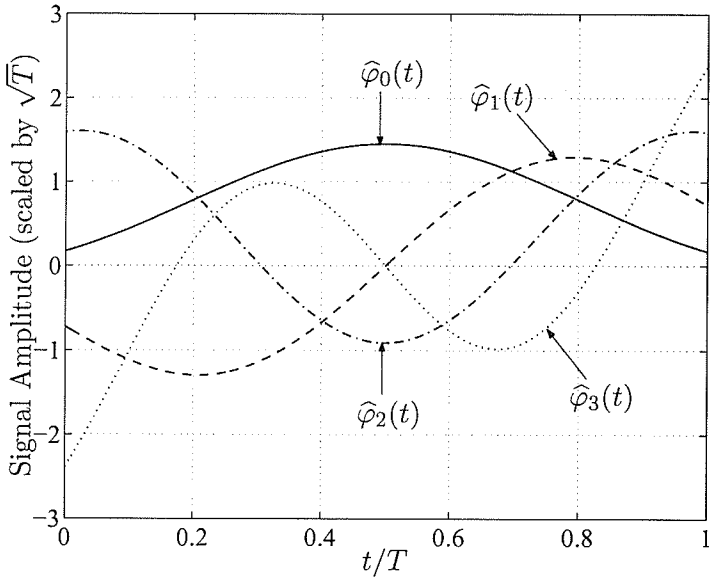

Figure 2.2: The first four shifted, normalized and time-truncated PSWFs as orthonormal bases

most concentrated in $[-W, W]$, etc. As an example, the set of the first four shifted, normalized and time-truncated PSWFs corresponding to $c = 4.0$ are plotted in Fig. 2.2.

Results similar to that of Nuttall but under FOBE bandwidth constraint are stated below [21].

Proposition 2.2 *(Fain and Varanasi, 1998).* Among all the signal set vectors $\mathbf{s}(t)$ that have the same prescribed $K \times K$ unit-diagonal correlation matrix $\mathbf{R}$, the optimal signal set vector that achieves the minimum average FOBE is given by

$$\mathbf{s}(t) = \mathbf{V}\mathbf{\Lambda}^{1/2}\mathbf{\Psi}(t) \tag{2.50}$$

where $\mathbf{\Lambda} = \text{diag}(\lambda_1, \ldots, \lambda_K), \lambda_i \geq \lambda_{i+1}$, are the ordered eigenvalues of $\mathbf{R}$, $\mathbf{V}$ is the matrix of eigenvectors of $\mathbf{R}$ in its singular-value decomposition $\mathbf{R} = \mathbf{V}\mathbf{\Lambda}\mathbf{V}^\top$ and

the vector of basis functions $\mathbf{\Psi}(t)$ contains the first K shifted, normalized and time-truncated PSWFs:

$$\mathbf{\Psi}(t) = \left[\widehat{\varphi}_0(t), \widehat{\varphi}_1(t), \ldots, \widehat{\varphi}_{K-1}(t)\right]^\top . \tag{2.51}$$

Furthermore the individual and average FOBE of the signals are given by,

$$\epsilon(s_k(t)) = \left(\mathbf{V}\mathbf{\Lambda}\mathbf{\Xi}\mathbf{V}^\top\right)_{kk} \tag{2.52}$$

$$\epsilon(\mathbf{s}(t)) = \frac{1}{K}\mathrm{tr}\left(\mathbf{\Lambda}\mathbf{\Xi}\right) \tag{2.53}$$

where $\mathbf{\Xi} = \mathrm{diag}\left(1-\chi_0, 1-\chi_1, \ldots, 1-\chi_{K-1}\right)$. $\triangle$

Chapter 3

Signature Waveforms for Maximizing the Network Capacity of S-CDMA Systems

In some CDMA systems it is sufficient to maintain the SIR (hence the bit-error-rate) for each user to be larger than some level α. In such systems the question of interest is how many users can be simultaneously supported for given values of α and available bandwidth W. Maximizing the number of users or the network capacity of the S-CDMA systems by means of signature waveforms is the problem considered in this chapter. The network capacity provided by proposed signature waveforms is also compared to that of suboptimal signature waveforms. Throughout this chapter we assume equal received power for all users, i.e., $p_k = P,\ k = 1, \ldots, K$. This assumption implies that there is a perfect power control.

3.1 Problem Formulation

The problem of characterizing the network capacity of S-CDMA systems can be formulated as follows.

Problem 3.1. Consider an S-CDMA system with either a correlation or MMSE receiver. Given T, W, $0 < \alpha < 1$, P and $0 < \eta < 1$ (this parameter is for FOBE

bandwidth only), find the largest set of signature waveforms $\{s_1(t), s_2(t), \ldots, s_K(t)\}$ subject to (i) $s_k(t) = 0$ for $t < 0$ and $t > T$; (ii) $\int_0^T s_k^2(t)\mathrm{d}t = 1$; (iii) $\mathrm{SIR}_k \geq \alpha$ and (iv) $\epsilon(\mathbf{s}(t)) \leq \eta$ (for FOBE bandwidth), or $b(\mathbf{s}(t)) \leq W$ (for RMS bandwidth).

The above problem is difficult to solve directly. However, by further restricting the signature waveforms to be spanned by a finite set of orthonormal basis functions, this problem can be solved in two steps as outlined below.

- *Step 1:* Assume there exists a set of orthonormal basis functions $\{\psi_1(t), \ldots, \psi_N(t);\ 0 \leq t \leq T\}$ for the construction of the signature waveforms. Then the maximum number of users, $K_{\max}$, and the corresponding signature sequences $\mathbf{s}_k$ are obtained in terms of the dimension N of the signature space and the SIR requirement α. This step does not take into account the bandwidth constraint of the signature set, hence it is valid for both bandwidth criteria.

- *Step 2:* The optimal basis functions for constructing the users' signature waveforms are identified according to each bandwidth criterion. By optimality is meant the *largest* set of orthonormal functions, which together with the signature sequences found in Step 1, will give the set of signature waveforms whose average bandwidth satisfies the corresponding criterion stated in (iv) above.

Step 1 is carried out in the next section for the MMSE receiver. However it will be shown that with the resulting signature sequences, the MMSE receiver becomes the correlation receiver. Here we would like to point out that the results in Section 3.2 can be inferred from the results in [15] with some modifications. In [15] the authors allow the user's received power to be controlled at any level and find the optimal power allocation. They also process the sufficient statistic $\mathbf{r}$ in (2.6) to obtain the results. Here the received power of every user is fixed and the sufficient statistic $\mathbf{y}$ in (2.3) is processed.

3.2 Optimal Signature Sequences: WBE Sequences

To obtain the maximum network capacity of the system, first find the upper bound on SIR for every user and the corresponding signature sequences that achieve that upper bound. Comparing this upper bound with the SIR requirement α will give an upper bound on the number of users, hence the maximum network capacity follows.

It can be seen from equation (2.24) in Chapter 2 that maximizing SIR_k is equivalent to minimizing MMSE_k for $k = 1, \ldots, K$. Instead of minimizing each MMSE_k individually, consider minimizing the sum of them, which is precisely the TMSE defined in (2.26). It can be shown that when the sum is minimized, the individual MMSE_k will be all equal, hence each of them is also minimized, i.e., each SIR_k will be maximized.

When the signature waveforms are spanned by a set of N ($N < K$) orthonormal basis functions, they are completely determined by the $N \times K$ signature matrix $\mathbf{S}$. Since $\mathbf{R} = \mathbf{S}^\top \mathbf{S}$ has rank $N < K$, it is a singular matrix and has only N nonzero eigenvalues. Because $\mathbf{R}$ is non-invertible, the MMSE linear filter is given by (2.17) and can be rewritten as follows,

$$\mathbf{C} = P\left(P\mathbf{R}^2 + \sigma^2\mathbf{R}\right)^{-}\mathbf{R}. \tag{3.1}$$

Using the decomposition $\mathbf{R} = \mathbf{V}\mathbf{\Lambda}\mathbf{V}^\top$ and $\mathbf{R}_k = \mathbf{V}\mathbf{\Lambda}\mathbf{u}_k$ it can be shown that

$$\mathbf{c}_k = P\mathbf{V}\left(P\mathbf{\Lambda} + \sigma^2\widetilde{\mathbf{I}}\right)^{-}\mathbf{u}_k \tag{3.2}$$

where $\mathbf{\Lambda} = \mathrm{diag}(\lambda_1, \ldots, \lambda_N, 0, \ldots, 0)$, $\mathbf{u}_k$ is the kth column of $\mathbf{V}^\top$ and $\widetilde{\mathbf{I}} = \mathrm{diag}(\underbrace{1, 1, \ldots, 1}_{N}, 0, \ldots, 0)$. The MMSE_k and the TMSE are given by

$$\mathrm{MMSE}_k = P\left[1 - P\mathbf{u}_k^\top\left(P\widetilde{\mathbf{I}} + \sigma^2\mathbf{\Lambda}^{-}\right)^{-}\mathbf{u}_k\right] \tag{3.3}$$

and

$$\mathrm{TMSE} = \sum_{k=1}^{K}\mathrm{MMSE}_k = (K-N)P + P\sum_{k=1}^{N}\frac{1}{\gamma\lambda_k + 1} \tag{3.4}$$

where $\gamma = P/\sigma^2$ is the signal-to-background noise ratio. Now the problem is to find N positive eigenvalues $\{\lambda_1, \ldots, \lambda_N\}$ that minimize $\sum_{k=1}^{N} \frac{1}{\gamma\lambda_k + 1}$, subject to $\sum_{k=1}^{N} \lambda_k = K$. The Lagrange method can be used to show that the optimal eigenvalues are all equal to K/N, i.e.,

$$\mathbf{\Lambda} = \mathrm{diag}\big(\underbrace{K/N, \ldots, K/N}_{N}, 0, \ldots, 0\big). \tag{3.5}$$

Substitute $\mathbf{\Lambda}$ from (3.5) into (3.3) and note that $\mathbf{u}_k^\top \mathbf{\Lambda} \mathbf{u}_k = \mathbf{R}_{kk} = 1$. Then

$$\mathrm{MMSE}_k = P\left[1 - \frac{\gamma}{\gamma(K/N) + 1}\right] \tag{3.6}$$

which is independent of k. This together with (2.24) implies that the SIR_k are all maximized and equal to

$$\mathrm{SIR}_{\max} = \frac{\gamma}{\gamma\,(K/N - 1) + 1}. \tag{3.7}$$

From the eigenvalues of the correlation matrix $\mathbf{R}$ one needs to find the $N \times K$ signature matrix $\mathbf{S}$ such that $\mathbf{R} = \mathbf{S}^\top \mathbf{S}$. Write the singular-value decomposition of $\mathbf{R}$ as follows,

$$\begin{aligned} \mathbf{R} &= \mathbf{V}\mathbf{\Lambda}\mathbf{V}^\top = [\mathbf{v}_1, \mathbf{v}_2, \ldots, \mathbf{v}_K]\, \mathbf{\Lambda}\, [\mathbf{v}_1, \mathbf{v}_2, \ldots, \mathbf{v}_K]^\top \\ &= [\mathbf{v}_1, \mathbf{v}_2, \ldots, \mathbf{v}_N] \left(\frac{K}{N}\mathbf{I}\right) [\mathbf{v}_1, \mathbf{v}_2, \ldots, \mathbf{v}_N]^\top = \frac{K}{N}\widetilde{\mathbf{V}}\widetilde{\mathbf{V}}^\top = \mathbf{S}^\top\mathbf{S} \end{aligned} \tag{3.8}$$

where $\mathbf{v}_1, \mathbf{v}_2, \ldots, \mathbf{v}_K$ are the eigenvectors which are orthogonal to each other, i.e., $\mathbf{v}_i^\top \mathbf{v}_j = \delta(i-j)$. It is obvious from the above equation that $\mathbf{S} = \sqrt{\frac{K}{N}}\widetilde{\mathbf{V}}^\top$, which also implies that $\mathbf{S}\mathbf{S}^\top = \frac{K}{N}\mathbf{I}$. The K sequences whose signature matrix satisfies this equality are called the Welch bound equality (WBE) sequences [13] since they achieve Welch's lower bound on the sum of the squared cross correlations of unit energy sequences [16]. The family of WBE sequences will be discussed in more detail in Chapter 4.

The fact that the MMSE receiver simplifies to a correlation receiver when the WBE signature sequences are employed can be seen as follows. From (3.2) the filter for the MMSE receiver is

$$\mathbf{C} = P\mathbf{V}\left(P\mathbf{\Lambda} + \sigma^2\widetilde{\mathbf{I}}\right)^{-}\mathbf{V}^{\top} = \frac{P(N/K)}{P(K/N)+\sigma^2}\mathbf{V}\mathbf{\Lambda}\mathbf{V}^{\top} = \frac{P(N/K)}{P(K/N)+\sigma^2}\mathbf{R}. \tag{3.9}$$

From the above expression and the fact that $\mathbf{R}^2 = \frac{K}{N}\mathbf{R}$, the output of the MMSE filter can be shown to be a scaled version of the sufficient statistic $\mathbf{y}$ as follows

$$\widehat{\mathbf{y}} = \mathbf{C}\mathbf{y} = \frac{P}{P(K/N)+\sigma^2}\left(\sqrt{P}\mathbf{R}\mathbf{b} + \sigma\widehat{\mathbf{n}}\right) = \frac{P}{P(K/N)+\sigma^2}\mathbf{y} \tag{3.10}$$

where the noise vector $\widehat{\mathbf{n}}$ has exactly the same statistics as the the noise vector $\mathbf{n}$, namely a zero-mean Gaussian vector with covariance matrix $\mathbf{R}$.

At this point, it is natural to ask a question about the performance of the decorrelating receiver with WBE sequences, or more generally, about the design of optimal signature sequences that maximize the SIR at the output of the decorrelating receiver. Regarding the performance of the decorrelating receiver with WBE sequences, it can be shown that the SIR at the output of a decorrelating receiver is given by,

$$\mathrm{SIR}_k = \frac{\gamma\mathbf{u}_k^{\top}\widetilde{\mathbf{I}}\mathbf{u}_k}{N/K + \gamma(1-\mathbf{u}_k^{\top}\widetilde{\mathbf{I}}\mathbf{u}_k)}. \tag{3.11}$$

Thus the performance of the decorrelating receiver depends on the matrix $\mathbf{V}$ in the decomposition $\mathbf{R} = \mathbf{V}\mathbf{\Lambda}\mathbf{V}^{\top}$, which is usually not unique. When the number of users K is a Hadamard dimension, one can choose $\mathbf{V}$ to be the normalized Hadamard matrix. With this choice of matrix $\mathbf{V}$ the SIR in (3.11) reduces to (3.7), suggesting that the decorrelating receiver in this case also becomes the correlation receiver. Mathematically, this fact can be easily proven following the same reasoning that leads to (3.9) and (3.10).

The optimal design of signature sequences for the decorrelating receiver is not available. This is mainly because no sensible design criterion for the decorrelating

receiver could be established. However, such a design is of no practical importance due to the fact that the MMSE receiver maximizes the SIR among all the linear receivers and with the optimal WBE sequences, the MMSE receiver simplifies to the correlation receiver.

Now returning to the condition $\mathrm{SIR}_{\max} \geq \alpha$, one has

$$K \leq N\left(1+\frac{1}{\alpha}-\frac{\sigma^2}{P}\right). \tag{3.12}$$

Thus given the dimension N of the signature space and the SIR requirement α for all users, the largest number of users that can be supported in a S-CDMA system is

$$K_{\max} = \left\lfloor N\left(1+\frac{1}{\alpha}-\frac{\sigma^2}{P}\right)\right\rfloor \tag{3.13}$$

where $\lfloor x \rfloor$ is the largest integer less than or equal to x.

The above equation shows that the maximum number of users is directly proportional to the dimension of the signature space. Therefore, to further maximize the network capacity, one needs to identify the largest set of orthonormal basis functions for a given available bandwidth. This issue is addressed in the next section.

3.3 Optimal Othonormal Basis Functions

The optimal basis functions depend on what bandwidth criterion is used. In what follows the optimal basis functions are first obtained for the FOBE bandwidth criterion. The same approach is then applied to find the optimal basis functions under an RMS bandwidth constraint.

3.3.1 FOBE Bandwidth Constraint

Define an $N \times N$ matrix $\mathbf{M}$, whose (m,n) element is

$$\mathbf{M}_{mn} = \int_{f>|W|} \Psi_m^*(f)\Psi_n(f)\mathrm{d}f, \qquad m,n=1,\ldots,N \tag{3.14}$$

where $\Psi_n(f)$ is the Fourier transform of $\psi_n(t)$ and * denotes the complex conjugate. In terms of the vector $\mathbf{\Psi}(f) = [\Psi_1(f), \ldots, \Psi_N(f)]^\top$, $\mathbf{M}$ can be written as

$$\mathbf{M} = \int_{f>|W|} \mathbf{\Psi}^*(f)\mathbf{\Psi}^\top(f)\mathrm{d}f. \tag{3.15}$$

The above definition implies that $\mathbf{M}_{nn} = \epsilon(\psi_n(t))$, the fractional out-of-band energy of the nth basis function. From (2.5),(2.42) and (3.14) it is not hard to verify that $\epsilon(s_k(t)) = \mathbf{s}_k^\top \mathbf{M}\mathbf{s}_k$, hence the average FOBE of the signature set defined in (2.44) becomes

$$\epsilon(\mathbf{s}(t)) = \frac{1}{K}\sum_{k=1}^{K} \mathbf{s}_k^\top \mathbf{M}\mathbf{s}_k = \frac{1}{K}\mathrm{tr}\left(\mathbf{S}^\top\mathbf{M}\mathbf{S}\right) = \frac{1}{K}\mathrm{tr}\left(\mathbf{M}\mathbf{S}\mathbf{S}^\top\right). \tag{3.16}$$

Now using the property that $\mathbf{S}\mathbf{S}^\top = \frac{K}{N}\mathbf{I}$ for WBE signature sequences, the FOBE bandwidth constraint of the signature set can be expressed in terms of the bandwidth constraint of the basis functions as follows,

$$\epsilon(\mathbf{s}(t)) = \frac{1}{N}\mathrm{tr}(\mathbf{M}) = \frac{1}{N}\sum_{n=1}^{N} \epsilon(\psi_n(t)) \leq \eta. \tag{3.17}$$

Thus when the signature sequences are the WBE sequences, finding the optimal basis functions is equivalent to finding the largest set of orthonormal functions whose average FOBE satisfies (3.17). Equation (3.17) also allows one to identify the largest set (with $N_{\max}$) of orthonormal functions in terms of prolate spheroidal wave functions (PSWFs). More precisely, by applying Proposition 2.2 for the special case of $\mathbf{R} = \mathbf{I}$ one can select the largest set of orthonormal functions to be the set of the first $N_{\max}$ functions $\{\widehat{\varphi}_0(t), \widehat{\varphi}_1(t), \ldots, \widehat{\varphi}_{N_{\max}-1}(t)\}$ whose eigenvalues satisfy

$$\frac{1}{N_{\max}+1}\sum_{i=0}^{N_{\max}} \chi_i(c) < 1-\eta \leq \frac{1}{N_{\max}}\sum_{i=0}^{N_{\max}-1} \chi_i(c). \tag{3.18}$$

From the above expression, it can be seen that the maximum dimension of the signature space, $N_{\max}$, depends only on the product WT (through $c = \pi WT$), and so does the user capacity $K_{\max}$ according to (3.13). Figure 3.1 plots $\frac{1}{N}\sum_{i=0}^{N-1}(1-\chi_i(c))$

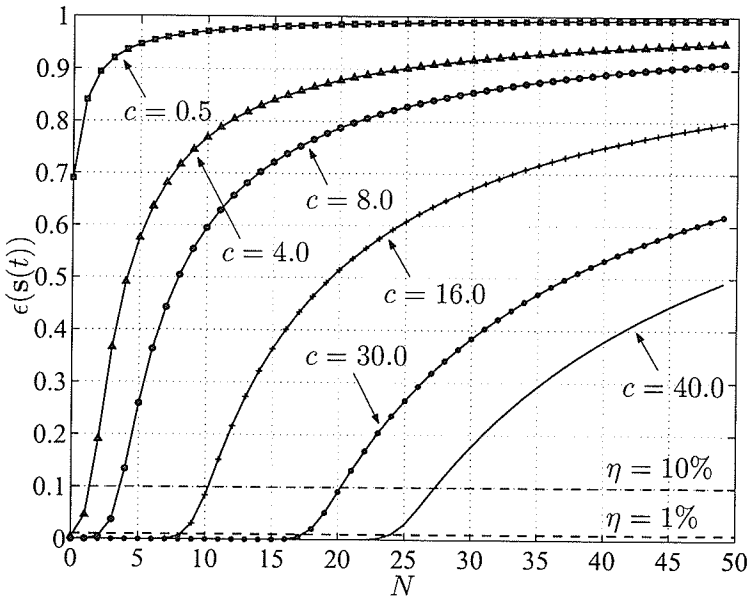

Figure 3.1: Average FOBE of signature set based on PSWFs

versus N for some values of c. The eigenvalues corresponding to these values of c are obtained from the data in [51] and they are also tabulated in Appendix A. Given η, the value $N_{\max}$ can be easily determined from such a figure. The levels of $\eta = 10\%$ and $\eta = 1\%$ are used later in Figs. 3.2 and 3.3 for this purpose.

3.3.2 RMS Bandwidth Constraint

Analogously, to deriving the optimal basis functions under the RMS bandwidth constraint, define the following $N \times N$ matrix $\mathbf{Q}$,

$$\mathbf{Q} = \int_{-\infty}^{\infty} f^2 \mathbf{\Psi}^*(f) \mathbf{\Psi}^\top(f) \mathrm{d}f. \tag{3.19}$$

Again using the fact that $\mathbf{S}\mathbf{S}^\top = \frac{K}{N}\mathbf{I}$, one can show that the constraint on the average RMS bandwidth of the signature set can be written in terms of the bandwidth constraint of the basis functions as follows.

$$b^2(\mathbf{s}(t)) = \frac{1}{N}\mathrm{tr}(\mathbf{Q}) \leq W^2. \tag{3.20}$$

Since $\mathbf{Q}_{nn} = b^2(\psi_n(t))$, $n = 1, 2, \ldots, N$, the maximum number of orthonormal functions, $N_{\max}$, is the largest integer satisfying [52]

$$WT \geq \sqrt{\frac{1}{12}\left(N_{\max} + \frac{1}{2}\right)(N_{\max} + 1)}. \tag{3.21}$$

One of the optimal sets of orthonormal functions is the set of sinusoids $\{\sin(n\pi t/T)\}_{n=1}^{N_{\max}}$.

Having constructed the signature waveforms from the WBE signature sequences and the optimal basis functions, it is interesting to investigate the effect of choosing suboptimal basis functions on the network capacity of the S-CDMA systems. This is studied in the next section.

3.4 Comparison with Suboptimal Signature Waveforms

The suboptimal basis functions considered here have the following form.

$$\psi_i(t) = p(t - iT_c), \qquad 0 \leq i \leq N - 1 \tag{3.22}$$

where $p(t)$ is some chip waveform limited to the chip interval $[0, T_c]$ and $\int_0^{T_c} p^2(t)\mathrm{d}t = 1$. Thus the suboptimal basis functions are just the delayed versions of some chip waveform. The dimension of the signature space spanned by the delayed chip waveforms is simply

$$N_c = \lfloor T/T_c \rfloor = \lfloor WT/WT_c \rfloor. \tag{3.23}$$

Therefore, to increase the dimension of the signature space (i.e., to increase the network capacity of the system) one needs to minimize WT_c. However the minimum value WT_c is limited by the bandwidth constraint of the signature set. Since the bandwidth of every basis function is the same as that of the chip waveform $p(t)$, the bandwidth constraints in (3.17) and (3.20) become $\epsilon(p(t)) \leq \eta$ and $b(p(t)) \leq W$ respectively.

3.4.1 FOBE Bandwidth Constraint

For a given η, among all the chip waveforms limited to $[0, T_c]$ the optimal chip waveform, which gives the smallest WT_c, is obviously the first normalized, time-truncated and shifted PSWF $\widehat{\varphi}_0(t)$ whose eigenvalue satisfies

$$\chi_0(\pi W T_c) = 1 - \eta. \tag{3.24}$$

Solving the above equation gives the smallest WT_c. If W is known, then T_c can be found and $\widehat{\varphi}_0(t)$ can be realized. Denote the dimension of the signature space based on this PSWF chip waveform by N_c^{opt}.

If the chip waveform is selected to be a rectangular pulse, which is common in many CDMA systems,

$$p(t) = \begin{cases} \frac{1}{\sqrt{T_c}}, & 0 \le t \le T_c \\ 0, & \text{otherwise} \end{cases} \tag{3.25}$$

then it can be shown that the minimum WT_c is determined by the following equation

$$1 - 2\int_0^{WT_c} \text{sinc}^2(x)\mathrm{d}x = \eta. \tag{3.26}$$

where $\text{sinc}(x) = \sin(\pi x)/(\pi x)$. Denote the dimension of the signature space based on this rectangular chip waveform by N_c^{rect}.

Finally, another chip waveform of interest is the half-sine wave

$$p(t) = \begin{cases} \sqrt{\frac{2}{T_c}} \sin\left(\frac{\pi t}{T_c}\right), & 0 \le t \le T_c \\ 0, & \text{otherwise.} \end{cases} \tag{3.27}$$

This waveform can be shown to have the minimum RMS bandwidth among all the waveforms limited to $[0, T_c]$. Furthermore, over a wide range of bandwidth, the energy concentration of this waveform is very close to that of the optimal chip waveform $\widehat{\varphi}_0(t)$ [52]. The minimum WT_c for this chip waveform satisfies

$$1 - \int_0^{WT_c} \left[\text{sinc}\left(x - \frac{1}{2}\right) + \text{sinc}\left(x + \frac{1}{2}\right)\right]^2 \mathrm{d}x = \eta. \tag{3.28}$$

Similarly, denote the dimension of the signature space based on this half-sine chip waveform by $N_c^{\sin}$.

Note that one always has $N_c^{\text{opt}} \geq N_c^{\text{rect}}$ and $N_c^{\text{opt}} \geq N_c^{\sin}$, but the relation between N_c^{rect} and $N_c^{\sin}$ depends on the value of η. Commonly used values for η are 10% and 1%, corresponding to the 90% and 99% bandwidth occupancies respectively [32]. Table 3.1 gives the values of WT_c found from (3.24), (3.26) and (3.28) for these two values of η.

Table 3.1: Values of WT_c for various chip waveforms.

	$\eta = 10\%$	$\eta = 1\%$
Optimal chip ($\widehat{\varphi}_0(t)$)	0.6750	1.1170
Rectangular chip	0.8487	10.2860
Half-sine chip	0.7769	1.1820

Figures 3.2 and 3.3 plot the values of $N_{\max}$ and N_cs versus $2WT$ for $\eta = 10\%$ and $\eta = 1\%$ respectively. The advantage of using optimal signature waveforms over the suboptimal ones are clearly observed from such figures. Furthermore, the gain in network capacity increases significantly as η decreases from 10% to 1%. Also it can be seen from these two figures that $N_c^{\sin} \geq N_c^{\text{rect}}$ and the difference becomes larger for smaller value of η. This relation between $N_c^{\sin}$ and N_c^{rect} is due to the following reasons. (i) The power spectral density (PSD) of the half-sine chip decays as $|f|^{-4}$ while the PSD of the rectangular chip decays as $|f|^{-2}$. (ii) For both $\eta = 1\%$ and $\eta = 10\%$, the mainlobe of the PSD of either half-sine chip or rectangular chip is well contained in the FOBE bandwidth.

To obtain $N_{\max}$ from (3.18) for different η, the eigenvalues $\{\chi_i(c)\}$ are calculated based on the data in [51]. For many practical CDMA systems, the value of WT is typically large (in the hundreds). Unfortunately data is not available on the behavior of $\chi_i(c)$ for large i and large $c = \pi WT$. However, for large WT one could use the

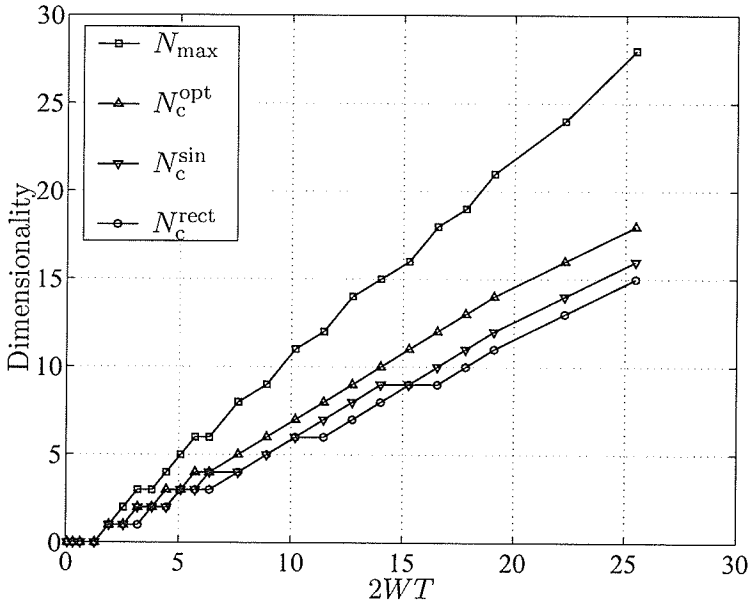

Figure 3.2: Dimensionality of signature space, $\eta = 10\%$.

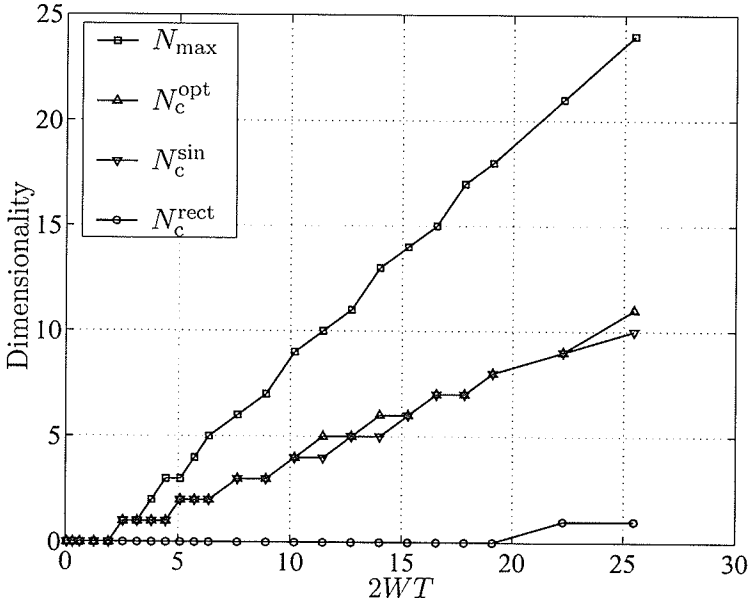

Figure 3.3: Dimensionality of signature space, $\eta = 1\%$.

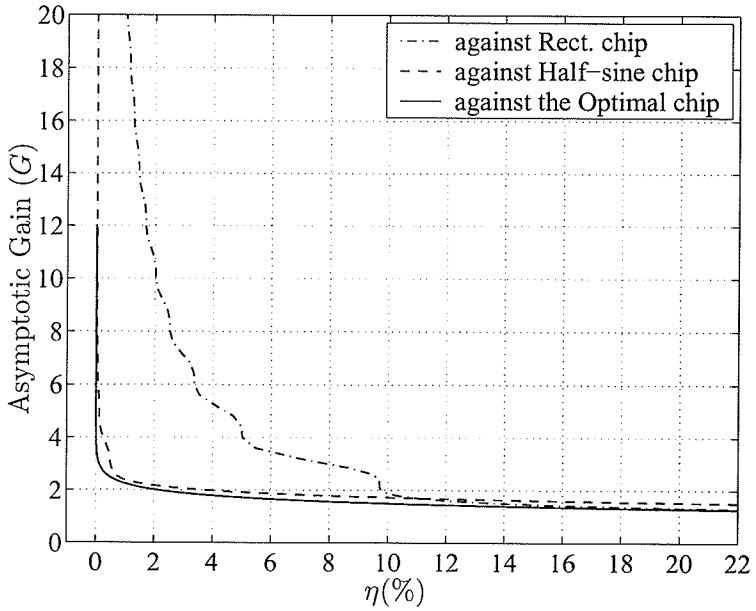

Figure 3.4: Asymptotic gain of network capacity as a function of η.

following close approximation [53]

$$\sum_{i=0}^{N-1} \chi_i(c) \cong 2WT. \tag{3.29}$$

Thus the condition to find $N_{\max}$ in (3.18) becomes

$$N_{\max} = \left\lfloor \frac{WT}{(1-\eta)/2} \right\rfloor. \tag{3.30}$$

Note that in the above equation, $(1-\eta)/2$ plays the role of WT_c as in (3.23). Thus dividing WT_c by $(1-\eta)/2$ gives the following asymptotic gain (for large WT) in network capacity when the optimal basis functions are used instead of suboptimal ones,

$$G = \frac{2WT_c}{1-\eta}. \tag{3.31}$$

The asymptotic gain G is plotted in Fig. 3.4 as a function of η. It can be seen that when η is small, the time-truncated PSWF $\widehat{\varphi}_0(t)$ and the half-sine wave have very favorable WT_c, while the rectangular chip requires much larger WT_c and therefore is

not efficient for constructing the signature space. On the other hand, when η is large ($\eta \geq 10\%$) all the chip waveforms have almost the same WT_c. Furthermore, it is interesting to note that for large η, the rectangular chip has a smaller WT_c than the half-sine chip even though the half-sine wave is a smoother function. This fact can be explained as follows. Although the PSD of the half-sine chip decays faster than that of the rectangular chip, its mainlobe is wider and lower in amplitude, therefore it may require a wider bandwidth to contain a small amount of the required in-band energy (i.e., when η is large).

In summary, Fig. 3.4 shows that there is always a gain of approximately 1.4 in network capacity when using optimal basis functions against suboptimal ones for large values of η. For small values of η the gain becomes very significant. For example when $\eta = 1\%$ a gain of 2.2 can be achieved versus the PSWF chip and the half-sine wave chip and a gain of 20.0 can be achieved over the rectangular chip.

3.4.2 RMS Bandwidth Constraint

Since both the rectangular chip and the first PSWF are discontinuous functions, the RMS bandwidths of these waveforms are infinite. Thus the only chip waveform considered under the RMS bandwidth criterion is the half-sine wave. Because the minimum value of WT_c for this chip waveform is 1/2, one has

$$N_c^{\sin} = \lfloor WT/WT_c \rfloor = 2WT. \tag{3.32}$$

From (3.21) and (3.32) one has the following relation between $N_{\max}$ and $N_c^{\sin}$ (for large WT)

$$N_c^{\sin} = \sqrt{\frac{\left(N_{\max} + \frac{1}{2}\right)\left(N_{\max} + 1\right)}{3}}. \tag{3.33}$$

This relation is plotted in Fig. 3.5. As can be seen from Fig. 3.5, an asymptotic gain of about 1.73 is achieved by employing optimal signature waveforms instead of suboptimal ones constructed from the half-sine chip waveform.

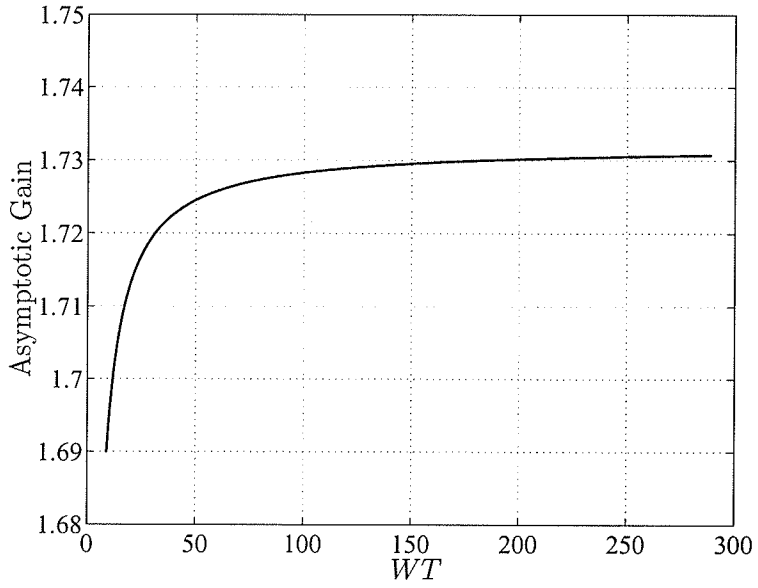

Figure 3.5: Asymptotic gain of network capacity as a function of WT.

3.5 Chapter Summary

We obtained the optimal basis functions for the construction of the bandwidth constrained signature waveforms in S-CDMA systems, where each user is equipped with a MMSE receiver and network capacity is the performance criterion. Both FOBE and RMS bandwidth criteria were considered. The network capacity of the systems was characterized through the signaling duration T, the available bandwidth W (with the corresponding η for FOBE bandwidth) and the SIR requirement α. Comparison to systems employing the suboptimal signature waveforms, which are constructed from the suboptimal, time-disjoint basis functions showed a significant improvement in the network capacity of the systems using the proposed signature waveforms. Since the MMSE receiver becomes a correlation receiver when the signature sequences are WBE sequences, all the results in this chapter are also applicable to S-CDMA systems that use correlation receivers.

Chapter 4

MAI-Minimized Signature Waveforms for S-CDMA Systems

In Chapter 3 the signature waveforms were obtained to maximize the total number of users of S-CDMA systems subject to the constraint on the available bandwidth as well as the constraint on the minimum allowable value of signal to interference ratio (SIR). In this chapter a different design problem is considered for S-CDMA systems. Here, the question of interest is: given a fixed number of users K, what signature waveforms optimize the users' performance subject to a bandwidth constraint. The optimization criterion chosen is minimization of multiple access interference (MAI). More precisely, the signature waveforms are designed to minimize either the TIP or the TMSE defined in (2.25) and (2.26), corresponding to the correlation receiver or the MMSE receiver respectively. In the special case when the number of user K is the size of a Hadamard matrix then the optimal signature waveforms are obtained to maximize the individual SIR at the output of the underlying receiver. The design is carried out under both RMS and FOBE bandwidth constraints. The performance of the proposed signature waveforms is also compared to that of the suboptimal ones constructed based on the Welch bound equality (WBE) sequences. In this chapter, equal received power for all users is also assumed.

4.1 RMS Bandwidth Constrained Signature Waveforms for Correlation Receivers

As mentioned earlier, the design criterion for the correlation receiver is to minimize the TIP in (2.25). Define the following total squared correlation (TSC) of the set of all signature waveforms

$$\text{TSC} = \sum_{i=1}^{K}\sum_{j=1}^{K}\left(\int_0^T s_i(t)s_j(t)\mathrm{d}t\right)^2 = \sum_{i=1}^{K}\sum_{j=1}^{K}\mathbf{R}_{ij}^2. \tag{4.1}$$

It is clear from (2.25) and (4.1) that the TIP for the correlation receiver can be written as

$$\text{TIP} = K\left(\sigma^2 - P\right) + P\cdot\text{TSC}. \tag{4.2}$$

Thus minimizing TIP is equivalent to minimizing TSC. The problem of designing signature waveforms for a correlation receiver to have the minimum value of TSC under the average RMS bandwidth constraint can be formulated as follows.

Problem 4.1. Given T and W. Design a set of K signals $\{s_1(t),\ldots,s_K(t)\}$ that minimizes the TSC in (4.1) subject to the following constraints. (i) $\forall k$, $s_k(t) = 0$ for $t < 0$ and $t > T$; (ii) $\int_0^T s_k^2(t)\mathrm{d}t = 1$, $\forall k$; and (iii) $b(\mathbf{s}(t)) \le W$.

It should be noted that the above design problem for $K = 2$ has been solved in [18] (where the solutions under the FOBE bandwidth constraint are also given). Furthermore, it can be seen that the above problem is very similar to the problem addressed in [20]. More precisely, in [20] the authors found signal sets whose correlation matrix has a maximum determinant, but here we find the set of signature waveforms whose correlation matrix gives the minimum sum of squares of its eigenvalues. The same approach as in [20] is used to transform the original problem into new finite-dimensional formulations.

4.1.1 Equivalent Problems

Note that the TSC in (4.1) can be rewritten as,

$$\text{TSC} = \sum_{i=1}^{K}\sum_{j=1}^{K}(\mathbf{R}_{ij})^2 = \text{tr}\left(\mathbf{R}\mathbf{R}^\top\right). \tag{4.3}$$

Let $b^2(\mathbf{R})$ denote the square of the minimum bandwidth of the optimal signal set corresponding to the correlation matrix $\mathbf{R}$. Then the following propositions provide different formulations for Problem 4.1.

Proposition 4.1. Problem 4.1 is equivalent to Problem 4.2 below, which is stated in terms of the correlation matrix $\mathbf{R}$.

Problem 4.2. Find the correlation matrix $\mathbf{R}$ that minimizes $\text{tr}(\mathbf{R}\mathbf{R}^\top)$ subject to

$$\mathbf{R} \geq 0; \quad \mathbf{R}_{kk} = 1, \ \forall k; \quad b^2(\mathbf{R}) \leq W^2. \tag{4.4}$$

△

Proof. Let $\mathbf{s}_1(t)$ be the solution to Problem 4.1 with the corresponding correlation matrix $\mathbf{R}_1$. Let $\mathbf{R}_2$ be the solution to the Problem 4.2 from which $\mathbf{s}_2(t)$ is found through (2.45). The results of Nuttall (Proposition 2.1) and the constraints in Problem 4.1 imply that $b^2(\mathbf{R}_1) \leq b^2(\mathbf{s}_1(t)) \leq W^2$. Since $\mathbf{R}_1$ satisfies the constraints in Problem 4.2, one has $\text{tr}(\mathbf{R}_1\mathbf{R}_1^\top) \geq \text{tr}(\mathbf{R}_2\mathbf{R}_2^\top)$. On the other hand, since $b^2(\mathbf{s}_2(t)) = b^2(\mathbf{R}_2) \leq W^2$, $\mathbf{s}_2(t)$ satisfies all the constraints in Problem 4.1, and hence $\text{tr}(\mathbf{R}_2\mathbf{R}_2^\top) \geq \text{tr}(\mathbf{R}_1\mathbf{R}_1^\top)$. Thus one concludes that $\text{tr}(\mathbf{R}_1\mathbf{R}_1^\top) = \text{tr}(\mathbf{R}_2\mathbf{R}_2^\top)$ and the two problems yield signal sets having the same minimum value for the TSC. □

Proposition 4.2. The signal design Problem 4.2 is equivalent to Problem 4.3 below, which is stated in terms of the eigenvalues of the correlation matrix $\mathbf{R}$.

Problem 4.3. Find the set of eigenvalues $\{\lambda_1, \ldots, \lambda_K\}$ that minimizes $\sum_{k=1}^{K} \lambda_k^2$, subject to[1]

$$\begin{aligned} &\lambda_k \geq \lambda_{k+1} \geq 0, \quad 1 \leq k < K; \\ &\mathrm{tr}(\mathbf{\Lambda}) = K; \quad \text{and } (K)^{-1}\mathrm{tr}(\mathbf{\Lambda\Pi}) \leq w_0^2 = (2WT)^2. \end{aligned} \tag{4.5}$$

△

Proof. The ordering constraint on the eigenvalues and the RMS bandwidth constraint in Problem 4.3 are the consequences of Proposition 2.1. It is well known that the eigenvalues of a non-negative definite matrix are non-negative and sum to $\mathrm{tr}(\mathbf{R}) = K$. The fact that the TSC can be expressed as the sum of squared eigenvalues of the correlation matrix is established below, using the orthogonality property of the matrix $\mathbf{V}$.

$$\begin{aligned} \text{TSC} &= \mathrm{tr}(\mathbf{R}\mathbf{R}^\top) = \mathrm{tr}(\mathbf{V}\mathbf{\Lambda}\mathbf{V}^\top\mathbf{V}\mathbf{\Lambda}\mathbf{V}^\top) = \mathrm{tr}(\mathbf{V}\mathbf{\Lambda}^2\mathbf{V}^\top) \\ &= \mathrm{tr}(\mathbf{\Lambda}^2\mathbf{V}^\top\mathbf{V}) = \mathrm{tr}(\mathbf{\Lambda}^2) = \sum_{k=1}^{K} \lambda_k^2. \end{aligned} \tag{4.6}$$

Algorithms to construct a correlation matrix which has a prescribed set of eigenvalues and diagonal entries (here $\mathbf{R}$ is a unit-diagonal matrix) are also known. One such algorithm using the *T-transform* is provided in [17] and given in Appendix B for ease of reference. Another algorithm can be found in [20]. Hence the equivalence of Problem 4.2 and 4.3 is demonstrated. □

Proposition 4.3. Problem 4.3 is equivalent to the following problem.

Problem 4.4. Find the set of eigenvalues $\{\lambda_1, \ldots, \lambda_K\}$ that minimizes $\sum_{k=1}^{K} \lambda_k^2$, subject to

$$\mathbf{\Lambda} \geq 0, \quad \mathrm{tr}(\mathbf{\Lambda}) = K, \quad \mathrm{tr}(\mathbf{\Lambda\Pi}) = Kw_0^2. \tag{4.7}$$

[1]Recall from Chapter 2.3 that $\mathbf{\Pi}$ is a $K \times K$ diagonal matrix with $\mathbf{\Pi}_{kk} = k^2$.

Δ

Proof. As in [20], it is first shown that the ordering of the eigenvalues will be a natural consequence of the optimization problem. Suppose that $\mathbf{\Lambda}$ minimizes $\mathrm{tr}(\mathbf{\Lambda}^2)$ and satisfies all the constraints of Problem 4.3 except for being well ordered. Assume $\lambda_k < \lambda_{k+1}$ for some $1 \leq k < K$ and consider $\mathbf{\Lambda}'$ that is obtained from $\mathbf{\Lambda}$ by modifying only the two diagonal entries kth and $(k+1)$th as $\lambda'_k = \lambda'_{k+1} = (\lambda_k + \lambda_{k+1})/2$. Then it can be verified that $\mathrm{tr}(\mathbf{\Lambda}) = \mathrm{tr}(\mathbf{\Lambda}') = K$ and $\mathrm{tr}(\mathbf{\Lambda}'\mathbf{\Pi}) < \mathrm{tr}(\mathbf{\Lambda}\mathbf{\Pi})$, but $\mathrm{tr}(\mathbf{\Lambda}'^2) < \mathrm{tr}(\mathbf{\Lambda}^2)$, a contradiction.

Next it is shown that the inequality on the bandwidth constraint can be replaced by an equality. Suppose there exists a solution $\mathbf{\Lambda}$ to Problem 4.3 where all diagonal entries are well ordered but with $\mathrm{tr}(\mathbf{\Lambda}\mathbf{\Pi}) = \sum_{k=1}^{K} k^2\lambda_k = Kw_0^2 - \epsilon_w < Kw_0^2$. Except for the trivial case when $\mathbf{R} = \mathbf{I}$, there always exists an integer $1 \leq k < K$ such that $\lambda_k - \lambda_{k+1} = \epsilon_\lambda > 0$. Consider $\mathbf{\Lambda}'$ obtained from $\mathbf{\Lambda}$ by modifying the kth and $(k+1)$th diagonal entries as $\lambda'_k = \lambda_k - \delta$ and $\lambda'_{k+1} = \lambda_{k+1} + \delta$ where $\delta = \min\{\epsilon_w/(2k+1), \epsilon_\lambda/2\} > 0$. Then it can be shown that $\mathbf{\Lambda}'$ satisfies all the constraints in Problem 4.3 but $\mathrm{tr}(\mathbf{\Lambda}'^2) < \mathrm{tr}(\mathbf{\Lambda}^2)$, a contradiction. Hence the proof. $\square$

4.1.2 Solutions

The following proposition follows from solving Problem 4.4.

Proposition 4.4. Given T, W and K. If $1 \leq (2WT)^2 < (K+1)(2K+1)/6$, then the minimum total squared correlation (MTSC) of the set of K signals of duration T and average RMS bandwidth less than or equal to W is

$$\mathrm{MTSC} = \frac{K^2}{N}\left(1 + \frac{5\left[(N+1)(2N+1) - 6(2WT)^2\right]^2}{(N-1)(N+1)(2N+1)(8N+11)}\right) \tag{4.8}$$

where N is the largest integer less than or equal to K such that

$$w_0^2 = (2WT)^2 \geq \frac{(N+1)(2N-1)(2N+1)}{5(4N+1)}. \tag{4.9}$$

The MTSC is achieved by the signal set

$$\mathbf{s}(t) = \sqrt{\frac{2}{T}}\mathbf{V}\mathbf{\Lambda}^{1/2}\left[\sin\left(\frac{\pi t}{T}\right), \sin\left(\frac{2\pi t}{T}\right), \ldots, \sin\left(\frac{K\pi t}{T}\right)\right]^{\top}, \quad 0 \le t \le T \tag{4.10}$$

where

$$\begin{aligned}
&\mathbf{\Lambda} = \operatorname{diag}(\lambda_1, \ldots, \lambda_K);\\
&\lambda_k = \frac{K}{N}\left(1 + \frac{5\left[(N+1)(2N+1) - 6(2WT)^2\right]\left[(N+1)(2N+1) - 6k^2\right]}{(N-1)(N+1)(2N+1)(8N+11)}\right),\\
&\text{for } k = 1, \ldots, N;\\
&\lambda_k = 0, \text{ for } k = N+1, \ldots, K;
\end{aligned} \tag{4.11}$$

and $\mathbf{V}$ is any $K \times K$ orthogonal matrix such that $\mathbf{V}\mathbf{\Lambda}\mathbf{V}^{\top}$ is a unit-diagonal matrix.

If $(2WT)^2 \ge (K+1)(2K+1)/6$, then MTSC $= K$ and the set of K orthonormal signals achieves the minimum TSC.

If $(2WT)^2 < 1$, then no signal of duration T and RMS bandwidth less than or equal to W exists. Δ

Proof. It is well-known that among all the signals time limited to $[0, T]$, the signal $\sin(\pi t/T)$ has the minimum RMS bandwidth of $W = 1/(2T)$. Thus when $w_0^2 = (2WT)^2 < 1$ there exists no signal of duration T and RMS bandwidth less than or equal to W. When $w_0^2 = 1$, K signals are identical to $\sin(\pi t/T)$ and MTSC $= K^2$.

If (2.48) is applied for $\mathbf{R} = \mathbf{I}$ then the minimum average RMS bandwidth of K orthonormal signals is $\frac{1}{2T}\sqrt{(K+1)(2K+1)/6}$ (see also [52]). Therefore, when $w_0^2 \ge (K+1)(2K+1)/6$, an orthonormal signal set is always available and MTSC $= K$. Nontrivial solutions for the optimal signal set exist only when

$$1 < w_0^2 < \frac{(K+1)(2K+1)}{6}. \tag{4.12}$$

To find the solutions to Problem 4.4, ignore the nonnegativity constraint of $\mathbf{\Lambda}$ for now and form the Lagrangian

$$L(\mathbf{\Lambda}, \alpha_1, \alpha_2) = \sum_{k=1}^{K}\lambda_k^2 - \alpha_1\left(\sum_{k=1}^{K}\lambda_k - K\right) - \alpha_2\left(\sum_{k=1}^{K}k^2\lambda_k - Kw_0^2\right).$$

By setting $\partial L/\partial \lambda_k = 0$ ones obtains

$$\lambda_k = \frac{1}{2}\left(\alpha_1 + \alpha_2 k^2\right). \tag{4.13}$$

But the constraints in (4.7) give a set of linear equations

$$\begin{cases} \alpha_1 + \frac{1}{6}(K+1)(2K+1)\alpha_2 &= 2 \\ \alpha_1 + \frac{1}{5}(3K^2+3K-1)\alpha_2 &= \dfrac{12w_0^2}{(K+1)(2K+1)} \end{cases} \tag{4.14}$$

from which one can solve for α_1 and α_2 as follows

$$\alpha_1 = 2 + \frac{10\left[(K+1)(2K+1) - 6w_0^2\right]}{(K-1)(8K+11)} \tag{4.15}$$

$$\alpha_2 = -\frac{60\left[(K+1)(2K+1) - 6w_0^2\right]}{(K-1)(K+1)(2K+1)(8K+11)}. \tag{4.16}$$

The optimal eigenvalues are found from (4.13) and are given by the following formula

$$\lambda_k = 1 + \frac{5\left[(K+1)(2K+1) - 6w_0^2\right]\left[(K+1)(2K+1) - 6k^2\right]}{(K-1)(K+1)(2K+1)(8K+11)}, \quad k = 1, \ldots, K. \tag{4.17}$$

Note that due to condition (4.12), $\alpha_1 > 0$ and $\alpha_2 < 0$, hence the λ_k are well ordered as required.

Now check the nonnegativity constraint of $\mathbf{\Lambda}$. Because of the ordering of the λ_k, it is sufficient to require that $\lambda_K \geq 0$, which implies the following

$$w_0^2 \geq \frac{(K+1)(2K-1)(2K+1)}{5(4K+1)}. \tag{4.18}$$

If the above condition is not satisfied, simply set $\lambda_K = 0$ and solve the whole problem again, but with only $K-1$ variables $\lambda_1, \ldots, \lambda_{K-1}$. In general one can assume the maximum number of nonzero eigenvalues to be N and require that $\lambda_N \geq 0$. Then it is not hard to see that N is determined by (4.9) and the new formula for the optimal eigenvalues is given by (4.11) as in the proposition. □

Since $\mathbf{V}$ can be any $K \times K$ orthogonal matrix that satisfies the requirement that $\mathbf{V}\mathbf{\Lambda}\mathbf{V}^\top$ has unit diagonal entries, the set of optimal signals that achieves the MTSC is not unique. As mentioned before, one method to generate the correlation matrix $\mathbf{R}$ (hence the matrix $\mathbf{V}$) is given in Appendix B. Furthermore, the optimal signals have different RMS bandwidths except when the size of the set is a Hadamard matrix dimension, as shown below.

From equation (4.13) one has

$$\mathbf{\Lambda\Pi} = \frac{1}{\alpha_2}\left(2\mathbf{\Lambda}^2 - \alpha_1\mathbf{\Lambda}\right) \tag{4.19}$$

which implies

$$\begin{aligned} \mathbf{V\Lambda\Pi V}^\top &= \frac{2}{\alpha_2}\mathbf{V\Lambda}^2\mathbf{V}^\top - \frac{\alpha_1}{\alpha_2}\mathbf{V\Lambda V}^\top \\ &= \frac{2}{\alpha_2}\mathbf{V\Lambda}^2\mathbf{V}^\top - \frac{\alpha_1}{\alpha_2}\mathbf{R}. \end{aligned} \tag{4.20}$$

Because the matrix $\mathbf{V\Lambda}^2\mathbf{V}^\top$ does not necessarily have equal diagonal entries, it follows from (2.47) and (4.20) that the individuals RMS bandwidths of the optimal signals are not all equal. Some signals have RMS bandwidths larger than W and some have smaller bandwidths. However when K is a Hadamard dimension, $\mathbf{V}$ can be chosen to be the normalized Hadamard matrix $\mathbf{H}$ whose components are $\pm 1/\sqrt{K}$ and hence $\mathbf{H\Lambda H}^\top$ has unit diagonal entries. With this choice of $\mathbf{V}$, the matrix $\mathbf{H\Lambda}^2\mathbf{H}^\top$ also has equal diagonal entries of $\frac{1}{K}\sum_{k=1}^{K}\lambda_k^2$ and therefore all the signals in the optimal set have the same RMS bandwidth of W.

Another interesting property of the optimal signal set whose cardinality is a Hadamard dimension is that the set maximizes the individual SIR at the output of each correlation receiver. This simply follows from the fact that with the choice

$\mathbf{V} = \mathbf{H}$ one has

$$\begin{aligned}\sum_{j=1}^{K} \mathbf{R}_{kj}^2 &= \left(\mathbf{R}\mathbf{R}^\top\right)_{kk} = \left(\mathbf{V}\boldsymbol{\Lambda}^2\mathbf{V}^\top\right)_{kk} \\ &= \left(\mathbf{H}\boldsymbol{\Lambda}^2\mathbf{H}^\top\right)_{kk} = \frac{1}{K}\sum_{k=1}^{K}\lambda_k^2 \end{aligned} \tag{4.21}$$

which is the same for every k and therefore minimum. From (2.19) the new expression for SIR_k is as follows,

$$\mathrm{SIR}_k = \frac{K\gamma}{K(1-\gamma)+\gamma\sum_{k=1}^{K}\lambda_k^2}. \tag{4.22}$$

Thus the SIR_k is equal and maximized for every k.

The above discussion means that when K is a Hadamard matrix dimension, the optimal signature waveforms can be obtained to maximize the individual SIR_k for every user. These optimal signature waveforms are also valid if the *maximum* RMS bandwidth constraint of the signature set defined in (2.41) is considered. As a special case, it can be verified that for a system with $K = 2$ users, Proposition 4.4 produces the same result as in [18].

To conclude this section, an example to design four signals that achieve the MTSC is given next. Note that when $K = 4$, in order to have nontrivial solutions w_0^2 should be in the range of $(1, 15/2)$. The MTSC is given below and it is plotted in Fig. 4.1 as a function of the time-bandwidth product.

$$\mathrm{MTSC} = \begin{cases} 8\left[1+\dfrac{(5-2w_0^2)^2}{9}\right] & 1 \le w_0^2 \le \dfrac{28}{13} \\ \dfrac{16}{3}\left[1+\dfrac{(14-3w_0^2)^2}{98}\right] & \dfrac{28}{13} \le w_0^2 \le \dfrac{63}{17} \\ 4\left[1+\dfrac{(15-2w_0^2)^2}{129}\right] & \dfrac{63}{17} \le w_0^2 \le \dfrac{15}{2} \\ 4 & \dfrac{15}{2} \le w_0^2 \end{cases} \tag{4.23}$$

Example 4.1. Let $WT = 1.25$, hence $w_0^2 = 6.25$. The optimal eigenvalues are found to be $\boldsymbol{\Lambda} = \mathrm{diag}(1.2519, 1.1357, 0.9419, 0.6705)$ and $\mathrm{MTSC} = 4.1938$. When $\mathbf{V}$ is a

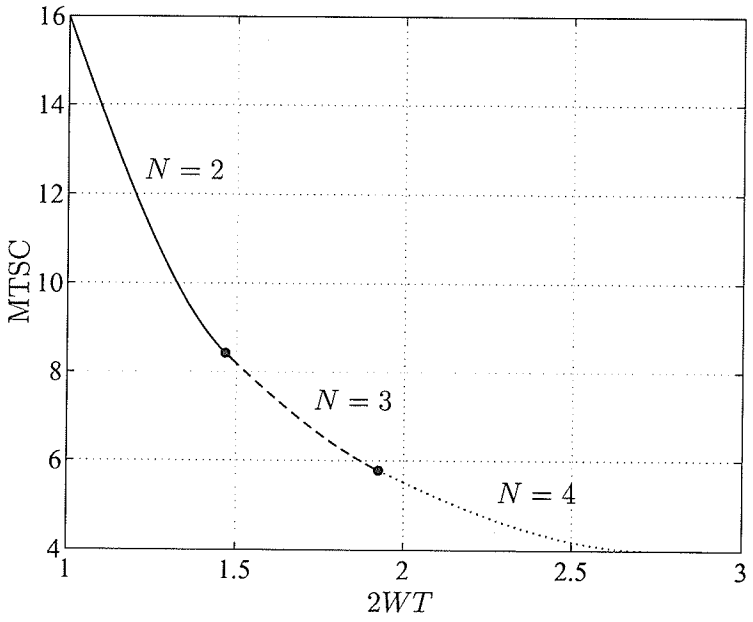

Figure 4.1: Minimum TSC versus time-bandwidth product: $K = 4$, RMS bandwidth constraint.

normalized Hadamard matrix

$$\mathbf{V} = \mathbf{H} = \frac{1}{2}\begin{bmatrix} 1 & 1 & 1 & 1 \\ 1 & -1 & 1 & -1 \\ 1 & 1 & -1 & -1 \\ 1 & -1 & -1 & 1 \end{bmatrix}$$

the optimal signals, all of which have the same RMS bandwidth of $W = 1.25/T$, are plotted in Fig. 4.2. Note that there are two pairs of signals which are mirror images of each other about $T/2$ in Fig. 4.2. Optimal signals obtained from the matrix $\mathbf{V}$ which is found by the recursive algorithm in Appendix B are plotted in Fig. 4.3. The RMS bandwidths of these signals are $1.1740/T$, $1.2919/T$, $1.3506/T$ and $1.1740/T$ respectively.

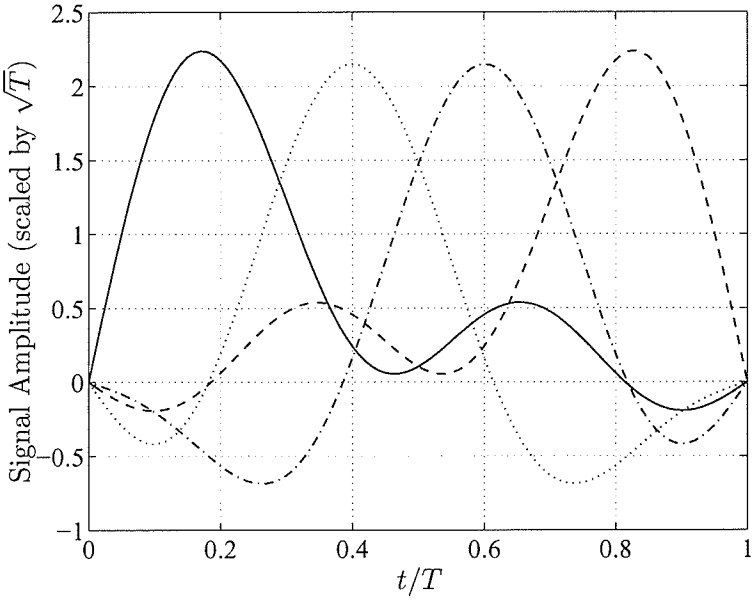

Figure 4.2: TSC-minimized signature waveforms under RMS bandwidth constraint: $K = 4$, $WT = 1.25$ with $\mathbf{V}$ a Hadamard matrix.

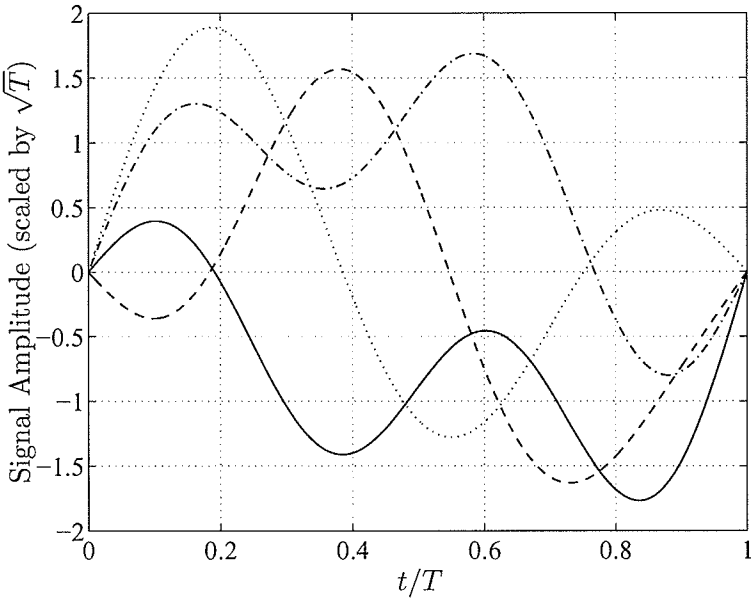

Figure 4.3: TSC-minimized signature waveforms under RMS bandwidth constraint: $K = 4$, $WT = 1.25$ with $\mathbf{V}$ obtained using the *T-transform.*

4.2 FOBE Bandwidth Constrained Signature Waveforms for Correlation Receivers

This section addresses the same problem of designing signal sets that achieve the minimum value of TSC, but under the FOBE bandwidth measurement. The design problem can be stated as follows.

Problem 4.5. Given T, W and $0 < \eta < 1$. Design a set of K signals $\{s_1(t), \ldots, s_K(t)\}$ that minimizes the TSC in (4.1) subject to the following constraints. (i) $\forall k$, $s_k(t) = 0$, for $t < 0$ and $t > T$; (ii) $\int_0^T s_k^2(t)\mathrm{d}t = 1$, $\forall k$; and (iii) $\epsilon(\mathbf{s}(t)) \leq \eta$.

The method to solve the the above problem is similar to the one presented in Section 4.1 for solving Problem 4.1. In particular, based on Proposition 2.2 it is shown in Appendix C that Problem 4.5 is equivalent to the following problem.

Problem 4.6. Find the set of eigenvalues $\{\lambda_1, \ldots, \lambda_K\}$ that minimizes $\sum_{k=1}^K \lambda_k^2$, subject to[2]

$$\mathbf{\Lambda} \geq 0; \quad \mathrm{tr}(\mathbf{\Lambda}) = K; \quad \mathrm{tr}(\mathbf{\Lambda\Xi}) = K\eta. \tag{4.24}$$

It can be seen that Problem 4.6 is basically the same as Problem 4.4 except for the last constraint in (4.24). The following proposition provides the solution to Problem 4.6.

Proposition 4.5. Given T, W, K and $0 < \eta < 1$. If $\frac{1}{K}\sum_{k=0}^{K-1} \chi_k < 1 - \eta \leq \chi_0$, then the minimum total squared correlation (MTSC) of the set of K signals of duration T and average FOBE bandwidth at level η less than or equal to W is

$$\mathrm{MTSC} = \frac{K^2}{N}\left[1 + \frac{(v(N) - \eta)^2}{u(N) - v^2(N)}\right] \tag{4.25}$$

where

$$u(N) = \frac{1}{N}\sum_{k=0}^{N-1}(1 - \chi_k)^2, \qquad v(N) = \frac{1}{N}\sum_{k=0}^{N-1}(1 - \chi_k) \tag{4.26}$$

[2]Recall from Chapter 2.3 that $\mathbf{\Xi} = \mathrm{diag}\,(1 - \chi_0, 1 - \chi_1, \ldots, 1 - \chi_{K-1})$.

and N is the largest integer less than or equal to K such that

$$(1-\chi_{N-1})(v(N)-\eta) \le u(N)-\eta v(N). \tag{4.27}$$

The MTSC is achieved by the signal set

$$\mathbf{s}(t) = \mathbf{V}\mathbf{\Lambda}^{1/2}\left[\widehat{\varphi}_0(t), \widehat{\varphi}_1(t), \ldots, \widehat{\varphi}_{K-1}(t)\right]^{\top} \tag{4.28}$$

where

$$\begin{aligned}
&\mathbf{\Lambda} = \operatorname{diag}(\lambda_1, \ldots, \lambda_K);\\
&\lambda_k = \frac{K}{N}\frac{(\eta v(N)-u(N))+(v(N)-\eta)(1-\chi_{k-1})}{v^2(N)-u(N)}, \qquad k=1,\ldots,N;\\
&\lambda_k = 0, \qquad k=N+1,\ldots,K
\end{aligned} \tag{4.29}$$

and $\mathbf{V}$ is any $K \times K$ orthogonal matrix such that $\mathbf{V}\mathbf{\Lambda}\mathbf{V}^{\top}$ is a unit-diagonal matrix.

If $\frac{1}{K}\sum_{k=0}^{K-1}\chi_k \ge 1-\eta$, then MTSC $= K$ and the set of K orthonormal signals achieves the minimum TSC.

If $1-\eta > \chi_0$, then no signal of duration T and FOBE bandwidth at level η less than or equal to W exists. Δ

Proof. The proof is similar to the proof of Proposition 4.4. From the properties of PSWFs it is known that the function $\widehat{\varphi}_0(t;c)$ is the unique signal which has the smallest FOBE of χ_0 among all signals of duration T. Thus when $1-\eta > \chi_0$ there exists no signal of duration T and FOBE bandwidth at level η less than or equal to W. When $1-\eta = \chi_0$, K signals are identical to $\widehat{\varphi}_0(t;c)$ and MTSC $= K^2$. By applying Proposition 2.2 for the case of an orthonormal set, i.e., $\mathbf{R} = \mathbf{I}$, the minimum average FOBE of K signals satisfies

$$\epsilon(\mathbf{s}(t)) = \frac{1}{K}\sum_{k=0}^{K-1}(1-\chi_k).$$

Thus when $\frac{1}{K}\sum_{k=0}^{K-1}\chi_k \ge 1-\eta$, orthonormal signals are always available, hence MTSC $= K$.

From the above discussion, nontrivial solutions for the optimal signal set exist only when

$$\frac{1}{K}\sum_{k=0}^{K-1}\chi_k < 1-\eta \leq \chi_0. \tag{4.30}$$

As in the proof of Proposition 4.4, first ignore the nonnegativity constraint on $\mathbf{\Lambda}$ and form the Lagrangian,

$$L\left(\mathbf{\Lambda},\alpha_1,\alpha_2\right) = \sum_{k=1}^{K}\lambda_k^2 - \alpha_1\left(\sum_{k=1}^{K}\lambda_k - K\right) - \alpha_2\left(\sum_{k=1}^{K}(1-\chi_{k-1})\lambda_k - K\eta\right).$$

Taking the derivative with respect to λ_k and setting it to 0 produce

$$\lambda_k = \frac{1}{2}\left[\alpha_1 + \alpha_2(1-\chi_{k-1})\right]. \tag{4.31}$$

But the constraints in (4.24) give a set of linear equations

$$\begin{cases} \alpha_1 v + \alpha_2 u &= 2\eta \\ \alpha_1 + \alpha_2 v &= 2 \end{cases} \tag{4.32}$$

where $u = u(K)$ and $v = v(K)$ are defined in (4.26). From the above equations one can find

$$\alpha_1 = \frac{2(\eta v - u)}{v^2 - u} \quad \text{and} \quad \alpha_2 = \frac{2(v-\eta)}{v^2-u} \tag{4.33}$$

and the optimal eigenvalues are found from (4.31) as

$$\lambda_k = \frac{(\eta v - u) + (v-\eta)(1-\chi_{k-1})}{v^2-u}. \tag{4.34}$$

Note that, due to condition (4.30), one has $v > \eta$. Furthermore, by applying the Cauchy-Schwarz inequality and from the fact that the χ_k are all distinct, one also has $u > v^2$, which together with $v\eta > 0$ implies $u > v\eta$. Thus one has $\alpha_1 > 0$ and $\alpha_2 < 0$. Since $1-\chi_0 < 1-\chi_1 < \ldots < 1-\chi_{K-1}$, from (4.31) it can be seen that the λ_k are well ordered, as required.

Now check the nonnegativity constraint of $\mathbf{\Lambda}$. It suffices to require that $\lambda_K \geq 0$, which implies

$$\chi_{K-1} \geq 1 + \frac{\eta v - u}{v - \eta}. \tag{4.35}$$

If the above condition is not satisfied, simply set $\lambda_K = 0$ and solve the whole problem again, but with only $K-1$ variables $\lambda_1, \ldots, \lambda_{K-1}$. It can be shown that the number of nonzero eigenvalues N is given in (4.27) and the corresponding formula for the optimal eigenvalues are given as in (4.29). □

Similar to the case of RMS bandwidth, the following observations can be made regarding the optimal signature waveforms given by Proposition 4.5.

- The set of optimal signature waveforms is not unique due to the fact that $\mathbf{V}$ can be any $K \times K$ orthogonal matrix that satisfies the requirement that $\mathbf{V\Lambda V}^\top$ has unit diagonal entries.

- The optimal signature waveforms have different FOBEs, except when the size of the set is a Hadamard matrix dimension. Thus when K is a Hadamard matrix dimension, the results of Proposition 4.5 are also valid if the *maximum* FOBE bandwidth constraint of the set is considered.

- When the number of users is a Hadamard dimension, the optimal signature waveforms can be obtained to maximize the individual SIR at the output of each correlation receiver.

- As a special case, when $K = 2$ the results of Proposition 4.5 agree with the results given in [18] for the minimum cross-correlation between two signals of duration T and with FOBE bandwidths at level η less than or equal to W.

Finally, an example is given next to illustrate the design of the optimal sets of four signals under the FOBE bandwidth constraint. The MTSC is plotted in Fig. 4.4 as a function of $w_0 = 2WT$ for various values of η.

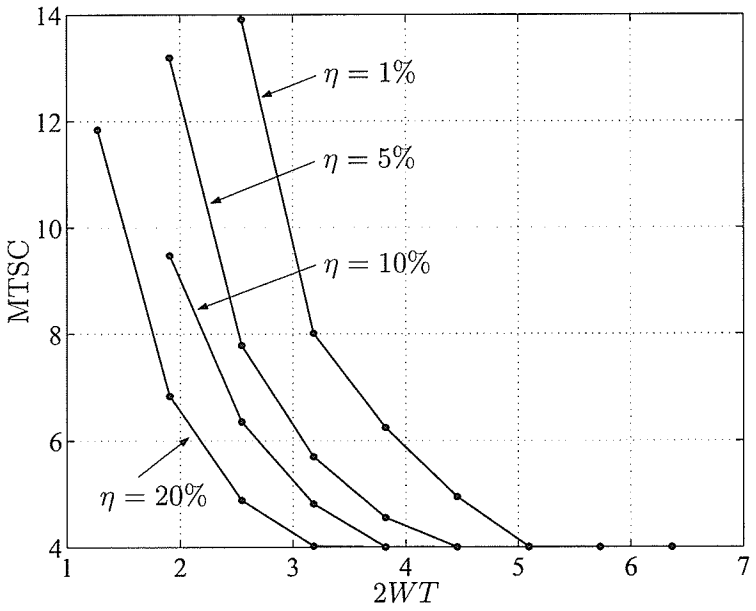

Figure 4.4: Minimum TSC versus time-bandwidth product: $K = 4$, FOBE bandwidth constraint.

Example 4.2. Consider $c = \pi WT = 4.0$ (or $W = 1.2732/T$) and $\eta = 0.1$, thus $\chi_0 = 9.9589 \times 10^{-1}$, $\chi_1 = 9.1211 \times 10^{-1}$, $\chi_2 = 5.1905 \times 10^{-1}$, $\chi_3 = 1.1021 \times 10^{-1}$. Proposition 4.5 yields $N = 3$ and MTSC $= 6.3551$. The corresponding set of optimal eigenvalues is $\{1.8580, 1.6228, 0.5192, 0.0\}$. The optimal signal sets are shown in Fig. 4.5 and Fig. 4.6 corresponding to two different ways of obtaining the matrix $\mathbf{V}$.

4.3 Signature Waveforms for MMSE Receivers

Sections 4.1 and 4.2 dealt with the design of signature waveforms for S-CDMA systems when the correlation receiver is employed. Though simple, the correlation receiver suffers from the near-far problem, i.e., the bit error rate of the correlation receiver is sensitive to differences in the received powers of the desired user and interfering users [2]. Even when perfect power control is assumed, the bit error rate of the correlation receiver is still orders of magnitude far from optimal. As explained before,

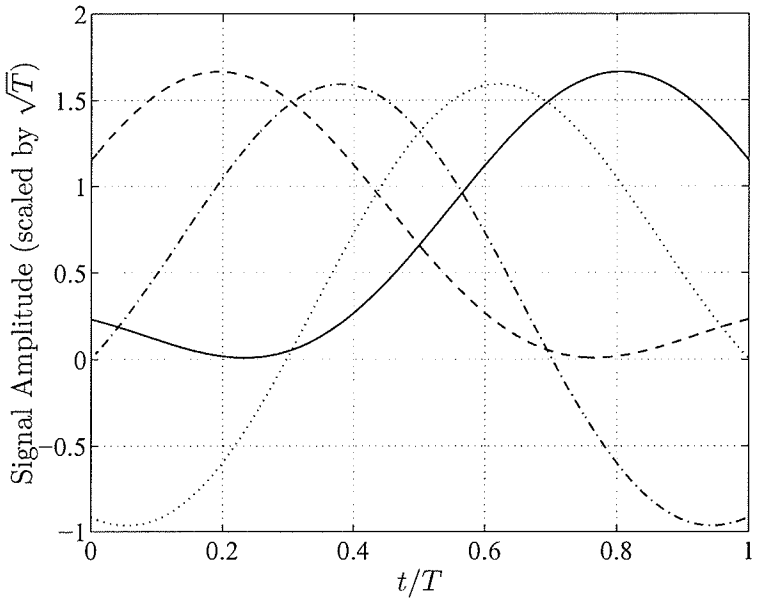

Figure 4.5: TSC-minimized signature waveforms under FOBE bandwidth constraint: $K = 4$, $c = 4.0$, $\eta = 0.1$ with $\mathbf{V}$ a Hadamard matrix.

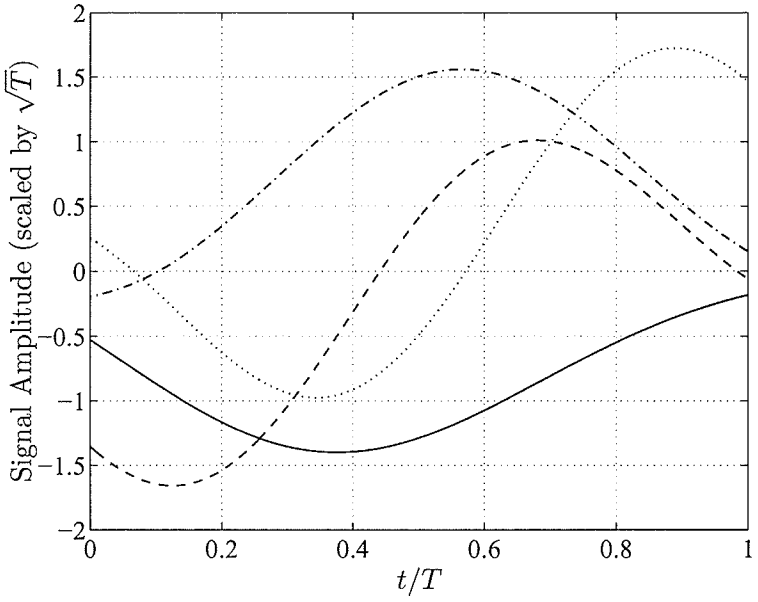

Figure 4.6: TSC-minimized signature waveforms under FOBE bandwidth constraint: $K = 4$, $c = 4.0$, $\eta = 0.1$ with $\mathbf{V}$ obtained using the *T-transform.*

this is due to the correlation of users through their signature waveforms (even though these signature waveforms have been optimally designed), which makes the interuser interference, not white Gaussian noise, the dominant degradation.

The linear MMSE receiver described in Chapter 2 is a more sophisticated receiver which accounts for the presence of the other interfering users in the CDMA channel. It has been shown that the MMSE receiver can dramatically improve the error performance over the correlation receiver [44, 45, 46]. When the MMSE receiver is employed, the signature waveforms obtained in Sections 4.1 and 4.2 are no longer optimal and therefore new sets of signature waveforms for this type of receiver need to be found. This is precisely the goal of this section.

The problem of designing signature waveforms for the MMSE receivers under either RMS or FOBE bandwidth constraint can be stated similarly to Problems 4.1 and 4.5 respectively. The only difference is due to the objective function. For the case of MMSE receiver, the objective is to minimize the TMSE given in (2.26). With the perfect power-control assumption (i.e., $p_k = P,\ k = 1, \ldots, K$), (2.26) can be written as

$$\begin{aligned} \text{TMSE} &= KP - P\text{tr}\left(\left[\mathbf{I} + \frac{\sigma^2}{P}\mathbf{R}^{-1}\right]^{-1}\right) && (4.36) \\ &= KP - P\sum_{k=1}^{K} \frac{P\lambda_k}{P\lambda_k + \sigma^2} \\ &= P\sum_{k=1}^{K} \frac{1}{(P/\sigma^2)\lambda_k + 1} = P\sum_{k=1}^{K}(\gamma\lambda_k + 1)^{-1} && (4.37) \end{aligned}$$

where, as before, $\lambda_k,\ k = 1, \ldots, K$, are the eigenvalues of the correlation matrix $\mathbf{R}$ and $\gamma = P/\sigma^2$ is the signal-to-background noise ratio.

Following the same procedure as in Section 4.1, Appendix D shows that it is possible to transform the original design problem (stated in Problem D.1) into a new finite-dimensional optimization problem for each bandwidth criterion. Let $\mathbf{\Delta} = \mathbf{\Pi}$,

$\nu = w_0^2 = (2WT)^2$ when the RMS bandwidth is considered and $\mathbf{\Delta} = \mathbf{\Xi}$, $\nu = \eta$ when the FOBE bandwidth constraint is used. Then the finite-dimensional optimization problem, under either an RMS or FOBE bandwidth constraint, can be formulated as follows.

Problem 4.7. Find the set of eigenvalues $\{\lambda_1, \ldots, \lambda_K\}$ that minimizes $\sum_{k=1}^{K} (\gamma\lambda_k + 1)^{-1}$ subject to (i) $\mathbf{\Lambda} \geq 0$; (ii) $\mathrm{tr}(\mathbf{\Lambda}) = K$; and (iii) $\mathrm{tr}(\mathbf{\Lambda\Delta}) = K\nu$.

To solve the above optimization problem, again the Lagrange method can be used. However, closed-form expressions for the solutions are not available due to the fact that one obtains a system of nonlinear equations to solve for the Lagrange multipliers. Nevertheless, Proposition 4.6 below gives a procedure to find optimal signature waveforms. Note that in Proposition 4.6, $\xi_k = k^2$, $k = 1, \ldots, K$ if the RMS bandwidth is considered and $\xi_k = 1 - \chi_{k-1}$, $k = 1, \ldots, K$ if the FOBE bandwidth is used.

Proposition 4.6. Given T, W, K and $0 < \eta < 1$ (η is only required for FOBE bandwidth). If $\xi_1 \leq \nu < \frac{1}{K}\sum_{k=1}^{K} \xi_k$, then the set of K signals of duration T with an average bandwidth less than or equal to W that minimizes the TMSE is given by

$$\mathbf{s}(t) = \mathbf{V}\mathbf{\Lambda}^{1/2}\mathbf{\Gamma}(t) \tag{4.38}$$

where

$$\mathbf{\Gamma}(t) = \begin{cases} \sqrt{\frac{2}{T}}\left[\sin\left(\frac{\pi t}{T}\right), \sin\left(\frac{2\pi t}{T}\right), \ldots, \sin\left(\frac{K\pi t}{T}\right)\right]^\top, \ 0 \leq t \leq T; & \text{for RMS bandwidth} \\ \left[\widehat{\varphi}_0(t), \widehat{\varphi}_1(t), \ldots, \widehat{\varphi}_{K-1}(t)\right]^\top; & \text{for FOBE bandwidth} \end{cases}$$

and

$$\begin{aligned} &\mathbf{\Lambda} = \mathrm{diag}(\lambda_1, \ldots, \lambda_K); \\ &\lambda_k = \gamma^{-1}\left(\sqrt{\frac{\gamma}{\alpha_1 + \alpha_2\xi_k}} - 1\right), \quad k = 1, \ldots, K. \end{aligned} \tag{4.39}$$

The quantities α_1, α_2 are the roots of the following system of nonlinear equations[3]

$$\begin{cases} \sum_{k=1}^{K} \dfrac{1}{\sqrt{\alpha_1 + \alpha_2 \xi_k}} &= K\left(\gamma^{1/2} + \gamma^{-1/2}\right) \\ \sum_{k=1}^{K} \dfrac{\xi_k}{\sqrt{\alpha_1 + \alpha_2 \xi_k}} &= K\nu\gamma^{1/2} + \gamma^{-1/2} \sum_{k=1}^{K} \xi_k \end{cases} \tag{4.40}$$

that satisfy the following constraints.

$$\begin{cases} -\alpha_2 < \alpha_1 \leq \gamma - \alpha_2 \\ -\xi_K \alpha_2 < \alpha_1 \leq \gamma - \xi_K \alpha_2. \end{cases} \tag{4.41}$$

The matrix $\mathbf{V}$ is any $K \times K$ orthogonal matrix such that $\mathbf{V}\mathbf{\Lambda}\mathbf{V}^\top$ is a unit-diagonal matrix.

If $\nu \geq \frac{1}{K}\sum_{k=1}^{K} \xi_k$, then the set of optimal signature waveforms is any set of orthonormal signals.

If $\nu < \xi_1$, then there is no signal of duration T whose bandwidth is less than or equal to W. Δ

The constraints on α_1 and α_2 in (4.41) are necessary and sufficient to have non-negative λ_ks, which is required. This can be easily verified based on the ordering of the χ_ks. The system of nonlinear equations given in (4.40), together with the constraints of (4.41), can be solved numerically in order to find the λ_ks, which give the optimal signature waveforms. If no solutions for α_1 and α_2 can be found then simply set $\lambda_K = 0$ and solve Problem 4.7 again but with only $K-1$ variables $\lambda_1, \ldots, \lambda_{K-1}$.

From equation (4.39), it can be shown that the optimal signature waveforms found in Proposition 4.6 have different FOBEs, except when K is a Hadamard matrix dimension. Similar to the TSC-minimized signature waveforms, when K is a Hadamard matrix dimension, the TMSE-minimized signature waveforms can also be made to maximize the individual SIR_ks in (2.24). This can be verified as follows. Substitute $\mathbf{R} = \mathbf{V}\mathbf{\Lambda}\mathbf{V}^\top$ and $\mathbf{R}_k = \mathbf{V}\mathbf{\Lambda}\mathbf{u}_k$, where $\mathbf{u}_k$ is the kth column of $\mathbf{V}^\top$, into (2.23). Using

[3]These two equations are to satisfy constraints (ii) and (iii) in Problem 4.7 respectively.

the orthogonality property of $\mathbf{V}$ one can write MMSE_k as

$$\text{MMSE}_k = P - P\mathbf{u}_k^\top \left(\mathbf{I} + \gamma^{-1}\mathbf{\Lambda}^{-1}\right)^{-1} \mathbf{u}_k. \tag{4.42}$$

Now if $\mathbf{V} = \mathbf{H}$ then the components of $\mathbf{u}_k$ are $\pm 1/\sqrt{K}$ and the MMSE_k becomes

$$\text{MMSE}_k = P - P\frac{1}{K}\sum_{k=1}^{K} \frac{1}{1 + (\gamma\lambda_k)^{-1}} = \frac{P}{K}\sum_{k=1}^{K}(1 + \gamma\lambda_k)^{-1}. \tag{4.43}$$

Since MMSE_ks are the same for every k and their sum is minimized, the individual MMSE_k is also minimized. This implies that the SIR_k in (2.24) is maximized and its value is given by

$$\text{SIR}_k = \frac{\sum_{k=1}^{K} \gamma\lambda_k (1 + \gamma\lambda_k)^{-1}}{\sum_{k=1}^{K}(1 + \gamma\lambda_k)^{-1}}. \tag{4.44}$$

Note that there is a major difference when finding the optimal signature waveforms for the correlation receivers (Propositions 4.4 and 4.5) and for the MMSE receivers (Proposition 4.6). The TSC-minimized signature set is found independently from the signal-to-noise ratio level γ, whereas the TMSE-minimized signature set needs to be found for each value of γ. However, when γ is large, the dependence on γ of the solutions given by Proposition 4.6 is very small, as shown in Tables 4.1 and 4.2 for different bandwidth criteria. Figures 4.7 to 4.10 plot the optimal signature waveforms for different bandwidth measurements and various ways of obtaining matrix $\mathbf{V}$. These signature waveforms are all obtained by setting $\gamma = 14\text{dB}$.

Finally, we would like to point out that although this chapter only considers signature waveforms designs for the correlation and MMSE receivers, the design for the decorrelating receiver can be carried out similarly. From the expression of SIR in (3.11), an obvious and sensible design criterion is to minimize $\sum_{k=1}^{K} (\mathbf{R}^{-1})_{kk} = \text{tr}\,(\mathbf{R}^{-1})$, or in terms of the eigenvalues, to minimize $\text{tr}\,(\mathbf{\Lambda}^{-1})$.

Table 4.1: Dependence of the optimal eigenvalues on γ: $K = 4$ and RMS bandwidth of $WT = 1.25$.

γ (dB)	λ_1	λ_2	λ_3	λ_4
6	1.3177	1.0907	0.8781	0.7136
7	1.3194	1.0892	0.8769	0.7145
8	1.3206	1.0882	0.8761	0.7151
9	1.3213	1.0875	0.8757	0.7155
10	1.3218	1.0871	0.8754	0.7157
11	1.3221	1.0869	0.8752	0.7159
12	1.3223	1.0867	0.8750	0.7160
13	1.3224	1.0866	0.8750	0.7160
14	1.3225	1.0865	0.8749	0.7161
15	1.3226	1.0865	0.8749	0.7161
16	1.3226	1.0864	0.8749	0.7161

Table 4.2: Dependence of the optimal eigenvalues on γ: $K = 4$ and FOBE bandwidth with $c = 4.0$ and $\eta = 0.1$.

γ (dB)	λ_1	λ_2	λ_3	λ_4
6	2.7397	0.7627	0.2961	0.2015
7	2.7695	0.7309	0.2938	0.2058
8	2.7887	0.7105	0.2923	0.2085
9	2.8009	0.6975	0.2914	0.2102
10	2.8087	0.6892	0.2908	0.2113
11	2.8136	0.6840	0.2904	0.2120
12	2.8167	0.6806	0.2902	0.2124
13	2.8187	0.6785	0.2901	0.2127
14	2.8199	0.6772	0.2900	0.2129
15	2.8207	0.6764	0.2899	0.2130
16	2.8212	0.6759	0.2899	0.2131

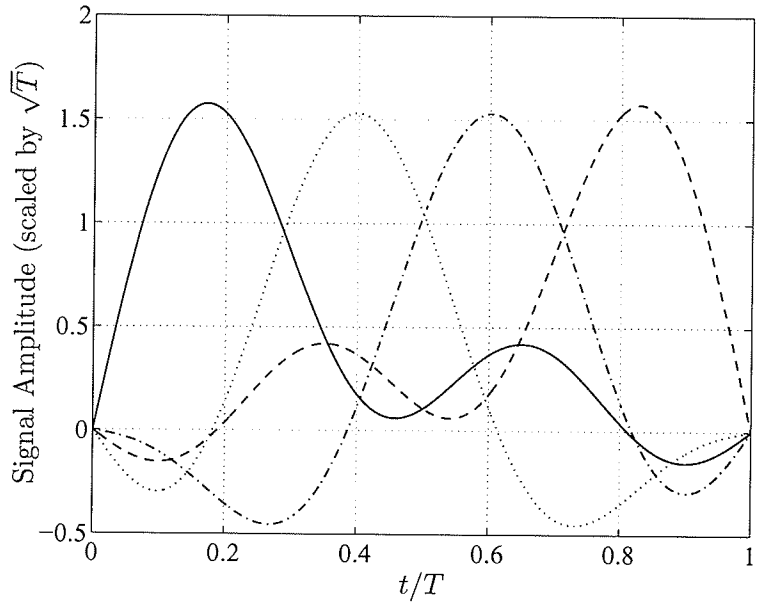

Figure 4.7: TMSE-minimized signature waveforms under RMS bandwidth constraint: $K = 4$, $WT = 1.25$ with $\mathbf{V}$ a Hadamard matrix.

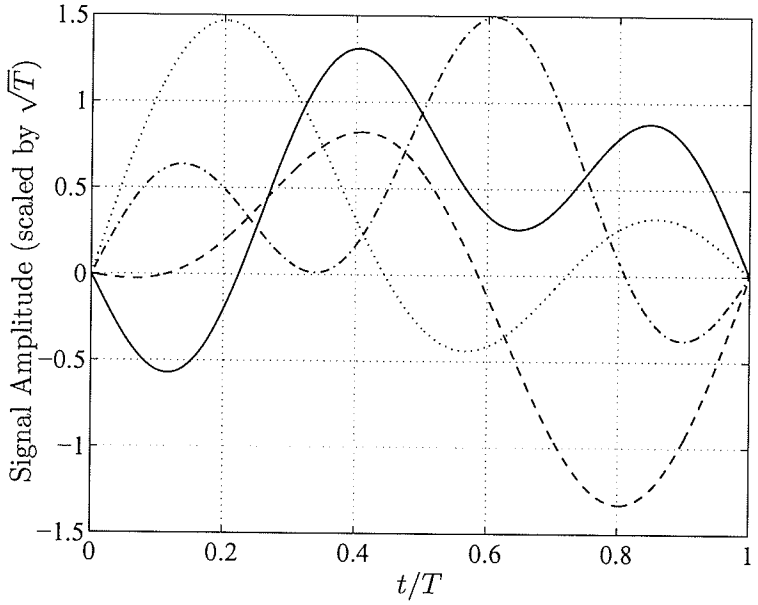

Figure 4.8: TMSE-minimized signature waveforms under RMS bandwidth constraint: $K = 4$, $WT = 1.25$ with $\mathbf{V}$ obtained using the *T-transform*.

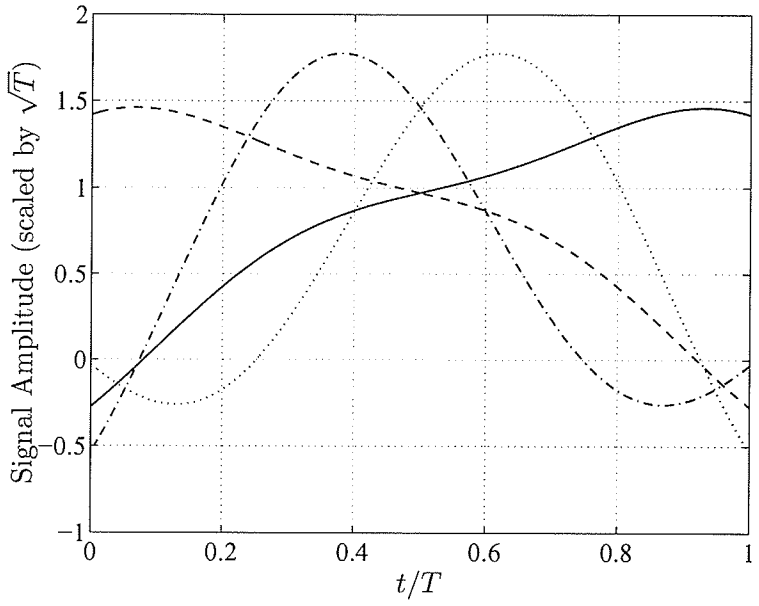

Figure 4.9: TMSE-minimized signature waveforms under FOBE bandwidth constraint: $K = 4$, $c = 4.0$, $\eta = 0.1$ with $\mathbf{V}$ a Hadamard matrix.

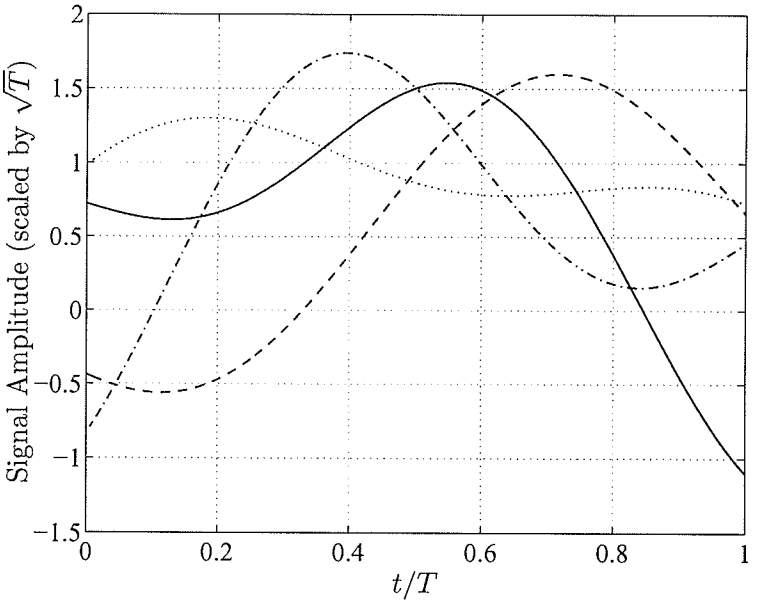

Figure 4.10: TMSE-minimized signature waveforms under FOBE bandwidth constraint: $K = 4$, $c = 4.0$, $\eta = 0.1$ with $\mathbf{V}$ obtained using the *T-transform*.

4.4 Comparison with Suboptimal Signature Waveforms Constructed from WBE Sequences

This section compares the performance of the optimal signature waveforms obtained in the previous sections with that of suboptimal signature waveforms. The suboptimal signature waveforms are constructed from Welch bound equality (WBE) sequences. This family of sequences is discussed next.

4.4.1 WBE Sequences and the Uniformly-Good Property

If the signature waveforms are constructed as linear combinations of some orthonormal basis functions as in (2.5), then the TSC in (4.1) can be written in terms of signature sequences as,

$$\text{TSC} = \sum_{i=1}^{K} \sum_{j=1}^{K} \left(\mathbf{s}_i^{\top} \mathbf{s}_j\right)^2 . \tag{4.45}$$

The lower bound of TSC for the set of K signature sequences, each of length N ($K > N$) is given by Welch [16] to be

$$\text{TSC} \geq \frac{K^2}{N}. \tag{4.46}$$

The sequences that achieve Welch's bound on TSC are called Welch bound equality (WBE) sequences [14]. The necessary and sufficient conditions for having WBE sequences for a given K and N was first established in [13] as,

$$\mathbf{S}\mathbf{S}^{\top} = \frac{K}{N}\mathbf{I} \tag{4.47}$$

where $\mathbf{I}$ is an $N \times N$ identity matrix. In general, for given K and N, the set of WBE sequences is not unique. One such set is identified in terms of *tight frames* in the wavelets literature [54],

$$\mathbf{s}_k = \begin{cases} \sqrt{\frac{2}{N}} \left[\frac{1}{\sqrt{2}}, \cos\left(\frac{2\pi k}{K}\right), \sin\left(\frac{2\pi k}{K}\right), \ldots, \cos\left(\frac{2\pi(N-1)k}{2K}\right), \sin\left(\frac{2\pi(N-1)k}{2K}\right)\right]^{\top}, & N \text{ odd} \\ \sqrt{\frac{2}{N}} \left[\cos\left(\frac{2\pi k}{K}\right), \sin\left(\frac{2\pi k}{K}\right), \ldots, \cos\left(\frac{2\pi Nk}{2K}\right), \sin\left(\frac{2\pi Nk}{2K}\right)\right]^{\top}, & N \text{ even} \end{cases}$$

Another set may be obtained by a recursive algorithm using the *T-transform* as provided in [17] (see Appendix B). The construction of *binary* WBE sequences from linear codes can also be found in [13].

It has been shown in Section 3.2 that the WBE signature sequences also minimize the TSME at the outputs of the MMSE receivers. Furthermore, using WBE signature sequences makes an MMSE receiver identical to a correlation receiver. When the WBE sequences are used, the SIRs at the outputs of the MMSE (or correlation) receivers are all equal and maximized. This property of WBE sequences is called the uniformly-good property (UGP) in [13]. In terms of maintaining fairness among users, UGP is desirable. Unfortunately, the UGP does not hold for the TSC-minimized and TSME-minimized waveforms in general. This property only holds when the number of users K is a Hadamard matrix dimension as discussed in the previous sections.

When K is not a Hadamard matrix dimension, one way to maintain the UGP is to assign the signature waveforms to users *cyclically* after each symbol interval. In this way each user will see the same *average* interference after K symbol intervals. Another straightforward way to have the UGP among the set of signature waveforms is to construct the signature waveforms based on the WBE sequences. In this manner, the UGP of the resulting signature set will be inherited from WBE sequence set. This construction of signature waveforms is exactly the same as the one considered in Chapter 3 and is described in the next section.

4.4.2 Signature Waveforms Constructed from WBE Sequences

As shown in Section 3.2, the maximum SIR at the output of each MMSE receiver (or correlation receiver) is given by (3.7). On the other hand, the TSC and TMSE assume the following expressions:

$$\text{TSC} = \frac{K^2}{N} \tag{4.48}$$

and

$$\text{TMSE} = KP\left(1 - \frac{\gamma}{\gamma(K/N)+1}\right). \tag{4.49}$$

It follows from the above two equations that it is necessary to maximize the dimension N of the signature space to minimize TSC or TMSE. Based on the property of WBE sequences, the maximum values of N, called $N_{\max}$, have been determined in (3.18) and (3.21) of Chapter 3 for FOBE and RMS bandwidth criteria respectively.

Obviously, the price paid for inheriting the UGP from WBE sequences of the suboptimal signature waveforms is the increase in TSC (or TMSE). In other words, the TSC (or TMSE) of WBE sequence sets is always larger than the TSC (or TMSE) of the optimal signature waveforms found previously. This is illustrated in Figs. 4.11 and 4.12 for the TSC in S-CDMA systems under RMS bandwidth constraint and with $K = 16$ and $K = 32$ users respectively. In each of these two figures, both the absolute values and the ratio of the TSCs achieved by the proposed signature waveforms and the signature waveforms constructed from WBE sequences are shown. Note also that the absolute values of TSCs are plotted using a log scale. The TSC achieved by the suboptimal signature waveforms in these figures can be determined from (3.18) and (4.48). They are given by

$$\text{TSC} = \frac{K^2}{\left\lfloor\left(\sqrt{1+48(2WT)^2}-3\right)/4\right\rfloor}. \tag{4.50}$$

As can be seen from Figs. 4.11 and 4.12, on the average, there is approximately 10% of TSC (i.e., total multiple access interference) that can be reduced by using the optimal signature waveforms. This reduction of multiple access interference provides a significant improvement of bit error rate (BER) as shown in Figs. 4.13 and 4.14 for S-CDMA systems with $K = 32$ users and with two different values of RMS bandwidth ($WT = 0.8$ and $WT = 0.9$). The error probabilities plotted in these figures are calculated based on the Gaussian approximation (equation (2.28)) and

they are also averaged over all users. Also shown in Figs. 4.13 and 4.14 are the performances of TMSE-minimized signature waveforms, i.e., the signature waveforms designed for MMSE receivers. Recall that the WBE sequences also minimize the TMSE. The improvement in BER is much larger for the MMSE receiver than for the correlation receiver and this is due to the more complicated structure of the MMSE receivers. Furthermore, it can be observed from Figs. 4.13 and 4.14 that the improvement in BER provided by the proposed signature waveforms decreases as the available bandwidth increases. If the available bandwidth is increased enough to afford orthogonal signature waveforms, then the performances of WBE, TSC-minimized and TMSE-minimized signature waveforms are all the same and equal to that of the single-user system.

Figures 4.15 and 4.16 show the improvement in BER when using the proposed signature waveforms for the case of FOBE bandwidth constraint. The bandwidth specifications used in these two figures are $c = 10.0$ (or $2WT = 6.37$) and $\eta = 0.1$. The error probability curves in Fig. 4.15 are obtained using both the exact formula and the Gaussian approximation of (2.27) and (2.28), respectively. On the other hand, only the exact formula is used for Fig. 4.16. In both Figs. 4.15 and 4.16 the BERs are averaged over all users. The inferiority of the WBE signature waveforms is clear from Figs. 4.15 and 4.16 and can be explained as follows. Using the Gaussian approximation (2.28), the probability of error when using the WBE sequences equals to $P_{\mathrm{e}} = Q\left(\sqrt{\mathrm{SIR}_{\max}}\right) = Q\left(\sqrt{\frac{\gamma}{\gamma(\frac{K}{N}-1)+1}}\right)$. When the signal-to-noise ratio γ is large, one can approximate $P_{\mathrm{e}} \simeq Q\left(\sqrt{\frac{N}{K-N}}\right)$. For the system under consideration, there can be up to $N_{\max} = 6$ orthogonal users, whose performance achieves the performance of a single-user system. However, adding one more user to the system ($K = 7$) causes $P_{\mathrm{e}} \simeq Q(\sqrt{6}) = 7.2 \times 10^{-3}$ and adding two users makes $P_{\mathrm{e}} \simeq Q(\sqrt{3}) = 4.16 \times 10^{-2}$. On the other hand, the TSCs of the optimal signature waveforms corresponding to seven and eight users are 7.0149 and 8.9122 respectively. This means that the

optimal signature waveforms are very close to orthogonal to maintain the good BER performance.

Recall that the SIR performance of the TSC-minimized or TMSE-minimized signature waveforms is not uniform over all users, except when the number of users is the size of a Hadamard matrix. Thought in all the previous discussions the BER is *averaged* over all the users, here we would like to point out that the user-specific BER performance of the proposed signature waveforms still outperforms the signature waveforms constructed from WBE sequences in most of the cases. As an example, Table 4.3 lists the SIRs at the outputs of both MF and MMSE receivers for different families of signature waveforms at $\gamma = 14$dB. The system under consideration has $c = 10$ and $\eta = 0.1$ (which means there can be up to $N_{\max} = 6$ orthogonal users). When using the MF receiver, there are seven users in the system, whereas there are eight users in the system using MMSE receiver. To compute the SIRs for either MF or MMSE receiver, the matrix $\mathbf{V}$ is generated using the T-transform algorithm given in [17] in order to realize the correlation matrix $\mathbf{R}$. Note that since a Hadamard matrix of size eight exists, the correlation matrix $\mathbf{R}$ in this case can also be chosen as a normalized Hadamard matrix so that the SIRs for all users are equal and individually maximized.

As can be seen from Table 4.3, when a normalized Hadamard matrix $\mathbf{H}$ is not available (or not used) for $\mathbf{R}$, the SIRs are not uniform. Nevertheless, the difference among SIRs is quite small and the worst SIR performance is still much better than the uniform SIR performance of the WBE signature waveforms. This is further illustrated in Figs. 4.17 and 4.18, where the performance of WBE signature waveforms is compared with the worst, the best and the average performances of the TSC-minimized and TMSE-minimized signature waveforms respectively. In computing the error probability for each user, the exact formula in [47] has been used.

Table 4.3: SIR_k (in dB): CDMA systems with $c = 10.0$, $\eta = 0.1$ and $\gamma = 14\mathrm{d}B$

User Index (k)	MF Receiver ($K = 7$)		MMSE Receiver ($K = 8$)		
				Optimal	
	WBE	Optimal	WBE	$\mathbf{V} \neq \mathbf{H}$	$\mathbf{V} = \mathbf{H}$
1	6.85	13.71	4.28	12.80	13.19
2	6.85	13.71	4.28	12.80	13.19
3	6.85	13.71	4.28	13.14	13.19
4	6.85	13.71	4.28	13.25	13.19
5	6.85	13.92	4.28	13.84	13.19
6	6.85	13.96	4.28	13.81	13.19
7	6.85	13.71	4.28	13.17	13.19
8	–	–	4.28	12.80	13.19

4.5 Chapter Summary

Bandwidth constrained signature waveforms that minimize the multiple access interference have been obtained for S-CDMA systems. Both the RMS or FOBE bandwidth constraints were considered. For the correlation receivers, closed-form expression for the optimal signature waveforms exists, whereas for the MMSE receivers a set of two non-linear equations (with constraints) can be numerically solved to realize the optimal signature waveforms. The performance of the optimal signature waveforms has been compared to that of the suboptimal ones constructed from WBE sequences. It general, it has been demonstrated that the reduction in multiple access interference achieved by the optimal signature waveforms can significantly improve the BER performance in S-CDMA systems.

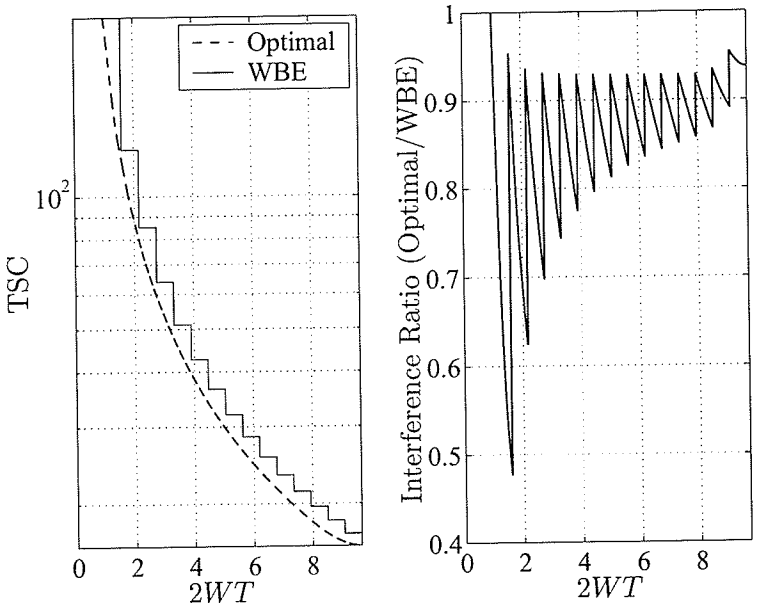

Figure 4.11: TSC achieved by the optimal signature waveforms and signature waveforms constructed from WBE sequences: $K = 16$, RMS bandwidth constraint.

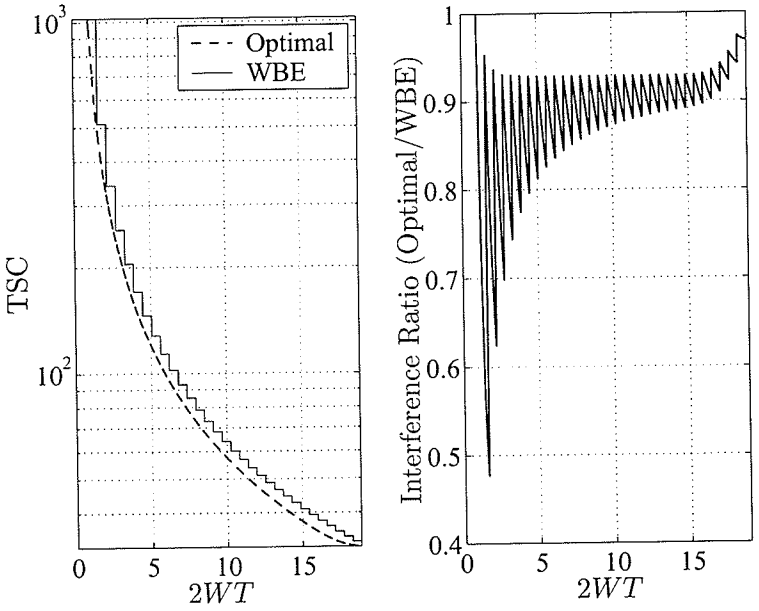

Figure 4.12: TSC achieved by the optimal signature waveforms and signature waveforms constructed from WBE sequences: $K = 32$, RMS bandwidth constraint.

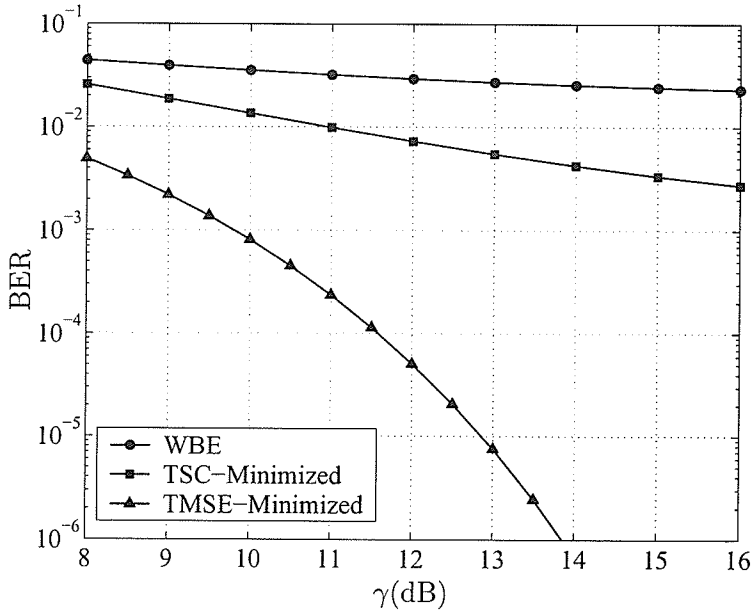

Figure 4.13: Error performance of WBE, TSC-minimized and TMSE-minimized signature waveforms in a S-CDMA system: $K = 32$ with RMS bandwidth of $WT = 8.0$.

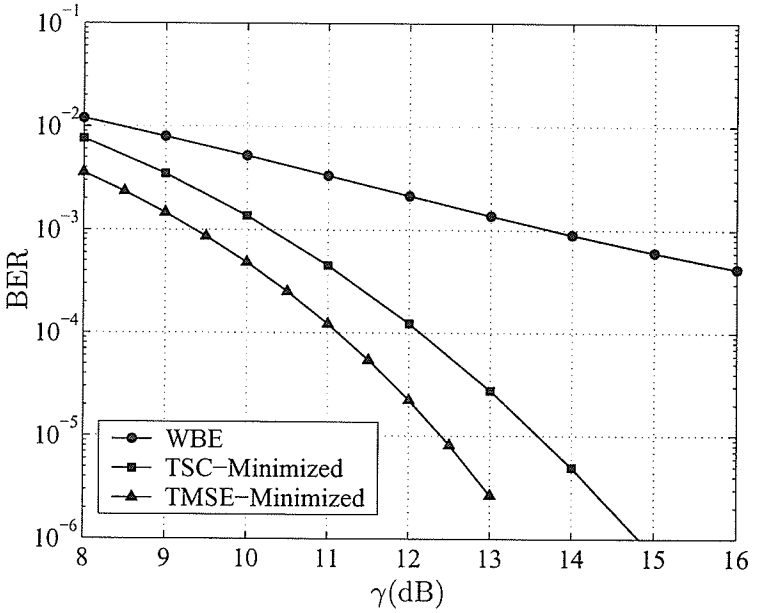

Figure 4.14: Error performance of WBE, TSC-minimized and TMSE-minimized signature waveforms in a S-CDMA system: $K = 32$ with RMS bandwidth of $WT = 9.0$.

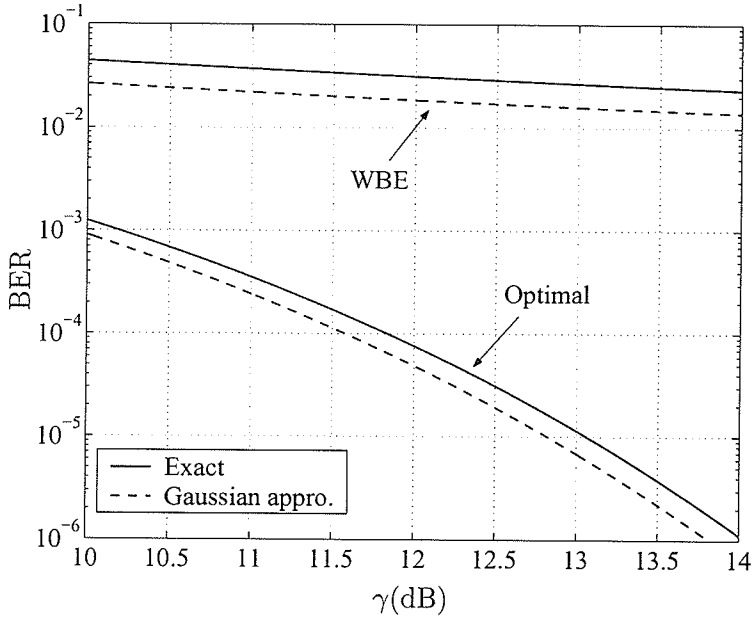

Figure 4.15: Error performances of WBE and TSC-minimized signature waveforms in a CDMA system: $c = 10.0$, $\eta = 0.1$ and $K = 7$.

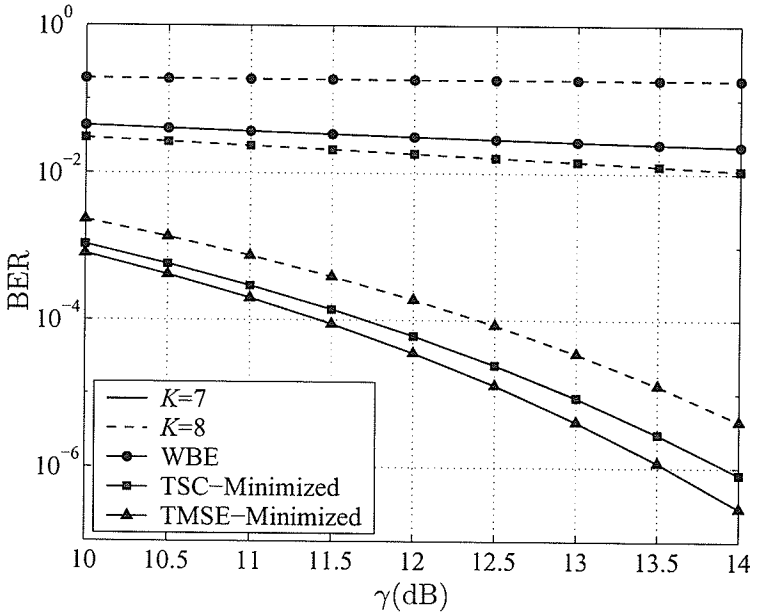

Figure 4.16: Error performances of WBE, TSC-minimized and TMSE-minimized signature waveforms in CDMA systems: $c = 10.0$, $\eta = 0.1$ and $K = 7$ or $K = 8$.

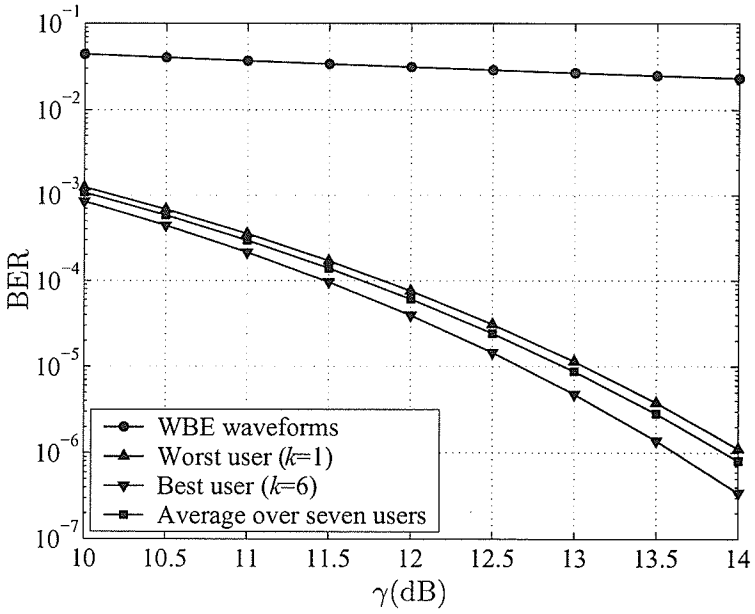

Figure 4.17: Worst-user error performance with TSC-minimized signature waveforms in a CDMA system: $c = 10.0$, $\eta = 0.1$ and $K = 7$.

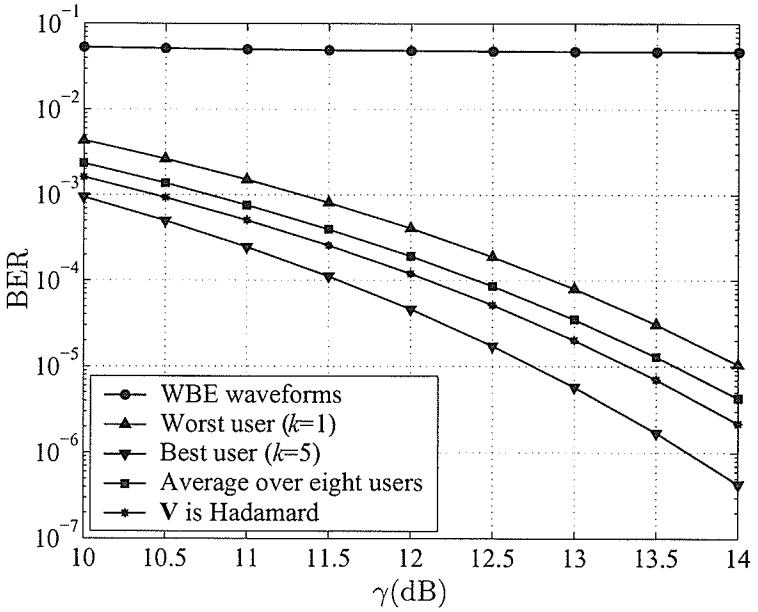

Figure 4.18: Worst-user error performance with TMSE-minimized signature waveforms in a CDMA system: $c = 10.0$, $\eta = 0.1$ and $K = 8$.

Chapter 5

Simplified Receiver in Walsh Signal Space

It was shown in Chapters 3 and 4 that when the bandwidth constraint is the FOBE bandwidth (which is typically a more practical measure than the RMS bandwidth), the optimal signature waveforms are constructed as linear combinations of the normalized, time-truncated and shifted prolate spheroidal wave functions (PSWFs). The block diagram of the receiver in Fig. 2.1 implies that, in order to obtain the sufficient statistic in the linear receiver, the signature waveforms need to be generated at the receiver. However when the signature waveforms are synthesized from the PSWFs, this is obviously not a simple task, taking into account the complicated nature of these functions.

This chapter is concerned with the practical implementation of the linear receiver when such optimal signature waveforms are used. In particular, the same approach as in [55, 56] of using a Walsh signal space to realize the simplified receiver is studied. As pointed out in [55], there are two main advantages when using the Walsh signal space:

(i) The Walsh functions form an orthogonal, complete basis for the L_2 signal space, a space that includes all the signature waveforms of interest. This means that

by increasing the dimensionality of the Walsh signal space, the receiver performance can approach the optimal performance (when no approximation for the receiver is made).

(ii) Since the approximated (projected) signature waveforms in the Walsh signal space are staircase functions, the bank of the correlators (or matched filters) in Fig. 2.1 can be replaced by an ordinary integrate-and-dump filter, followed by a sampler which samples at a higher rate. The advantage of the latter operation is that it is easier to implement in hardware.

It should be noted that the second advantage discussed above is considerably more important when the whole vector of sufficient statistics $\mathbf{y}$ (or most of its elements) is required at the receiver, for example as in an MMSE receiver.

5.1 Structure of the Simplified Receiver

Let $\mathbf{w}(t) = [w_1(t), w_2(t), \ldots, w_L(t)]^\top$, $0 \leq t \leq T$, be the basis vector for a Walsh signal space of dimension $L = 2^D$. Write the index k ($k \neq 0$) as follows [55]

$$k = \sum_{d=0}^{D-1} k_d 2^d \tag{5.1}$$

where $k_d \in \{0, 1\}$ and D is the smallest integer such that $k_{D-1} \neq 0$. Then the Walsh functions can be expressed in terms of coefficients k_ds as

$$w_k(t) = \begin{cases} \frac{1}{\sqrt{T}} \prod_{d=0}^{D-1} \operatorname{sgn}\left(\cos\left[k_d 2^d \frac{\pi t}{T}\right]\right), & 0 \leq t < T \\ 0, & \text{otherwise} \end{cases} \tag{5.2}$$

where $\operatorname{sgn}(x) = 1$ if $x \geq 0$ and $\operatorname{sgn}(x) = -1$ if $x < 0$. As an example, the first eight Walsh functions are plotted in Fig. 5.1 for $T = 1.0$.

To obtain the simplified receivers, consider the approximation of the optimal signature waveforms using the first L orthonormal Walsh functions as follows:

$$\widehat{\mathbf{s}}(t) = [\widehat{s}_1(t), \widehat{s}_2(t), \ldots, \widehat{s}_K(t)]^\top = \mathbf{A}\mathbf{w}(t) \tag{5.3}$$

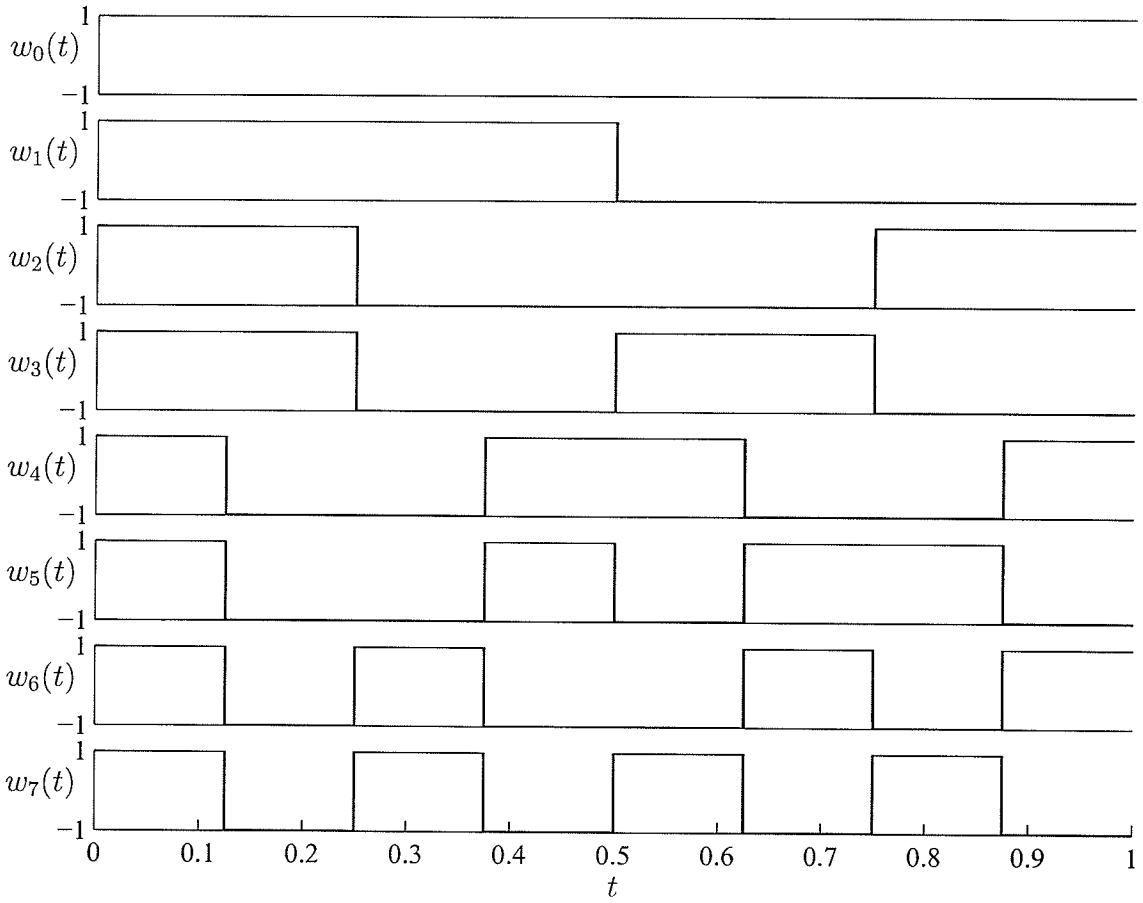

Figure 5.1: The first eight Walsh functions ($T = 1.0$).

where $\widehat{\mathbf{s}}(t)$ is the approximation of the optimal signature waveform vector $\mathbf{s}(t) = [s_1(t), \ldots, s_K(t)]^\top$ and the $K \times L$ coefficient matrix $\mathbf{A}$ is given by

$$\mathbf{A} = \int_0^T \mathbf{s}(t)\mathbf{w}^\top(t)\mathrm{d}t. \tag{5.4}$$

Recall from the results established in Chapters 3 and 4 that the optimal signature waveform vector under FOBE bandwidth constraint can be commonly expressed as

$$\mathbf{s}(t) = \mathbf{S}^\top \mathbf{\Psi}(t) \tag{5.5}$$

where $\mathbf{S}$ is an $N \times K$ signature matrix and $\mathbf{\Psi}(t)$ contains the first K shifted, normalized and time-truncated PSWFs, i.e., $\mathbf{\Psi}(t) = \left[\widehat{\varphi}_0(t), \widehat{\varphi}_1(t), \ldots, \widehat{\varphi}_{K-1}(t)\right]^\top$. For the signature waveforms obtained in Chapter 3, $N < K$ and the columns of matrix $\mathbf{S}$ are the WBE sequences. On the other hand, for the optimal signature waveforms in Chapter 4 one has $N = K$ and the signature matrix $\mathbf{S}$ is given by Proposition 4.5.

It follows from (5.3), (5.4) and (5.5) that

$$\widehat{\mathbf{s}}(t) = \mathbf{S}^\top \left(\int_0^T \mathbf{\Psi}(t)\mathbf{w}^\top(t)\mathrm{d}t \right) \mathbf{w}(t) = \mathbf{S}^\top \mathbf{B}\mathbf{w}(t) = \mathbf{S}^\top \widehat{\mathbf{\Psi}}(t). \tag{5.6}$$

Thus the approximation of optimal signature waveforms is essentially the approximation of the first N shifted, normalized and time-truncated PSWFs. Given L, the $N \times L$ matrix $\mathbf{B} = \int_0^T \mathbf{\Psi}(t)\mathbf{w}^\top(t)\mathrm{d}t$ can be pre-computed and stored in the memory at the receiver. Note also that $\mathbf{A} = \mathbf{S}^\top \mathbf{B}$.

Having obtained the approximated signature waveforms at the receiver, the sufficient statistics at the output of the bank of matched filters (filter k is matched to $\widehat{s}_k(t)$) in Fig. 2.1 can be calculated as follows:

$$\widehat{\mathbf{y}} = \int_0^T y(t)\widehat{\mathbf{s}}(t)\mathrm{d}t = \mathbf{A} \int_0^T y(t)\mathbf{w}(t)\mathrm{d}t. \tag{5.7}$$

Since at any point in the interval $[0, T]$ the Walsh functions receive only one of the two values $\pm 1/\sqrt{T}$, the integration in the above equation should be very simple. Let

the interval $[0, T]$ be partitioned into L sub-intervals and index these sub-intervals by $l = 0, 1, \ldots, L-1$. From (5.2) it can be seen that the kth Walsh function $w_k(t)$ is constant in the lth sub-interval $[lT/L, (l+1)T/L)$ and its value is given by

$$w_k(l) = \frac{1}{\sqrt{T}} \prod_{d=0}^{D-1} \operatorname{sgn}\left(\cos\left[k_d 2^d \pi \left(l + \frac{1}{2}\right)\frac{L}{T}\right]\right), \quad k, l = 0, 1, \ldots, L-1. \tag{5.8}$$

Define an $L \times L$ matrix $\mathbf{H}$ such that $\mathbf{H}_{kl} = w_{k-1}(l-1)$ and let $\mathbf{h}_k^\top$ be its kth row. Then it is not hard to see that

$$\int_0^T y(t) w_k(t) \mathrm{d}t = \sum_{l=0}^{L-1} w_k(l) \int_{lT/L}^{(l+1)T/L} y(t)\mathrm{d}t = \mathbf{h}_k^\top \widetilde{\mathbf{y}}, \quad k = 1, 2, \ldots, L \tag{5.9}$$

where $\widetilde{\mathbf{y}} = \left[\int_0^{T/L} y(t)\mathrm{d}t, \int_{T/L}^{2T/L} y(t)\mathrm{d}t, \ldots, \int_{(L-1)T/L}^{T} y(t)dt\right]^\top$. It follows from (5.7) and (5.9) that the approximated sufficient statistic can be produced from $\widetilde{\mathbf{y}}$ as follows

$$\widehat{\mathbf{y}} = \mathbf{A}\mathbf{H}\widetilde{\mathbf{y}} = \mathbf{S}^\top \mathbf{B}\mathbf{H}\widetilde{\mathbf{y}}. \tag{5.10}$$

It is important to realize that $\widetilde{\mathbf{y}}$ can be generated from the received signal $y(t)$ in a very simple manner. It requires only one integrate-and-dump filter followed by a sampler which samples the output at L time instants $t = (l+1)T/L$, $l = 0, 1, \ldots, L-1$. This observation allows one to replace the linear receiver in Fig. 2.1 by a simpler structure which is shown in Fig. 5.2. We would like to point out here that the higher sampling rate required in the simplified receivers should not be a major implementation problem. This is because the original sampling rate (in the receiver of Fig. 2.1) is at the symbol rate, which is typically quite low[1].

Technically, the approximated sufficient statistic $\widehat{\mathbf{y}}$ generated in (5.10) can be made as close to the sufficient statistic $\mathbf{y}$ in (2.3) as desired by increasing the dimensionality L of the Walsh signal space. Thus it may be appropriate to refer to $\widehat{\mathbf{y}}$ as the

[1]In many current CDMA systems, the sampling rate is equal to the "chip" rate, which is much higher than the symbol rate.

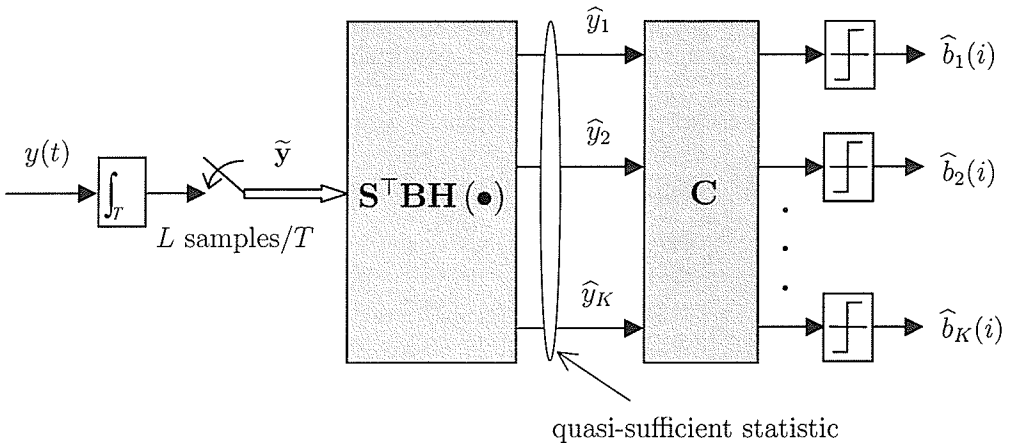

Figure 5.2: A simplified linear receiver in Walsh signal space.

quasi-sufficient statistic. However, since the optimal signature waveforms are continuous functions in $(0, T)$, the Walsh signal space has to have an infinite dimension to truly represent all the signature waveforms. But this also implies an infinite number of samples in one symbol duration T, which is impossible in practice. Therefore, although it can be approached as closely as desired by increasing L, the sufficient statistic can never be produced by the receiver structure in Fig. 5.2. Obviously, an important question is how small L can be so that near-optimal performance can be achieved by the simplified receiver in Fig. 5.2. This is investigated in the next section.

5.2 Error Performance of the Simplified Receiver

In this section, the error performances of both simplified correlation and MMSE receivers in the Walsh signal space are evaluated under various system configurations. In particular, the performance of the first user in the system, who is considered to be a typical user is evaluated. The calculation of error probability is based on the exact formula in (2.27). It should be noted that, for the simplified receiver, the correlation matrix in (2.27) is given by $\widetilde{\mathbf{R}} = \int_0^T \widehat{\mathbf{s}}(t)\mathbf{s}^\top(t)\mathrm{d}t$.

Figs. 5.3 and 5.4 present the error performances of the simplified correlation and MMSE receivers for a S-CDMA system loaded with six users and having a bandwidth specification of $c = 10.0$ and $\eta = 0.01$, respectively. Shown in each of these figures are the performance curves of the simplified receiver in Walsh signal spaces of different dimensionalities. Also shown in each of these figures is the optimal performance curve, i.e., the performance of the receiver in Fig. 2.1 when the true optimal signature waveforms are available at the receivers. Similar error performances are presented in Figs. 5.5 to 5.8 but for systems with bandwidth specification of $c = 10.0$, $\eta = 0.1$ and loaded with seven or eight users. Note that there can be up to five orthogonal users in a S-CDMA system with $c = 10.0$ and $\eta = 0.01$, whereas increasing η to 0.1 increases the number of orthogonal users to six.

It is clear from these figures that the optimal performance can be closely approached by increasing the dimensionality of the Walsh signal space. It also appears from these figures that to achieve a near-optimal performance, the dimension of the Walsh signal space needs to be increased as the number of users in the system increases. For example Figs. 5.3, 5.5, 5.7 show that $L = 16$ is sufficient to realize a simplified correlation receiver if there are six users in the system, but it requires $L = 32$ for the systems loaded with seven or eight users. Moreover, compared to the simplified correlation receiver, the simplified MMSE receiver can be realized with a smaller Walsh signal space in order to achieve a near-optimal performance. As an example, Figs. 5.6 and 5.5 show that it requires $L = 16$ Walsh functions to approach the optimal performance for the MMSE receivers, but $L = 32$ functions are needed for the correlation receivers. Finally, the same observations hold for systems with different FOBE bandwidth specifications and different number of users.

5.3 Chapter Summary

A simplified linear (multiuser) receiver in Walsh signal space has been developed for S-CDMA systems. The need for this receiver structure arises from the fact that the optimal signature waveforms under FOBE bandwidth constraint are generated from the complicated prolate spheroidal wave functions. Investigation of the error performances of the simplified receivers show that the optimal performance can be closely approached by increasing the dimensionality of the Walsh signal space. In general, only a relatively small number of Walsh functions is required for the simplified receiver to achieve a near-optimal performance.

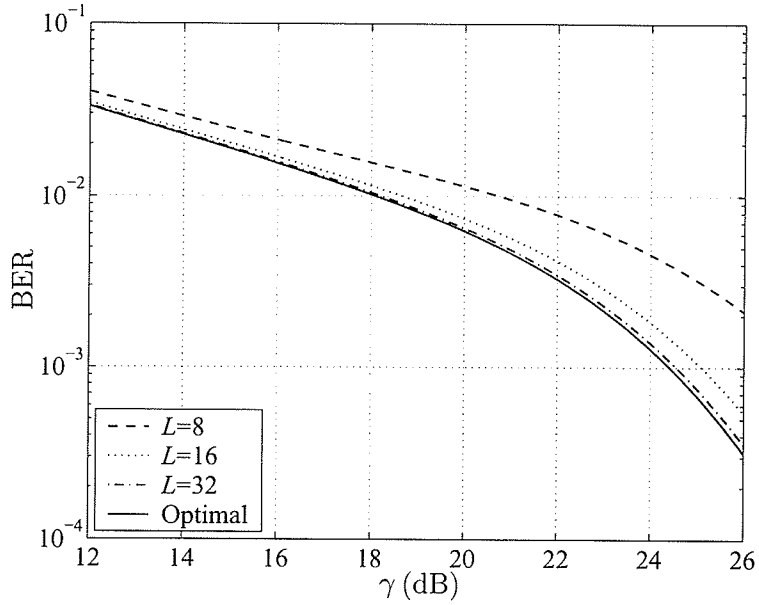

Figure 5.3: Error performance of the simplified correlation receiver in a CDMA system: $c = 10.0$, $\eta = 0.01$ and $K = 6$.

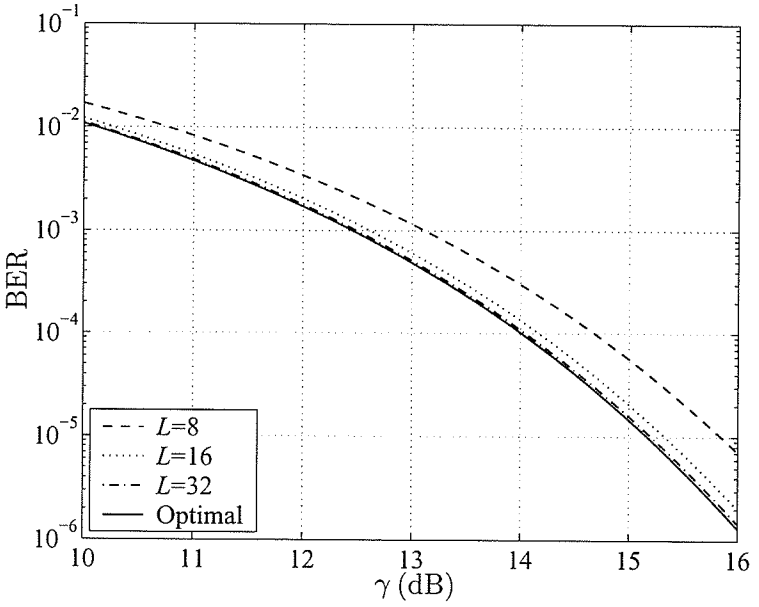

Figure 5.4: Error performance of the simplified MMSE receiver in a CDMA system: $c = 10.0$, $\eta = 0.01$ and $K = 6$.

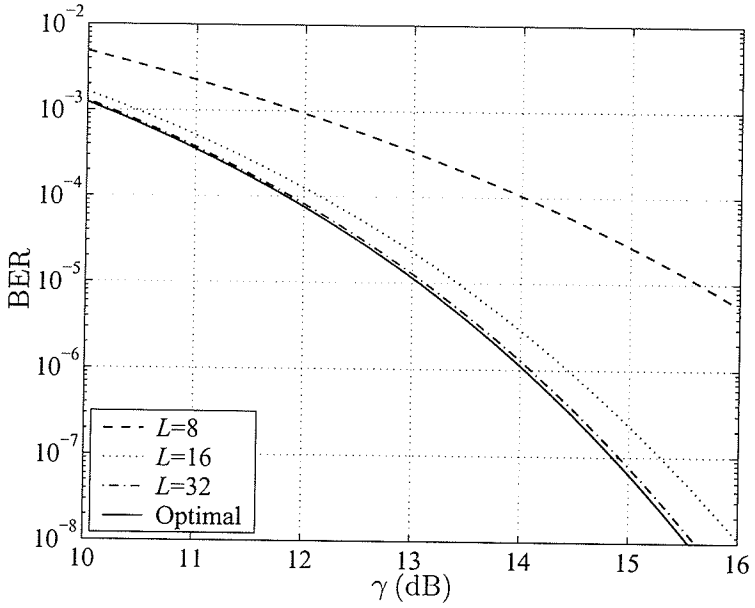

Figure 5.5: Error performance of the simplified correlation receiver in a CDMA system: $c = 10.0$, $\eta = 0.1$ and $K = 7$.

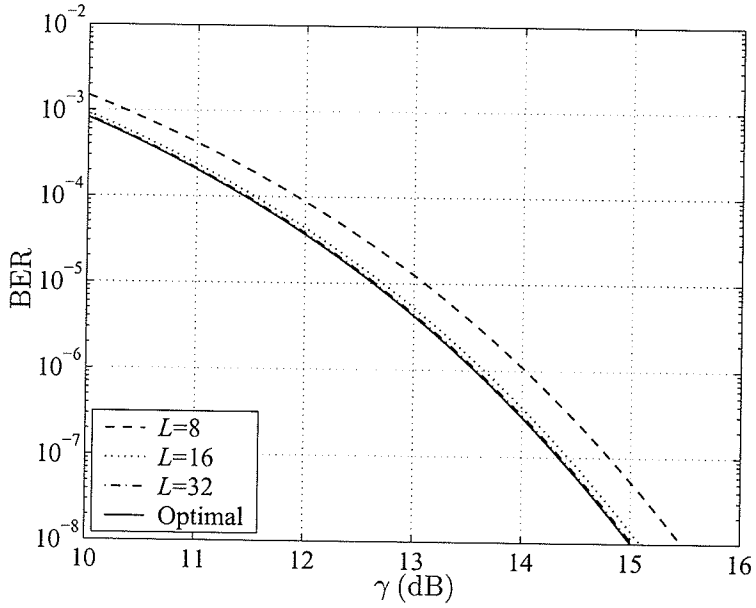

Figure 5.6: Error performance of the simplified MMSE receiver in a CDMA system: $c = 10.0$, $\eta = 0.1$ and $K = 7$.

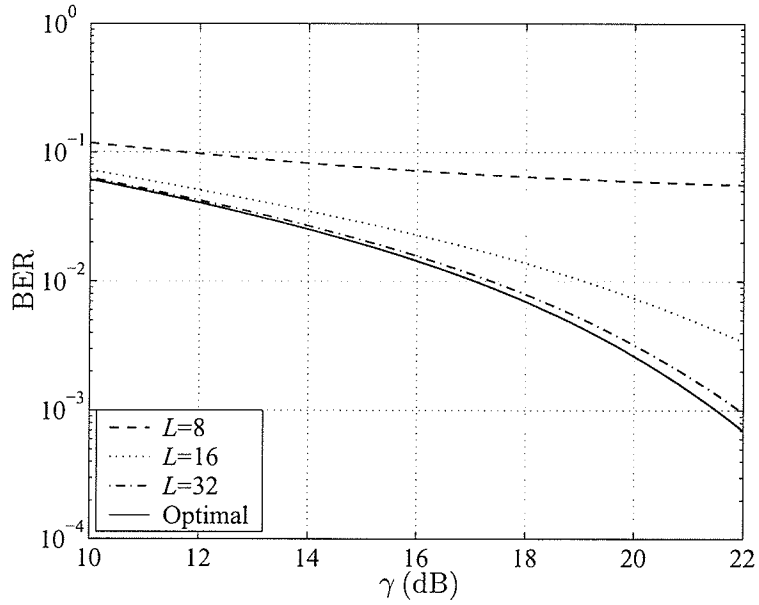

Figure 5.7: Error performance of the simplified correlation receiver in a CDMA system: $c = 10.0$, $\eta = 0.1$ and $K = 8$.

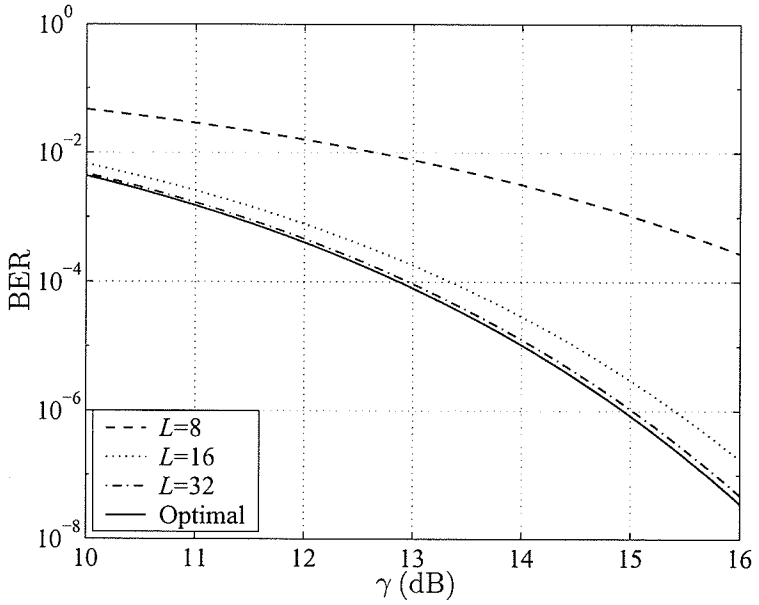

Figure 5.8: Error performance of the simplified MMSE receiver in a CDMA system: $c = 10.0$, $\eta = 0.1$ and $K = 8$.

Chapter 6

Signature and Chip Waveform Design for A-CDMA Systems

As discussed before, signature waveform design for CDMA systems, especially for *asynchronous* systems, has received little attention. This chapter is a contribution to this important area. Specifically, signature waveform design is considered for asynchronous CDMA systems equipped with a correlation receiver. The correlation receiver is preferred to other multiuser receivers because the complexity of multiuser detection is usually prohibitive in asynchronous systems with a large number of users and a correlation receiver is still the only practical solution.

As in the case of synchronous CDMA systems, a common and important performance measure for the correlation receiver is the signal-to-interference ratio (SIR). In order to maximize the SIR, it is necessary to minimize the variance of MAI at the output of each correlation receiver. Ideally, the signature waveforms should be designed so that the MAI is zero. However this is likely impossible due to the limitation of the transmission bandwidth as well as the asynchronous nature of the transmitted signals. Nevertheless, for a given transmission bandwidth, the set of signature waveforms that produces a minimum MAI is desired. Finding such signature waveforms is precisely one goal of this chapter. To quantify the transmission bandwidth, both the

RMS and FOBE bandwidth criteria can be used. If the FOBE bandwidth is considered, then the Fourier transforms of the optimal signature waveforms can be found through a series expansion in prolate spheroidal wave functions, which is similar to the approach in [32]. On the other hand, if the RMS bandwidth is used, then the optimal signature waveforms can be found through a series expansion in sinusoids.

The signature waveforms obtained as described above essentially may admit any shape as long as they are limited to the symbol duration and have a specified energy. There is, however, a popular form of CDMA known as direct-sequence CDMA (DS-CDMA) where more structure is imposed on the signature waveforms. In particular, each signature waveform is constructed by modulating a given chip waveform with the corresponding binary *signature sequence*. Clearly with these signature waveforms, the SIR at the output of each correlation receiver depends on both the signature sequences and the shape of the chip waveform employed. To maximize the SIR in this case, one needs to jointly optimize the signature sequences and the chip waveform. Recently, *random* signature sequences have been widely used to analyze the performance of DS-CDMA systems [32, 33, 34, 35, 57]. Some reasons for using random signature sequences are as follows [34]. First, random signature sequences are often used in an attempt to match certain characteristics of extremely complex signature sequences with a very long period. Second, random signature sequence models may serve as substitutes for deterministic models when there is little or no information about the structure of the signature sequences to be used. Finally, for a system with a large number of users and very long signature sequences, the use of random signature sequences remains the only hope to obtain computable closed-form expressions for the system analysis. With random signature sequences, the average SIR depends only on the chip pulse shape.

As mentioned in Chapter 1 the chip pulse shape can be either time-limited or band-limited. With band-limited chip waveforms, the signature waveforms are not

time-limited to the symbol interval T. This means that the CDMA systems models introduced in Chapter 2 need to be re-formulated. The designs of band-limited chip waveforms to minimize the MAI in A-CDMA systems were studied in [57, 58, 59, 60], whereas the design of time-limited chip pulse appeared in [32]. In this chapter only the design of time-limited chip waveforms are considered.

It is important to note that when a time-limited single chip waveform is used and when the delays between the desired user and the interfering users are exactly multiples of the chip duration, the chip pulse shape has no effect on the MAI. In such situations the MAI depends only on the cross correlations of the signature sequences, which can be large if the signature sequences are chosen randomly (or not well designed, for deterministic signature sequences). Instead of using a single chip waveform, suppose that two *orthogonal* chip pulses are alternatively employed for the construction of signature waveforms. Now if the delays of the interfering users are exactly odd multiples of the chip duration, the signals from interfering users will be orthogonal to that of the desired user (which means that the MAI is zero), no matter what are the signature sequences (random or deterministic). This discussion is graphically illustrated in Fig. 6.1 where the signature waveform of the kth user (the desired user) and the signature waveform of the jth user (the interfering user) delayed by one chip duration (T_c) are shown. In this particular example, the single chip waveform is a half-sinusoid and the double orthogonal chip waveforms are the half-sinusoid and half-cosine. Furthermore, for convenience, the maximum absolute value of each chip waveform is normalized to be one.

Motivated by the above observation, in this chapter we also introduce the use of multiple chip waveforms as a means of reducing MAI in asynchronous DS-CDMA systems. Again, the series expansion method can be used to obtain the optimal chip waveforms. Numerical results show that a significant gain can be achieved by using multiple chip waveforms instead of a single chip waveform.

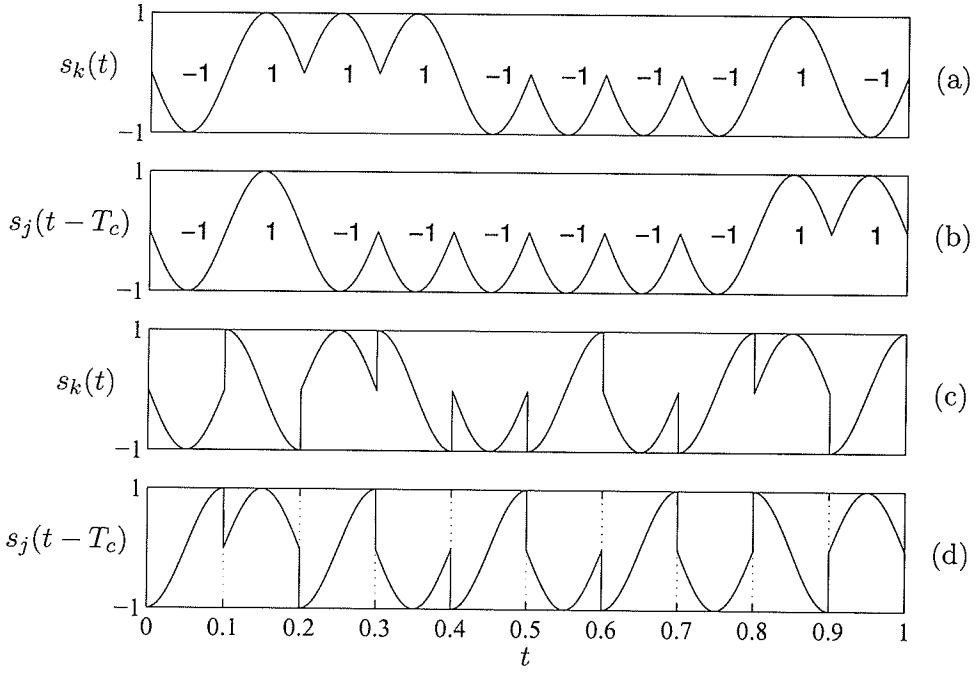

Figure 6.1: Signature waveforms constructed from a single chip waveform (figures (a) and (b)) and from double orthogonal chip waveforms (figures (c) and (d)). $T = 1.0$ and $T/T_c = 10$.

The chapter is organized as follows. In Section 6.1, the SIR at the output of the correlation receiver is evaluated for both the asynchronous CDMA system and the DS-CDMA system using random signature sequences and multiple chip waveforms. In each case, the SIR is expressed in terms of the Fourier transforms of the signature waveforms or the chip waveforms respectively. These expressions suggest a method to obtain the signature and chip waveforms via a series expansion. Bandwidth constraint and problems under consideration are discussed in Section 6.2. The series expansion method is used to obtain optimal signature waveforms and multiple chip waveforms in Section 6.3 and Section 6.4 respectively. Section 6.5 investigates the advantage of multiple chip waveforms technique for some common chip waveforms. Finally, Section 6.6 summarizes the chapter.

6.1 SIR Evaluation

6.1.1 Asynchronous CDMA systems

Recall from Section 2.2 that the signal received over an A-CDMA channel is

$$y(t) = \sum_{k=1}^{K} \sum_{i=-\infty}^{\infty} \sqrt{2P} b_k(i) s_k(t - iT - \tau_k) \cos(2\pi f_c t + \varphi_k) + n(t) \tag{6.1}$$

where τ_k and φ_k are the delay and the overall phase shift of the kth user, which are modeled as uniform random variables over $[0, T]$ and $[0, 2\pi]$ respectively. The noise $n(t)$ is additive white Gaussian noise (AWGN) with a two-sided power spectral density of $N_0/2$. The output of the kth correlation receiver for the detection of $b_k(0)$ is

$$Z_k = \sqrt{P/2} b_k(0) T + \sqrt{P/2} \sum_{i=1, i\neq k}^{K} I_{k,i} + n \tag{6.2}$$

where n is a Gaussian random variable with zero mean and variance $N_0 T/4$. The random variable $I_{k,i}$ is the interference caused by the ith user and is related to the

partial cross-correlation functions between the kth and the ith signature waveforms through (2.34).

The random variables $I_{k,i}$ and n can be shown to be uncorrelated and have zero mean. Furthermore, due to the symmetry involved, it can be assumed that $b_k(0) = +1$ was transmitted, thus the SIR at the output of the kth correlation receiver is given by

$$\mathrm{SIR}_k = \frac{[E(Z_k|b_k(0)=+1)]^2}{\mathrm{var}(Z_k|b_k(0)=+1)} = \left[\left(\frac{2E_b}{N_0}\right)^{-1} + \frac{1}{T^2}\sum_{i=1,i\neq k}^{K}\mathrm{var}(I_{k,i})\right]^{-1} \tag{6.3}$$

where $E_b = PT$ is the energy per symbol. Note that $I_{k,i}$ depends on the random variables $\mathbf{b}_i = [b_i(-1), b_i(0)]$, φ_i and τ_i. As usual, these random variables are assumed to be mutually statistically independent, hence the variance of $I_{k,i}$ can be computed as follows:

$$\begin{aligned}
\mathrm{var}(I_{k,i}) &= E_{\tau_i}\left\{E_{\varphi_i}\left(E_{\mathbf{b}_i}(I_{k,i}^2|\mathbf{b}_i,\varphi_i,\tau_i)\right)\right\} \\
&= \frac{1}{T}\int_0^T\left[\frac{1}{2\pi}\int_0^{2\pi}\left(\frac{1}{4}\sum_{\mathbf{b}_i\in\{+1,-1\}^2} I_{k,i}^2\right)\mathrm{d}\varphi_i\right]\mathrm{d}\tau_i \\
&= \frac{1}{2T}\int_0^T\left[R_{k,i}^2(\tau)+\widehat{R}_{k,i}^2(\tau)\right]\mathrm{d}\tau.
\end{aligned} \tag{6.4}$$

Though (6.4) is useful to evaluate the variance of MAI for a given set of signature waveforms, it is not convenient to use when finding the optimal signature waveforms. In what follows, it is shown that $\mathrm{var}(I_{k,i})$ can be written in terms of the Fourier transforms of $s_k(t)$ and $s_i(t)$. As will be seen later, the new expression for $\mathrm{var}(I_{k,i})$ is very helpful when formulating and solving the optimization problem considered in this chapter.

Since $s_k(t)$ and $s_i(t)$ are time limited to $[0,T]$, it follows that $R_{k,i}(\tau) = \widehat{R}_{i,k}(T-\tau)$ and $\int_0^T R_{k,i}^2(\tau)\mathrm{d}\tau = \int_0^T \widehat{R}_{i,k}^2(\tau)\mathrm{d}\tau$. Therefore the integral in (6.4) becomes

$$\int_0^T\left[R_{k,i}^2(\tau)+\widehat{R}_{k,i}^2(\tau)\right]\mathrm{d}\tau = \int_0^T\left[R_{k,i}^2(\tau)+R_{i,k}^2(\tau)\right]\mathrm{d}\tau \tag{6.5}$$

Define $v_{k,i}(\tau) = \int_{-\infty}^{\infty} s_k(t)s_i(t+T-\tau)\mathrm{d}t$ and let $V_{k,i}(f) = \mathcal{F}\{v_{k,i}(\tau)\}$, where $\mathcal{F}\{\cdot\}$ denotes the Fourier transform. Since $v_{k,i}(\tau) = s_k(\tau) \circledast \widetilde{s}_i(-\tau)$, where $\circledast$ denotes the convolution operation and $\widetilde{s}_i(\tau) = s_i(\tau+T)$, then $V_{k,i}(f) = S_k(f)S_i^*(f)\mathrm{e}^{-j2\pi fT}$ and $|V_{k,i}(f)|^2 = |S_k(f)|^2|S_i(f)|^2$. Let $f(\tau)=v_{k,i}^2(\tau) + v_{i,k}^2(\tau)$, then $f(\tau)$ is time-limited to $[0, 2T]$. Furthermore, it can be shown that $f(\tau) = f(2T-\tau)$, i.e., $f(\tau)$ is an even function about T. Since $f(\tau) = R_{k,i}^2(\tau) + R_{i,k}^2(\tau)$ for $0 \le \tau \le T$, the right hand side of (6.5) can be written as

$$\begin{aligned}\int_0^T \left[R_{k,i}^2(\tau) + R_{i,k}^2(\tau)\right] \mathrm{d}\tau &= \frac{1}{2}\int_0^{2T} \left[v_{k,i}^2(\tau) + v_{i,k}^2(\tau)\right] \mathrm{d}\tau \\ &= \frac{1}{2}\int_{-\infty}^{\infty} \left(|V_{k,i}(f)|^2 + |V_{i,k}(f)|^2\right) \mathrm{d}f \\ &= \int_{-\infty}^{\infty} |S_k(f)|^2|S_i(f)|^2\mathrm{d}f. \end{aligned} \tag{6.6}$$

Now, combining (6.4), (6.5) and (6.6) gives

$$\mathrm{var}(I_{k,i}) = \frac{1}{2T}\int_{-\infty}^{\infty} |S_k(f)|^2|S_i(f)|^2\mathrm{d}f \tag{6.7}$$

and the SIR in (6.3) becomes

$$\mathrm{SIR}_k = \left[\left(\frac{2E_b}{N_0}\right)^{-1} + \frac{1}{2T^3}\sum_{i=1,i\neq k}^{K}\int_{-\infty}^{\infty} |S_k(f)|^2|S_i(f)|^2\mathrm{d}f\right]^{-1}. \tag{6.8}$$

6.1.2 Asynchronous DS-CDMA Systems with Random Signature Sequences

In this section, the model of asynchronous DS-CDMA systems using random signature sequences and multiple chip waveforms is introduced. The SIR at the output of a correlation receiver is also obtained as a function of the number of users, the processing gain and the Fourier transforms of the multiple chip waveforms.

Let $g_1(t), g_2(t), \ldots, g_D(t)$ be D distinct chip waveforms each time-limited to $[0, T_c]$ whose energies are normalized so that

$$\int_0^{T_c} g_m^2(t)\mathrm{d}t = T_c, \qquad m = 1, 2, \ldots, D. \tag{6.9}$$

Then the signature waveform of user k is constructed as follows

$$\begin{aligned} s_k(t) &= \sum_{j=0}^{M-1} \left[s_k(Dj) g_1(t - DjT_c) + s_k(Dj+1) g_2(t-(Dj+1)T_c) \right. \\ &\quad \left. + \ldots + s_k(Dj+D-1) g_D(t-(Dj+D-1)T_c) \right] \end{aligned} \tag{6.10}$$

where $\mathbf{s}_k = [s_k(0), s_k(1), \ldots, s_k(N-1)]$ is modeled as a vector of i.i.d. random variables taking values in $\{-1, +1\}$ with equal probability. To simplify our analysis, it has been assumed in (6.10) that the processing gain $N = T/T_c$ is an integer multiple of D, i.e., $N = DM$.

To evaluate the SIR in this case, the variance of $I_{k,i}$ in (6.3) needs to be re-evaluated, taking into account the randomness of the signature sequences. That is,

$$\begin{aligned} \mathrm{var}(I_{k,i}) &= E_{\mathbf{s}_k,\mathbf{s}_i} \left\{ E_{\tau_i} \left[E_{\varphi_i} \left(E_{\mathbf{b}_i} (I_{k,i}^2 | \mathbf{s}_k, \mathbf{s}_i, \mathbf{b}_i, \varphi_i, \tau_i) \right) \right] \right\} \\ &= E_{\mathbf{s}_k,\mathbf{s}_i} \left\{ \frac{1}{2T} \int_0^T \left[R_{k,i}^2(\tau) + R_{i,k}^2(\tau) \right] \mathrm{d}\tau \right\}. \end{aligned} \tag{6.11}$$

Note that the index i of the delay τ_i in (6.11) has been removed for simplicity. Let[1] $v_k(\tau) = \int_{-\infty}^{\infty} s_k(t) s_k(t-\tau) \mathrm{d}t$ and $V_k(f) = \mathcal{F}\{v_k(\tau)\}$. Then $V_k(f) = |S_k(f)|^2$. Since $v_k(\tau)$ is an even function, time-limited to $[-T, T]$ and $\widehat{R}_k(\tau) = v_k(\tau)$ for $0 \le \tau \le T$, one has

$$\begin{aligned} 2\int_0^T \widehat{R}_k(\tau)\widehat{R}_i(\tau)\mathrm{d}\tau &= \int_{-T}^{T} v_k(\tau) v_i(\tau) \mathrm{d}\tau \\ &= \int_{-\infty}^{\infty} V_k(f) V_i(f) \mathrm{d}f \\ &= \int_{-\infty}^{\infty} |S_k(f)|^2 |S_i(f)|^2 \mathrm{d}f. \end{aligned} \tag{6.12}$$

Comparing (6.6) and (6.12) leads to the following identity,

$$\int_0^T \left[R_{k,i}^2(\tau) + R_{i,k}^2(\tau) \right] \mathrm{d}\tau = 2\int_0^T \widehat{R}_k(\tau)\widehat{R}_i(\tau)\mathrm{d}\tau. \tag{6.13}$$

[1]Note that with this definition, $v_k(\tau)$ is different from $v_{k,k}(\tau)$ defined in Section 6.1.1.

Thus (6.11) becomes

$$\begin{aligned} \mathrm{var}(I_{k,i}) &= E_{\mathbf{s}_k,\mathbf{s}_i}\left\{\frac{1}{T}\int_0^T \widehat{R}_k(\tau)\widehat{R}_i(\tau)\mathrm{d}\tau\right\} \\ &= \frac{1}{T}\int_0^T E_{\mathbf{s}_k}\left\{\widehat{R}_k(\tau)\right\} E_{\mathbf{s}_i}\left\{\widehat{R}_i(\tau)\right\}\mathrm{d}\tau \end{aligned} \tag{6.14}$$

To further evaluate (6.14), let $l = \lfloor \tau/T_c \rfloor$ be the integer part of τ/T_c and $r = \tau - lT_c$. It follows that l and r are random variables uniformly distributed over $\{0, 1, \ldots, N-1\}$ and $[0, T_c)$ respectively. Since the components of vector $\mathbf{s}_k$ are i.i.d. random variables, it is not hard to see that $E_{\mathbf{s}_k}\left\{\widehat{R}_k(\tau)\right\}$ is nonzero only when $0 \le \tau \le T_c$ (i.e., when $l = 0$). More precisely,

$$E_{\mathbf{s}_k}\left\{\widehat{R}_k(\tau)\right\} = \begin{cases} \frac{N}{D}\sum_{m=1}^{D}\widehat{h}_m(r), & \text{if } l = 0 \\ 0, & \text{otherwise.} \end{cases} \tag{6.15}$$

In (6.15), $\widehat{h}_m(r) = \int_r^{T_c} g_m(t)g_m(t-r)\mathrm{d}t$, $0 \le r \le T_c$, is the partial correlation function of the chip waveform $g_m(t)$. Thus the variance of $I_{k,i}$ in (6.14) can be written as follows

$$\mathrm{var}(I_{k,i}) = \frac{N}{D^2T_c}\int_0^{T_c}\left(\sum_{m=1}^{D}\widehat{h}_m(r)\right)^2 \mathrm{d}r \tag{6.16}$$

which is the same for all i ($i \neq k$). Let $I = \frac{1}{D^2T_c^3}\int_0^{T_c}\left(\sum_{m=1}^{D}\widehat{h}_m(r)\right)^2\mathrm{d}r$ be the normalized *interference parameter*, then the SIR in (6.3) is the same for every user and given by

$$\mathrm{SIR} = \left[\left(\frac{2E_b}{N_0}\right)^{-1} + \frac{K-1}{N}I\right]^{-1}. \tag{6.17}$$

Note that when $g_1(t) = g_2(t) = \ldots = g_D(t)$, I is just the normalized *mean-squared partial chip correlation* defined in [32, 34] and the SIR in (6.17) agrees with the result given in [34] for the single chip waveform.

To facilitate the design of optimal multiple chip waveforms, it is convenient, as in Section 6.1.1, to express the parameter I in terms of the Fourier transforms of

the chip waveforms. This can be done as follows. For $m = 1, 2, \ldots, D$, let $u_m(\tau) = \int_{-\infty}^{\infty} g_m(t) g_m(t-\tau) \mathrm{d}t$ be the autocorrelation function of the chip waveform $g_m(t)$. Then $u_m(\tau)$ is an even function confined to $[-T_c, T_c]$ with $U_m(f) = |G_m(f)|^2$. Now using the fact that $\widehat{h}_m(\tau) = u_m(\tau)$ for $0 \leq \tau \leq T_c$ and applying Parseval's theorem one has

$$\begin{aligned} I &= \frac{1}{D^2 T_c^3} \int_0^{T_c} \left(\sum_{m=1}^{D} \widehat{h}_m(\tau) \right)^2 \mathrm{d}\tau = \frac{1}{D^2 T_c^3} \int_0^{T_c} \left(\sum_{m=1}^{D} u_m(\tau) \right)^2 \mathrm{d}\tau \\ &= \frac{1}{2D^2 T_c^3} \int_{-T_c}^{T_c} \left(\sum_{m=1}^{D} u_m(\tau) \right)^2 \mathrm{d}\tau = \frac{1}{2D^2 T_c^3} \int_{-\infty}^{\infty} \left| \sum_{m=1}^{D} U_m(f) \right|^2 \mathrm{d}f \\ &= \frac{1}{2D^2 T_c^3} \int_{-\infty}^{\infty} \left(\sum_{m=1}^{D} |G_m(f)|^2 \right)^2 \mathrm{d}f. \end{aligned} \tag{6.18}$$

Again, when $g_1(t) = g_2(t) = \ldots = g_D(t)$, (6.18) reduces to the normalized integration of the fourth power of the magnitude spectrum of the single chip waveform as shown in [32] and [35].

6.2 Design Problems

6.2.1 Design of Signature Waveforms

Similar to the case of synchronous systems, it is desired to obtain the signature waveforms that maximize the SIR in (6.3) for *every* user. Again this is a very difficult (if not an impossible) task. Thus an alternative objective, namely to minimize the average MAI variance at the outputs of all correlation receivers is considered here. The (normalized) average MAI variance is defined by

$$\begin{aligned} J = \frac{1}{KT^2} \sum_{k=1}^{K} \sum_{\substack{i=1 \\ i \neq k}}^{K} \mathrm{var}(I_{k,i}) &= \frac{1}{2KT^3} \sum_{k=1}^{K} \sum_{\substack{i=1 \\ i \neq k}}^{K} \int_{-\infty}^{\infty} |S_k(f)|^2 |S_i(f)|^2 \mathrm{d}f \\ &= \frac{1}{KT^3} \sum_{k=1}^{K} \sum_{i=k+1}^{K} \int_{-\infty}^{\infty} |S_k(f)|^2 |S_i(f)|^2 \mathrm{d}f \end{aligned} \tag{6.19}$$

where J has been normalized to be independent of T. Minimizing J ensures an average performance level over all users. It is conceivable that, when the number of users K is fixed, the minimum value of J decreases as the transmission bandwidth of the system increases. Thus, for a given bandwidth W, the optimal set of signature waveforms is the one that minimizes J.

As in the case of S-CDMA systems, here both the RMS and FOBE bandwidths can be considered. Recall that the energies of the signature waveforms in A-CDMA systems are normalized to equal the symbol duration T as in (2.31). Thus the RMS and FOBE bandwidth constraints in (2.40) and (2.44) become

$$\frac{1}{KT}\sum_{k=1}^{K}\int_{-\infty}^{\infty} f^2|S_k(f)|^2\mathrm{d}f = W^2 \tag{6.20}$$

and

$$\frac{1}{KT}\sum_{k=1}^{K}\int_{|f|>W} |S_k(f)|^2\mathrm{d}f = \eta \tag{6.21}$$

respectively. Now the design problem for signature waveforms in A-CDMA systems with bandwidth constraint is as follows.

Problem 6.1. Consider an asynchronous CDMA system equipped with a correlation receiver. Given a signaling interval T and a transmission bandwidth W, find a set of K signature waveforms $\{s_1(t), s_2(t), \ldots, s_K(t)\}$ that minimize J in (6.19) subject to the energy constraint of (2.31) and the RMS bandwidth constraint of (6.20) (or the FOBE bandwidth constraint of (6.21)).

6.2.2 Design of Multiple Chip Waveforms

In asynchronous DS-CDMA systems using random signature sequences, the SIR is the same for every user. It follows from (6.17) that to maximize SIR, one needs to find multiple chip waveforms to minimize I in (6.18). Furthermore, the chip waveforms also determine the bandwidth of the system as discussed below.

When the signature waveforms are constructed from random signature sequences and multiple chip waveforms, the PSD of the transmitted signal in (2.32) can be shown to be proportional to $\sum_{m=1}^{D} |G_m(f)|^2$. Thus the RMS bandwidth constraint is as follows:

$$\frac{1}{DT_c} \sum_{m=1}^{D} \int_{-\infty}^{\infty} f^2 |G_m(f)|^2 \mathrm{d}f = W^2. \tag{6.22}$$

Likewise, for $0 < \eta < 1$, the FOBE bandwidth constraint can be written as

$$\frac{1}{DT_c} \sum_{m=1}^{D} \int_{|f|>W} |G_m(f)|^2 \mathrm{d}f = \eta. \tag{6.23}$$

From (6.18), (6.22) and (6.23) one may suggest that by choosing a single chip waveform with power spectral density

$$|G(f)|^2 = \frac{1}{D} \sum_{m=1}^{D} |G_m(f)|^2 \tag{6.24}$$

then the SIR performance of any choice of multiple chip waveforms can be obtained by the corresponding single chip waveform with the same bandwidth. This is not possible in general. Granted one can readily obtain the energy density spectrum as indicated in (6.24). However to obtain the time waveform $g(t)$, one must also specify the phase spectrum. The single chip waveform $g(t)$ obtained through the inverse Fourier transform of $G(f)$ now will not be necessarily a *time-limited* (to the interval $[0, T_c]$) function as required. Though an analytical proof for this claim was not found the following conjecture, based on the above discussion and the numerical results in Section 6.4.2 (see Fig. 6.10), is proposed.

Conjecture 6.1. Given D arbitrary chip waveforms $g_1(t), g_2(t), \ldots, g_D(t)$, each time-limited to $[0, T_c]$ whose energies are normalized to be T_c. Let $G_1(f), G_2(f), \ldots, G_D(f)$ be the corresponding Fourier transforms of these chip waveforms. Then it is not always possible to generate a chip waveform $g(t)$ which is also time-limited to $[0, T_c]$ whose Fourier transform satisfies (6.24). Δ

Note that, if the restriction on time limitation is lifted, the expression of the interference parameter in (6.18) does not hold for the single chip waveform obtained via (6.24). This is because for a chip waveform that spans multiple chip interval, there is generally a nonzero interchip interference (ICI). It can be shown that the interference parameter for a chip waveform whose support is longer than a chip interval is given by [61],

$$I = \frac{1}{2T_c^3}\int_{-\infty}^{\infty}|G(f)|^4\mathrm{d}f + \frac{1}{(K-1)T_c^2}\sum_{m\neq 0}\left[\int_{-\infty}^{\infty}\cos(2\pi m f T_c)|G(f)|^2\mathrm{d}f\right]^2 \qquad (6.25)$$

where the second term accounts for the ICI.

The design problem for multiple chip waveforms can be stated as follows.

Problem 6.2. Consider a K-user asynchronous DS-CDMA system using random signature sequences and multiple chip waveforms. Given a signaling interval, T, and a transmission bandwidth, W, find a set of D chip waveforms $\{g_1(t), g_2(t), \ldots, g_D(t)\}$ that minimize I in (6.18) subject to the energy constraint of (6.9) and the RMS bandwidth constraint of (6.22) (or the FOBE bandwidth constraint of (6.23)).

The two optimization problems stated in this section concern finite sets of time-limited waveforms and they are very similar. The only difference lies in the objective functions. These problems are very difficult to solve explicitly due to the complexity of the objectives and the constraints. Nevertheless, the expansion technique employed in [32] can be applied here to simplify the design problems.

In [32] the authors obtain the optimal *single* chip waveforms for offset quadrature DS-CDMA systems under bandwidth, phase and envelope constraints. The method is to approximate the solution by using a finite series expansion over a complete set of basis functions. As pointed out in [32], the choice of a proper set of basis functions is very important to reduce the dimensionality of the equivalent discrete optimization problem. Which basis set is chosen is governed by the bandwidth criterion under consideration. If the FOBE bandwidth is used, it is suggested in [32] that the prolate

spheroidal functions should be used to expand the Fourier transforms of the signature waveforms (and chip waveforms respectively). For the RMS bandwidth constraint, the set of time-truncated sinuisoids $\{\sin(n\pi t/T), 0 \le t \le T\}_{n=1}^{\infty}$ is selected for the expansion of the signature waveforms (and chip waveforms respectively). This selection is natural since the functions $\{\sin(n\pi t/T), 0 \le t \le T\}_{n=1}^{\infty}$ form a complete set for all *continuous* functions time limited to $[0, T]$ and, more importantly, they achieve the minimum RMS bandwidth [52]. For brevity of presentation, only the RMS bandwidth constraint is pursued in this chapter.

6.3 Optimal Signature Waveforms

6.3.1 Problem Simplification

Let $\psi_n(t) = \sqrt{2/T}\sin(n\pi t/T)p_T(t)$, where $p_T(t) = 1$ for $0 \le t \le T$ and $p_T(t) = 0$ otherwise. Then the RMS bandwidth of $\psi_n(t)$ is $b(\psi_n(t)) = n/(2T)$. To simplify the calculation of the objective function in (6.19) introduce the shifted (and possibly negated) versions of $\psi_n(t)$, defined by[2]

$$\phi_n(t,T) = \begin{cases} \sqrt{\frac{2}{T}}\cos\left(\frac{n\pi t}{T}\right), & -\frac{T}{2} \le t \le \frac{T}{2}, \quad \text{if } n \text{ is odd} \\ \sqrt{\frac{2}{T}}\sin\left(\frac{n\pi t}{T}\right), & -\frac{T}{2} \le t \le \frac{T}{2}, \quad \text{if } n \text{ is even.} \end{cases} \tag{6.26}$$

Let $\Phi_n(f,T) = \mathcal{F}\{\phi_n(t,T)\}$. Note that when n is odd, the function $\phi_n(t,T)$ is even, hence $\Phi_n(f,T)$ is a real function. On the other hand, when n is even, $\phi_n(t,T)$ is an odd function and $\Phi_n(f,T)$ is purely imaginary. Write $\Phi_n(f,T) = X_l(f,T)$ when $n = 2l-1$ and $\Phi_n(f,T) = jY_l(f,T)$ when $n = 2l$, then

$$\begin{cases} X_l(f,T) &= \sqrt{\frac{T}{2}}\left[\text{sinc}(fT-(l-0.5)) + \text{sinc}(fT+(l-0.5))\right] \\ Y_l(f,T) &= \sqrt{\frac{T}{2}}\left[\text{sinc}(fT-l) - \text{sinc}(fT+l)\right] \end{cases} \tag{6.27}$$

where $\text{sinc}(x) = \sin(\pi x)/(\pi x)$.

[2]Instead of $\phi_n(t)$, we write $\phi_n(t,T)$ to emphasize that $\phi_n(t)$ has a duration of T. Later $\phi_n(t,T_c)$ is used to discuss the design of chip waveforms.

Let $\widehat{s}_k(t) = s_k(t+T/2)$ be the shifted version of the signature waveform $s_k(t)$. Since $\{\phi_n(t)\}_{n=1}^{\infty}$ forms a complete set for all continuous functions that are time limited to $[-T/2, T/2]$, $\widehat{s}_k(t)$ can be expanded as follows

$$\widehat{s}_k(t) = \sum_{l=1}^{\infty} x_{kl}\phi_{2l-1}(t,T) + \sum_{l=1}^{\infty} y_{kl}\phi_{2l}(t,T) \tag{6.28}$$

where the coefficients x_{kl} and y_{kl} are given by $x_{kl} = \int_{-T/2}^{T/2} \widehat{s}_k(t)\phi_{2l-1}(t,T)\mathrm{d}t$ and $y_{kl} = \int_{-T/2}^{T/2} \widehat{s}_k(t)\phi_{2l}(t,T)\mathrm{d}t$. The RMS bandwidths of $s_k(t)$ and $\widehat{s}_k(t)$ are the same. They can be computed as shown below [52],

$$\begin{aligned} b^2(s_k(t)) = b^2(\widehat{s}_k(t)) &= \frac{1}{(2\pi)^2 T}\int_{-T/2}^{T/2}\left(\frac{\mathrm{d}\widehat{s}_k(t)}{\mathrm{d}t}\right)^2 \mathrm{d}t \\ &= \sum_{l=1}^{\infty}\left[x_{kl}^2 b^2(\phi_{2l-1}(t,T)) + y_{kl}^2 b^2(\phi_{2l}(t,T))\right] \\ &= \frac{1}{4T^3}\sum_{l=1}^{\infty}\left[(2l-1)^2 x_{kl}^2 + 4l^2 y_{kl}^2\right]. \end{aligned} \tag{6.29}$$

Due to the constraint on the system bandwidth in (6.20), it follows from (6.29) that the coefficients x_{kl} and y_{kl} should be very small when l is large. Therefore, for all practical purposes, it is sufficient to truncate each sum in (6.28) to a finite length of L terms, that is

$$\widehat{s}_k(t) \cong \sum_{l=1}^{L} x_{kl}\phi_{2l-1}(t,T) + \sum_{l=1}^{L} y_{kl}\phi_{2l}(t,T). \tag{6.30}$$

Using the truncated expansion in (6.30), the constraints in (2.31) and (6.20) can be written in terms of x_{kl} and y_{kl}, $k = 1, 2\ldots, K$ and $l = 1, 2, \ldots, L$ as follows.

$$\sum_{l=1}^{L}\left(x_{kl}^2 + y_{kl}^2\right) = T, \qquad k = 1, 2, \ldots, K \tag{6.31}$$

and

$$\sum_{k=1}^{K}\sum_{l=1}^{L}\left[(2l-1)^2 x_{kl}^2 + 4l^2 y_{kl}^2\right] = 4K(WT)^2 T. \tag{6.32}$$

Appendix E also shows that the objective J in (6.19) can be written in terms of x_{kl} and y_{kl} (see Eqn. (E.3)). Thus Problem 6.1 is now equivalent to the following finite-dimensional optimization problem.

Problem 6.3. Find the $2KL$ coefficients x_{kl} and y_{kl}, $k = 1, 2 \ldots, K$ and $l = 1, 2, \ldots, L$, that minimize $J(L)$ in (E.3) subject to the constraints in (6.31) and (6.32).

The above optimization problem can be solved numerically, for example, by means of sequential quadratic programming routines. Here the program code was written based on the MATLAB optimization toolbox and it is documented in a separate report [62]. Since the number of users K is not controllable, to reduce the dimensionality of the optimization problem, it is important to use as a small value for L as possible. In general, such a value of L depends on the bandwidth-time product WT (due to the bandwidth constraint). No analytical expression was found to determine the convergence properties of the approximation. Therefore a heuristic approach was used. Simply the approximated objective funtion $J^*(L)$ is plotted versus L for each value of RMS bandwidth considered. A judgement is then made regarding the value of L at which $J^*(L)$ reaches an "asymptote".

6.3.2 Numerical Examples

Some numerical results are given in this section to demonstrate the optimal signature waveforms obtained from solving Problem 6.3. Although results for systems with a large number of users are of practical interest, solving Problem 6.3 for large K is quite time consuming. For this reason only CDMA systems with $K = 2$ and $K = 4$ are examined as illustrative examples. The RMS bandwidth value ranges from $0.525/T$ to $1.1/T$ for the two-user system and from $0.6/T$ to $2.0/T$ for the four-user system.

Given the number of users and the RMS bandwidth, different values of L were used in Problem 6.3 to obtain the corresponding signature waveforms and the minimum value of the objective function, namely $J^*(L)$. Plotting $J^*(L)$ versus L reveals that,

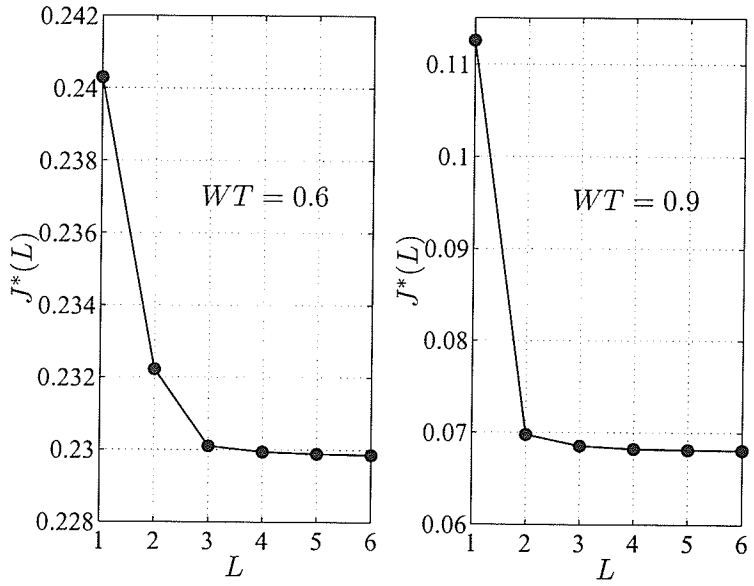

Figure 6.2: Influence of L on the minimum value of the objective function, $K = 2$.

for all RMS bandwidth values considered and for both the two-user and the four-user systems, the asymptote of $J^*(L)$ is reached practically for $L \geq 4$. For example, Fig. 6.2 plots $J^*(L)$ for two-user systems with $WT = 0.6$ and $WT = 0.9$, whereas Fig. 6.3 plots $J^*(L)$ for four-user systems with $WT = 1.4$ and $WT = 2.0$. Thus $L = 4$ is used for the remaining examples of this section to obtain the signature waveforms. It should be noted, however, that for systems with a larger number of users and wider bandwidth the value of L may become large and therefore obtaining the solutions to Problem 6.3 would become time consuming.

To evaluate the performance of the designed signature waveforms, the average MAI variance (J) achieved by the optimal signature waveforms in two-user and four-user systems is plotted in Figs. 6.4 and 6.5 respectively as a function of the time-bandwidth product WT. As expected, the MAI reduces as the bandwidth increases. For a given bandwidth, MAI increases as the number of users increases. In Figs. 6.4 and 6.5, the performance of the designed signature waveforms is also compared with that of the signature waveforms optimally designed for *synchronous* CDMA systems. Such design

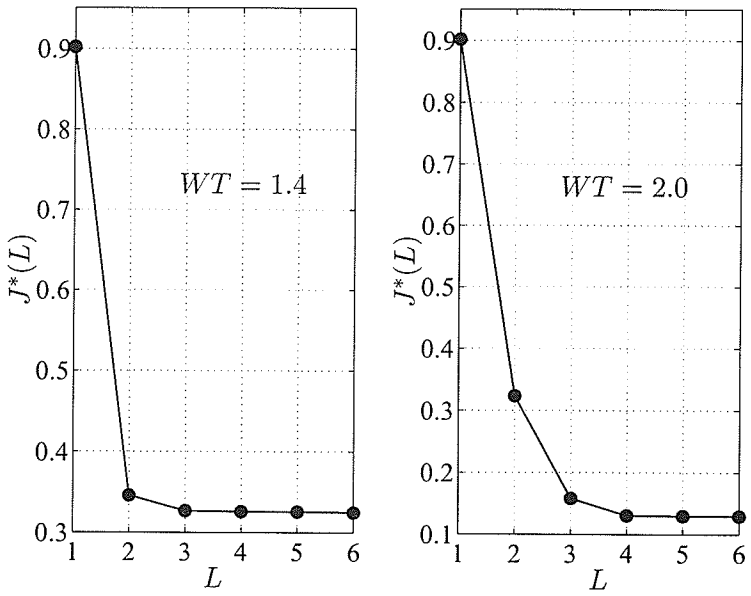

Figure 6.3: Influence of L on the minimum value of the objective function, $K = 4$.

of signature waveforms has been considered in Chapter 4 with the same optimality criterion and bandwidth constraint. For convenience, we shall refer to the waveforms designed specifically for A-CDMA systems in this chapter as the *asynchronous signature waveforms* and the waveforms designed for S-CDMA systems in Chapter 4 as the *synchronous signature waveforms.* In each of Figs. 6.4 and 6.5 two curves are plotted for the performance of the synchronous signature waveforms: one over synchronous systems and the other over asynchronous systems (system-mismatch situation).

As already known from Chapter 4, orthogonal signature waveforms are available in S-CDMA systems when $(2WT)^2 \geq (K+1)(2K+1)/6$. Therefore the MAI produced by the synchronous signature waveforms in synchronous systems is zero when $WT \geq 0.791$ and $WT \geq 1.369$ as shown in Figs 6.4 and 6.5 respectively. Assuming that the same orthogonal synchronous signature waveforms are used for larger bandwidths, then the MAI produced by the synchronous signature waveforms in asynchronous systems stays the same for $WT \geq 0.791$ and $WT \geq 1.369$, as can be seen in Figs 6.4

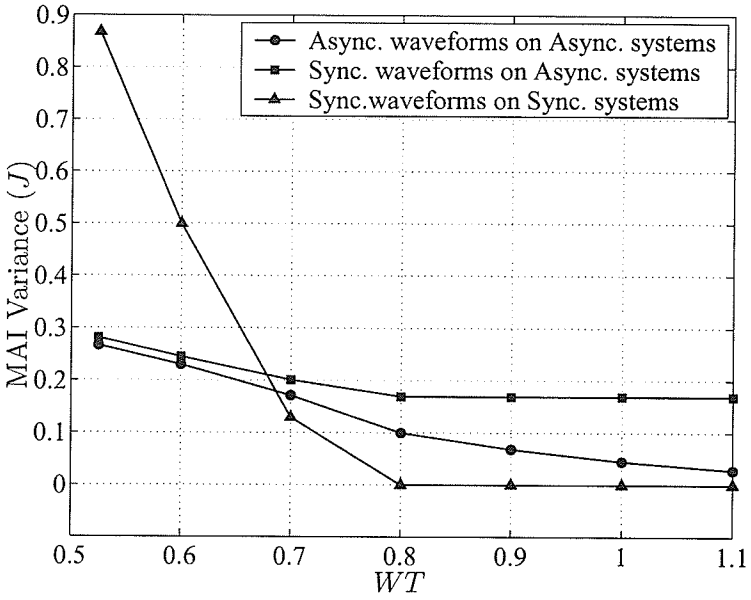

Figure 6.4: Minimum MAI variance J as a function of time-bandwidth product WT, $K = 2$.

and 6.5 respectively. The superiority of the asynchronous signature waveforms over synchronous ones in asynchronous systems is clearly observed from Figs 6.4 and 6.5 for all values of RMS bandwidth under consideration.

It is also of interest to notice from Figs 6.4 and 6.5 that, for very small values of a RMS bandwidth, the MAI produced by synchronous waveforms in synchronous systems is larger than that produced by the asynchronous waveforms in asynchronous systems. This is counterintuitive since the performance of synchronous systems is usually taken as the lower bound for the performance of the asynchronous ones. This observation can be explained as follows. When the bandwidth is very small, all the signature waveforms possess very similar shapes (in order to satisfy the bandwidth constraint). This means that the synchronous correlations among signature waveforms are very high, causing a huge MAI in synchronous systems. On the other hand, the MAI in the asynchronous systems depends on the particular delays among users and can be very small for certain delays. Therefore, after averaging over the

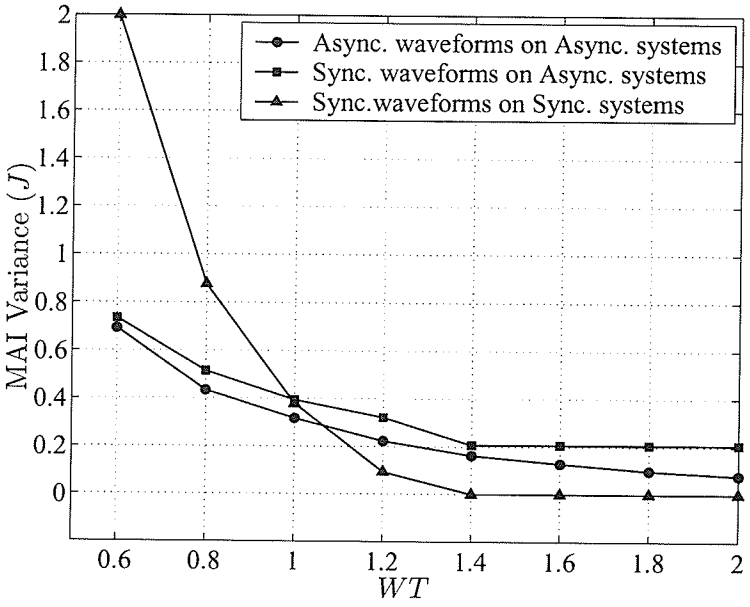

Figure 6.5: Minimum MAI variance J as a function of time-bandwidth product WT, $K = 4$.

entire range of the delays (the symbol duration T), the average MAI in asynchronous systems can be significantly smaller than that in synchronous ones. Nevertheless, when the bandwidth increases, the MAI in synchronous systems approaches zero much faster than that in asynchronous systems. In other words, it requires much larger bandwidth for the asynchronous system to perform at a satisfactory level (i.e., when MAI is small) compared to that of synchronous systems, even though optimal signature waveforms are used in both scenarios.

Finally, asynchronous signature waveforms for two-user and four-user systems are demonstrated in Figs. 6.6 to 6.9 for selected values of RMS bandwidth occupancies. Note that the signature waveforms in Figs. 6.7, 6.8 and 6.9 possess (even or odd) symmetry about the midpoint of the symbol duration. The synchronous signature waveforms for two-user synchronous systems are also shown in Figs. 6.6 and 6.7 for comparison. We would like to point out that these synchronous signature waveforms

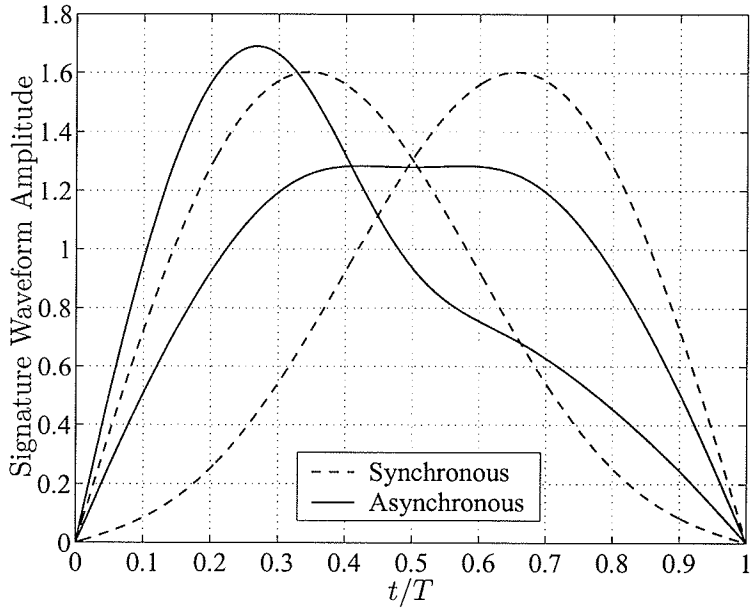

Figure 6.6: Optimal signature waveforms for synchronous and asynchronous CDMA systems: $K = 2$ with RMS bandwidth of $WT = 0.6$.

were first obtained in [18] to achieve each point inside the capacity region of the two-user Gaussian multiple access channel. It turns out that they are also the optimal signature waveforms that minimize the MAI in synchronous CDMA systems (see Chapter 4).

6.4 Optimal Chip Waveforms

6.4.1 Problem Simplification

Similar to signature waveform design, the problem of designing multiple chip waveforms (Problem 6.2) can be reduced to a finite-dimensional optimization problem. To this end, expand the delayed version of each chip waveform as follows

$$\begin{aligned} \widehat{g}_m(t) &= g_m(t + T_c/2) \\ &\cong \sum_{l=1}^{L} x_{ml}\phi_{2l-1}(t, T_c) + \sum_{l=1}^{L} y_{ml}\phi_{2l}(t, T_c), \qquad m = 1, 2, \ldots, D \end{aligned} \tag{6.33}$$

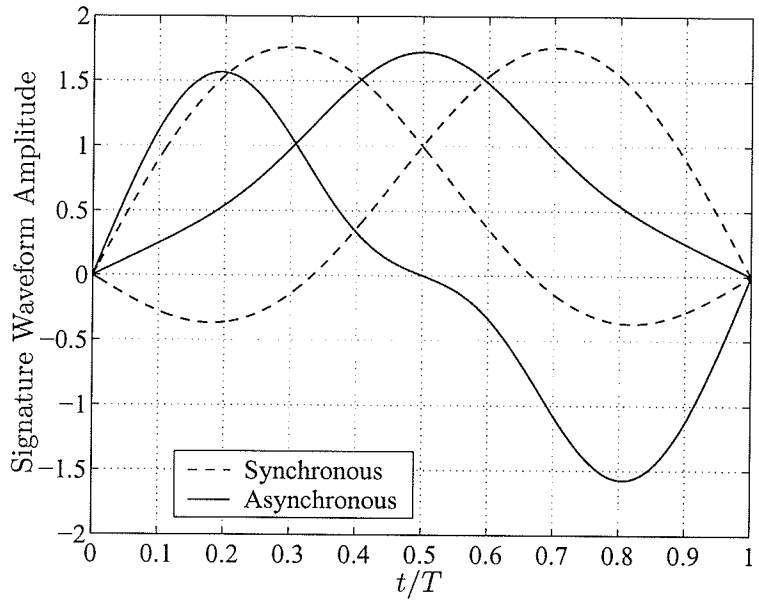

Figure 6.7: Optimal signature waveforms for synchronous and asynchronous CDMA systems: $K = 2$ with RMS bandwidth of $WT = 0.9$.

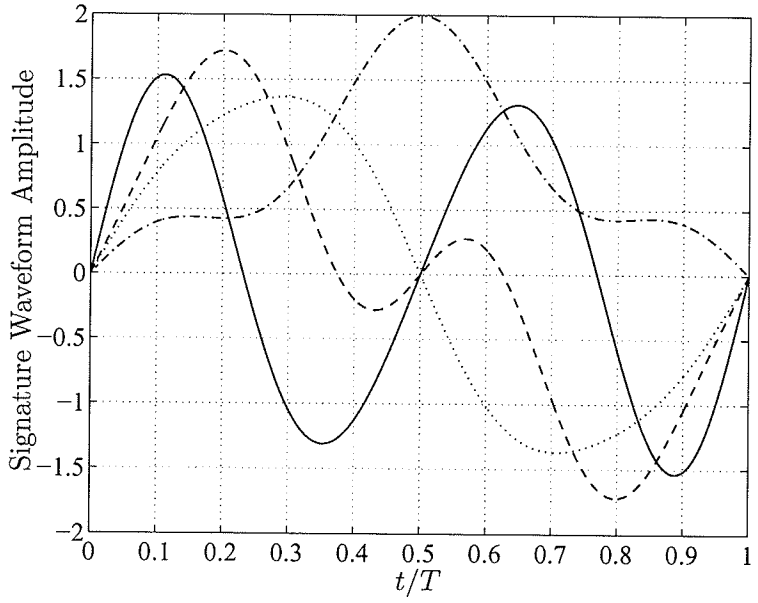

Figure 6.8: Optimal signature waveforms for an asynchronous CDMA system: $K = 4$ with RMS bandwidth of $WT = 1.4$.

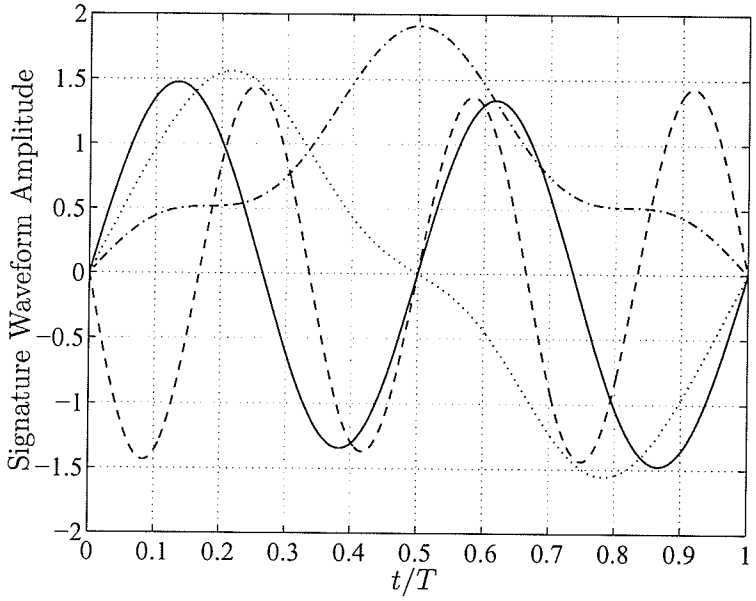

Figure 6.9: Optimal signature waveforms for an asynchronous CDMA system: $K = 4$ with RMS bandwidth of $WT = 2.0$.

where $x_{ml} = \int_{-T_c/2}^{T_c/2} \widehat{g}_m(t)\phi_{2l-1}(t, T_c)\mathrm{d}t$ and $y_{ml} = \int_{-T_c/2}^{T_c/2} \widehat{g}_m(t)\phi_{2l}(t, T_c)\mathrm{d}t$. Using this expansion, the constraints in (6.9) and (6.22) can be written in terms of x_{ml} and y_{ml}, $m = 1, 2 \ldots, D$ and $l = 1, 2, \ldots, L$, as follows.

$$\sum_{l=1}^{L} \left(x_{ml}^2 + y_{ml}^2\right) = T_c, \qquad m = 1, 2, \ldots, D \tag{6.34}$$

and

$$\sum_{m=1}^{D} \sum_{l=1}^{L} \left[(2l-1)^2 x_{ml}^2 + 4l^2 y_{ml}^2\right] = 4D(WT_c)^2 T_c. \tag{6.35}$$

Furthermore, the objective in (6.18) can also be expressed in terms of x_{ml} and y_{ml} as shown in Appendix F (see Eqn. (F.10)). Therefore Problem 6.2 is now equivalent to the following finite-dimensional optimization problem.

Problem 6.4. Find $2DL$ coefficients x_{ml} and y_{ml}, $m = 1, 2 \ldots, D$ and $l = 1, 2, \ldots, L$, that minimize $I(D, L)$ in (F.10) subject to the constraints given in (6.34) and (6.35).

As for Problem 6.3, Problem 6.4 can be solved numerically. It should be noted,

however, that the dimensionality of Problem 6.4 does not depend on the number of users, K, and it is usually much smaller than that of Problem 6.3. This is due to the following two reasons. First, the number of unknowns in Problem 6.4 depends only on D and L, which can be selected to achieve a compromise between performance and complexity. Secondly, since the value of WT_c is usually less than 3.0 for DS-CDMA systems, a practical value of L in Problem 6.4 is much smaller than that in Problem 6.3.

Finally, the following proposition justifies the advantage of using multiple chip waveforms in DS-CDMA systems with random signature sequences.

Proposition 6.1. Consider a DS-CDMA system using random signature sequences and D chip waveforms. Let the D chip waveforms be the solutions of Problem 6.4 for some fixed value of L. Let $I^*(D, L)$ be the corresponding interference parameter and κ be an integer number. Then

$$I^*(\kappa D, L) \leq I^*(D, L) \tag{6.36}$$

△

Proof. The proof is trivial, by noting that the equality in (6.36) is achieved when using κ copies of the set of D optimal chip waveforms for the set of κD chip waveforms. □

6.4.2 Numerical Results

Several multiple chip waveforms obtained from solving Problem 6.4 are presented in this section. Up to $D = 3$ is considered. The values of W are from $0.5/T_c$ to $3.0/T_c$, which is the range of interest for us. For this range of RMS bandwidth, it has been determined that using $L = 6$ yields sufficient accuracy for optimal chip waveforms.

Numerical results indicate that the improvement from using multiple chip waveforms over single chip waveforms is quite significant. This is illustrated in Fig. 6.10 where the interference parameters I achieved by the optimal single, double and triple

chip waveforms (denoted by I_{1c}, I_{2c} and I_{3c} respectively) are plotted versus WT_c. From Fig. 6.10 it can be seen that the largest gain is achieved by moving from a single chip waveform to double chip waveforms and there is not much improvement with triple chip waveforms. A closer investigation of Fig. 6.10 reveals that, for a fixed level of interference I, it is possible to save about 10% of the transmission bandwidth when using double chip waveforms compared to a single chip waveform. Fig. 6.10 therefore also supports Conjecture 6.1.

Fig. 6.11 plots the ratios I_{2c}/I_{1c} and I_{3c}/I_{1c} to compare the performances of multiple chip waveforms with that of a single chip waveform but from a different perspective. Note that when $W = 0.5/T_c$ there exists only one chip waveform of duration T_c, namely the half-sine waveform $\sqrt{2/T_c}\sin(\pi t/T_c)\,p_{T_c}(t)$. Therefore there is no advantage to use multiple chip waveforms for interference suppression. However, as the bandwidth increases, the interference reduction capability of multiple chip waveforms increases and saturates at about $W = 2.4/T_c$. At $W = 2.4/T_c$, the interference can be reduced by about 10% by using multiple chip waveforms instead of a single chip waveform.

It is also of interest to compare the performance of optimal chip waveforms (single, double or triple) among themselves when varying the chip duration T_c. For a fair comparison, the bandwidth W and the symbol duration T are fixed. Since $N = T/T_c$, it follows from (6.17) that to maximize SIR, one needs to minimize IT_c, or equivalently to minimize IWT_c. This parameter is plotted against WT_c in Fig. 6.12[3]. It can be seen that the performance improves with increasing chip duration T_c and saturates at about $T_c = 1.4/W$ for the single chip waveform and $2.4/W$ for both double and trip chip waveforms. Thus in general, there exists a minimum value of WT_c for multiple chip waveforms that minimizes the multiple access interference. Note that the RMS

[3]Note that, since the bandwidth expansion has been taken into account in the parameter IWT_c, the WT_c axis in Figs. 6.12 and 6.13, in essence, is irrelevant for the comparison.

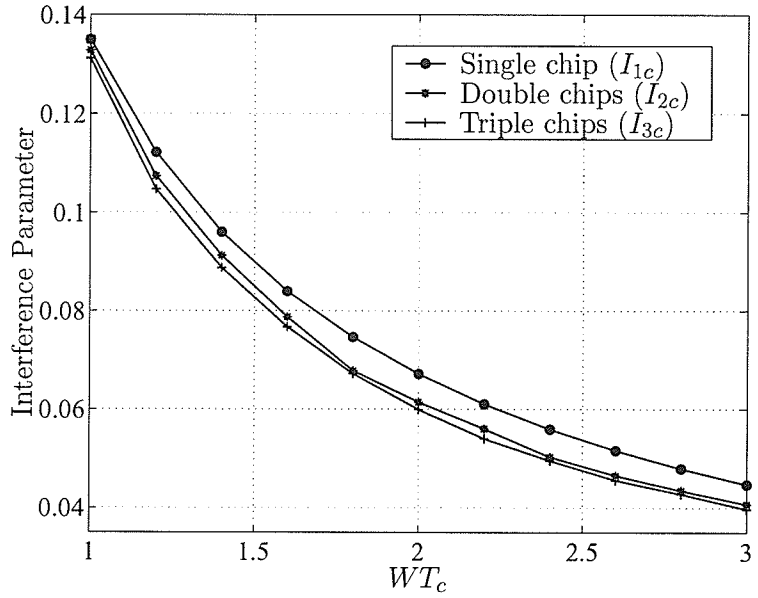

Figure 6.10: Minimum interference parameter as a function of WT_c for single, double and triple chip waveforms.

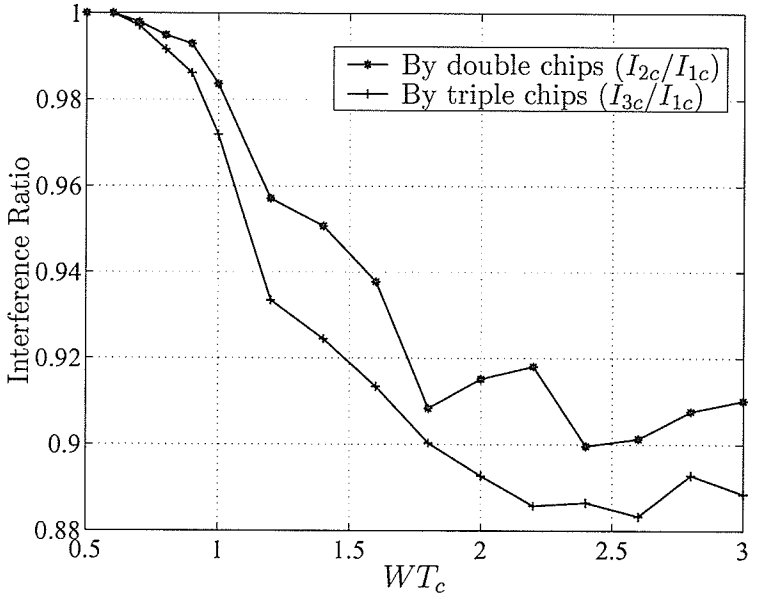

Figure 6.11: Interference reduction compared to single chip waveform.

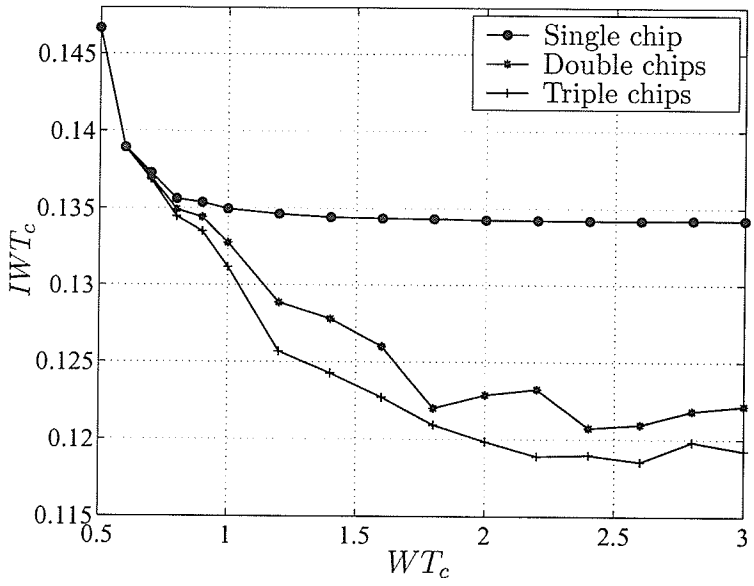

Figure 6.12: IWT_c as a function of WT_c for single, double and triple chip waveforms.

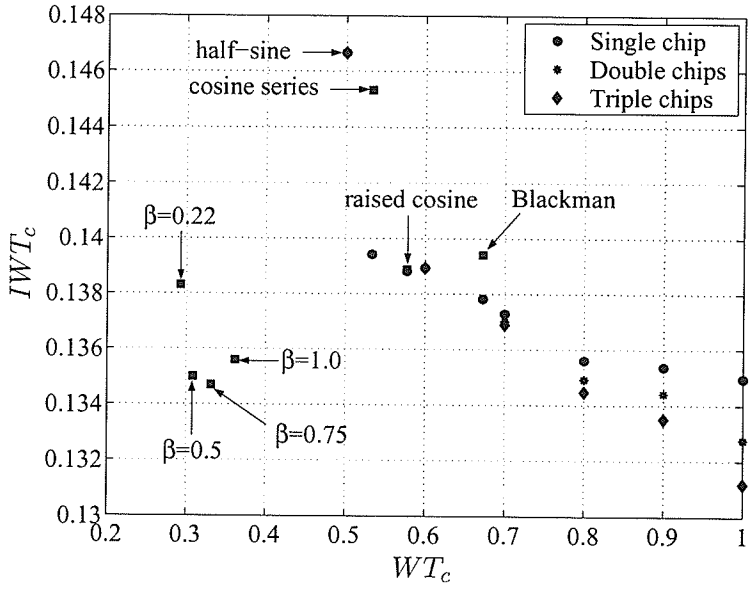

Figure 6.13: IWT_c as a function of WT_c for optimal single, double, triple and some common chip waveforms. The parameter β refers to different roll-off factors for the square-root raised cosine waveform.

bandwidths of some common time-limited chip waveforms are relatively small, which make them inefficient in terms of minimizing MAI. This is illustrated in Fig. 6.13 where the IWT_c that is achieved by the raised cosine, Blackman and four-term odd cosine series chip waveforms are shown (in the range of small WT_c). The equations for these chip waveforms can be found in Section 6.5. It can be seen from Fig. 6.13 that the performance of the raised cosine chip is closest to that of the optimal single chip, followed by the Blackman and cosine series chips.

The advantage of the proposed optimal chip waveforms over the square-root raised cosine (SRRC) waveforms with various roll-off factors can also be observed from Fig. 6.13. Note that a SRRC waveform spans more than a chip interval. The SRRC waveform corresponding to a roll-off factor of 0.22 is proposed for Wideband-CDMA systems [63], whereas the chip shape used in the IS-95 standard is also similar to a SRRC pulse [64]. The expression for a SRRC pulse is given by [65]

$$g(t) = \frac{4\beta}{\pi} \frac{\cos\left[(1+\beta)\pi t/T_c\right] + T_c \sin\left[(1-\beta)\pi t/T_c\right]/(4\beta t)}{1-(4\beta t/T_c)^2} \tag{6.37}$$

where β $(0 \leq \beta \leq 1)$ is the roll-off parameter. The square of the Fourier transform (i.e., the energy spectral density) of $g(t)$ is [65]

$$G^2(f) = \begin{cases} 1, & 0 \leq |f| \leq \frac{1-\beta}{2T_c} \\ \frac{1}{2}\left\{1+\cos\left[\frac{\pi T_c}{\beta}\left(|f|-\frac{1-\beta}{2T_c}\right)\right]\right\}, & \frac{1-\beta}{2T_c} \leq |f| \leq \frac{1+\beta}{2T_c} \\ 0, & |f| \geq \frac{1+\beta}{2T_c}. \end{cases} \tag{6.38}$$

To evaluate the performance of the SRRC chip waveforms one needs to calculate the parameter IWT_c. The RMS bandwidth of an SRRC pulse can be easily shown to satisfy

$$WT_c = \left[\frac{(1-\beta)^3+(1+\beta)^3}{24} - \frac{2\beta^2}{\pi^2}\right]^{1/2}. \tag{6.39}$$

Because an SRRC pulse spans more than one chip interval, its performance parameter I should be calculated based on (6.25). However, it is well known that the SRRC

pulses satisfy the Nyquist criterion, hence the ICI term in (6.25) disappears. The interference parameter I for the SRRC pulses therefore is simply given by

$$I = \frac{1}{2T_c^3}\int_{-\infty}^{\infty} |G(f)|^4 \mathrm{d}f = \frac{1}{2} - \frac{\beta}{8}. \tag{6.40}$$

From (6.39) and (6.40), the parameter IWT_c assumes the following expression

$$IWT_c = \left(\frac{1}{2} - \frac{\beta}{8}\right)\left[\frac{(1-\beta)^3 + (1+\beta)^3}{24} - \frac{2\beta^2}{\pi^2}\right]^{1/2}. \tag{6.41}$$

Finally, examples of optimal single, double and triple chip waveforms are plotted in Figs. 6.14 to 6.16 for $WT_c = 2.4$. This value of WT_c is chosen since it gives the optimal chip duration for double and triple chip waveforms as discussed above. The advantage of using optimal single and double chip waveforms in terms of bit error rate is also shown in Figs. 6.17 and 6.18 for a CDMA system having $K = 32$ users and a RMS bandwidth value such that $N = 32$ if the optimal double chip waveforms are used (i.e., $WT = 32 \times 2.4$). Note that Fig. 6.17 is obtained by using a standard Gaussian approximation (GA) to the error probability (see Chapter 7), whereas the improved Gaussian approximation developed in Chapter 7 is used to produce Fig 6.18. The standard GA uses only the parameter IWT_c of the chip waveforms to approximate the error probability and it is quite loose for high signal-to-noise ratios. On the other hand, the improved GA takes into account the actual shapes of the chip waveforms (through their correlation functions) to approximate the error probability. It will be shown in Chapter 7 that this approximation is very accurate. The relative performances of different chip waveform(s) given in Fig. 6.18 agree very well with the values of parameter IWT_c plotted in Fig. 6.13. It can be seen from Fig. 6.18 that, at the BER level of 10^{-4}, a gain of about 2dB in E_b/N_0 can be attained by using the optimal double chip waveforms.

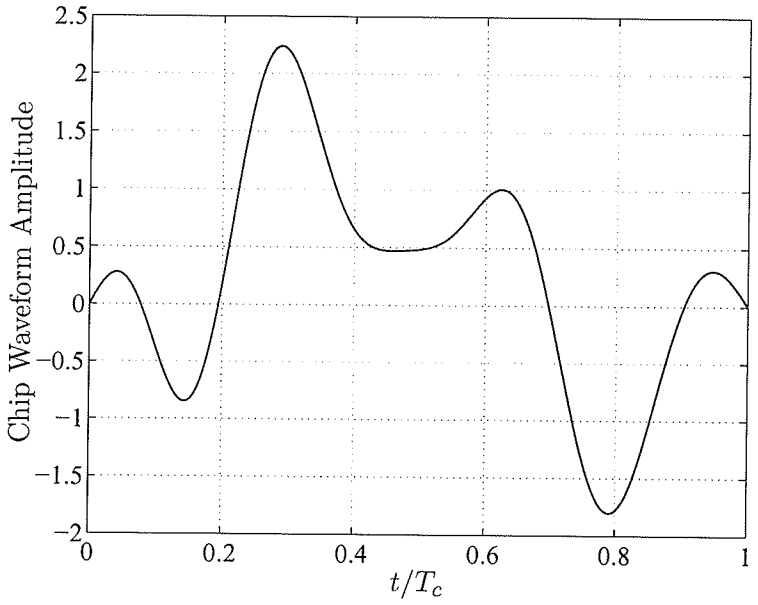

Figure 6.14: Optimal single chip waveform for RMS bandwidth of $WT_c = 2.4$.

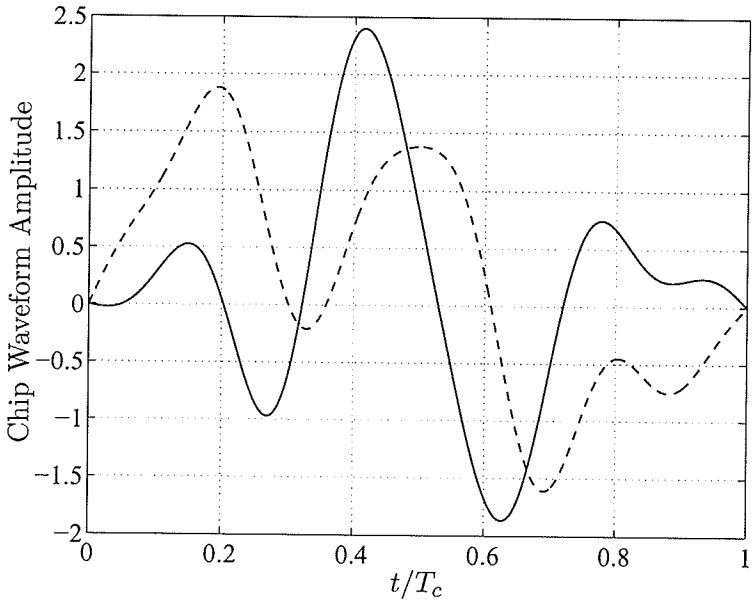

Figure 6.15: Optimal double chip waveforms for RMS bandwidth of $WT_c = 2.4$.

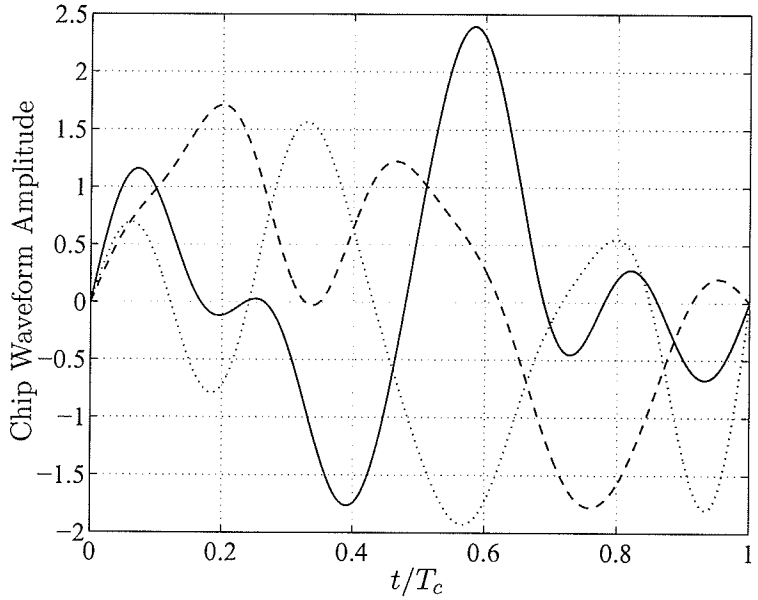

Figure 6.16: Optimal triple chip waveforms for RMS bandwidth of $WT_c = 2.4$.

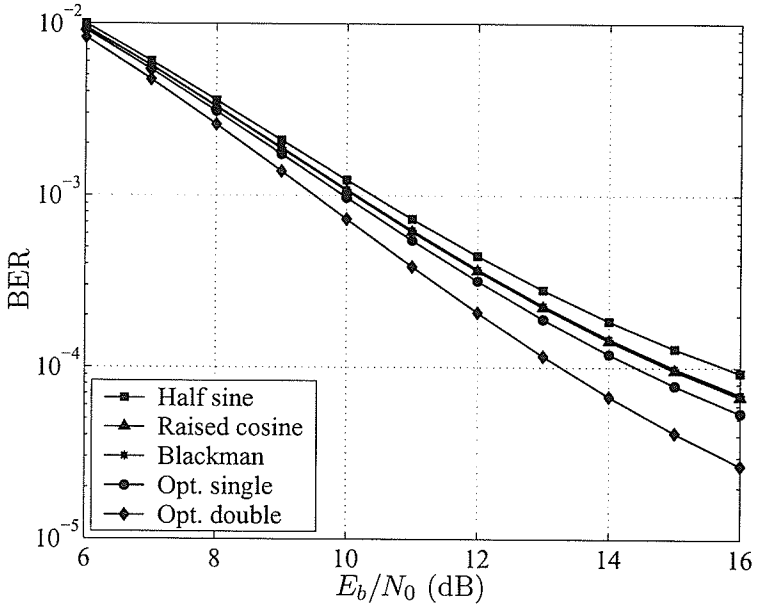

Figure 6.17: Gaussian approximation of error probabilities of asynchronous DS-CDMA systems using different chip waveforms: $K = 32$ with RMS bandwidth of $WT = 32 \times 2.4$.

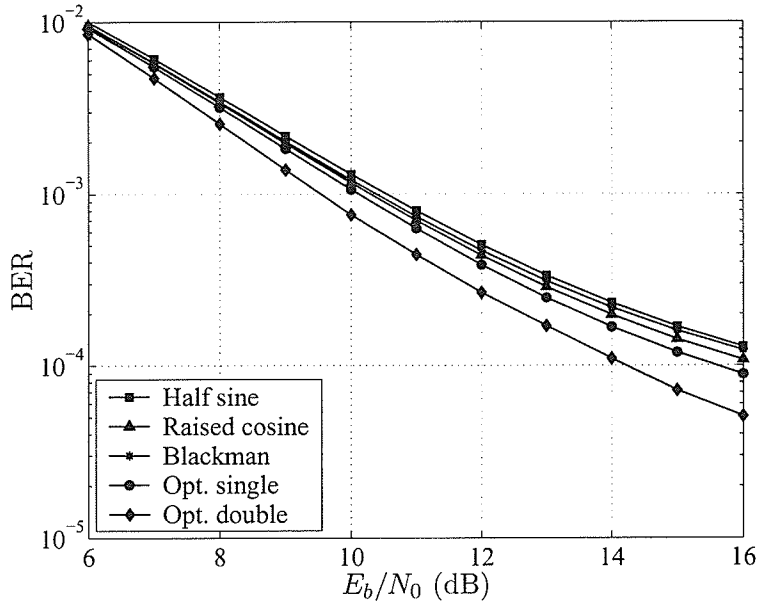

Figure 6.18: Improved Gaussian approximation of error probabilities of asynchronous DS-CDMA systems using different chip waveforms: $K = 32$ with RMS bandwidth of $WT = 32 \times 2.4$.

6.5 Combinations of Common Chip Waveforms

In the previous section, optimal multiple chip waveforms have been obtained to minimize MAI in asynchronous DS-CDMA systems under the RMS bandwidth constraint. Given the technique of using multiple chip waveforms to combat MAI, the question of interest is whether the advantage of this technique can be realized for commonly used signature waveforms without relying on optimal chip waveforms. The answer to this question is investigated in this section. More precisely, this section studies double combinations of the following common chip waveforms.

1) Rectangular pulse: $p_1(t) = p_{T_c}(t)$, where $p_{T_c}(t) = 1$ for $0 \leq t \leq T_c$ and $p_{T_c}(t) = 0$ otherwise.

2) Half-sine: $p_2(t) = \sqrt{2} \sin\left(\frac{\pi t}{T_c}\right) p_{T_c}(t)$.

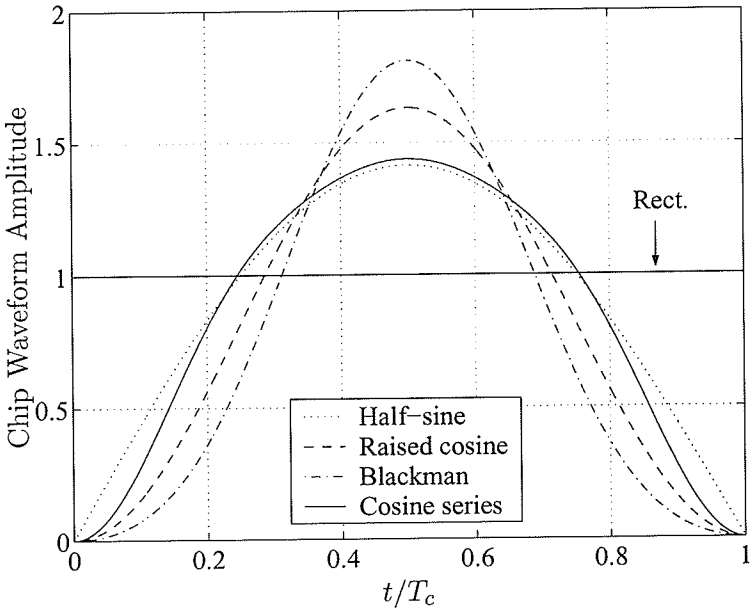

Figure 6.19: Chip waveforms that are even about $T_c/2$.

3) Raised cosine: $p_3(t) = \sqrt{\frac{2}{3}}\left[1 - \cos\left(\frac{2\pi t}{T_c}\right)\right] p_{T_c}(t)$.

4) Blackman [38]: $p_4(t) = c\left[k_1 - k_2\cos\left(\frac{2\pi t}{T_c}\right) + k_3\cos\left(\frac{4\pi t}{T_c}\right)\right] p_{T_c}(t)$, where $c^2 = (k_1^2 + k_2^2/2 + k_3^2/2)^{-1}$ and $k_1 = 0.42$, $k_2 = 0.5$ and $k_3 = 0.08$.

5) Four-term odd cosine series [39]:
$p_5(t) = \left[0.868 - 0.686\cos\left(\frac{2\pi t}{T_c}\right) - 0.149\cos\left(\frac{4\pi t}{T_c}\right) - 0.033\cos\left(\frac{6\pi t}{T_c}\right)\right] p_{T_c}(t)$.

6) Half-cosine: $p_6(t) = \sqrt{2}\cos\left(\frac{\pi t}{T_c}\right) p_{T_c}(t)$.

7) Full-sine: $p(t) = \sqrt{2}\sin\left(\frac{2\pi t}{T_c}\right) p_{T_c}(t)$.

Note that the first five chips are even about $T_c/2$, while the last two are odd. The "even" chip waveforms are plotted in Fig. 6.19 while the "odd" chip waveforms are shown in Fig. 6.20.

The normalized interference parameter, I, is given in Table 6.1 for all combinations of the above chip waveforms. As expected, using the even chips in combination with

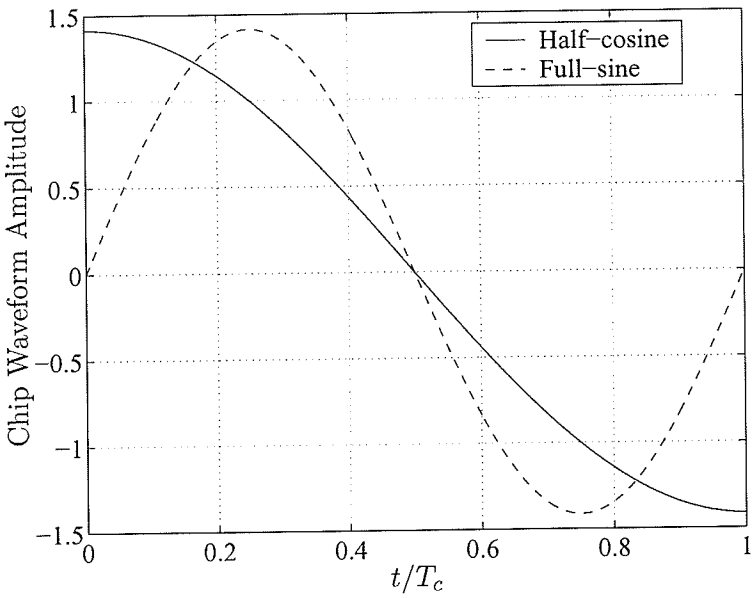

Figure 6.20: Chip waveforms that are odd about $T_c/2$.

the odd chips reduces the interference significantly (see columns 6 and 7 of Table 6.1). It is also of interest to note that using two odd chips offers lower interference compared to using two even chips. However, it should be noted from Table 6.1 that the huge reduction of interference by using odd chip waveforms comes at the expense of expanding the transmission bandwidth. As mentioned in the previous section, for a fair comparison of different chip waveform combinations, the issue of bandwidth needs to be taken into account and the quantity IWT_c is the performance measure of interest. Here the transmission bandwidth is quantified through the FOBE bandwidth criterion which is governed by Eqn. (6.23). The values of the time-bandwidth product WT_c for some typical values of η are tabulated in Table 6.2. Based on Tables 6.1 and 6.2, the parameter IWT_c is tabulated in Table 6.3.

From Table 6.3 one can see that, even when the effect of increasing the bandwidth of the odd chip is taken into account, it is still beneficial to combine the full-cosine chip (odd chip) with the even chips for most of the FOBE bandwidth criteria. The use

of two even chips offers better performance only when the requirement for fractional out-of-band power is very strict ($\eta = 0.1\%$). This is expected since, if η is very small, the FOBE bandwidth of the full-cosine chip can be very large, which eventually offsets the interference reduction. However, if an odd chip with a narrower FOBE bandwidth can be found, then the advantage of combining an odd chip with an even chip should remain even when $\eta = 0.1\%$. Another observation is that, although the half-cosine is an odd chip, it has a very large FOBE bandwidth (due to its discontinuties) when η is small ($\eta < 10\%$). Hence there is no advantage to combine this odd chip with other even chips in a system with a very strict requirement for fractional out-of-band energy.

Finally, Figs. 6.21 and 6.22 show the advantage of using double chip waveforms over a single chip waveform in terms of the bit error rate for systems with $\eta = 10\%$ and $\eta = 1\%$ respectively. The error probabilities are calculated based on the improved Gaussian approximation derived later in Chapter 7. Note that in both cases, the FOBE transmission bandwidth is selected so that the processing gain of the corresponding system using a single raised cosine waveform equals $N = 64$ (i.e., $WT = 64 \times 0.9501$ for $\eta = 10\%$ and $WT = 64 \times 1.4093$ for $\eta = 1\%$). The number of users in both systems is $K = 8$. The advantage of using double chip waveforms is clearly observed from these figures.

6.6 Chapter Summary

Two problems of designing signature waveforms and multiple chip waveforms for *asynchronous* CDMA systems have been considered in this chapter. The bandwidth constraint is explicitly taken into account in the design process so that the available bandwidth of the system is optimally utilized. Appropriate performance parameters have been derived for both design problems when correlation receivers are used. These performance parameters are expressed in terms of the Fourier transforms of

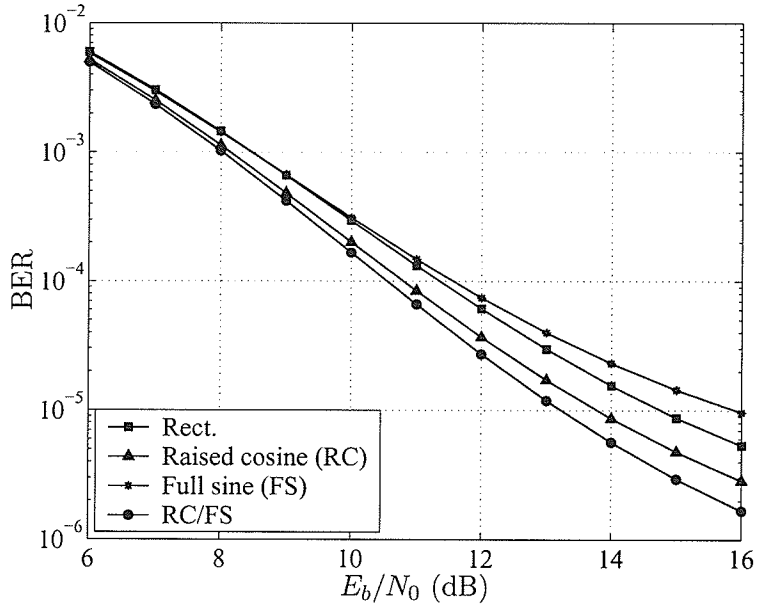

Figure 6.21: Error performance of asynchronous DS-CDMA systems using different chip waveform combinations: $K = 8$ with FOBE bandwidth of $WT = 64 \times 0.9501$, $\eta = 10\%$.

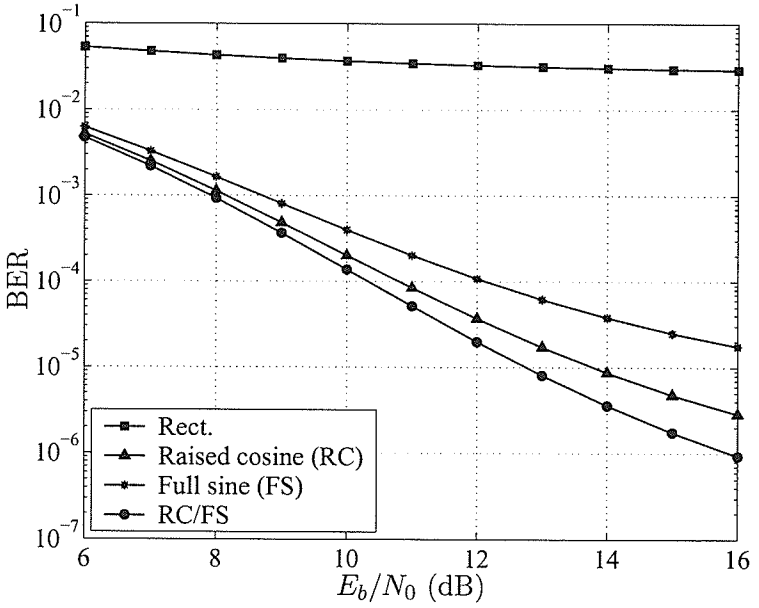

Figure 6.22: Error performance of asynchronous DS-CDMA systems using different chip waveform combinations: $K = 8$ with FOBE bandwidth $WT = 64 \times 1.4093$, $\eta = 1\%$.

Table 6.1: Values of I for all combinations of chip waveforms.

	$p_1(t)$	$p_2(t)$	$p_3(t)$	$p_4(t)$	$p_5(t)$	$p_6(t)$	$p_7(t)$
$p_1(t)$	0.3333	0.3086	0.2757	0.2537	0.2960	0.1820	0.1709
$p_2(t)$		0.2933	0.2648	0.2447	0.2826	0.1920	0.1792
$p_3(t)$			0.2406	0.2230	0.2556	0.1832	0.1744
$p_4(t)$				0.2073	0.2364	0.1746	0.1692
$p_5(t)$					0.2724	0.1889	0.1772
$p_6(t)$						0.1920	0.1877
$p_7(t)$							0.1983

$p_1(t)$–rectangular, $p_2(t)$–half-sine, $p_3(t)$–raised cosine
$p_4(t)$–Blackman, $p_5(t)$–cosine series, $p_6(t)$–half-cosine, $p_7(t)$–full-sine

the signature and chip waveforms, respectively, which facilitates the use of the series expansion method to simplify design problems. The method is most effective for the design of multiple chip waveforms since the dimensionality of the optimization problem is small and independent of the number of users. For the design of signature waveforms, the method generally involves solving an optimization problem whose dimensionality increases with the number of users. Various design examples have also been given to demonstrate the superiority of the optimally designed signature and multiple chip waveforms. In particular, it has been shown that in DS-CDMA systems with random signature sequences, either 10% of transmission bandwidth or 10% of MAI can be reduced by using two chip waveforms instead of a conventional single chip waveform. Finally, the performance investigation of combining several commonly used chip waveforms has been carried out to justify the advantage of the proposed technique. The technique of using multiple chip waveforms is very simple and can be easily accommodated in many current DS-CDMA systems.

Table 6.2: Values of WT_c for all combinations of chip waveforms and for different values of η.

(a) $\eta = 10\%$

	$p_1(t)$	$p_2(t)$	$p_3(t)$	$p_4(t)$	$p_5(t)$	$p_6(t)$	$p_7(t)$
$p_1(t)$	0.8487	0.7885	0.9432	1.0987	0.8381	1.6249	1.3257
$p_2(t)$		0.7769	0.8665	0.9523	0.8070	1.1413	1.2026
$p_3(t)$			0.9501	1.0305	0.8946	1.2029	1.2304
$p_4(t)$				1.1091	0.9784	1.3040	1.2750
$p_5(t)$					0.8366	1.1603	1.2112
$p_6(t)$						2.0669	1.4671
$p_7(t)$							1.3564

(b) $\eta = 1\%$

	$p_1(t)$	$p_2(t)$	$p_3(t)$	$p_4(t)$	$p_5(t)$	$p_6(t)$	$p_7(t)$
$p_1(t)$	10.2860	5.2471	5.2154	5.2154	4.8336	15.1610	5.3346
$p_2(t)$		1.1820	1.3490	1.5966	1.2472	10.0823	1.7272
$p_3(t)$			1.4093	1.5720	1.3811	10.0780	1.6834
$p_4(t)$				1.6805	1.6265	10.0790	1.7660
$p_5(t)$					1.3055	9.9859	1.7714
$p_6(t)$						20.1467	9.1275
$p_7(t)$							2.1971

(c) $\eta = 0.1\%$

	$p_1(t)$	$p_2(t)$	$p_3(t)$	$p_4(t)$	$p_5(t)$	$p_6(t)$	$p_7(t)$
$p_1(t)$	31.1677	31.0413	31.0410	31.0414	31.0008	63.6900	12.0099
$p_2(t)$		2.7355	2.1640	2.1662	2.4237	31.8190	3.5608
$p_3(t)$			1.7290	2.0110	2.3016	31.8191	3.4474
$p_4(t)$				2.0689	2.2778	31.8193	3.4384
$p_5(t)$					2.4046	31.8018	3.4148
$p_6(t)$						31.8750	18.2568
$p_7(t)$							4.3127

$p_1(t)$–rectangular, $p_2(t)$–half-sine, $p_3(t)$–raised cosine
$p_4(t)$–Blackman, $p_5(t)$–cosine series, $p_6(t)$–half-cosine, $p_7(t)$–full-sine

Table 6.3: Values of IWT_c for all combinations of chip waveforms and for different values of η (the bold entries highlight the best combinations).

(a) $\eta = 10\%$

	$p_1(t)$	$p_2(t)$	$p_3(t)$	$p_4(t)$	$p_5(t)$	$p_6(t)$	$p_7(t)$
$p_1(t)$	0.2829	0.2434	0.2601	0.2787	0.2481	0.2957	0.2266
$p_2(t)$		0.2279	0.2294	0.2330	0.2281	0.2191	0.2155
$p_3(t)$			0.2286	0.2298	0.2287	0.2203	**0.2146**
$p_4(t)$				0.2299	0.2313	0.2276	0.2157
$p_5(t)$					0.2279	0.2192	**0.2146**
$p_6(t)$						0.3968	0.2753
$p_7(t)$							0.2690

(b) $\eta = 1\%$

	$p_1(t)$	$p_2(t)$	$p_3(t)$	$p_4(t)$	$p_5(t)$	$p_6(t)$	$p_7(t)$
$p_1(t)$	3.4286	1.6195	1.4379	1.3230	1.4308	2.7593	0.9117
$p_2(t)$		0.3467	0.3572	0.3906	0.3524	1.9358	0.3095
$p_3(t)$			0.3390	0.3505	0.3530	1.8461	**0.2936**
$p_4(t)$				0.3483	0.3845	1.7595	0.2988
$p_5(t)$					0.3557	1.8866	0.3139
$p_6(t)$						3.8682	1.7128
$p_7(t)$							0.4358

(c) $\eta = 0.1\%$

	$p_1(t)$	$p_2(t)$	$p_3(t)$	$p_4(t)$	$p_5(t)$	$p_6(t)$	$p_7(t)$
$p_1(t)$	10.3890	9.5809	8.5580	7.8744	9.1762	11.5916	2.0525
$p_2(t)$		0.8024	0.5730	0.5300	0.6849	6.1093	0.6381
$p_3(t)$			**0.4159**	0.4485	0.5884	5.8285	0.6013
$p_4(t)$				0.4288	0.5385	5.5549	0.5817
$p_5(t)$					0.6551	6.0081	0.6051
$p_6(t)$						6.1200	3.4259
$p_7(t)$							0.8553

$p_1(t)$–rectangular, $p_2(t)$–half-sine, $p_3(t)$–raised cosine
$p_4(t)$–Blackman, $p_5(t)$–cosine series, $p_6(t)$–half-cosine, $p_7(t)$–full-sine

Chapter 7

Error Probabilities of Asynchronous DS-CDMA Systems using Random Signature Sequences

Perhaps the error probability is the most important performance index in any communication systems. It is therefore important to calculate the error probabilities of users in CDMA systems. For the synchronous CDMA systems, this has been discussed in Chapter 2 where both the exact formula and Gaussian approximation (GA) are provided. The primary purpose of this chapter is to study the error probabilities of asynchronous DS-CDMA systems using random signature sequences and the multiple chip waveforms proposed in Chapter 6.

The exact calculation of the error probabilities of asynchronous DS-CDMA communications systems is often intractable and computationally difficult due to the complexity of asynchronous CDMA systems. Thus, most previous work on this problem has concerned approximations and bounds [36, 66, 67, 33, 40, 68, 69]. Among these contributions, the approximation derived by Holtzman [40] seems very attractive since it is simple but it gives good accuracy. This approximation has been widely used [68, 70, 71] and is generally referred to as the improved Gaussian approximation (IGA). In [40] the improved GA is originally obtained and evaluated for DS-CDMA

systems using random signature sequences and a rectangular chip waveform only. It should be noted, however, that the chip waveform influences the inter-user interference, and hence the error probabilities of DS-CDMA systems. In this chapter, the Holtzman's approximation is first extended to include an arbitrary *single* chip waveform. More importantly, it is also applied to approximate the error probabilities of DS-CDMA systems using double chip waveforms[1] proposed in Chapter 6. Comparison to either an exact calculation (for the case of single chip waveform) or a simulation result (for the case of double chip waveforms) is also carried out to justify the accuracy of Holtzman's approximation.

It is acknowledged that[2] Yoon has also applied Holtzman's improved Gaussian approximation for the case of arbitrary chip waveforms [72]. More precisely the "arbitrary" chip waveforms in [72] are band-limited chip waveforms and also constrained to have no inter-chip interference (ICI) and inter-bit-symbol interference (ISI). Since the time-limited waveforms are both ICI and ISI free, the result in [72] is also applicable to the time-limited chip waveforms. However, although the work in [72] appears to be more general than the one developed in Section 7.1.1, the expression of Holtzman's improved Gaussian approximation developed here is simpler and more convenient than the one found in [72] for time-limited chip waveforms.

[1]Recall from Chapter 6 that there is a little gain by using more than double chip waveforms.

[2]The author would like to thank one of the members of the examining committee who pointed out reference [72].

7.1 Error Probabilities for DS-CDMA Systems with Single Chip Waveform

7.1.1 Holtzman's Improved Gaussian Approximation

Using the result established in [33], the decision statistic at the output of the kth correlation receiver can be written as

$$Z_k = \sqrt{P/2}b_1(0)T + \sqrt{P/2}\sum_{i=1,i\neq k}^{K} W_i \cos\varphi_i + n \tag{7.1}$$

where n is a Gaussian random variable with zero mean and variance $N_0T/4$. The random variable W_i is given by

$$W_i = \widehat{h}_1(r_i)P_i + h_1(r_i)Q_i + \left(\widehat{h}_1(r_i) + h_1(r_i)\right)X_i + \left(\widehat{h}_1(r_i) - h_1(r_i)\right)Y_i \tag{7.2}$$

recalling that, $r_i = \tau_i - l_iT_c$, $l_i = \lfloor \tau_i/T_c \rfloor$ and that these random variables are uniformly distributed over $[0, T_c)$ and $\{0, 1, \ldots, N-1\}$ respectively. In (7.2), the functions $h_1(r)$ and $\widehat{h}_1(r)$ are the continuous-time, partial autocorrelation of the *single* chip waveform, $g_1(t)$. The function $\widehat{h}_1(r)$ was defined in Chapter 6 as $\widehat{h}_1(r) = \int_r^{T_c} g_1(t)g_1(t-r)\mathrm{d}t$, and $h_1(r) = \widehat{h}_1(T_c - r)$ for $0 \leq r \leq T_c$. The random variables P_i and Q_i are uniform on $\{0, 1\}$. The densities of X_i and Y_i are given in [33] but only their first and second moments are needed in deriving the improved GA. Another important observation is that W_i depends on r_i, φ_i and a random variable $|B|$, which represents the number of chip boundaries in the signature sequence of the first user (where a transition to a different value occurs)[3]. Furthermore, given $|B|$, the random variables P_i, Q_i, X_i and Y_i are conditionally independent.

The second term of (7.1) is the multiple access interference (MAI). The most straightforward approximation to the error probabilities is the standard GA, where the MAI is approximated by a Gaussian random variable. Using a Gaussian approximation, the error probability is given by $P_e^G = Q\left(\sqrt{\mathrm{SIR}}\right)$, where SIR is the

[3]More precisely, $|B|$ is the cardinality of the set B which is defined in [33].

signal-to-interference ratio at the output of the correlation receiver. The standard GA is clearly very simple but is not accurate, in general. As will be seen later, it is very optimistic when the signal to noise ratio increases.

Let $\mathbf{r} = [r_1, r_2 \ldots, r_K]$, $\boldsymbol{\varphi} = [\varphi_1, \varphi_2, \ldots, \varphi_K]$ and $\Psi \equiv \text{var}\,(\text{MAI}|\mathbf{r}, \boldsymbol{\varphi}, |B|)$. Since Ψ is a function of $\mathbf{r}$, $\boldsymbol{\varphi}$ and $|B|$, Ψ can be thought of as a random variable. Let μ and σ be the mean and standard deviation of Ψ, then the Holtzman's improved GA for the error probabilities is as follows [40].

$$\begin{aligned} P_e^H = & \frac{2}{3} Q\left(\left[\gamma_e^{-1} + 2\mu/(PT^2)\right]^{-1/2}\right) \\ & + \frac{1}{6} Q\left(\left[\gamma_e^{-1} + 2(\mu + \sqrt{3}\sigma)/(PT^2)\right]^{-1/2}\right) \\ & + \frac{1}{6} Q\left(\left[\gamma_e^{-1} + 2(\mu - \sqrt{3}\sigma)/(PT^2)\right]^{-1/2}\right) \end{aligned} \tag{7.3}$$

where $E_b = PT$ is the energy per symbol and $\gamma_e = \frac{2E_b}{N_0}$. One disadvantage of Holtzman's IGA is that μ can be smaller than $\sqrt{3}\sigma$ (depending on the particular values of N and K) and therefore the last term in (7.3) cannot be evaluated. Nevertheless, as μ and $\sqrt{3}\sigma$ approach equality, the last term goes to zero and the second term becomes dominant. In this chapter the last term of (7.3) is set to zero whenever $\mu \leq \sqrt{3}\sigma$.

The mean and standard deviation of Ψ can be found as follows. Recall that the random variables P_i, Q_i, X_i and Y_i are conditionally independent, given $|B|$. Furthermore, these random variables have zero mean and variances $E(P_i^2) = E(Q_i^2) = 1$, $E(X_i^2||B|) = N - |B| - 1$, $E(Y_i^2||B|) = |B|$. Thus it can be shown from (7.2) that $\Psi = \sum_{i=1, i\neq k}^{K} L_i$, where

$$L_i = \frac{P}{4}\left[1 + \cos(2\varphi_i)\right]\left[N\left(\widehat{h}_1^2(r_i) + h_1^2(r_i)\right) + 2(N - 1 - 2|B|)\widehat{h}_1(r_i)h_1(r_i)\right] \tag{7.4}$$

are identically distributed and conditionally independent random variables, given $|B|$. Now from the fact that the random variables $\mathbf{r}$ and $\boldsymbol{\varphi}$ are statistically independent

and $E(|B|) = (N-1)/2$, $E(|B|^2) = N(N-1)/4$, it follows that

$$\mu = \frac{(K-1)PT^2}{2N} m_1 \tag{7.5}$$

and

$$\sigma = \frac{PT^2}{2N}(K-1)^{1/2}\left[\frac{3}{8}w_1 + \frac{3(N-1)}{2N^2}\widehat{w}_1 - m_1^2 + \frac{(K-2)(N-1)}{N^2}\widehat{m}_1^2\right]^{1/2} \tag{7.6}$$

where

$$m_1 = \frac{1}{T_c^3}\int_0^{T_c} h_1^2(r)\mathrm{d}r = \frac{1}{T_c^3}\int_0^{T_c} \widehat{h}_1^2(r)\mathrm{d}r \tag{7.7}$$

$$\widehat{m}_1 = \frac{1}{T_c^3}\int_0^{T_c} \widehat{h}_1(r)h_1(r)\mathrm{d}r \tag{7.8}$$

$$w_1 = \frac{1}{T_c^5}\int_0^{T_c} \left[\widehat{h}_1^2(r) + h_1^2(r)\right]^2 \mathrm{d}r \tag{7.9}$$

$$\widehat{w}_1 = \frac{1}{T_c^5}\int_0^{T_c} \widehat{h}_1^2(r)h_1^2(r)\mathrm{d}r. \tag{7.10}$$

All the above correlation parameters of the chip waveform are normalized so that they are independent of the chip duration, T_c. Also note that the standard GA is the first term in (7.3) without the scaling factor 2/3, i.e.,

$$P_e^G = Q\left(\left[\gamma_e^{-1} + \frac{K-1}{N}m_1\right]^{-1/2}\right). \tag{7.11}$$

This standard GA is also given in [34].

7.1.2 Exact Calculation

To evaluate the accuracy of both the standard and improved GAs discussed in the previous sub-section, the exact error probability derived in [34] is employed and reproduced below.

$$P_e = Q\left(\gamma_e^{1/2}\right) + \pi^{-1}\int_0^{\infty} u^{-1}\sin u \cdot \exp\left[-u^2/(2\gamma_e)\right]\left[1 - \overline{\phi}(u)\right]\mathrm{d}u \tag{7.12}$$

where

$$\overline{\phi}(u) = 2^{1-N} \sum_{n=0}^{N-1} \binom{N-1}{n} [\Phi_{N,n}(u)]^{K-1} \tag{7.13}$$

$$\Phi_{N,n}(u) = \frac{4}{\pi T_c} \int_0^{\pi/2} \int_0^{T_c/2} f(N,n,u;r,\theta) \mathrm{d}r\mathrm{d}\theta \tag{7.14}$$

$$\begin{aligned} f(N,n,u;r,\theta) &= \cos\left[\frac{u}{T} h_1(r)\cos\theta\right] \cos\left[\frac{u}{T}\widehat{h}_1(r)\cos\theta\right] \\ &\quad \cdot \cos^n\left\{\frac{u}{T}\left[h_1(r)+\widehat{h}_1(r)\right]\cos\theta\right\} \\ &\quad \cdot \cos^{N-n-1}\left\{\frac{u}{T}\left[h_1(r)-\widehat{h}_1(r)\right]\cos\theta\right\}. \end{aligned} \tag{7.15}$$

Although (7.12) is exact, only an approximation to P_e can be calculated due to the fact that the definite integral in (7.12) extends to infinity. However, since any desirable value of the truncation and integration errors can be achieved, the results obtained via (7.12) are usually referred to as "exact" [34].

7.1.3 Numerical Examples

In this section the accuracy of the standard GA and Holtzman's improved GA are evaluated for some of the common chip waveforms given in Section 6.5.

1) Rectangular pulse: $g_1(t) = p_{T_c}(t)$. For this waveform one has $h_1(r) = r$, $\widehat{h}_1(r) = T_c - r$, $m_1 = 1/3$, $\widehat{m}_1 = 1/6$, $w_1 = 7/15$ and $\widehat{w}_1 = 1/30$.

2) Half-sine: $g_1(t) = \sqrt{2}\sin\left(\frac{\pi t}{T_c}\right) p_{T_c}(t)$. The autocorrelation functions of this chip waveform are

$$h_1(r) = -r\cos\left(\frac{\pi r}{T_c}\right) + \frac{T_c}{\pi}\sin\left(\frac{\pi r}{T_c}\right) \tag{7.16}$$

$$\widehat{h}_1(r) = (T_c - r)\cos\left(\frac{\pi r}{T_c}\right) + \frac{T_c}{\pi}\sin\left(\frac{\pi r}{T_c}\right) \tag{7.17}$$

and $m_1 = 5/(4\pi^2) + 1/6$, $\widehat{m}_1 = 5/(4\pi^2) - 1/12$.

3) Raised Cosine: $g_1(t) = \sqrt{\frac{2}{3}}\left[1 - \cos\left(\frac{2\pi t}{T_c}\right)\right] p_{T_c}(t)$. It can be shown that the autocorrelations of this waveform are

$$h_1(r) = \frac{2}{3}r + \frac{1}{3}r\cos\left(\frac{2\pi r}{T_c}\right) - \frac{T_c}{2\pi}\sin\left(\frac{2\pi r}{T_c}\right) \tag{7.18}$$

$$\widehat{h}_1(r) = \frac{2}{3}(T_c - r) + \frac{1}{3}(T_c - r)\cos\left(\frac{2\pi r}{T_c}\right) + \frac{T_c}{2\pi}\sin\left(\frac{2\pi r}{T_c}\right) \tag{7.19}$$

and $m_1 = 1/6 + 35/(48\pi^2)$, $\widehat{m}_1 = 1/12 - 35/(48\pi^2)$.

4) Blackman: $g_1(t) = c\left[k_1 - k_2\cos\left(\frac{2\pi t}{T_c}\right) + k_3\cos\left(\frac{4\pi t}{T_c}\right)\right] p_{T_c}(t)$, where $c^2 = (k_1^2 + k_2^2/2 + k_3^2/2)^{-1}$ and $k_1 = 0.42$, $k_2 = 0.5$ and $k_3 = 0.08$. The partial autocorrelations of the Blackman chip are as follows:

$$\begin{aligned} h_1(r) = c^2\Bigg[& k_1^2 r + \frac{k_2^2 r}{2}\cos\left(\frac{2\pi r}{T_c}\right) + \frac{k_3^2 r}{2}\cos\left(\frac{4\pi r}{T_c}\right) - \frac{k_1 k_2 T_c}{\pi}\sin\left(\frac{2\pi r}{T_c}\right) \\ & + \frac{k_2^2 T_c}{4\pi}\sin\left(\frac{2\pi r}{T_c}\right) + \frac{k_2 k_3 T_c}{3\pi}\sin\left(\frac{2\pi r}{T_c}\right) + \frac{k_1 k_3 T_c}{2\pi}\sin\left(\frac{4\pi r}{T_c}\right) \\ & - \frac{2k_2 k_3 T_c}{3\pi}\sin\left(\frac{4\pi r}{T_c}\right) + \frac{k_3^2 T_c}{8\pi}\sin\left(\frac{4\pi r}{T_c}\right)\Bigg] \end{aligned} \tag{7.20}$$

$$\begin{aligned} \widehat{h}_1(r) = c^2\Bigg[& k_1^2(T_c - r) + \frac{k_2^2}{2}(T_c - r)\cos\left(\frac{2\pi r}{T_c}\right) + \frac{k_3^2}{2}(T_c - r)\cos\left(\frac{4\pi r}{T_c}\right) \\ & + \frac{k_1 k_2 T_c}{\pi}\sin\left(\frac{2\pi r}{T_c}\right) - \frac{k_2^2 T_c}{4\pi}\sin\left(\frac{2\pi r}{T_c}\right) - \frac{k_2 k_3 T_c}{3\pi}\sin\left(\frac{2\pi r}{T_c}\right) \\ & - \frac{k_1 k_3 T_c}{2\pi}\sin\left(\frac{4\pi r}{T_c}\right) + \frac{2k_2 k_3 T_c}{3\pi}\sin\left(\frac{4\pi r}{T_c}\right) - \frac{k_3^2 T_c}{8\pi}\sin\left(\frac{4\pi r}{T_c}\right)\Bigg] \end{aligned} \tag{7.21}$$

Table 7.1: Correlation parameters for different chip waveforms.

Waveform	m_1	$\widehat{m}_1$	w_1	$\widehat{w}_1$
Rectangular	3.333E-1	1.667E-1	4.667E-1	3.333E-2
Half-sine	2.933E-1	4.332E-2	4.229E-1	3.237E-3
Raised cosine	2.406E-1	9.453E-3	3.437E-1	1.904E-4
Blackman	2.073E-1	2.553E-3	2.949E-1	1.475E-5

and the correlation parameters m_1 and $\widehat{m}_1$ are given by

$$\begin{aligned} m_1 &= c^4[576k_1^3(4k_2-k_3)+608k_2^3k_3+960k_2^2k_3^2+32k_2k_3^3 \\ &\quad +432k_1^2(4k_2^2+k_3^2)-72k_1(4k_2^3+16k_2^2k_3+16k_2k_3^2-k_3^3) \\ &\quad +768k_1^4\pi^2+12k_2^4(3+8\pi^2)+3k_3^4(3+32\pi^2)]/(2304\pi^2) \qquad (7.22) \\ \widehat{m}_1 &= c^4[-576k_1^3(4k_2-k_3)-608k_2^3k_3-960k_2^2k_3^2-32k_2k_3^3 \\ &\quad -432k_1^2(4k_2^2+k_3^2)+72k_1(4k_2^3+16k_2^2k_3+16k_2k_3^2-k_3^3) \\ &\quad +384k_1^4\pi^2+12k_2^4(-3+4\pi^2)+3k_3^4(-3+16\pi^2)]/(2304\pi^2). \qquad (7.23) \end{aligned}$$

Since obtaining the exact expressions of w_1 and $\widehat{w}_1$ for the half-sine, raised-cosine and Blackman waveforms is tedious, the values of these parameters are evaluated numerically. They are listed in Table 7.1.

The standard GA, Holtzman's improved GA and the exact calculation of the error probabilities have been evaluated for DS-CDMA systems using the above chip waveforms and different values of N and K. For brevity of presentation, only the numerical results for systems with $N = 31$; $K = 3$ and $N = 63$; $K = 6$ are presented in Tables 7.2 and 7.3 respectively. As can be seen from these tables, the standard GA is very conservative for high signal-to-noise ratios ($E_b/N_0 \geq 8$dB), whereas the accuracy of Holtzman's improved GA should be acceptable for most values of the signal-to-noise ratio. In general, the accuracy of the standard GA improves as the number of users increases [67]. This is also observed from Tables 7.2 and 7.3. Comparing

the different chip waveforms under consideration shows that the Blackman chip gives the best performance, followed by the raised cosine, the half-sine and the rectangular chips. However, it should be noted that this comparison is on the basis of an equal processing gain N, not an equal transmission bandwidth. For the latter case, the reader is referred to Section 6.5.

Table 7.2: Error probabilities of a DS-CDMA system: $K = 3$ and $N = 31$.

	Rectangular			Half-sine			Raised cosine			Blackman			
E_b/N_0	P_e^G	P_e^H	P_e	P_e^G	P_e^H	P_e	P_e^G	P_e^H	P_e	P_e^G	P_e^H	P_e	
2	4.248	4.248	4.248	4.188	4.188	4.188	4.109	4.109	4.109	4.060	4.060	4.060	$(\times 10^{-2})$
4	1.662	1.666	1.666	1.610	1.616	1.615	1.543	1.549	1.548	1.502	1.507	1.507	$(\times 10^{-2})$
6	4.563	4.667	4.660	4.263	4.380	4.373	3.883	3.999	3.993	3.653	3.765	3.759	$(\times 10^{-3})$
8	8.150	9.166	9.104	7.073	8.154	8.133	5.801	6.809	6.814	5.083	6.012	6.030	$(\times 10^{-4})$
10	0.921	1.430	1.406	0.698	1.196	1.217	0.468	0.878	0.922	0.356	0.702	0.755	$(\times 10^{-4})$
12	0.707	2.333	2.241	0.427	1.866	2.014	0.202	1.197	1.429	0.119	0.854	1.106	$(\times 10^{-5})$
14	0.446	5.067	4.500	0.194	3.921	4.464	0.054	2.186	3.137	0.021	1.373	2.299	$(\times 10^{-6})$

(P_e^G: Gaussian approximation, P_e^H: Holtzman's approximation, P_e: Exact calculation)

Table 7.3: Error probabilities of a DS-CDMA system: $K = 6$ and $N = 63$.

	Rectangular			Half-sine			Raised cosine			Blackman			
E_b/N_0	P_e^G	P_e^H	P_e	P_e^G	P_e^H	P_e	P_e^G	P_e^H	P_e	P_e^G	P_e^H	P_e	
2	4.362	4.362	4.362	4.289	4.289	4.289	4.192	4.192	4.192	4.131	4.131	4.131	$(\times 10^{-2})$
4	1.761	1.764	1.764	1.697	1.700	1.700	1.614	1.617	1.617	1.562	1.565	1.565	$(\times 10^{-2})$
6	5.166	5.227	5.225	4.775	4.844	4.841	4.282	4.351	4.349	3.985	4.052	4.050	$(\times 10^{-3})$
8	10.496	11.144	11.123	8.948	9.638	9.630	7.140	7.785	7.785	6.133	6.727	6.731	$(\times 10^{-4})$
10	1.493	1.866	1.859	1.103	1.466	1.474	0.711	1.006	1.021	0.524	0.770	0.788	$(\times 10^{-4})$
12	1.647	3.051	3.041	0.974	2.172	2.251	0.442	1.230	1.332	0.250	0.809	0.991	$(\times 10^{-5})$
14	1.706	6.207	6.197	0.747	4.085	4.481	0.205	1.923	2.359	0.078	1.083	1.475	$(\times 10^{-6})$

(P_e^G: Gaussian approximation, P_e^H: Holtzman's approximation, P_e: Exact calculation)

7.2 Error Probabilities for DS-CDMA Systems with Double Chip Waveforms

7.2.1 Holtzman's Improved Gaussian Approximation

For DS-CDMA systems using double chip waveforms, the output of the kth correlation receiver is also given as in (7.1). As shown in Appendix G, the random variables W_i can be expressed in one of the following two forms, depending whether l_i is even or not. If l_i is *even* then

$$\begin{aligned} W_i = W_i^e &= X_i\left[\widehat{h}_2(r_i) + h_{1,2}(r_i)\right] + Y_i\left[\widehat{h}_2(r_i) - h_{1,2}(r_i)\right] \\ &+ P_i\widehat{h}_2(r_i) + Q_i h_{1,2}(r_i) \\ &+ U_i\left[h_{2,1}(r_i) + \widehat{h}_1(r_i)\right] + V_i\left[h_{2,1}(r_i) - \widehat{h}_1(r_i)\right]. \end{aligned} \tag{7.24}$$

On the other hand if l_i is *odd*, one has

$$\begin{aligned} W_i = W_i^o &= X_i\left[\widehat{h}_{2,1}(r_i) + h_1(r_i)\right] + Y_i\left[\widehat{h}_{2,1}(r_i) - h_1(r_i)\right] \\ &+ P_i\widehat{h}_{2,1}(r_i) + Q_i h_1(r_i) \\ &+ U_i\left[h_2(r_i) + \widehat{h}_{1,2}(r_i)\right] + V_i\left[h_2(r_i) - \widehat{h}_{1,2}(r_i)\right]. \end{aligned} \tag{7.25}$$

In (7.24) and (7.25), the continuous partial cross-correlation functions between the two chip waveforms are defined as follows

$$h_{m,n}(r) = \int_0^r g_m(t)g_n(t + T_c - r)\mathrm{d}t \tag{7.26}$$

$$\widehat{h}_{m,n}(r) = \int_r^{T_c} g_m(t)g_n(t - r)\mathrm{d}t \tag{7.27}$$

for $m, n \in \{1, 2\}$ and for $0 \le r \le T_c$. Also denote $h_m(r) = h_{m,n}(r)$ and $\widehat{h}_m(r) = \widehat{h}_{m,n}(r)$ when $m = n$. Moreover, it is important to note that $h_{m,n}(r) = \widehat{h}_{n,m}(T_c - r)$ and therefore one has the following useful identity

$$\int_0^{T_c} h_{m,n}^k(r)\widehat{h}_{p,q}^l(r)\mathrm{d}r = \int_0^{T_c} \widehat{h}_{n,m}^k(r)h_{q,p}^l(r)\mathrm{d}r \tag{7.28}$$

where $m, n, p, q \in \{1, 2\}$ and k, l are any (positive) integer number.

From the definitions of the random variables X_i, Y_i, P_i, Q_i, U_i and Y_i given in Appendix G, it is not hard to see that these random variables are mutually independent given $|B|$ and $|D|$ (which, respectively, are the cardinalities of sets B and D defined in Appendix G). Furthermore, the random variables W_i^e and W_i^o, $i = 1, \ldots, k-1, k+1, \ldots, K$ are also mutually independent. This follows from the fact that these random variables are functions of elements in disjoint subsets of mutually independent random variables [33]. The random variables P_i and Q_i are uniformly distributed over $\{0, 1\}$. Given $|B|$ and $|D|$, the density functions of X_i, Y_i, U_i and V_i can be determined by elementary combinatorial arguments [33] but they are not needed in deriving Holtzman's approximation for double chip waveforms. Only the first and second moments of these random variables are important and they are given by $E(X_i) = E(Y_i) = E(U_i) = E(V_i) = 0$, $E(X_i^2) = |A| = N/2 - |B| - 1$, $E(Y_i^2) = |B|$, $E(U_i^2) = |C| = N/2 - |D|$, $E(V_i^2) = |D|$. Furthermore, the first and second moments of $|B|$ and $|D|$ can be shown to be $E(|B|) = (N-2)/4$, $E(|B|^2) = N(N-2)/16$, $E(|D|) = N/4$ and $E(|D|^2) = N(N+2)/16$.

As in Section 7.1.1, define $\Psi \equiv \text{var}\,(\text{MAI}|\mathbf{r}, \boldsymbol{\varphi}, |B|, |D|)$ and let μ and σ be the mean and standard deviation of Ψ, respectively. Then the Holtzman's approximation to calculate the error probabilities of DS-CDMA systems using double chip waveforms is exactly the same as that used in (7.3). Thus it remains to determine μ and σ. The random variable Ψ can be written as $\Psi = \sum_{i=1, i\neq k}^{K} L_i$, where

$$L_i = \frac{P}{4}[1 + \cos(2\varphi_i)]\text{var}\,(W_i|r_i, |B|, |D|)\,. \tag{7.29}$$

Note that the random variables L_is are identically distributed and conditionally independent, given $|B|$ and $|D|$. Let $\alpha_i = \text{var}\,(W_i^e|r_i, |B|, |D|)$ and $\beta_i = \text{var}\,(W_i^o|r_i, |B|, |D|)$.

Then it can be shown that

$$\begin{aligned}
\alpha_i &= \frac{N}{2}\left[\widehat{h}_2^2(r_i)+h_{1,2}^2(r_i)\right]+2\left(\frac{N}{2}-1-2|B|\right)\widehat{h}_2(r_i)h_{1,2}(r_i) \\
&+ \frac{N}{2}\left[\widehat{h}_1^2(r_i)+h_{2,1}^2(r_i)\right]+2\left(\frac{N}{2}-2|D|\right)\widehat{h}_1(r_i)h_{2,1}(r_i) \qquad (7.30)\\
\beta_i &= \frac{N}{2}\left[\widehat{h}_{2,1}^2(r_i)+h_1^2(r_i)\right]+2\left(\frac{N}{2}-1-2|B|\right)\widehat{h}_{2,1}(r_i)h_1(r_i) \\
&+ \frac{N}{2}\left[\widehat{h}_{1,2}^2(r_i)+h_2^2(r_i)\right]+2\left(\frac{N}{2}-2|D|\right)\widehat{h}_{1,2}(r_i)h_2(r_i). \qquad (7.31)
\end{aligned}$$

Since l_i takes even or odd integers of the set $\{0,1,\ldots,N-1\}$ with the same probability, var $(W_i|r_i,|B|,|D|)$ equals α_i or β_i with probability $1/2$.

Now the mean of Ψ can be obtained by averaging over the random variables φ_i, r_i, $|B|$ and $|D|$. It is given by

$$\begin{aligned}
\mu &= \sum_{i=1,i\neq k}^{K} E(L_i) = (K-1)E(L_i) \\
&= \frac{(K-1)PT^2}{16N}\frac{1}{T_c^3}\int_0^{T_c}\Big[\widehat{h}_1^2(r)+\widehat{h}_2^2(r)+\widehat{h}_{1,2}^2(r)+\widehat{h}_{2,1}^2(r) \\
&\quad +h_1^2(r)+h_2^2(r)+h_{1,2}^2(r)+h_{2,1}^2(r)\Big]\mathrm{d}r \\
&= \frac{(K-1)PT^2}{8N}\frac{1}{T_c^3}\int_0^{T_c}\left[h_1^2(r)+h_2^2(r)+\widehat{h}_{1,2}^2(r)+\widehat{h}_{2,1}^2(r)\right]\mathrm{d}r \qquad (7.32)
\end{aligned}$$

where the last equality follows from (7.28). Define

$$m_2 = \frac{1}{4T_c^3}\int_0^{T_c}\left[h_1^2(r)+h_2^2(r)+\widehat{h}_{1,2}^2(r)+\widehat{h}_{2,1}^2(r)\right]\mathrm{d}r. \qquad (7.33)$$

Then it follows from (6.13) and (7.28) that $m_2 = \frac{1}{4T_c^3}\int_0^{T_c}\left(\widehat{h}_1(r)+\widehat{h}_2(r)\right)^2\mathrm{d}r$, which is precisely the normalized interference parameter, I, defined in Section 6.1.2. Now the mean of Ψ can be written as

$$\mu = \frac{(K-1)PT^2}{2N}m_2 \qquad (7.34)$$

which is the same form as in (7.5) for the case of single chip waveform. The variance of Ψ is calculated as follows

$$\begin{aligned}\sigma^2 &= E(\Psi^2) - \mu^2 \\ &= (K-1)E(L_i^2) + (K-1)(K-2)E(L_iL_j) - \mu^2 \end{aligned} \tag{7.35}$$

where i and j are any index not equal to k and not equal to each other. The second moment of L_i is given by

$$E(L_i^2) = \frac{3P^2}{64}\left[E(\alpha_i^2) + E(\beta_i^2)\right] = \frac{3(PT^2)^2}{128N^2}w_N \tag{7.36}$$

where the parameter w_N depends on N and it is given in (H.4) of Appendix H. The correlation between L_i and L_j $(i \neq j)$ is given by

$$E(L_iL_j) = \frac{P^2}{64}\left[E(\alpha_i\alpha_j) + E(\alpha_i\beta_j) + E(\beta_i\alpha_j) + E(\beta_i\beta_j)\right] = \frac{(PT^2)^2}{256N^2}\widehat{w}_N \tag{7.37}$$

where $\widehat{w}_N$ is given in (I.7) of Appendix I[4]. Now, combining (7.34), (7.36) and (7.37), one has

$$\sigma = \frac{PT^2}{16N}(K-1)^{1/2}\left[6w_N + (K-2)\widehat{w}_N - 64(K-1)m_2^2\right]^{1/2}. \tag{7.38}$$

Though the expressions for μ and σ obtained above appear to be complicated, they are quite simple to evaluate. Also note that, although there are eight possible correlation functions that can be defined for the two chip waveforms, only four of them are needed in the evaluation of μ and σ. Furthermore, if the chip waveforms $g_1(t)$ and $g_2(t)$ posses an (even or odd) symmetry about $T_c/2$, then only three correlation functions are required and the expressions for w_N and $\widehat{w}_N$ significantly simplify to (H.6) and (I.8), respectively. Finally, it is not hard to see that (7.34) and (7.38) reduce to (7.5) and (7.6), respectively, when the two chip waveforms are identical, i.e., $g_1(t) = g_2(t)$.

[4]Note that m_2, w_N and $\widehat{w}_N$ have all been normalized to be independent of the chip duration, T_c.

7.2.2 Numerical Examples

This section evaluates the accuracy of Holtzman's improved Gaussian approximation derived in the previous section for the case of double chip waveforms. The combinations of two chip waveforms selected are "rectangular/half-sine", "rectangular/raised-cosine" and "rectangular/Blackman". Since the exact calculation of the error probability for the case of double chip waveforms is not available, the results produced by standard GA and improved GA are compared with simulation results. The error probabilities obtained by different methods are listed in Tables 7.4 and 7.5 for two systems with $K = 3$; $N = 32$ and $K = 6$; $N = 64$ respectively.

From Tables 7.4 and 7.5, similar observations as for the case of a single chip waveform can be made regarding the accuracy of the standard GA and improved GA when the double chip waveforms are used. More specifically, the accuracy of the improved GA is acceptable for all the signal-to-noise ratios, whereas the standard GA is quite loose for $E_b/N_0 \geq 8$dB. As for the single chip waveform, the improved GA for double chip waveforms is clearly very simple to use once the double chip waveforms are specified. This improved GA was used in Section 6.5 to evaluate the error performances of different combinations of double chip waveforms.

7.3 Chapter Summary

This chapter extends Holtzman's improved Gaussian approximation of error probability in asynchronous DS-CDMA systems to include both arbitrary single and double chip waveforms. The accuracy of the approximation has also been verified by either exact calculation or simulation results. Due to its simplicity and accuracy, the improved GA is very attractive for evaluating the error performance of the asynchronous DS-CDMA systems using the random signature sequences and multiple chip waveforms proposed in Chapter 6.

Table 7.4: Error probabilities of DS-CDMA systems with double chip waveforms: $K = 3$ and $N = 32$.

	Rect./Half-sine				Rect./Raised cosine				Rect./Blackman			
E_b/N_0	P_e^G	P_e^H	P_e		P_e^G	P_e^H	P_e		P_e^G	P_e^H	P_e	
2	4.196	4.196	4.226	$(\times 10^{-2})$	4.149	4.149	4.152	$(\times 10^{-2})$	4.117	4.117	4.124	$(\times 10^{-2})$
4	1.617	1.622	1.644	$(\times 10^{-2})$	1.577	1.581	1.611	$(\times 10^{-2})$	1.550	1.553	1.593	$(\times 10^{-2})$
6	4.305	4.397	4.399	$(\times 10^{-3})$	4.072	4.152	4.205	$(\times 10^{-3})$	3.920	3.992	3.983	$(\times 10^{-3})$
8	7.220	8.079	8.113	$(\times 10^{-4})$	6.420	7.143	7.256	$(\times 10^{-4})$	5.919	6.557	6.516	$(\times 10^{-4})$
10	0.727	1.125	1.159	$(\times 10^{-4})$	5.746	8.848	9.122	$(\times 10^{-5})$	4.874	7.457	7.832	$(\times 10^{-5})$
12	0.460	1.581	1.620	$(\times 10^{-5})$	0.298	1.062	1.154	$(\times 10^{-5})$	2.184	7.930	9.091	$(\times 10^{-6})$
14	0.220	2.939	3.213	$(\times 10^{-6})$	0.106	1.661	1.712	$(\times 10^{-6})$	0.062	1.084	1.231	$(\times 10^{-6})$

(P_e^G: Gaussian approximation, P_e^H: Holtzman's approximation, P_e: Simulation)

Table 7.5: Error probabilities of DS-CDMA systems with double chip waveforms: $K = 6$ and $N = 64$.

	Rect./Half-sine				Rect./Raised cosine				Rect./Blackman			
E_b/N_0	P_e^G	P_e^H	P_e		P_e^G	P_e^H	P_e		P_e^G	P_e^H	P_e	
2	4.308	4.308	4.421	$(\times 10^{-2})$	4.248	4.248	4.290	$(\times 10^{-2})$	4.209	4.209	4.282	$(\times 10^{-2})$
4	1.714	1.716	1.815	$(\times 10^{-2})$	1.662	1.664	1.718	$(\times 10^{-2})$	1.628	1.630	1.648	$(\times 10^{-2})$
6	4.876	4.932	4.796	$(\times 10^{-3})$	4.567	4.616	4.662	$(\times 10^{-3})$	4.366	4.410	4.471	$(\times 10^{-3})$
8	9.339	9.906	10.021	$(\times 10^{-4})$	8.164	8.642	8.657	$(\times 10^{-4})$	7.435	7.856	8.034	$(\times 10^{-4})$
10	1.197	1.503	1.476	$(\times 10^{-4})$	0.925	1.161	1.119	$(\times 10^{-4})$	7.699	9.662	9.491	$(\times 10^{-5})$
12	1.124	2.153	2.242	$(\times 10^{-5})$	0.712	1.407	1.424	$(\times 10^{-5})$	0.511	1.031	1.104	$(\times 10^{-5})$
14	0.938	3.811	4.356	$(\times 10^{-6})$	0.450	2.070	2.432	$(\times 10^{-6})$	0.262	1.314	1.223	$(\times 10^{-6})$

(P_e^G: Gaussian approximation, P_e^H: Holtzman's approximation, P_e: Simulation)

Chapter 8

Conclusions and Suggestions for Further Study

8.1 Conclusions

This thesis was mainly devoted to signature waveform design to minimize the MAI (or maximize the number of users for a given MAI level) in CDMA systems under a bandwidth constraint. For synchronous CDMA systems, closed-form solutions were obtained for the optimal signature waveforms under either FOBE or RMS bandwidth constraints. In general, the optimal signature waveforms were constructed based on sinusoids when the RMS bandwidth is considered, whereas they were constructed from prolate spheroidal wave functions under the FOBE bandwidth criterion. Comparisons to other signature waveform constructions showed significant improvements of the proposed signature waveforms, both in terms of the network capacity and the bit error rate performance. Due to the complexity of the receiver working with prolate spheroidal wave functions, a simplified receiver based on Walsh signal space was also developed for a more practical implementation. It was shown that, by using a relatively small number of Walsh functions, the performance of the simplified receiver can approach very closely that of the true receiver.

Signature waveform design was also carried out for asynchronous CDMA systems

equipped with correlation receivers. The design procedure was based on the series expansion method. For the FOBE bandwidth constraint, it is suggested that the prolate spheroidal wave functions be used to expand the Fourier transforms of the optimal signature waveforms. On the other hand, sinusoids were used to expand the optimal signature waveforms under the RMS bandwidth criterion. Although several examples were given to demonstrate the superiority of the proposed signature waveforms, this method is quite time consuming, in general, for systems with a large number of users. Nevertheless, the method was successfully applied to find the optimal multiple chip waveforms to minimize the MAI in asynchronous DS-CDMA systems using random signature sequences. It was demonstrated that using double chip waveforms instead of a single chip waveform can reduce the MAI by about 10% (corresponding to about 2.0dB gain in E_b/N_0 for a BER level of 10^{-4} to 10^{-5}) for a given bandwidth, or conversely save about 10% of the transmission bandwidth for a given MAI level.

Finally, to evaluate the error performance of the proposed DS-CDMA systems using random signature sequences and double chip waveforms, an expression for error probabilities was developed based on Holtzman's approximation. Since the derived expression is very simple and accurate, it is very useful for a performance analysis of the proposed DS-CDMA systems.

8.2 Suggestions for Further Study

The signature waveform designs have only been considered for additive white Gaussian noise (AWGN) CDMA channels in this thesis. Since a fading channel is a more practical model for wireless communications, it would be interesting to extend the designs to fading CDMA channels. Furthermore, in both synchronous and asynchronous CDMA systems, it has been assumed that perfect power control can be implemented. This assumption can be easily removed for the design of multiple chip waveforms for DS-CDMA systems but not for the designs of the signature waveforms (for both

synchronous and asynchronous CDMA systems) considered in this thesis. Therefore, designing optimal signature waveforms for CDMA systems with arbitrary received power levels of all users remains to be studied.

The signature and chip waveforms considered in this thesis are limited to the family of time-limited waveforms. Because most of practical systems use band-limited waveforms (such as the square root raised cosine), it is natural to extend the ideas elaborated in this work to include the family of band-limited waveforms. Such extension would benefit the systems proposed for 3G (IMT2000, UMTS, etc.,).

In this thesis, the accuracy of the derived approximation of the error probability for the case of double chip waveforms was verified with a computer simulation. It would be useful to obtain an exact expression of the error probabilities in this case. Moreover, a semi-analytical approach combined with *importance sampling*, as in [69], can be developed for an efficient evaluation of the error probabilities for DS-CDMA systems with double chip waveforms.

Recently, the technique of multicarrier CDMA has been received much attention [58, 73, 74, 75, 76, 77, 78, 12]. Thus, designing optimal signature waveforms for multicarrier CDMA seems very attractive. In multicarrier CDMA, the transmission bandwidth associated with an individual carrier is usually much smaller than the total available bandwidth. This means that signature waveform design using the series expansion method is more effective in this situation. However, it should be noted that, in multicarrier CDMA systems, the signature waveforms need to be designed to minimize not only the MAI caused by the signals of the users using the same carrier but also the MAI caused by the signals from the other carriers. This could make the design problem more challenging.

In this thesis the signature waveforms are optimally designed for a particular type of (linear) receiver. It is believed that the users' performance in CDMA systems can be further improved if the signature waveforms and the receiver are jointly designed. If

the receiver is constrained to be a linear receiver, then an iterative procedure similar to that proposed for joint optimization of the transmitter and receiver in CDMA systems [10, 11, 12] may be of interest.

Appendix A

Table of Eigenvalues $\chi_n(c)$

n	$c = 0.1$	$c = 0.2$	$c = 0.3$	$c = 0.4$	$c = 0.5$	$c = 0.6$
0	6.3591E-002	1.2676E-001	1.8909E-001	2.5019E-001	3.0969E-001	3.6724E-001
1	7.0651E-005	5.6318E-004	1.8894E-003	4.4411E-003	8.5811E-003	1.4634E-002
2	1.2574E-008	4.0222E-007	3.0525E-006	1.2852E-005	3.9175E-005	9.7326E-005
3	9.2386E-013	1.1824E-010	2.0199E-009	1.5128E-008	7.2114E-008	2.5829E-007
4	3.7244E-017	1.9068E-014	7.3298E-013	9.7610E-012	7.2714E-011	3.7512E-010
5	9.5001E-022	1.9456E-018	1.6828E-016	3.9841E-015	4.6378E-014	3.4456E-013
6	1.6725E-026	1.3701E-022	2.6664E-020	1.1223E-018	2.0413E-017	2.1840E-016
7	2.1552E-031	7.0621E-027	3.0924E-024	2.3140E-022	6.5766E-021	1.0132E-019
8	2.1212E-036	2.7803E-031	2.7393E-028	3.6441E-026	1.6183E-024	3.5902E-023
9	1.6469E-041	8.6344E-036	1.9141E-032	4.5269E-030	3.1411E-028	1.0035E-026
10	1.0345E-046	2.1694E-040	1.0821E-036	4.5496E-034	4.9326E-032	2.2692E-030
11	5.3655E-052	4.5009E-045	5.0512E-041	3.7756E-038	6.3961E-036	4.2372E-034
12	2.3369E-057	7.8413E-050	1.9800E-045	2.6311E-042	6.9644E-040	6.6437E-038
13	8.6680E-063	1.1634E-054	6.6098E-050	1.5615E-046	6.4581E-044	8.8714E-042
14	2.7711E-068	1.4877E-059	1.9018E-054	7.9871E-051	5.1615E-048	1.0210E-045
15	7.7146E-074	1.6567E-064	4.7651E-059	3.5577E-055	3.5924E-052	1.0233E-049
16	1.8871E-079	1.6210E-069	1.0491E-063	1.3925E-059	2.1969E-056	9.0114E-054
17	4.0883E-085	1.4047E-074	2.0454E-068	4.8265E-064	1.1898E-060	7.0279E-058
18	7.8985E-091	1.0856E-079	3.5565E-073	1.4920E-068	5.7469E-065	4.8881E-062
19	1.3694E-096	7.5281E-085	5.5494E-078	4.1386E-073	2.4908E-069	3.0508E-066
20	2.1423E-102	4.7110E-090	7.8136E-083	1.0360E-077	9.7420E-074	1.7182E-070
21	3.0396E-108	2.6737E-095	9.9777E-088	2.3518E-082	3.4556E-078	8.7764E-075
22	3.9292E-114	1.3824E-100	1.1608E-092	4.8640E-087	1.1167E-082	4.0842E-079
23	4.6466E-120	6.5395E-106	1.2355E-097	9.2035E-092	3.3016E-087	1.7388E-083
24	5.0463E-126	2.8408E-111	1.2076E-102	1.5992E-096	8.9639E-092	6.7980E-088
25	5.0503E-132	1.1372E-116	1.0877E-107	2.5608E-101	2.2428E-096	2.4492E-092
26	4.6727E-138	4.2088E-122	9.0573E-113	3.7910E-106	5.1878E-101	8.1580E-097

n	$c = 0.1$	$c = 0.2$	$c = 0.3$	$c = 0.4$	$c = 0.5$	$c = 0.6$
27	4.0089E-144	1.4443E-127	6.9934E-118	5.2038E-111	1.1127E-105	2.5196E-101
28	3.1979E-150	4.6086E-133	5.0208E-123	6.6418E-116	2.2190E-110	7.2358E-106
29	2.3780E-156	1.3708E-138	3.3602E-128	7.9021E-121	4.1251E-115	1.9370E-110
30	1.6523E-162	3.8099E-144	2.1013E-133	8.7850E-126	7.1656E-120	4.8452E-115
31	1.0751E-168	9.9165E-150	1.2306E-138	9.1463E-131	1.1657E-124	1.1350E-119
32	6.5654E-175	2.4222E-155	6.7630E-144	8.9363E-136	1.7795E-129	2.4951E-124
33	3.7697E-181	5.5632E-161	3.4949E-149	8.2098E-141	2.5545E-134	5.1576E-129
34	2.0390E-187	1.2036E-166	1.7013E-154	7.1050E-146	3.4542E-139	1.0043E-133
35	1.0407E-193	2.4574E-172	7.8154E-160	5.8023E-151	4.4077E-144	1.8454E-138
36	5.0210E-200	4.7422E-178	3.3934E-165	4.4788E-156	5.3161E-149	3.2050E-143
37	2.2931E-206	8.6631E-184	1.3948E-170	3.2728E-161	6.0698E-154	5.2695E-148
38	9.9286E-213	1.5004E-189	5.4353E-176	2.2673E-166	6.5702E-159	8.2136E-153
39	4.0811E-219	2.4669E-195	2.0108E-181	1.4911E-171	6.7517E-164	1.2154E-157
40	1.5947E-225	3.8557E-201	7.0713E-187	9.3226E-177	6.5955E-169	1.7097E-162
41	5.9309E-232	5.7360E-207	2.3669E-192	5.5475E-182	6.1324E-174	2.2891E-167
42	2.1020E-238	8.1315E-213	7.5497E-198	3.1457E-187	5.4334E-179	2.9206E-172
43	7.1070E-245	1.0997E-218	2.2974E-203	1.7018E-192	4.5928E-184	3.5550E-177
44	2.2949E-251	1.4205E-224	6.6767E-209	8.7925E-198	3.7077E-189	4.1327E-182
45	7.0849E-258	1.7541E-230	1.8551E-214	4.3430E-203	2.8616E-194	4.5930E-187
46	2.0932E-264	2.0730E-236	4.9326E-220	2.0530E-208	2.1135E-199	4.8850E-192
47	5.9236E-271	2.3466E-242	1.2563E-225	9.2957E-214	1.4953E-204	4.9768E-197
48	1.6072E-277	2.5467E-248	3.0679E-231	4.0355E-219	1.0143E-209	4.8612E-202
49	4.1846E-284	2.6523E-254	7.1888E-237	1.6811E-224	6.6021E-215	4.5565E-207

n	$c = 0.7$	$c = 0.8$	$c = 0.9$	$c = 1.0$	$c = 2.0$	$c = 3.0$
0	4.2254E-001	4.7533E-001	5.2540E-001	5.7258E-001	8.8056E-001	9.7583E-001
1	2.2881E-002	3.3551E-002	4.6816E-002	6.2791E-002	3.5564E-001	7.0996E-001
2	2.0994E-004	4.0829E-004	7.3348E-004	1.2375E-003	3.5868E-002	2.0514E-001
3	7.5946E-007	1.9327E-006	4.4047E-006	9.2010E-006	1.1522E-003	1.8204E-002
4	1.5254E-009	4.9935E-009	1.4409E-008	3.7179E-008	1.8882E-005	7.0815E-004
5	1.8777E-012	8.1560E-012	2.9791E-011	9.4914E-011	1.9359E-007	1.6551E-005
6	1.6200E-015	9.1915E-015	4.2494E-014	1.6716E-013	1.3661E-009	2.6410E-007
7	1.0230E-018	7.5813E-018	4.4361E-017	2.1544E-016	7.0489E-012	3.0737E-009
8	4.9341E-022	4.7759E-021	3.5369E-020	2.1207E-019	2.7768E-014	2.7281E-011
9	1.8771E-025	2.3732E-024	2.2244E-023	1.6466E-022	8.6267E-017	1.9086E-013
10	5.7777E-029	9.5407E-028	1.1318E-026	1.0344E-025	2.1680E-019	1.0798E-015
11	1.4684E-032	3.1671E-031	4.7551E-030	5.3650E-029	4.4987E-022	5.0431E-018
12	3.1338E-036	8.8281E-035	1.6776E-033	2.3367E-032	7.8383E-025	1.9775E-020
13	5.6958E-040	2.0957E-038	5.0402E-037	8.6675E-036	1.1630E-027	6.6033E-023
14	8.9225E-044	4.2879E-042	1.3052E-040	2.7710E-039	1.4873E-030	1.9003E-025
15	1.2172E-047	7.6400E-046	2.9432E-044	7.7143E-043	1.6564E-033	4.7620E-028

n	$c = 0.7$	$c = 0.8$	$c = 0.9$	$c = 1.0$	$c = 2.0$	$c = 3.0$
16	1.4589E-051	1.1961E-049	5.8317E-048	1.8871E-046	1.6208E-036	1.0485E-030
17	1.5487E-055	1.6584E-053	1.0233E-051	4.0881E-050	1.4045E-039	2.0445E-033
18	1.4661E-059	2.0505E-057	1.6014E-055	7.8983E-054	1.0854E-042	3.5552E-036
19	1.2455E-063	2.2752E-061	2.2489E-059	1.3693E-057	7.5274E-046	5.5476E-039
20	9.5477E-068	2.2781E-065	2.8498E-063	2.1423E-061	4.7106E-049	7.8114E-042
21	6.6379E-072	2.0686E-069	3.2752E-067	3.0395E-065	2.6734E-052	9.9753E-045
22	4.2044E-076	1.7114E-073	3.4293E-071	3.9291E-069	1.3824E-055	1.1605E-047
23	2.4363E-080	1.2953E-077	3.2849E-075	4.6465E-073	6.5391E-059	1.2352E-050
24	1.2965E-084	9.0028E-082	2.8897E-079	5.0462E-077	2.8406E-062	1.2074E-053
25	6.3579E-089	5.7664E-086	2.3425E-083	5.0503E-081	1.1372E-065	1.0875E-056
26	2.8825E-093	3.4146E-090	1.7556E-087	4.6727E-085	4.2087E-069	9.0561E-060
27	1.2117E-097	1.8749E-094	1.2200E-091	4.0088E-089	1.4443E-072	6.9926E-063
28	4.7364E-102	9.5717E-099	7.8829E-096	3.1979E-093	4.6085E-076	5.0203E-066
29	1.7258E-106	4.5553E-103	4.7480E-100	2.3780E-097	1.3708E-079	3.3598E-069
30	5.8758E-111	2.0257E-107	2.6722E-104	1.6523E-101	3.8098E-083	2.1011E-072
31	1.8735E-115	8.4360E-112	1.4085E-108	1.0751E-105	9.9162E-087	2.3776E-075
32	5.6057E-120	3.2969E-116	6.9666E-113	6.5654E-110	2.4221E-090	6.7626E-079
33	1.5772E-124	1.2115E-120	3.2401E-117	3.7697E-114	5.5630E-094	3.4947E-082
34	4.1801E-129	4.1940E-125	1.4196E-121	2.0390E-118	1.2036E-097	1.7012E-085
35	1.0455E-133	1.3700E-129	5.8690E-126	1.0407E-122	2.4573E-101	7.8150E-089
36	2.4714E-138	4.2301E-134	2.2934E-130	5.0209E-127	4.7421E-105	3.3933E-092
37	5.5306E-143	1.2364E-138	8.4842E-135	2.2931E-131	8.6630E-109	1.3948E-095
38	1.1734E-147	3.4262E-143	2.9755E-139	9.9285E-136	1.5003E-112	5.4351E-099
39	2.3633E-152	9.0134E-148	9.9069E-144	4.0811E-140	2.4669E-116	2.0107E-102
40	4.5250E-157	2.2541E-152	3.1356E-148	1.5947E-144	3.8557E-120	7.0710E-106
41	8.2462E-162	5.3652E-157	9.4459E-153	5.9309E-149	5.7359E-124	2.3668E-109
42	1.4320E-166	1.2169E-161	2.7117E-157	2.1019E-153	8.1315E-128	7.5495E-113
43	2.3725E-171	2.6334E-166	7.4265E-162	7.1069E-158	1.0997E-131	2.2973E-116
44	3.7540E-176	5.4423E-171	1.9425E-166	2.2949E-162	1.4205E-135	6.6765E-120
45	5.6788E-181	1.0753E-175	4.8574E-171	7.0849E-167	1.7541E-139	1.8551E-123
46	8.2209E-186	2.0331E-180	1.1624E-175	2.0931E-171	2.0729E-143	4.9325E-127
47	1.1400E-190	3.6824E-185	2.6645E-180	5.9236E-176	2.3466E-147	1.2563E-130
48	1.5156E-195	6.3945E-190	5.8560E-185	1.6072E-180	2.5467E-151	3.0678E-134
49	1.9336E-200	1.0655E-194	1.2350E-189	4.1846E-185	2.6523E-155	7.1887E-138

n	$c = 4.0$	$c = 5.0$	$c = 6.0$	$c = 7.0$	$c = 8.0$	$c = 9.0$
0	9.9589E-001	9.9935E-001	9.9990E-001	9.9998E-001	1.0000E-000	1.0000E-000
1	9.1211E-001	9.7986E-001	9.9606E-001	9.9929E-001	9.9988E-001	9.9998E-001
2	5.1905E-001	7.9992E-001	9.4017E-001	9.8571E-001	9.9700E-001	9.9942E-001
3	1.1021E-001	3.4356E-001	6.4679E-001	8.6457E-001	9.6055E-001	9.9040E-001
4	8.8279E-003	5.6016E-002	2.0735E-001	4.7705E-001	7.4790E-001	9.1013E-001

n	$c = 4.0$	$c = 5.0$	$c = 6.0$	$c = 7.0$	$c = 8.0$	$c = 9.0$
5	3.8129E-004	4.1821E-003	2.7387E-002	1.1572E-001	3.2028E-001	5.9910E-001
6	1.0951E-005	1.9331E-004	1.9550E-003	1.3056E-002	6.0784E-002	1.9694E-001
7	2.2786E-007	6.3591E-006	9.4849E-005	9.0657E-004	6.1263E-003	3.0565E-002
8	3.6066E-009	1.5823E-007	3.4368E-006	4.5624E-005	4.1825E-004	2.8466E-003
9	4.4938E-011	3.0917E-009	9.7321E-008	1.7775E-006	2.1663E-005	1.9231E-004
10	4.5252E-013	4.8757E-011	2.2190E-009	5.5526E-008	8.9304E-007	1.0194E-005
11	3.7603E-015	6.3403E-013	4.1662E-011	1.4251E-009	3.0137E-008	4.3974E-007
12	2.6228E-017	6.9173E-015	6.5575E-013	3.0622E-011	8.4966E-010	1.5796E-008
13	1.5576E-019	6.4236E-017	8.7804E-015	5.5929E-013	2.0334E-011	4.8069E-010
14	7.9711E-022	5.1393E-019	1.0126E-016	8.7927E-015	4.1853E-013	1.2565E-011
15	3.5519E-024	3.5798E-021	1.0164E-018	1.2027E-016	7.4905E-015	2.8534E-013
16	1.3906E-026	2.1905E-023	8.9611E-021	1.4446E-018	1.1767E-016	5.6843E-015
17	4.8211E-029	1.1869E-025	6.9951E-023	1.5359E-020	1.6359E-018	1.0017E-016
18	1.4905E-031	3.4047E-014	4.8688E-025	1.4559E-022	2.0270E-020	1.5728E-018
19	4.1353E-034	2.4865E-030	3.0405E-027	1.2381E-024	2.2530E-022	2.2145E-020
20	1.0352E-036	9.7274E-033	1.7133E-029	9.4989E-027	2.2589E-024	2.8124E-022
21	2.3503E-039	3.4511E-035	8.7544E-032	6.6085E-029	2.0535E-026	3.2379E-024
22	4.8615E-042	1.1155E-037	4.0752E-034	4.1882E-031	1.7005E-028	3.3953E-026
23	9.1992E-045	3.2983E-040	1.7354E-036	2.4281E-033	1.2880E-030	3.2563E-028
24	1.5986E-047	8.9560E-043	6.7865E-039	1.2926E-035	8.9585E-033	2.8675E-030
25	2.5599E-050	2.2410E-045	2.4456E-041	6.3411E-038	5.7412E-035	2.3265E-032
26	3.7897E-053	5.1842E-048	8.1472E-044	2.8757E-040	3.4013E-037	1.7449E-034
27	5.2023E-056	1.1120E-050	2.5166E-046	1.2092E-042	1.8683E-039	1.2134E-036
28	6.6400E-059	2.2177E-053	7.2280E-049	4.7275E-045	9.5419E-042	7.8444E-039
29	7.9003E-062	4.1230E-056	1.9351E-051	1.7229E-047	4.5425E-044	4.7271E-041
30	8.7832E-065	7.1624E-059	4.8409E-054	5.8667E-050	2.0205E-046	2.6616E-043
31	9.1446E-068	1.1652E-061	1.1341E-056	1.8708E-052	8.4165E-049	1.4034E-045
32	8.9348E-071	1.7789E-064	2.4933E-059	5.5986E-055	3.2900E-051	6.9437E-048
33	8.2085E-074	2.5536E-067	5.1542E-062	1.5753E-057	1.2092E-053	3.2304E-050
34	7.1039E-077	3.4531E-070	1.0037E-064	4.1756E-060	4.1867E-056	1.4157E-052
35	5.8016E-080	4.4064E-073	1.8443E-067	1.0444E-062	1.3678E-058	5.8542E-055
36	4.4783E-083	5.3147E-076	3.2034E-070	2.4692E-065	4.2239E-061	2.2881E-057
37	3.2724E-086	6.0683E-079	5.2670E-073	5.5260E-068	1.2347E-063	8.4660E-060
38	2.2670E-089	6.5687E-082	8.2100E-076	1.1725E-070	3.4219E-066	2.9696E-062
39	1.4910E-092	6.7502E-085	1.2149E-078	2.3617E-073	9.0028E-069	9.8888E-065
40	9.3217E-096	6.5942E-088	1.7091E-081	4.5220E-076	2.2516E-071	3.1303E-067
41	5.5470E-099	6.1313E-091	2.2883E-084	8.2412E-079	5.3598E-074	9.4310E-070
42	3.1455E-102	5.4325E-094	2.9197E-087	1.4312E-081	1.2158E-076	2.7077E-072
43	1.7017E-105	4.5920E-097	3.5540E-090	2.3713E-084	2.6311E-079	7.4163E-075
44	8.7919E-109	3.7071E-100	4.1315E-093	3.7522E-087	5.4378E-082	1.9400E-077
45	4.3427E-112	2.8612E-103	4.5918E-096	5.6761E-090	1.0745E-084	4.8516E-080
46	2.0528E-115	2.1133E-106	4.8838E-099	8.2173E-093	2.0317E-087	1.1611E-082

n	$c = 4.0$	$c = 5.0$	$c = 6.0$	$c = 7.0$	$c = 8.0$	$c = 9.0$
47	9.2952E-119	1.4951E-109	4.9757E-102	1.1395E-095	3.6799E-090	2.6617E-085
48	4.0353E-122	1.0142E-112	4.8602E-105	1.5150E-098	6.3904E-093	5.8502E-088
49	1.6810E-125	6.6014E-116	4.5555E-108	1.9329E-101	1.0649E-095	1.2338E-090

n	$c = 10.0$	$c = 12.0$	$c = 14.0$	$c = 16.0$	$c = 18.0$	$c = 20.0$
0	1.0000E-000	1.0000E-000	9.9999E-001	9.9995E-001	9.9994E-001	9.9993E-001
1	1.0000E-000	1.0000E-000	9.9999E-001	9.9995E-001	9.9994E-001	9.9993E-001
2	9.9989E-001	9.9994E-001	9.9999E-001	9.9995E-001	9.9994E-001	9.9993E-001
3	9.9790E-001	9.9989E-001	9.9999E-001	9.9995E-001	9.9994E-001	9.9993E-001
4	9.7446E-001	9.9856E-001	9.9993E-001	9.9995E-001	9.9994E-001	9.9993E-001
5	8.2515E-001	9.8365E-001	9.9903E-001	9.9995E-001	9.9994E-001	9.9993E-001
6	4.4015E-001	8.8172E-001	9.8962E-001	9.9937E-001	9.9994E-001	9.9993E-001
7	1.1232E-001	5.5733E-001	9.2169E-001	9.9345E-001	9.9960E-001	9.9993E-001
8	1.4920E-002	1.8342E-001	6.6362E-001	9.4897E-001	9.9588E-001	9.9972E-001
9	1.3146E-003	3.1054E-002	2.7255E-001	7.5365E-001	9.6717E-001	9.9736E-001
10	8.8213E-005	3.3744E-003	5.7771E-002	3.7483E-001	8.2538E-001	9.7906E-001
11	4.7664E-006	2.7742E-004	7.5603E-003	9.8343E-002	4.8298E-001	8.7968E-001
12	2.1340E-007	1.8475E-005	7.3608E-004	1.5326E-002	1.5521E-001	5.8877E-001
13	8.0707E-009	1.0282E-006	5.8096E-005	1.7310E-003	2.8697E-002	2.2896E-001
14	2.6170E-010	4.8758E-008	3.8541E-006	1.5775E-004	3.7161E-003	5.0245E-002
15	7.3635E-012	1.9980E-009	2.1921E-007	1.2117E-005	3.8416E-004	7.4209E-003
16	1.8159E-013	7.1570E-011	1.0846E-008	8.0200E-007	3.3476E-005	8.5983E-004
17	3.9590E-015	2.2619E-012	4.7180E-010	4.6393E-008	2.5213E-006	8.3737E-005
18	7.6871E-017	6.3575E-014	1.8208E-011	2.3710E-009	1.6661E-007	7.0600E-006
19	1.3381E-018	1.6002E-015	6.2816E-013	1.0801E-010	9.7665E-009	5.2371E-007
20	2.1002E-020	3.6289E-017	1.9498E-014	4.4178E-012	5.1225E-010	3.4574E-008
21	2.9878E-022	7.4547E-019	5.4770E-016	1.6323E-013	2.4209E-011	2.0484E-009
22	3.8707E-024	1.3939E-020	1.3991E-017	5.4782E-015	1.0373E-012	1.0972E-010
23	4.5860E-026	2.3827E-022	3.2654E-019	1.6782E-016	4.0504E-014	5.3441E-012
24	4.9882E-028	3.7380E-024	6.9910E-021	4.7119E-018	1.4480E-015	2.3786E-013
25	4.9987E-030	5.4014E-026	1.3782E-022	1.2173E-019	4.7586E-017	9.7201E-015
26	4.6302E-032	7.2132E-028	2.5097E-024	2.9037E-021	1.4428E-018	3.6607E-016
27	3.9762E-034	8.9271E-030	4.2355E-026	6.4167E-023	4.0500E-020	1.2750E-017
28	3.1745E-036	1.0273E-031	6.6427E-028	1.3173E-024	1.0556E-021	4.1212E-019
29	2.3623E-038	1.1017E-033	9.7068E-030	2.5192E-026	2.5618E-023	1.2396E-020
30	1.6424E-040	1.1037E-035	1.3250E-031	4.4989E-028	5.8038E-025	3.4788E-022
31	1.0693E-042	1.0352E-037	1.6934E-033	7.5204E-030	1.2305E-026	9.1317E-024
32	6.5330E-045	9.1131E-040	2.0306E-035	1.1791E-031	2.4464E-028	2.2472E-025
33	3.7528E-047	7.5420E-042	2.2888E-037	1.7379E-033	4.5710E-030	5.1948E-027
34	2.0306E-049	5.8788E-044	2.4300E-039	2.4122E-035	8.0414E-032	1.1305E-028
35	6.7227E-038	4.3238E-046	2.4338E-041	3.1588E-037	1.3341E-033	2.3202E-030

n	$c = 10.0$	$c = 12.0$	$c = 14.0$	$c = 16.0$	$c = 18.0$	$c = 20.0$
36	5.0035E-054	3.0057E-048	2.3042E-043	3.9086E-039	2.0918E-035	4.4982E-032
37	2.2857E-056	1.9778E-050	2.0646E-045	4.5780E-041	3.1039E-037	8.2515E-034
38	9.8991E-059	1.2337E-052	1.7536E-047	5.0822E-043	4.3649E-039	1.4344E-035
39	4.0699E-061	7.3055E-055	1.4141E-049	5.3551E-045	5.8265E-041	2.3661E-037
40	1.5906E-063	4.1126E-057	1.0837E-051	5.3635E-047	7.3907E-043	3.7096E-039
41	5.9168E-066	2.2031E-059	7.9056E-054	5.1123E-049	8.9218E-045	5.5340E-041
42	2.0973E-068	1.1248E-061	5.4949E-056	4.6430E-051	1.0262E-046	7.8644E-043
43	7.0924E-071	5.4781E-064	3.6434E-058	4.0228E-053	1.1259E-048	1.0660E-044
44	2.2905E-073	2.5481E-066	2.3071E-060	3.3282E-055	1.1795E-050	1.3798E-046
45	7.0722E-076	1.1330E-068	1.3967E-062	2.6324E-057	1.1813E-052	1.7071E-048
46	2.0896E-078	4.8214E-071	8.0905E-065	1.9922E-059	1.1320E-054	2.0208E-050
47	5.9142E-081	1.9650E-073	4.4896E-067	1.4444E-061	1.0390E-056	2.2911E-052
48	1.6048E-083	7.6792E-076	2.3884E-069	1.0039E-063	9.1425E-059	2.4903E-054
49	4.1788E-086	2.8798E-078	1.2192E-071	6.6949E-066	7.7196E-061	2.5969E-056

n	$c = 24.0$	$c = 26.0$	$c = 28.0$	$c = 30.0$	$c = 35.0$	$c = 40.0$
0	9.9999E-001	9.9996E-001	9.9997E-001	9.9998E-001	9.9992E-001	9.9994E-001
1	9.9999E-001	9.9996E-001	9.9997E-001	9.9998E-001	9.9992E-001	9.9994E-001
2	9.9999E-001	9.9996E-001	9.9997E-001	9.9998E-001	9.9992E-001	9.9994E-001
3	9.9999E-001	9.9996E-001	9.9997E-001	9.9998E-001	9.9992E-001	9.9994E-001
4	9.9999E-001	9.9996E-001	9.9997E-001	9.9998E-001	9.9992E-001	9.9994E-001
5	9.9999E-001	9.9996E-001	9.9997E-001	9.9998E-001	9.9992E-001	9.9994E-001
6	9.9999E-001	9.9996E-001	9.9997E-001	9.9998E-001	9.9992E-001	9.9994E-001
7	9.9999E-001	9.9996E-001	9.9997E-001	9.9998E-001	9.9992E-001	9.9994E-001
8	9.9999E-001	9.9996E-001	9.9997E-001	9.9998E-001	9.9992E-001	9.9994E-001
9	9.9999E-001	9.9996E-001	9.9997E-001	9.9998E-001	9.9992E-001	9.9994E-001
10	9.9983E-001	9.9996E-001	9.9997E-001	9.9998E-001	9.9992E-001	9.9994E-001
11	9.9897E-001	9.9988E-001	9.9997E-001	9.9998E-001	9.9992E-001	9.9994E-001
12	9.9164E-001	9.9931E-001	9.9988E-001	9.9998E-001	9.9992E-001	9.9994E-001
13	9.4647E-001	9.9476E-001	9.9954E-001	9.9989E-001	9.9992E-001	9.9994E-001
14	7.6732E-001	9.6512E-001	9.9667E-001	9.9971E-001	9.9992E-001	9.9994E-001
15	4.1647E-001	8.3341E-001	9.7746E-001	9.9788E-001	9.9992E-001	9.9994E-001
16	1.2910E-001	5.1885E-001	8.8389E-001	9.8561E-001	9.9992E-001	9.9994E-001
17	2.4867E-002	1.9068E-001	6.1768E-001	9.2093E-001	9.9973E-001	9.9994E-001
18	3.5542E-003	4.2240E-002	2.6732E-001	7.0691E-001	9.9822E-001	9.9994E-001
19	4.1970E-004	6.6919E-003	6.8527E-002	3.5648E-001	9.8834E-001	9.9994E-001
20	4.2826E-005	8.6217E-004	1.2067E-002	1.0628E-001	9.3657E-001	9.9973E-001
21	3.8569E-006	9.5618E-005	1.6912E-003	2.0909E-002	7.5585E-001	9.9852E-001
22	3.1039E-007	9.3590E-006	2.0272E-004	3.1856E-003	4.2212E-001	9.9057E-001
23	2.2528E-008	8.1958E-007	2.1420E-005	4.1101E-004	1.4288E-001	9.4932E-001
24	1.4853E-009	6.4841E-008	2.0265E-006	4.6633E-005	3.1566E-002	7.9833E-001

n	$c = 24.0$	$c = 26.0$	$c = 28.0$	$c = 30.0$	$c = 35.0$	$c = 40.0$
25	8.9457E-011	4.6678E-009	1.7339E-007	4.7379E-006	5.3270E-003	4.8727E-001
26	4.9479E-012	3.0759E-010	1.3521E-008	4.3570E-007	7.5923E-004	1.8525E-001
27	2.5233E-013	1.8644E-011	9.6662E-010	3.6554E-008	9.5447E-005	4.5551E-002
28	1.1913E-014	1.0442E-012	6.3674E-011	2.8152E-009	1.0796E-005	8.4174E-003
29	5.2233E-016	5.4232E-014	3.8814E-012	2.0009E-010	1.1112E-006	1.3055E-003
30	2.1332E-017	2.6199E-015	2.1971E-013	1.3177E-011	1.0490E-007	1.7876E-004
31	8.1388E-019	1.1813E-016	1.1592E-014	8.0709E-013	9.1360E-009	2.2118E-005
32	2.9075E-020	4.9826E-018	5.7147E-016	4.6128E-014	7.3779E-010	2.4946E-006
33	9.7489E-022	1.9709E-019	2.6397E-017	2.4668E-015	5.5469E-011	2.5935E-007
34	3.0743E-023	7.3287E-021	1.1450E-018	1.2378E-016	3.8963E-012	2.4978E-008
35	9.1360E-025	2.5667E-022	4.6755E-020	5.8407E-018	2.5644E-013	2.2391E-009
36	2.5632E-026	8.4827E-024	1.8004E-021	2.5970E-019	1.5862E-014	1.8757E-010
37	6.8013E-028	2.6500E-025	6.5506E-023	1.0904E-020	9.2402E-016	1.4733E-011
38	1.7093E-029	7.8395E-027	2.2558E-024	4.3307E-022	5.0804E-017	1.0882E-012
39	4.0749E-031	2.1992E-028	7.3641E-026	1.6298E-023	2.6426E-018	7.5776E-014
40	9.2296E-033	5.8597E-030	2.2822E-027	5.8202E-025	1.3022E-019	4.9861E-015
41	1.9884E-034	1.4848E-031	6.7254E-029	1.9755E-026	6.0897E-021	3.1066E-016
42	4.0799E-036	3.5821E-033	1.8866E-030	6.3814E-028	2.7076E-022	1.8362E-017
43	7.9830E-038	8.2408E-035	5.0446E-032	1.9641E-029	1.1458E-023	1.0313E-018
44	1.4912E-039	1.8095E-036	1.2872E-033	5.7683E-031	4.6216E-025	5.5128E-020
45	2.6618E-041	3.7966E-038	3.1380E-035	1.6181E-032	1.7792E-026	2.8086E-021
46	4.5459E-043	7.6197E-040	7.3167E-037	4.3400E-034	6.5451E-028	1.3655E-022
47	7.4340E-045	1.4643E-041	1.6332E-038	1.1143E-035	2.3028E-029	6.3451E-024
48	1.1654E-046	2.6967E-043	3.4935E-040	2.7406E-037	7.7601E-031	2.8203E-025
49	1.7526E-048	4.7644E-045	7.1675E-042	6.4660E-039	2.5064E-032	1.2007E-026

Appendix B

Constructing a Correlation Matrix with Prescribed Diagonal Entries and Eigenvalues

Let $\mathbf{x}$ be the vector of diagonal entries of a correlation matrix, $\mathbf{R}$, and $\mathbf{y}$ be the vector of its eigenvalues. A well-known condition for the existence of matrix $\mathbf{R}$ is that vector $\mathbf{y}$ majorizes[1] vector $\mathbf{x}$. Given $\mathbf{x}$ and $\mathbf{y}$, a recursive procedure to construct such a matrix $\mathbf{R}$ based on the *T-transform* is outlined below. For the justification of this procedure, readers are referred to [17].

1) Initialization:

   Let $\mathbf{y}^{(0)} = \mathbf{y}$. Define $\mathbf{\Lambda}$ be a $K \times K$ diagonal matrix having $\mathbf{y}^{(0)}$ as its diagonal.

   Let $\mathbf{V} = \mathbf{I}$, and $j = 0$.

2) Find the largest integer k such that $y_k^{(j)} > x_k$ and the smallest integer l such that $y_l^{(j)} < x_l$ and $l > k$.

   Find $\delta = \min(y_k^{(j)} - x_k, x_l - y_l^{(j)})$ and $\omega = \dfrac{\delta}{y_k^{(j)} - y_l^{(j)}}$

   Define $\mathbf{T}^{(j+1)} = \mathbf{U}^{(j+1)} = \mathbf{I}$, an $K \times K$ identity matrix. Then set

[1]For $\mathbf{x}, \mathbf{y} \in \Re^K$, one says that $\mathbf{x}$ is majorized by $\mathbf{y}$ (or $\mathbf{y}$ majorizes $\mathbf{x}$) if (i) $\sum_{i=1}^{k} \mathbf{x}_{[i]} \leq \sum_{i=1}^{k} \mathbf{y}_{[i]}$, for $k = 1, 2, \ldots K-1$ and (ii) $\sum_{i=1}^{K} \mathbf{x}_{[i]} = \sum_{i=1}^{K} \mathbf{y}_{[i]}$.

$$\mathbf{T}_{kk}^{(j+1)} = \mathbf{T}_{ll}^{(j+1)} = \omega,\ \mathbf{T}_{kl}^{(j+1)} = \mathbf{T}_{lk}^{(j+1)} = 1-\omega$$
$$\mathbf{U}_{kk}^{(j+1)} = \mathbf{U}_{ll}^{(j+1)} = \sqrt{\omega},\ \mathbf{T}_{kl}^{(j+1)} = \sqrt{1-\omega}, \mathbf{T}_{lk}^{(j+1)} = -\sqrt{1-\omega}$$

Compute $\mathbf{y}^{(j+1)} = \mathbf{T}^{(j+1)}\mathbf{y}^{(j)}$, $\mathbf{V} = (\mathbf{U}^{(j+1)})^{\top}\mathbf{V}$ and $\mathbf{R} = (\mathbf{U}^{(j+1)})^{\top}\mathbf{\Lambda}\mathbf{U}^{(j+1)}$.

If $\mathbf{y}^{(j+1)} = \mathbf{x}$ then go to 3), otherwise increase $j \rightarrow j+1$ and go back to 2).

3) Stop and output $\mathbf{R}$ and $\mathbf{V}$.

The above recursive algorithm is guaranteed to terminate after $K-1$ steps at most (corresponding to $j = K-2$). The singular-value decomposition of $\mathbf{R}$ is

$$\mathbf{R} = \mathbf{V}\mathbf{\Lambda}\mathbf{V}^{\top} \tag{B.1}$$

where $\mathbf{V} = [\mathbf{v}_1, \mathbf{v}_2, \ldots, \mathbf{v}_K]$ is an orthogonal matrix of the eigenvectors of $\mathbf{R}$.

Appendix C

The Equivalence of Problem 4.5 and Problem 4.6

Let $\epsilon(\mathbf{R})$ denote the minimum average FOBE of the optimal signal set corresponding to the correlation matrix $\mathbf{R}$. Then the proof consists of the following three steps.

- The first step is to show that Problem 4.5 is equivalent to the following problem, which is stated in terms of the correlation matrix $\mathbf{R}$: Find the correlation matrix $\mathbf{R}$ that minimizes $\mathrm{tr}(\mathbf{R}\mathbf{R}^\top)$ subject to (i) $\mathbf{R} \geq 0$; (ii) $\mathbf{R}_{kk} = 1$, $\forall k$; (iii) $\epsilon(\mathbf{R}) \leq \eta$. Proving this fact can be carried out similarly as for the proof of Proposition 4.1. Note, however, that one now relies on Proposition 2.2 to deal with metric $\epsilon(\mathbf{R})$ instead of metric $b^2(\mathbf{R})$.

- In the second step one needs to show that the design problem in Step 1 above is equivalent to the following problem, which is stated in terms of the eigenvalues of the correlation matrix $\mathbf{R}$: Find the set of eigenvalues $\{\lambda_1, \lambda_2, \ldots, \lambda_K\}$ that minimizes $\sum_{k=1}^{K} \lambda_k^2$, subject to (i) $\lambda_k \geq \lambda_{k+1} \geq 0$, $1 \leq k < K$; (ii) $\mathrm{tr}(\mathbf{\Lambda}) = K$; and (iii) $\mathrm{tr}(\mathbf{\Lambda\Xi}) \leq K\eta$. Again, proving this equivalence is exactly the same as the proof for Proposition 4.2 with the only exception that the ordering constraint on the eigenvalues and the FOBE bandwidth constraint are the consequences of Proposition 2.2.

- This final step is to prove that the design problem in Step 2 is equivalent to Problem 4.6. The proof is as follows. As in the proof of Proposition 4.3, it is first shown that the ordering of the eigenvalues will be a natural consequence of the optimization problem. Suppose that $\mathbf{\Lambda}$ minimizes $\mathrm{tr}(\mathbf{\Lambda}^2)$ and satisfies all the constraints of the problem in Step 2 except for being well ordered. Assume $\lambda_k < \lambda_{k+1}$ for some $1 \leq k < K$ and consider $\mathbf{\Lambda}'$ obtained from $\mathbf{\Lambda}$ by modifying only the kth and $(k+1)$th diagonal entries as $\lambda'_k = \lambda'_{k+1} = (\lambda_k + \lambda_{k+1})/2$. Then it can be verified that $\mathrm{tr}(\mathbf{\Lambda}) = \mathrm{tr}(\mathbf{\Lambda}') = K$ and $\mathrm{tr}(\mathbf{\Lambda}'\mathbf{\Xi}) < \mathrm{tr}(\mathbf{\Lambda}\mathbf{\Xi})$, but $\mathrm{tr}(\mathbf{\Lambda}'^2) < \mathrm{tr}(\mathbf{\Lambda}^2)$, a contradiction.

  Next it is shown that the inequality on bandwidth constraint can be replaced by the equality. Suppose there exists a solution $\mathbf{\Lambda}$ to the design problem in Step 2 where all diagonal entries are well ordered but with $\mathrm{tr}(\mathbf{\Lambda}\mathbf{\Xi}) = \sum_{k=1}^{K}(1-\chi_{k-1})\lambda_k = K\eta - \epsilon_\eta < K\eta$. Except for the trivial case when $\mathbf{R} = \mathbf{I}$, there always exists an integer $1 \leq k < K$ such that $\lambda_k - \lambda_{k+1} = \epsilon_\lambda > 0$. Consider $\mathbf{\Lambda}'$ obtained from $\mathbf{\Lambda}$ by modifying the kth and $(k+1)$th diagonal entries as $\lambda'_k = \lambda_k - \delta$ and $\lambda'_{k+1} = \lambda_{k+1} + \delta$ where $\delta = \min\{\epsilon_\eta/(\chi_{k-1} - \chi_k), \epsilon_\lambda/2\} > 0$. Then it can be shown that $\mathbf{\Lambda}'$ satisfies all the constraints of the design problem in Step 2 but $\mathrm{tr}(\mathbf{\Lambda}'^2) < \mathrm{tr}(\mathbf{\Lambda}^2)$, a contradiction. Hence the proof.

Appendix D

The Equivalence of Problem 4.7 and Problem D.1

The original design problem of optimal signature waveforms for MMSE can be stated as follows.

Problem D.1. Given T and W. Design a set of K signals $\{s_1(t), \ldots, s_K(t)\}$ that minimizes the TMSE in (4.36) subject to the following constraints. (i) $\forall k$, $s_k(t) = 0$ for $t < 0$ and $t > T$; (ii) $\int_0^T s_k^2(t)\mathrm{d}t = 1$, $\forall k$; and (iii) $b(\mathbf{s}(t)) \leq W$ (for RMS bandwidth) or $\epsilon(\mathbf{s}(t)) \leq \eta$ (for FOBE bandwidth).

Using the notation introduced in Section 4.3, the following three steps justify the equivalence of Problems D.1 and 4.7.

- The first step is to shows that Problem D.1 is equivalent to the following problem, which is stated in terms of the correlation matrix $\mathbf{R}$: Find the correlation matrix $\mathbf{R}$ that minimizes $KP - P\mathrm{tr}\left([\mathbf{I} + \gamma^{-1}\mathbf{R}^{-1}]^{-1}\right)$ subject to (i) $\mathbf{R} \geq 0$; (ii) $\mathbf{R}_{kk} = 1$, $\forall k$; (iii) $b^2(\mathbf{R}) \leq W^2$ (RMS), or $\epsilon(\mathbf{R}) \leq \eta$ (FOBE). Proof of this fact is similar to that of Proposition 4.1.

- The second step is to show that the signal design problem in Step 2 is equivalent to the following problem, which is stated in terms of the eigenvalues of the correlation matrix $\mathbf{R}$: Find the set of eigenvalues $\{\lambda_1, \lambda_2, \ldots, \lambda_K\}$ that minimizes

$\sum_{k=1}^{K}(\gamma\lambda_k+1)^{-1}$, subject to (i) $\lambda_k \geq \lambda_{k+1} \geq 0$, $1 \leq k < K$; (ii) $\mathrm{tr}(\mathbf{\Lambda}) = K$; (iii) $\mathrm{tr}(\mathbf{\Lambda\Delta}) \leq K\nu$. The proof of this fact is the same as the proof of Proposition 4.2.

- Finally one needs to prove that the design problem in Step 2 is equivalent to Problem 4.7. The proof is as follows. As before, it is first shown that the ordering of the eigenvalues is a natural consequence of the optimization problem. Suppose that $\mathbf{\Lambda}$ minimizes $\sum_{k=1}^{K}(\gamma\lambda_k+1)^{-1}$ and satisfies all the constraints of problem in Step 2 except for being well ordered. Assume $\lambda_k < \lambda_{k+1}$ for some $1 \leq k < K$ and consider $\mathbf{\Lambda}'$ obtained from $\mathbf{\Lambda}$ by modifying only the two diagonal entries kth and $(k+1)$th as $\lambda'_k = \lambda'_{k+1} = (\lambda_k + \lambda_{k+1})/2$. Then it can be verified that $\mathrm{tr}(\mathbf{\Lambda}) = \mathrm{tr}(\mathbf{\Lambda}') = K$ and $\mathrm{tr}(\mathbf{\Lambda}'\mathbf{\Delta}) < \mathrm{tr}(\mathbf{\Lambda\Delta})$, but $\sum_{k=1}^{K}(\gamma\lambda'_k+1)^{-1} < \sum_{k=1}^{K}(\gamma\lambda_k+1)^{-1}$, a contradiction.

  Next it is shown that the inequality on bandwidth constraint can be replaced by the equality. Let $\mathbf{\Delta} = \mathrm{diag}(\delta_1, \delta_2, \ldots, \delta_K)$, where $\delta_k < \delta_{k+1}$ for $1 \leq k < K$. Suppose there exists a solution $\mathbf{\Lambda}$ to problem in Step 2 where all diagonal entries are well ordered but with $\mathrm{tr}(\mathbf{\Lambda\Delta}) = \sum_{k=1}^{K}\delta_k\lambda_k = K\nu - \epsilon_\nu < K\nu$. Except for the trivial case when $\mathbf{R} = \mathbf{I}$, there always exists an integer $1 \leq k < K$ such that $\lambda_k - \lambda_{k+1} = \epsilon_\lambda > 0$. Consider $\mathbf{\Lambda}'$ obtained from $\mathbf{\Lambda}$ by modifying the kth and $(k+1)$th diagonal entries as $\lambda'_k = \lambda_k - \delta^*$ and $\lambda'_{k+1} = \lambda_{k+1} + \delta^*$ where $\delta^* = \min\{\epsilon_\nu/(\delta_{k+1} - \delta_k), \epsilon_\lambda/2\} > 0$. Then it can be shown that $\mathbf{\Lambda}'$ satisfies all the constraints of problem in Step 2 but $\sum_{k=1}^{K}(\gamma\lambda'_k+1)^{-1} < \sum_{k=1}^{K}(\gamma\lambda_k+1)^{-1}$, a contradiction. Hence the proof.

Appendix E

Objective Function for Signature Waveform Design

Let $\widehat{S}_k(f) = \mathcal{F}\{\widehat{s}_k(t)\}$. From (6.30) one has

$$\begin{aligned}\widehat{S}_k(f) &= \sum_{l=1}^{L} x_{kl}\mathcal{F}\{\phi_{2l-1}(t,T)\} + \sum_{l=1}^{L} y_{kl}\mathcal{F}\{\phi_{2l}(t,T)\} \\ &= \sum_{l=1}^{L} x_{kl}X_l(f,T) + j\sum_{l=1}^{L} y_{kl}Y_l(f,T). \end{aligned} \tag{E.1}$$

Thus

$$|S_k(f)|^2 = |\widehat{S}_k(f)|^2 = \left(\sum_{l=1}^{L} x_{kl}X_l(f,T)\right)^2 + \left(\sum_{l=1}^{L} y_{kl}Y_l(f,T)\right)^2. \tag{E.2}$$

It then follows from (6.19) that

$$J(L) = \frac{1}{KT^3}\sum_{k=1}^{K}\sum_{i=k+1}^{K}\int_{-\infty}^{\infty}|S_k(f)|^2|S_i(f)|^2\mathrm{d}f \tag{E.3}$$

where

$$\begin{aligned}\int_{-\infty}^{\infty}|S_k(f)|^2|S_i(f)|^2\mathrm{d}f &= \sum_{l=1}^{L}\sum_{m=1}^{L}\sum_{p=1}^{L}\sum_{q=1}^{L}(x_{kl}x_{km}x_{ip}x_{iq})\,\alpha_{l,m,p,q}(T)\\ &+\sum_{l=1}^{L}\sum_{m=1}^{L}\sum_{p=1}^{L}\sum_{q=1}^{L}(x_{kl}x_{km}y_{ip}y_{iq})\,\beta_{l,m,p,q}(T)\\ &+\sum_{l=1}^{L}\sum_{m=1}^{L}\sum_{p=1}^{L}\sum_{q=1}^{L}(y_{kl}y_{km}x_{ip}x_{iq})\,\lambda_{l,m,p,q}(T)\\ &+\sum_{l=1}^{L}\sum_{m=1}^{L}\sum_{p=1}^{L}\sum_{q=1}^{L}(y_{kl}y_{km}y_{ip}y_{iq})\,\mu_{l,m,p,q}(T). \quad \text{(E.4)}\end{aligned}$$

The quantities $\alpha_{l,m,p,q}(T)$, $\beta_{l,m,p,q}(T)$, $\lambda_{l,m,p,q}(T)$ and $\mu_{l,m,p,q}(T)$, $l,m,p,q=1,2\ldots,L$, in (E.4) are defined as:

$$\alpha_{l,m,p,q}(T) = \int_{-\infty}^{\infty}X_l(f,T)X_m(f,T)X_p(f,T)X_q(f,T)\mathrm{d}f \quad \text{(E.5)}$$

$$\beta_{l,m,p,q}(T) = \int_{-\infty}^{\infty}X_l(f,T)X_m(f,T)Y_p(f,T)Y_q(f,T)\mathrm{d}f \quad \text{(E.6)}$$

$$\lambda_{l,m,p,q}(T) = \int_{-\infty}^{\infty}Y_l(f,T)Y_m(f,T)X_p(f,T)X_q(f,T)\mathrm{d}f \quad \text{(E.7)}$$

$$\mu_{l,m,p,q}(T) = \int_{-\infty}^{\infty}Y_l(f,T)Y_m(f,T)Y_p(f,T)Y_q(f,T)\mathrm{d}f. \quad \text{(E.8)}$$

It should be noted that (E.4) is not the most efficient expression in terms of calculation effort. However, what is important to point out here is that all the integrals involving $J(L)$ can be precomputed based on (6.27). For a more efficient expression, each term

in (E.4) can be rewritten similarly as follows.

$$\begin{aligned}\sum_{l=1}^{L}\sum_{m=1}^{L}\sum_{p=1}^{L}\sum_{q=1}^{L}\left(x_{kl}x_{km}y_{ip}y_{iq}\right)\beta_{l,m,p,q}(T) &= \sum_{l=1}^{L}\sum_{p=1}^{L}\left(x_{kl}^2y_{ip}^2\right)\beta_{l,l,p,p}(T)\\ &+2\sum_{l=1}^{L}\sum_{p=1}^{L}\sum_{q=p+1}^{L}\left(x_{kl}^2y_{ip}y_{iq}\right)\beta_{l,l,p,q}(T)\\ &+2\sum_{l=1}^{L}\sum_{m=l+1}^{L}\sum_{p=1}^{L}\left(x_{kl}x_{km}y_{ip}^2\right)\beta_{l,m,p,p}(T)\\ &+4\sum_{l=1}^{L}\sum_{m=l+1}^{L}\sum_{p=1}^{L}\sum_{q=p+1}^{L}\left(x_{kl}x_{km}y_{ip}y_{iq}\right)\beta_{l,m,p,q}(T). \qquad \text{(E.9)}\end{aligned}$$

Appendix F

Objective Function for Multiple Chip Waveform Design

Rewrite (6.18) as follows:

$$\begin{aligned} I &= \frac{1}{2D^2T_c^3}\sum_{m=1}^{D}\int_{-\infty}^{\infty}|G_m(f)|^4\mathrm{d}f \\ &\quad +\frac{1}{D^2T_c^3}\sum_{m=1}^{D}\sum_{n=m+1}^{D}\int_{-\infty}^{\infty}|G_m(f)|^2|G_n(f)|^2\mathrm{d}f. \end{aligned} \tag{F.1}$$

The second term in the above equation can be expressed in terms of x_{ml} and y_{ml} in exactly the same form as (E.3) in Appendix E. In particular, let $J(L, D, T_c)$ be the expression in (E.3) when replacing K by D and T by T_c, that is

$$\frac{1}{D^2T_c^3}\sum_{m=1}^{D}\sum_{n=m+1}^{D}\int_{-\infty}^{\infty}|G_m(f)|^2|G_n(f)|^2\mathrm{d}f = \frac{J(L, D, T_c)}{D}. \tag{F.2}$$

Let $\widehat{G}_m(f) = \mathcal{F}\{\widehat{g}_m(t)\}$. Then from (6.33) one has

$$\widehat{G}_m(f) = \sum_{l=1}^{L} x_{ml}X_l(f, T_c) + j\sum_{l=1}^{L} y_{ml}Y_l(f, T_c). \tag{F.3}$$

Thus the integral in the first term of (F.1) can be calculated as follows.

$$\begin{aligned}\int_{-\infty}^{\infty}|G_m(f)|^4\mathrm{d}f &= \int_{-\infty}^{\infty}|\widehat{G}_m(f)|^4\mathrm{d}f \\ &= \int_{-\infty}^{\infty}\left(\sum_{l=1}^{L}x_{ml}X_l(f,T_c)\right)^4\mathrm{d}f+\int_{-\infty}^{\infty}\left(\sum_{l=1}^{L}y_{ml}Y_l(f,T_c)\right)^4\mathrm{d}f \\ &\quad +2\int_{-\infty}^{\infty}\left(\sum_{l=1}^{L}x_{ml}X_l(f,T_c)\right)^2\left(\sum_{l=1}^{L}y_{ml}Y_l(f,T_c)\right)^2\mathrm{d}f. \qquad \text{(F.4)}\end{aligned}$$

The first two terms of (F.4) can be written as follows [32]

$$\int_{-\infty}^{\infty}\left(\sum_{l=1}^{L}x_{ml}X_l(f,T_c)\right)^4\mathrm{d}f=\sum_{k_0,\ldots,k_L:\sum_{l=0}^{L}k_l=4}\gamma(k_0,\ldots,k_L)\prod_{l=0}^{L}x_{ml}^{k_l} \qquad \text{(F.5)}$$

$$\int_{-\infty}^{\infty}\left(\sum_{l=1}^{L}y_{ml}Y_l(f,T_c)\right)^4\mathrm{d}f=\sum_{k_0,\ldots,k_L:\sum_{l=0}^{L}k_l=4}\chi(k_0,\ldots,k_L)\prod_{l=0}^{L}y_{ml}^{k_l} \qquad \text{(F.6)}$$

where

$$\gamma(k_0,\ldots,k_L)=\frac{4!}{k_0!k_1!\cdots k_L!}\left(\int_{-\infty}^{\infty}\prod_{l=0}^{L}X_l^{k_l}(f,T)\mathrm{d}f\right) \qquad \text{(F.7)}$$

and

$$\chi(k_0,\ldots,k_L)=\frac{4!}{k_0!k_1!\cdots k_L!}\left(\int_{-\infty}^{\infty}\prod_{l=0}^{L}Y_l^{k_l}(f,T)\mathrm{d}f\right). \qquad \text{(F.8)}$$

The last term of (F.4) can be expressed as

$$\begin{aligned}&2\int_{-\infty}^{\infty}\left(\sum_{l=1}^{L}x_{ml}X_l(f,T_c)\right)^2\left(\sum_{l=1}^{L}y_{ml}Y_l(f,T_c)\right)^2\mathrm{d}f \\ &\quad=2\sum_{l=1}^{L}\sum_{n=1}^{L}\sum_{p=1}^{L}\sum_{q=1}^{L}\left(x_{ml}x_{mn}y_{mp}y_{mq}\right)\beta_{l,n,p,q}(T_c). \qquad \text{(F.9)}\end{aligned}$$

Finally, combining (F.1), (F.2), (F.4), (F.5), (F.6) and (F.9) gives

$$\begin{aligned}I(D,L)=&\frac{1}{2D^2T_c^3}\sum_{m=1}^{D}\sum_{k_0,\ldots,k_L:\sum_{l=0}^{L}k_l=4}\left(\gamma(k_0,\ldots,k_L)\prod_{l=0}^{L}x_{ml}^{k_l}+\chi(k_0,\ldots,k_L)\prod_{l=0}^{L}y_{ml}^{k_l}\right) \\ &+\frac{1}{D^2T_c^3}\sum_{m=1}^{D}\sum_{l=1}^{L}\sum_{n=1}^{L}\sum_{p=1}^{L}\sum_{q=1}^{L}\left(x_{ml}x_{mn}y_{mp}y_{mq}\right)\beta_{l,n,p,q}(T_c)+\frac{J(L,D,T_c)}{D}. \qquad \text{(F.10)}\end{aligned}$$

Appendix G

Derivation of W_i for Double Chip Waveforms

The expression for W_i in (7.1) can be readily obtained from (2.34). It is given by

$$W_i = b_i(-1)R_{k,i}(\tau_i) + b_i(0)\widehat{R}_{k,i}(\tau_i) \tag{G.1}$$

where τ_i is the delay of the ith user's signal relative to the signal of the kth user, which is the user of interest. Recall that $l_i = \lfloor \tau_i/T_c \rfloor$ and $r_i = \tau_i - l_i T_c$. At this point, to simplify the notation, we set $l = l_i$ and $r = r_i$. When necessary, the appropriate indexes of l and r can be restored.

Now if l is *even*, then W_i can be written as

$$\begin{aligned}
W_i^e &= b_i(-1)\Bigg[h_{1,2}(r)\sum_{j=0}^{l/2} s_k(2j)s_i(N-l+2j-1) + \widehat{h}_1(r)\sum_{j=0}^{l/2-1} s_k(2j)s_i(N-l+2j) \\
&+ h_{2,1}(r)\sum_{j=0}^{l/2-1} s_k(2j+1)s_i(N-l+2j) + \widehat{h}_2(r)\sum_{j=0}^{l/2-1} s_k(2j+1)s_i(N-l+2j+1)\Bigg] \\
&+ b_i(0)\Bigg[\widehat{h}_1(r)\sum_{j=0}^{(N-l)/2-1} s_i(2j)s_k(l+2j) + h_{2,1}(r)\sum_{j=0}^{(N-l)/2-1} s_i(2j)s_k(l+2j+1) \\
&+ \widehat{h}_2(r)\sum_{j=0}^{(N-l)/2-1} s_i(2j+1)s_k(l+2j+1) + h_{1,2}(r)\sum_{j=0}^{(N-l)/2-2} s_i(2j+1)s_k(l+2j+2)\Bigg].
\end{aligned} \tag{G.2}$$

Note that the last four summations in (G.2) can be rewritten as follows

$$\sum_{j=0}^{(N-l)/2-1} s_i(2j)s_k(l+2j) = \sum_{j=l/2}^{N/2-1} s_k(2j)s_i(2j-l) \tag{G.3}$$

$$\sum_{j=0}^{(N-l)/2-1} s_i(2j)s_k(l+2j+1) = \sum_{j=l/2}^{N/2-1} s_k(2j+1)s_i(2j-l) \tag{G.4}$$

$$\sum_{j=0}^{(N-l)/2-1} s_i(2j+1)s_k(l+2j+1) = \sum_{j=l/2}^{N/2-1} s_k(2j+1)s_i(2j-l+1) \tag{G.5}$$

$$\sum_{j=0}^{(N-l)/2-2} s_i(2j+1)s_k(l+2j+2) = \sum_{j=l/2+1}^{N/2-1} s_k(2j)s_i(2j-l-1). \tag{G.6}$$

Therefore

$$\begin{aligned} W_i^e &= b_i(-1)\sum_{j=0}^{l/2-1} s_i(N+2j-l+1)\left[s_k(2j+2)h_{1,2}(r)+s_k(2j+1)\widehat{h}_2(r)\right] \\ &+ b_i(0)\sum_{j=l/2}^{N/2-2} s_i(2j-l+1)\left[s_k(2j+2)h_{1,2}(r)+s_k(2j+1)\widehat{h}_2(r)\right] \\ &+ b_i(-1)s_k(0)s_i(N-l-1)h_{1,2}(r)+b_i(0)s_k(N-1)s_i(N-l-1)\widehat{h}_2(r) \\ &+ b_i(-1)\sum_{j=0}^{l/2-1} s_i(N+2j-l)\left[s_k(2j)\widehat{h}_1(r)+s_k(2j+1)h_{2,1}(r)\right] \\ &+ b_i(0)\sum_{j=l/2}^{N/2-1} s_i(2j-l)\left[s_k(2j)\widehat{h}_1(r)+s_k(2j+1)h_{2,1}(r)\right]. \end{aligned} \tag{G.7}$$

As in [33], with the motivation of reducing complexity, it is important to consider (G.7) conditioned on the signature sequence of the kth user and the random variable l, i.e., $\{s_k(j)\} = \{\widehat{s}_k(j)\}$ and $l = \widehat{l}$ ($\widehat{l}$ is even). In order to simplify (G.7), define the following $N+1$ random variables

$$F_j = \begin{cases} b_i(-1)s_i(N+2j-\widehat{l}+1)\widehat{s}_k(2j+1), & j = 0,1\ldots\frac{\widehat{l}}{2}-1 \\ b_i(0)s_i(2j-\widehat{l}+1)\widehat{s}_k(2j+1), & j = \frac{\widehat{l}}{2},\frac{\widehat{l}}{2}+1\ldots\frac{N}{2}-2 \\ b_i(0)s_i(N-\widehat{l}-1)\widehat{s}_k(N-1), & j = \frac{N}{2}-1 \\ b_i(-1)s_i(N-\widehat{l}-1)\widehat{s}_k(0), & j = \frac{N}{2} \end{cases} \tag{G.8}$$

and

$$G_j = \begin{cases} b_i(-1)s_i(N+2j-\widehat{l})\widehat{s}_k(2j+1), & j=0,1\ldots\frac{\widehat{l}}{2}-1 \\ b_i(0)s_i(2j-\widehat{l})\widehat{s}_k(2j+1), & j=\frac{\widehat{l}}{2},\frac{\widehat{l}}{2}+1\ldots\frac{N}{2}-1. \end{cases} \tag{G.9}$$

For any $\widehat{l}$ in the set $\{0,2,\ldots,\frac{N}{2}-2\}$, the random variables F_j and G_j are mutually independent and satisfy

$$\Pr(F_j=+1)=\Pr(F_j=-1)=\Pr(G_j=+1)=\Pr(G_j=-1)=\frac{1}{2}. \tag{G.10}$$

Using the definitions of the random variables F_j and G_j and the fact that $\widehat{s}_k^2(j)=1$ for every j, (G.7) can be simplified to

$$\begin{aligned} W_i^e &= \sum_{j=0}^{N/2-2} F_j\left[\widehat{h}_2(r)+\widehat{s}_k(2j+1)\widehat{s}_k(2j+2)h_{1,2}(r)\right] \\ &+ F_{\frac{N}{2}-1}\widehat{h}_2(r)+F_{\frac{N}{2}}h_{1,2}(r) \\ &+ \sum_{j=0}^{N/2-1} G_j\left[h_{2,1}(r)+\widehat{s}_k(2j)\widehat{s}_k(2j+1)\widehat{h}_1(r)\right]. \end{aligned} \tag{G.11}$$

Define the set A to be the set of all nonegative integers less than $\frac{N}{2}-1$ such that $\widehat{s}_k(2j+1)\widehat{s}_k(2j+2)=+1$ and B to be the set of all nonegative integers less than $\frac{N}{2}-1$ such that $\widehat{s}_k(2j+1)\widehat{s}_k(2j+2)=-1$. Similarly, define the set C to be the set of all nonegative integers less than $\frac{N}{2}$ such that $\widehat{s}_k(2j)\widehat{s}_k(2j+1)=+1$ and D to be the set of all nonegative integers less than $\frac{N}{2}$ such that $\widehat{s}_k(2j)\widehat{s}_k(2j+1)=-1$. It follows from the definitions of the sets A, B, C and D that (G.11) can be written as follows

$$\begin{aligned} W_i^e &= \sum_{j\in A} F_j\left[\widehat{h}_2(r)+h_{1,2}(r)\right]+\sum_{j\in B} F_j\left[\widehat{h}_2(r)-h_{1,2}(r)\right] \\ &+ F_{\frac{N}{2}-1}\widehat{h}_2(r)+F_{\frac{N}{2}}h_{1,2}(r) \\ &+ \sum_{j\in C} G_j\left[h_{2,1}(r)+\widehat{h}_1(r)\right]+\sum_{j\in D} G_j\left[h_{2,1}(r)-\widehat{h}_1(r)\right]. \end{aligned} \tag{G.12}$$

Now restore the index i and define $X_i = \sum_{j\in A} F_j$, $Y_i = \sum_{j\in B} F_j$, $P_i = F_{\frac{N}{2}-1}$, $Q_i = F_{\frac{N}{2}}$ and $U_i = \sum_{j\in C} G_j$, $V_i = \sum_{j\in D} G_j$. Then

$$\begin{aligned} W_i^e &= X_i\left[\widehat{h}_2(r_i) + h_{1,2}(r_i)\right] + Y_i\left[\widehat{h}_2(r_i) - h_{1,2}(r_i)\right] \\ &+ P_i\widehat{h}_2(r_i) + Q_i h_{1,2}(r_i) \\ &+ U_i\left[h_{2,1}(r_i) + \widehat{h}_1(r_i)\right] + V_i\left[h_{2,1}(r_i) - \widehat{h}_1(r_i)\right]. \end{aligned} \tag{G.13}$$

Similarly, if l is *odd*, then it can be shown that W_i in (G.1) is given by

$$\begin{aligned} W_i^o &= X_i\left[\widehat{h}_{2,1}(r_i) + h_1(r_i)\right] + Y_i\left[\widehat{h}_{2,1}(r_i) - h_1(r_i)\right] \\ &+ P_i\widehat{h}_{2,1}(r_i) + Q_i h_1(r_i) \\ &+ U_i\left[h_2(r_i) + \widehat{h}_{1,2}(r_i)\right] + V_i\left[h_2(r_i) - \widehat{h}_{1,2}(r_i)\right]. \end{aligned} \tag{G.14}$$

Finally, define the following random varibales

$$R = \sum_{j=0}^{N/2-2} \widehat{s}_k(2j+1)\widehat{s}_k(2j+2) \tag{G.15}$$

$$S = \sum_{j=0}^{N/2-1} \widehat{s}_k(2j)\widehat{s}_k(2j+1). \tag{G.16}$$

Then the density functions of R and S are given by

$$p_R(j) = \binom{\frac{N}{2}-1}{\frac{j+\frac{N}{2}-1}{2}} 2^{1-\frac{N}{2}}, \quad j = 1-\frac{N}{2}, 3-\frac{N}{2}, \ldots, \frac{N}{2}-3, \frac{N}{2}-1 \tag{G.17}$$

$$p_S(j) = \binom{\frac{N}{2}}{\frac{j+\frac{N}{2}}{2}} 2^{-\frac{N}{2}}, \quad j = -\frac{N}{2}, \frac{N}{2}+2, \ldots, \frac{N}{2}-2, \frac{N}{2}. \tag{G.18}$$

Let $|\cdot|$ denote the cardinality of the set. It is obvious that $R = |A| - |B|$ and $S = |C| - |D|$. Furthermore, note that $|A| + |B| = N/2 - 1$ and $|C| + |D| = N/2$. Thus, given R and S, one has $|A| = (N/2 - 1 + R)/2$, $|B| = (N/2 - 1 - R)/2$, $|C| = (N/2 + S)/2$ and $|D| = (N/2 - S)/2$. This fact also implies that, in order to obtain (G.13) and (G.14), it is not necessary to condition the signature sequence of user k. It is sufficient to condition the two random variables R and S defined above.

Appendix H

Derivation of w_N

For simplicity and without loss of accuracy, the index i of the normalized delay, r_i, is removed in this section. Using the first and second moments of $|B|$ and $|D|$ given in Section 7.2.1, it is not hard to see that

$$\begin{aligned}
E(\alpha_i^2|r) &= \frac{N^2}{4}\left[\widehat{h}_2^2(r)+h_{1,2}^2(r)\right]^2+\frac{N^2}{4}\left[\widehat{h}_1^2(r)+h_{2,1}^2(r)\right]^2 \\
&\quad +2(N-2)\widehat{h}_2^2(r)h_{1,2}^2(r)+2N\widehat{h}_1^2(r)h_{2,1}^2(r) \\
&\quad +\frac{N^2}{2}\left[\widehat{h}_2^2(r)+h_{1,2}^2(r)\right]\left[\widehat{h}_1^2(r)+h_{2,1}^2(r)\right] \\
&= \frac{N^2}{4}\left[\widehat{h}_1^4(r)+\widehat{h}_2^4(r)+h_{1,2}^4(r)+h_{2,1}^4(r)\right] \\
&\quad +\left[\frac{N^2}{2}+2(N-2)\right]\widehat{h}_2^2(r)h_{1,2}^2(r)+\left[\frac{N^2}{2}+2N\right]\widehat{h}_1^2(r)h_{2,1}^2(r) \\
&\quad +\frac{N^2}{2}\left[\widehat{h}_2^2(r)\widehat{h}_1^2(r)+\widehat{h}_2^2(r)h_{2,1}^2(r)+h_{1,2}^2(r)\widehat{h}_1^2(r)+h_{1,2}^2(r)h_{2,1}^2(r)\right]. \qquad \text{(H.1)}
\end{aligned}$$

Likewise,

$$\begin{aligned}
E(\beta_i^2|r) &= \frac{N^2}{4}\left[h_1^4(r)+h_2^4(r)+\widehat{h}_{1,2}^4(r)+\widehat{h}_{2,1}^4(r)\right] \\
&\quad +\left[\frac{N^2}{2}+2(N-2)\right]\widehat{h}_{2,1}^2(r)h_1^2(r)+\left[\frac{N^2}{2}+2N)\right]\widehat{h}_{1,2}^2(r)h_2^2(r) \\
&\quad +\frac{N^2}{2}\left[\widehat{h}_{2,1}^2(r)\widehat{h}_{1,2}^2(r)+\widehat{h}_{2,1}^2(r)h_2^2(r)+h_1^2(r)\widehat{h}_{1,2}^2(r)+h_1^2(r)h_2^2(r)\right]. \qquad \text{(H.2)}
\end{aligned}$$

Combining (H.1), (H.2) and using (7.28) produces

$$\begin{aligned}
E(\alpha_i^2)+E(\beta_i^2) &= \frac{1}{T_c}\int_0^{T_c}\left[E(\alpha_i^2|r)+E(\beta_i^2|r)\right]\mathrm{d}r \\
&= \frac{N^2}{2T_c}\int_0^{T_c}\left[h_1^4(r)+h_2^4(r)+\widehat{h}_{1,2}^4(r)+\widehat{h}_{2,1}^4(r)\right]\mathrm{d}r \\
&+\frac{N^2}{T_c}\int_0^{T_c} h_1^2(r)h_2^2(r)\mathrm{d}r+\frac{N^2}{T_c}\int_0^{T_c}\widehat{h}_{2,1}^2(r)\widehat{h}_{1,2}^2(r)\mathrm{d}r \\
&+\frac{N(N+2)-4}{T_c}\int_0^{T_c}\left[h_1^2(r)+h_2^2(r)\right]\widehat{h}_{2,1}^2(r)\mathrm{d}r \\
&+\frac{N(N+2)}{T_c}\int_0^{T_c}\left[h_1^2(r)+h_2^2(r)\right]\widehat{h}_{1,2}^2(r)\mathrm{d}r \\
&= \frac{N^2}{2T_c}\int_0^{T_c}\left[h_1^2(r)+h_2^2(r)+\widehat{h}_{1,2}^2(r)+\widehat{h}_{2,1}^2(r)\right]^2\mathrm{d}r \\
&+\frac{2}{T_c}\int_0^{T_c}\left[h_1^2(r)+h_2^2(r)\right]\left[N\widehat{h}_{1,2}^2(r)+(N-2)\widehat{h}_{2,1}^2(r)\right]\mathrm{d}r. \qquad \text{(H.3)}
\end{aligned}$$

Comparing (H.3) and (7.36) gives

$$\begin{aligned}
w_N &= \frac{1}{T_c^5}\int_0^{T_c}\Bigg\{\left[h_1^2(r)+h_2^2(r)+\widehat{h}_{1,2}^2(r)+\widehat{h}_{2,1}^2(r)\right]^2 \\
&+ 4\left[h_1^2(r)+h_2^2(r)\right]\left[\frac{1}{N}\widehat{h}_{1,2}^2(r)+\frac{N-2}{N^2}\widehat{h}_{2,1}^2(r)\right]\Bigg\}\mathrm{d}r. \qquad \text{(H.4)}
\end{aligned}$$

If the chip waveforms are symmetrical around $T_c/2$, it can be shown that

$$\widehat{h}_{1,2}(r) = \pm\widehat{h}_{2,1}(r) \qquad \text{(H.5)}$$

where the sign is a plus if the two chip waveforms are both even or both odd about $T_c/2$. Otherwise the sign is a minus. Therefore (H.4) simplifies to

$$\begin{aligned}
w_N &= \frac{1}{T_c^5}\int_0^{T_c}\Bigg\{\left[h_1^2(r)+h_2^2(r)+2\widehat{h}_{1,2}^2(r)\right]^2 \\
&+ \frac{8(N-1)}{N}\left[h_1^2(r)+h_2^2(r)\right]\widehat{h}_{1,2}^2(r)\Bigg\}\mathrm{d}r. \qquad \text{(H.6)}
\end{aligned}$$

Appendix I

Derivation of $\widehat{w}_N$

From (7.30) and (7.31) one has

$$\begin{aligned}
E(\alpha_i\alpha_j|r_i,r_j) = &\frac{N^2}{4}\left[\widehat{h}_2^2(r_i)+h_{1,2}^2(r_i)\right]\left[\widehat{h}_2^2(r_j)+h_{1,2}^2(r_j)\right]\\
&+\frac{N^2}{4}\left[\widehat{h}_2^2(r_i)+h_{1,2}^2(r_i)\right]\left[\widehat{h}_1^2(r_j)+h_{2,1}^2(r_j)\right]\\
&+\frac{N^2}{4}\left[\widehat{h}_1^2(r_i)+h_{2,1}^2(r_i)\right]\left[\widehat{h}_2^2(r_j)+h_{1,2}^2(r_j)\right]\\
&+\frac{N^2}{4}\left[\widehat{h}_1^2(r_i)+h_{2,1}^2(r_i)\right]\left[\widehat{h}_1^2(r_j)+h_{2,1}^2(r_j)\right]\\
&+2(N-2)\widehat{h}_2(r_i)h_{1,2}(r_i)\widehat{h}_2(r_j)h_{1,2}(r_j)\\
&+2N\widehat{h}_1(r_i)h_{2,1}(r_i)\widehat{h}_1(r_j)h_{2,1}(r_j). \qquad \text{(I.1)}
\end{aligned}$$

Thus

$$\begin{aligned}
E(\alpha_i\alpha_j) &= \frac{1}{T_c^2}\int_0^{T_c}\int_0^{T_c} E(\alpha_i,\alpha_j|r_i,r_j)\mathrm{d}r_i\mathrm{d}r_j\\
&= \frac{N^2}{4T_c^2}\left[\int_0^{T_c}\left(\widehat{h}_2^2(r)+h_{1,2}^2(r)\right)\mathrm{d}r\right]^2+\frac{N^2}{4T_c^2}\left[\int_0^{T_c}\left(\widehat{h}_1^2(r)+h_{2,1}^2(r)\right)\mathrm{d}r\right]^2\\
&+\frac{N^2}{2T_c^2}\int_0^{T_c}\left(\widehat{h}_2^2(r)+h_{1,2}^2(r)\right)\mathrm{d}r\int_0^{T_c}\left(\widehat{h}_1^2(r)+h_{2,1}^2(r)\right)\mathrm{d}r\\
&+\frac{2(N-2)}{T_c^2}\left[\int_0^{T_c}\widehat{h}_2(r)h_{1,2}(r)\mathrm{d}r\right]^2+\frac{2N}{T_c^2}\left[\int_0^{T_c}\widehat{h}_1(r)h_{2,1}(r)\mathrm{d}r\right]^2. \qquad \text{(I.2)}
\end{aligned}$$

Similarly, it can be shown that

$$
\begin{aligned}
E(\beta_i\beta_j) &= \frac{1}{T_c^2}\int_0^{T_c}\int_0^{T_c} E(\beta_i,\beta_j|r_i,r_j)\mathrm{d}r_i\mathrm{d}r_j \\
&= \frac{N^2}{4T_c^2}\left[\int_0^{T_c}\left(\widehat{h}_{2,1}^2(r)+h_1^2(r)\right)\mathrm{d}r\right]^2+\frac{N^2}{4T_c^2}\left[\int_0^{T_c}\left(\widehat{h}_{1,2}^2(r)+h_2^2(r)\right)\mathrm{d}r\right]^2 \\
&+\frac{N^2}{2T_c^2}\int_0^{T_c}\left(\widehat{h}_{2,1}^2(r)+h_1^2(r)\right)\mathrm{d}r\int_0^{T_c}\left(\widehat{h}_{1,2}^2(r)+h_2^2(r)\right)\mathrm{d}r \\
&+\frac{2(N-2)}{T_c^2}\left[\int_0^{T_c}\widehat{h}_{2,1}(r)h_1(r)\mathrm{d}r\right]^2+\frac{2N}{T_c^2}\left[\int_0^{T_c}\widehat{h}_{1,2}(r)h_2(r)\mathrm{d}r\right]^2. \qquad \text{(I.3)}
\end{aligned}
$$

Due to the symmetry, it is obvious that $E(\alpha_i\beta_j)=E(\beta_i\alpha_j)$. To calculate $E(\alpha_i\beta_j)$, first obtain $E(\alpha_i\beta_j|r_i,r_j)$ as follows

$$
\begin{aligned}
E(\alpha_i\beta_j|r_i,r_j) &= \frac{N^2}{4}\left[\widehat{h}_2^2(r_i)+h_{1,2}^2(r_i)\right]\left[\widehat{h}_{2,1}^2(r_j)+h_1^2(r_j)\right] \\
&+\frac{N^2}{4}\left[\widehat{h}_2^2(r_i)+h_{1,2}^2(r_i)\right]\left[\widehat{h}_{1,2}^2(r_j)+h_2^2(r_j)\right] \\
&+\frac{N^2}{4}\left[\widehat{h}_1^2(r_i)+h_{2,1}^2(r_i)\right]\left[\widehat{h}_{2,1}^2(r_j)+h_1^2(r_j)\right] \\
&+\frac{N^2}{4}\left[\widehat{h}_1^2(r_i)+h_{2,1}^2(r_i)\right]\left[\widehat{h}_{1,2}^2(r_j)+h_2^2(r_j)\right] \\
&+2(N-2)\widehat{h}_2(r_i)h_{1,2}(r_i)\widehat{h}_{2,1}(r_j)h_1(r_j) \\
&+2N\widehat{h}_1(r_i)h_{2,1}(r_i)\widehat{h}_{1,2}(r_j)h_2(r_j). \qquad \text{(I.4)}
\end{aligned}
$$

Therefore

$$
\begin{aligned}
E(\alpha_i\beta_j) &= \frac{1}{T_c^2}\int_0^{T_c}\int_0^{T_c} E(\alpha_i\beta_j|r_i,r_j)\mathrm{d}r_i\mathrm{d}r_j \\
&= \frac{N^2}{4T_c^2}\int_0^{T_c}\left(\widehat{h}_2^2(r)+h_{1,2}^2(r)\right)\mathrm{d}r\int_0^{T_c}\left(\widehat{h}_{2,1}^2(r)+h_1^2(r)\right)\mathrm{d}r \\
&+\frac{N^2}{4T_c^2}\int_0^{T_c}\left(\widehat{h}_2^2(r)+h_{1,2}^2(r)\right)\mathrm{d}r\int_0^{T_c}\left(\widehat{h}_{1,2}^2(r)+h_2^2(r)\right)\mathrm{d}r \\
&+\frac{N^2}{4T_c^2}\int_0^{T_c}\left(\widehat{h}_1^2(r)+h_{2,1}^2(r)\right)\mathrm{d}r\int_0^{T_c}\left(\widehat{h}_{2,1}^2(r)+h_1^2(r)\right)\mathrm{d}r \\
&+\frac{N^2}{4T_c^2}\int_0^{T_c}\left(\widehat{h}_1^2(r)+h_{2,1}^2(r)\right)\mathrm{d}r\int_0^{T_c}\left(\widehat{h}_{1,2}^2(r)+h_2^2(r)\right)\mathrm{d}r \\
&+\frac{2(N-2)}{T_c^2}\int_0^{T_c}\widehat{h}_2(r)h_{1,2}(r)\mathrm{d}r\int_0^{T_c}\widehat{h}_{2,1}(r)h_1(r)\mathrm{d}r \\
&+\frac{2N}{T_c^2}\int_0^{T_c}\widehat{h}_1(r)h_{2,1}(r)\mathrm{d}r\int_0^{T_c}\widehat{h}_{1,2}(r)h_2(r)\mathrm{d}r. \qquad \text{(I.5)}
\end{aligned}
$$

Now, by combining (I.2), (I.3), (I.5), using (7.28), and after some algebraic manipulations one obtains

$$
\begin{aligned}
&E(\alpha_i\alpha_j)+2E(\alpha_i\beta_j)+E(\beta_i\beta_j) = \\
&= \frac{N^2}{4T_c^2}\left[\int_0^{T_c}\left(h_2^2(r)+\widehat{h}_{2,1}^2(r)\right)\mathrm{d}r\right]^2+\frac{N^2}{4T_c^2}\left[\int_0^{T_c}\left(h_1^2(r)+\widehat{h}_{1,2}^2(r)\right)\mathrm{d}r\right]^2 \\
&+\frac{N^2}{4T_c^2}\left[\int_0^{T_c}\left(\widehat{h}_{2,1}^2(r)+h_1^2(r)\right)\mathrm{d}r\right]^2+\frac{N^2}{4T_c^2}\left[\int_0^{T_c}\left(\widehat{h}_{1,2}^2(r)+h_2^2(r)\right)\mathrm{d}r\right]^2 \\
&+\frac{2(N-2)}{T_c^2}\left[\int_0^{T_c}h_2(r)\widehat{h}_{2,1}(r)\mathrm{d}r+\int_0^{T_c}\widehat{h}_{2,1}(r)h_1(r)\mathrm{d}r\right]^2 \\
&+\frac{2N}{T_c^2}\left[\int_0^{T_c}h_1(r)\widehat{h}_{1,2}(r)\mathrm{d}r+\int_0^{T_c}\widehat{h}_{1,2}(r)h_2(r)\mathrm{d}r\right]^2 \\
&+\frac{N^2}{2T_c^2}\left[\int_0^{T_c}\left(h_1^2(r)+h_2^2(r)+\widehat{h}_{1,2}^2(r)+\widehat{h}_{2,1}^2(r)\right)\mathrm{d}r\right]^2 \\
&+\frac{N^2}{T_c^2}\left[\int_0^{T_c}h_1^2(r)\mathrm{d}r\int_0^{T_c}h_2^2(r)\mathrm{d}r+\int_0^{T_c}\widehat{h}_{1,2}^2(r)\mathrm{d}r\int_0^{T_c}\widehat{h}_{2,1}^2(r)\mathrm{d}r\right] \\
&+\frac{N^2}{2T_c^2}\left[\int_0^{T_c}h_1^2(r)\mathrm{d}r+\int_0^{T_c}h_2^2(r)\mathrm{d}r\right]\left[\int_0^{T_c}\widehat{h}_{1,2}^2(r)\mathrm{d}r+\int_0^{T_c}\widehat{h}_{2,1}^2(r)\mathrm{d}r\right]. \qquad \text{(I.6)}
\end{aligned}
$$

Comparing (I.6) and (7.37) shows that

$$\begin{aligned}\widehat{w}_N = &\frac{1}{T_c^6}\left[\int_0^{T_c}\left(h_2^2(r)+\widehat{h}_{2,1}^2(r)\right)\mathrm{d}r\right]^2+\frac{1}{T_c^6}\left[\int_0^{T_c}\left(h_1^2(r)+\widehat{h}_{1,2}^2(r)\right)\mathrm{d}r\right]^2\\
&+\frac{1}{T_c^6}\left[\int_0^{T_c}\left(\widehat{h}_{2,1}^2(r)+h_1^2(r)\right)\mathrm{d}r\right]^2+\frac{1}{T_c^6}\left[\int_0^{T_c}\left(\widehat{h}_{1,2}^2(r)+h_2^2(r)\right)\mathrm{d}r\right]^2\\
&+\frac{8(N-2)}{N^2T_c^6}\left[\int_0^{T_c}h_2(r)\widehat{h}_{2,1}(r)\mathrm{d}r+\int_0^{T_c}\widehat{h}_{2,1}(r)h_1(r)\mathrm{d}r\right]^2\\
&+\frac{8}{NT_c^6}\left[\int_0^{T_c}h_1(r)\widehat{h}_{1,2}(r)\mathrm{d}r+\int_0^{T_c}\widehat{h}_{1,2}(r)h_2(r)\mathrm{d}r\right]^2\\
&+\frac{2}{T_c^6}\left[\int_0^{T_c}\left(h_1^2(r)+h_2^2(r)+\widehat{h}_{1,2}^2(r)+\widehat{h}_{2,1}^2(r)\right)\mathrm{d}r\right]^2\\
&+\frac{4}{T_c^6}\left[\int_0^{T_c}h_1^2(r)\mathrm{d}r\int_0^{T_c}h_2^2(r)\mathrm{d}r+\int_0^{T_c}\widehat{h}_{1,2}^2(r)\mathrm{d}r\int_0^{T_c}\widehat{h}_{2,1}^2(r)\mathrm{d}r\right]\\
&+\frac{2}{T_c^6}\left[\int_0^{T_c}h_1^2(r)\mathrm{d}r+\int_0^{T_c}h_2^2(r)\mathrm{d}r\right]\left[\int_0^{T_c}\widehat{h}_{1,2}^2(r)\mathrm{d}r+\int_0^{T_c}\widehat{h}_{2,1}^2(r)\mathrm{d}r\right]. \qquad \text{(I.7)}\end{aligned}$$

As for the w_N used in Appendix H, when the chip waveforms are symmetrical around $T_c/2$, the above expression for $\widehat{w}_N$ simplifies to the following expression

$$\begin{aligned}\widehat{w}_N = &\frac{2}{T_c^6}\left[\int_0^{T_c}\left(h_2^2(r)+\widehat{h}_{1,2}^2(r)\right)\mathrm{d}r\right]^2+\frac{2}{T_c^6}\left[\int_0^{T_c}\left(h_1^2(r)+\widehat{h}_{1,2}^2(r)\right)\mathrm{d}r\right]^2\\
&+\frac{16(N-1)}{N^2T_c^6}\left[\int_0^{T_c}\Big(h_1(r)+h_2(r)\Big)\widehat{h}_{1,2}(r)\mathrm{d}r\right]^2\\
&+\frac{2}{T_c^6}\left[\int_0^{T_c}\left(h_1^2(r)+h_2^2(r)+2\widehat{h}_{1,2}^2(r)\right)\mathrm{d}r\right]^2\\
&+\frac{4}{T_c^6}\left[\int_0^{T_c}h_1^2(r)\mathrm{d}r\int_0^{T_c}h_2^2(r)\mathrm{d}r+\left(\int_0^{T_c}\widehat{h}_{1,2}^2(r)\mathrm{d}r\right)^2\right]\\
&+\frac{4}{T_c^6}\left[\int_0^{T_c}h_1^2(r)\mathrm{d}r+\int_0^{T_c}h_2^2(r)\mathrm{d}r\right]\int_0^{T_c}\widehat{h}_{1,2}^2(r)\mathrm{d}r. \qquad \text{(I.8)}\end{aligned}$$

References

[1] J. M. Wozencraft and I. M. Jacobs, *Principles of Communication Engineering.* John Wiley & Sons, 1965.

[2] S. Verdú, *Multiuser Detection.* Cambridge University Press, 1998.

[3] K. S. Gilhousen, I. M. Jacobs, R. Padovani, A. J. Viterbi, L. A. Weaver Jr., and C. E. Wheatley III, "On the capacity of a cellular CDMA system," *IEEE Trans. Veh. Technol.*, vol. 40, pp. 303–312, May 1991.

[4] R. Prasad, J. S. Dasilva, and B. Arroyo Fernández (Eds.), "Air interface access schemes for wireless communications (Part I)," *IEEE Commun. Mag.*, vol. 37, pp. 104–138, Sept. 1999.

[5] R. Prasad, J. S. Dasilva, and B. Arroyo Fernández (Eds.), "Air interface access schemes for wireless communications (Part II)," *IEEE Commun. Mag.*, vol. 37, pp. 70–88, Dec. 1999.

[6] S. Verdú, "Minimum probability of error for asynchronous gaussian multiple access channels," *IEEE Trans. Inform. Theory*, vol. 32, pp. 85–96, Jan. 1986.

[7] S. Verdú, "Computational complexity of optimum multiuser detection," *Algorithmica*, vol. 4, pp. 303–312, 1989.

[8] A. Duel-Hallen, J. Holtzman, and Z. Zvonar, "Multiuser detection for CDMA systems," *IEEE Personal Commun.*, pp. 46–95, Apr. 1995.

[9] S. Moshavi, "Multi-User detection for DS-CDMA communications," *IEEE Commun. Mag.*, pp. 124–136, Oct. 1996.

[10] J. Yang and S. Roy, "On joint transmitter and receiver optimization multiple-input-multiple-output transmission systems," *IEEE Trans. Commun.*, vol. 42, pp. 3221–3231, Dec. 1994.

[11] W. M. Jang, B. R. Vojčić, and R. L. Pickholtz, "Joint transmitter-receiver optimization in synchronous multiuser communications over multipath channels," *IEEE Trans. Commun.*, vol. 46, pp. 269–278, Feb. 1998.

[12] T. M. Lok and T. F. Wong, "Transmitter and receiver optimization in multi-carrier CDMA systems," *IEEE Trans. Commun.*, vol. 48, pp. 1197–1207, July 2000.

[13] J. L. Massey and T. Mittelholzer, "Welch's bound and sequence sets for code-division multiple access systems," in *Sequences II, Methods in Communication, Security and Computer Sciences* (R. Capocelli, A. D. Santis, and U. Vaccaro, eds.), New York: Springer-Verlag, 1993.

[14] M. Rupf and J. L. Massey, "Optimum sequence multisets for synchronous code-division multiple-access channels," *IEEE Trans. Inform. Theory*, vol. 40, pp. 1261–1266, July 1994.

[15] P. Viswanath, V. Anantharam, and D. N. C. Tse, "Optimal sequences, power control and user capacity of synchronous cdma systems with linear MMSE multiuser receiver," *IEEE Trans. Inform. Theory*, vol. 45, pp. 1968–1983, Sept. 1999.

[16] L. R. Welch, "Lower bound on the maximum cross correlation of signals," *IEEE Trans. Inform. Theory*, vol. IT-20, pp. 397–399, May 1974.

[17] P. Viswanath and V. Anantharam, "Optimal sequences and sum capacity of synchronous CDMA systems," *IEEE Trans. Inform. Theory*, vol. 45, pp. 1984–1991, Sept. 1999.

[18] R. S. Cheng and S. Verdú, "Optimal signal design for band-limited PAM synchronous multiple-access channels," in *Proc. 23rd. Conf. Information Sciences and Systems*, (The Johns Hopkins University, Baltimore, MD), pp. 321–326, Mar. 1989.

[19] R. S. Cheng and S. Verdú, "Capacity of root mean square bandlimited Gaussian multiuser channels," *IEEE Trans. Inform. Theory*, vol. 37, pp. 453–465, May 1991.

[20] D. Parsavand and M. K. Varanasi, "RMS bandwidth constrained signature waveforms that maximize the total capacity of PAM-synhcronous CDMA channels," *IEEE Trans. Commun.*, vol. 44, pp. 65–74, Jan. 1996.

[21] M. K. Varanasi and E. A. Fain, "Optimum signal design and power control for multiuser wireless communications under location-invariant bandwidth constraints," in *Proc. Thirty-Sixth Allerton Conf. Commun. Contr. and Comp.*, Sept. 1998.

[22] F. Amoroso, "The bandwidth of digital signals," *IEEE Commun. Mag.*, vol. 18, pp. 13–24, Nov. 1980.

[23] D. Slepian and H. O. Pollak, "Prolate spheroidal wave functions, Fourier analysis, and uncertainty–I," *Bell System Tech. J.*, vol. 40, pp. 43–64, Jan. 1961.

[24] H. J. Landau and H. O. Pollak, "Prolate spheroidal wave functions, Fourier analysis and uncertainty–II," *Bell System Tech. J.*, vol. 40, pp. 65–84, Jan. 1961.

[25] D. P. Sarwate and M. B. Pursley, "Crosscorrelation properties of pseudorandom and related sequences," *Proc. IEEE*, vol. 68, pp. 593–619, May 1980.

[26] D. V. Sarwate, "Mean-square correlation of shift-register sequences," *IEE Proc.*, vol. 131, part F, pp. 101–106, Apr. 1984.

[27] F. W. Sun and H. Leib, "Optimal phases for a family of quadriphase CDMA sequences," *IEEE Trans. Inform. Theory*, vol. 43, pp. 1205–1217, July 1997.

[28] D. P. Sarwate, "Bounds on crosscorrelation and autocorrelation of sequences," *IEEE Trans. Inform. Theory*, vol. IT-25, pp. 720–724, Nov. 1979.

[29] D. V. Sarwate, "Meeting the Welch bound with equality," in *Proc. IEEE Int. Conf. Sequences. and Their Appl.*, pp. 79–102, 1998.

[30] S. Boztas, R. Hammons, and P. V. Kumar, "4-phase sequences with near optimum correlation properties," *IEEE Trans. Inform. Theory*, vol. 38, pp. 1101–1113, May 1992.

[31] G. Chandran and J. S. Jaffe, "Signal set design with constrained amplitude spectrum and specified time-bandwidth product," *IEEE Trans. Commun.*, vol. 44, pp. 725–731, June 1996.

[32] M. A. Landolsi and W. E. Stark, "DS-CDMA chip waveform design for minimal interference under bandwidth, phase and envelope constraints," *IEEE Trans. Commun.*, vol. 47, pp. 1737–1746, Nov. 1999.

[33] J. S. Lehnert and M. B. Pursley, "Error probabilities for binary direct-sequence spread-spectrum communications with random signature sequences," *IEEE Trans. Commun.*, vol. COM-35, pp. 87–98, Jan. 1987.

[34] E. Geraniotis and B. Ghaffari, "Performance of binary and quaternary direct-sequence spread-spectrum multiple-access systems with random signature sequences," *IEEE Trans. Commun.*, vol. 39, pp. 713–724, May 1991.

[35] J. P. Chaib and H. Leib, "Chip shaping and channel coding for CDMA," *European Trans. Telecommun. Related Technol.*, vol. 7, pp. 133–143, Mar./Apr. 1996.

[36] M. B. Pursley, "Performance evaluation for phase-coded spread-spectrum multiple-access communication-Part I: System analysis," *IEEE Trans. Commun.*, vol. COM-25, pp. 795–799, Aug. 1977.

[37] M. B. Pursley, F. D. Garber, and J. S. Lehnert, "Analysis of generalized quadriphase spread-spectrum communications," in *Proc. IEEE Int. Conf. Commun.*, pp. 15.3.1–15.3.5, 1980.

[38] P. I. Dallas and F.-N. Pavlidou, "Innovative chip waveforms in microcellular DS/CDMA packet mobile radio," *IEEE Trans. Commun.*, vol. 44, pp. 1413–1416, Nov. 1996.

[39] M. A. Landolsi and W. E. Stark, "Optimal chip waveforms for DS-CDMA with generalized OQPSK modulation," *European Trans. Telecommun. Related Technol.*, vol. 8, pp. 527–536, Sep./Oct. 1997.

[40] J. M. Holtzman, "A simple, accurate method to calcualte spread-spectrum multiple-access error probabilities," *IEEE Trans. Commun.*, vol. 40, pp. 461–464, Mar. 1992.

[41] T. Kailath and H. V. Poor, "Detection of stochastic processes," *IEEE Trans. Inform. Theory*, vol. 44, pp. 2230–2259, Oct. 1998.

[42] C. Sankaran and A. Ephremides, "Solving a class of optimum multiuser detection problems with polynomial complexity," *IEEE Trans. Inform. Theory*, vol. 44, pp. 1958–1961, Sept. 1998.

[43] R. E. Learned, A. S. Willsky, and D. M. Boroson, "Low complexity optimal joint detection for oversaturated multiple access communications," *IEEE Trans. Signal Process.*, vol. 45, pp. 113–123, Jan. 1997.

[44] R. Lupas and S. Verdú, "Linear multiuser detectors for synchronous code-division multiple-access channels," *IEEE Trans. Inform. Theory*, vol. 35, pp. 123–136, Jan. 1989.

[45] Z. Xie, R. Short, and C. Rushforth, "A family of suboptimum detectors for coherent multiuser communications," *IEEE J. Select. Areas in Commun.*, vol. 8, pp. 683–690, May 1990.

[46] U. Madhow and M. L. Honig, "MMSE interference suppression for direct-sequence spread spectrum CDMA," *IEEE Trans. Commun.*, vol. 42, pp. 3178–3188, Dec. 1994.

[47] H. V. Poor and S. Verdú, "Probability of error in MMSE multiuser detection," *IEEE Trans. Inform. Theory*, vol. 43, pp. 858–871, May 1997.

[48] P. V. Rooyen and F. Solms, "Maximum entropy investigation of the inter user interference distribution in a DS/SSMA system," in *Proc. PIMRC*, 1995.

[49] G. Proakis, *Digital Communications*. McGraw-Hill Inc., 1995.

[50] A. H. Nuttall, "Minimum rms bandwidth of M time-limited signals with specified code or correlation matrix," *IEEE Trans. Inform. Theory*, vol. IT-14, pp. 699–707, Sept. 1968.

[51] S. Hanish, R. V. Baier, A. L. Van Buren, and B. J. King, "NRL report 7088: Tables of radial spheroidal wave functions," tech. rep., Naval Research Laboratory, Washington, D. C., June 1970.

[52] A. H. Nuttall and F. Amoroso, "Minimum Gabor bandwidth of M orthogonal signals," *IEEE Trans. Inform. Theory*, vol. IT-11, pp. 440–444, July 1965.

[53] T. P. McGree and G. R. Cooper, "Upper bounds and construction techniques for signal sets with constrained synchronous correlation and specified time-bandwidth product," *IEEE Trans. Inform. Theory*, vol. IT-30, pp. 439–443, Mar. 1984.

[54] I. Daubechies, *Ten Lectures on Wavelets.* SIAM, 1992.

[55] W. Tang, *A Receiver for Continuous Phase Modulation in Walsh Signal Space.* PhD thesis, University of Manitoba, Winnipeg, Manitoba, Canada, Sept. 1998.

[56] W. Tang and E. Shwedyk, "A quasi-optimum receiver for continuous phase modulation," *IEEE Trans. Commun.*, vol. 48, pp. 1087–1090, July 2000.

[57] T. F. Wong, T. M. Lok, and J. S. Lehnert, "Asynchronous multiple-access interference suppression and chip waveform selection with aperiodic random sequences," *IEEE Trans. Commun.*, vol. 47, pp. 103–114, Jan. 1999.

[58] V. M. DaSilva and E. S. Sousa, "Multicarrier orthogonal CDMA signals for quasi-synchronous communications systems," *IEEE J. Select. Areas in Commun.*, vol. 12, pp. 842–852, June 1994.

[59] J. H. Cho and J. S. Lehnert, "Optimum chip waveforms for DS/CDMA communications with random spreading sequences and a matched filter receiver," in *Proc. IEEE Wireless Commun. and Networking. Conf.*, pp. 574–578, 1999.

[60] W. Gao, J. H. Cho, and J. S. Lehnert, "Chip waveform design for DS/SSMA systems with aperiodic random spreading sequences," in *Proc. IEEE Military Commun. Conf.*, pp. 856–860, 2000.

[61] A. J. Viterbi, *CDMA: Principles of Spread Spectrum Communication.* Addison-Wesley Publishing Company, 1995.

[62] H. H. Nguyen, *Optimization Routines to Obtain Signature and Chip Waveforms for Asynchronous CDMA Systems.* Research report (unpublished), Dept. of Electrical & Computer Engineering, University of Manitoba, Winnipeg, MB, Canada, Aug. 2001.

[63] T. Ojanpera and R. Prasad, "An overview of air interface multiple access for IMT-2000/UMTS," *IEEE Commun. Mag.*, vol. 36, pp. 82–95, Sept. 1998.

[64] TIA/EIA/IS-95, "Mobile station-base station compatability standard for dual-mode wideband spread spectrum cellular system," tech. rep., Tech. Rep., TIA/EIA, July 1993.

[65] E. A. Lee and D. G. Messerschmitt, *Digital Communication.* Kluwer Academic Publishers, 2 ed.

[66] K. Yao, "Error probability of asynchronous spread spectrum multiple access communication systems," *IEEE Trans. Commun.*, vol. COM-25, pp. 803–809, Aug. 1977.

[67] R. K. Morrow and L. S. Lehnert, "Bit-to-bit error dependence in slotted DS/SSMA packet systems with random signature sequences," *IEEE Trans. Commun.*, vol. 37, pp. 1052–1061, Oct. 1989.

[68] T. M. Lok and J. S. Lehnert, "Error probabilities for generalized quadriphase DS/SSMA communication systems with random signature sequences," *IEEE Trans. Commun.*, vol. 44, pp. 876–885, July 1996.

[69] K. B. Letaief, "Efficient evaluation of the error probabilities of spread-spectrum multiple-access communications," *IEEE Trans. Commun.*, vol. 45, pp. 239–246, Feb. 1997.

[70] R. M. Buehrer and B. D. Woerner, "Analysis of adaptive multistage interference cancellation for CDMA using an improved gaussian approximation," *IEEE Trans. Commun.*, vol. 44, pp. 1308–1321, Oct. 1996.

[71] S. J. Lee, T. S. Kim, and D. K. Sung, "Bit-error probabilities of multicode direct-sequence spread-spectrum multiple-access systems," *IEEE Trans. Commun.*, vol. 49, pp. 31–34, Jan. 2001.

[72] Y. C. Yoon, "Simple and accurate BER analysis of bandlimited DS-CDMA systems with multi-class services," in *Proc. IEEE Int. Conf. 3rd Generation Wireless Commun.*, 2000.

[73] L. Vandendorpe, "Multitone spread spectrum multiple access communications system in a multipath rician fading channel," *IEEE Trans. Veh. Technol.*, vol. 44, pp. 327–337, May 1995.

[74] E. A. Sourour and M. Nakagawa, "Performance of orthogonal multicarrier CDMA in a multipath fading channel," *IEEE Trans. Commun.*, vol. 44, pp. 356–366, Mar. 1996.

[75] S. K. Kondo and L. B. Milstein, "Performance of multicarrier DS CDMA systems," *IEEE Trans. Commun.*, vol. 44, pp. 238–245, Feb. 1996.

[76] S. Hara and R. Prasad, "Overview of multicarrier CDMA," *IEEE Commun. Mag.*, pp. 126–133, Dec. 1997.

[77] K. W. Yip, X. Zhang, T. S. Ng, and J. Wang, "On the multiple access capacity of multitone-CDMA communications," *IEEE Commun. Letters*, vol. 4, pp. 40–42, Feb. 2000.

[78] S. M. Tseng and M. R. Bell, "Asynchronous multicarrier DS-CDMA using mutually orthogonal complementary sets of sequences," *IEEE Trans. Commun.*, vol. 48, pp. 53–59, Jan. 2000.